4.5 Metal sorption capacity by bentonite and zeolite after biofunctionalisation with *Penicillium simplicissimum*

The description of the preparation of biosorbents based on *Penicillium simplicissimum* is given in Chapter 3. In this section, adsorption of heavy metals on zeolite/bentonite-*Penicillium simplicissimum* was studied based on equilibrium and kinetic processes.

The following parameters were assessed: pH, concentration, contact time, temperature and adsorbent mass. Mathematical models (pseudo 1st and 2nd order, Elovich, intraparticle and film diffusion models) were employed for the prediction and comparison of the binding capacity and to design the sorption process. Thermodynamic parameters as well as adsorption rates as a function of temperature were calculated.

4.5.1 Growth and morphological identification of Penicillium simplicissimum

The growth of *Penicillium simplicissimum* in Schott bottles after 5 days at pH 5 and 6, immobilized and non immobilised are shown in Figure 4.45.

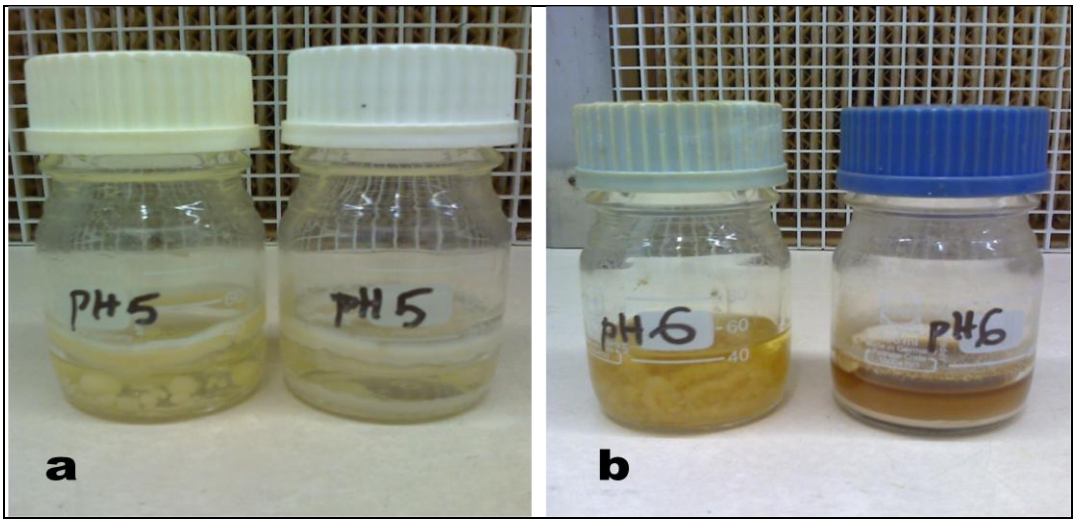

Figure 4.45 Growth of *P. simplicissimum* **(a)** left bottle: zeolite + liquid medium; right bottle: liquid medium without zeolite **(b)** left bottle: liquid medium without bentonite; right bottle: bentonite + liquid medium

The fungus grew rapidly in zeolite/bentonite and produced woolly to cottony, spreading colonies. This indicates the possibility of the *Penicillium* sp. to utilise zeolite/bentonite as a source of nutrients. These results were confirmed by the growth curves in Figure 4.47.

The fungal strain was identified by using standard identification techniques such as colony morphology and microscopic examination under light microscope (Figure 4.46).

On the basis of microscopic examination and morphologic characteristics, the fungal strain was identified as *Penicillium simplicissimum*. The identification was performed in the School of Molecular and Cell Biology. The images in Figure 4.46 showed the production of well defined aerial conidiophore from which a complex arrangement of branches arises. The chains of conidia contain several hundred spores, which are the feature of *Penicillium* sp. The conidiospores of *Penicillium* sp. have the following characeristics: length, 2.5 – 4.0 μm and width, 2.2 – 3.5μm.

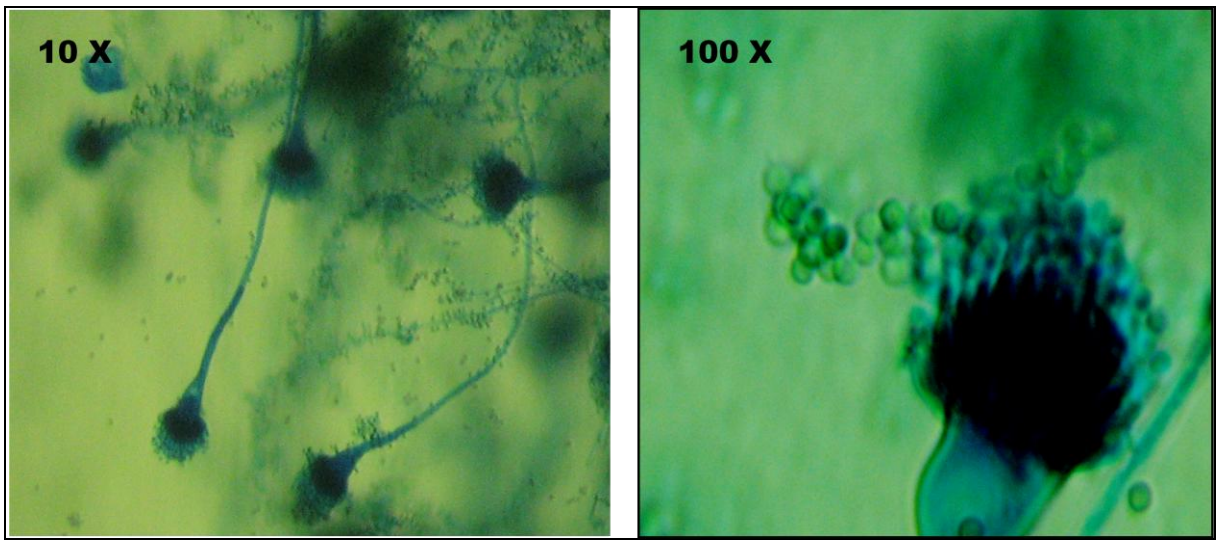

Figure 4.46 Light microscope images of sporulating culture of *P. simplicissimum*

4.5.2 Bentonite-*Penicillium simplicissimum*

4.5.2.1 Growth curve of P. simplicissimum on bentonite

This experiment determined the optimum conditions for the growth of *P. simplicissimum* as a function of medium pH and days of incubation. The graphs in Figure 4.47 show that 100 mg g^{-1} of biomass were harvested after 10 days of incubation at pH 5 for the fungus grown in liquid medium and 60 mg g^{-1} of biomass were obtained after 5 days at pH 4.

When the fungal biomass was grown in a matrix e.g. bentonite in the liquid medium, 600 mg g^{-1} of biomass were harvested after 5 days at pH 4. In general, a decrease of biomass was

observed after 10 days of incubation. This could be due to the lack or decrease of nutrients in the medium since no further nutrients were added in the growth medium.

The growth of *P. simplicissimum* showed a 10-fold increase in biomass when immobilized on bentonite (600 mg g^{-1}) at pH 4.

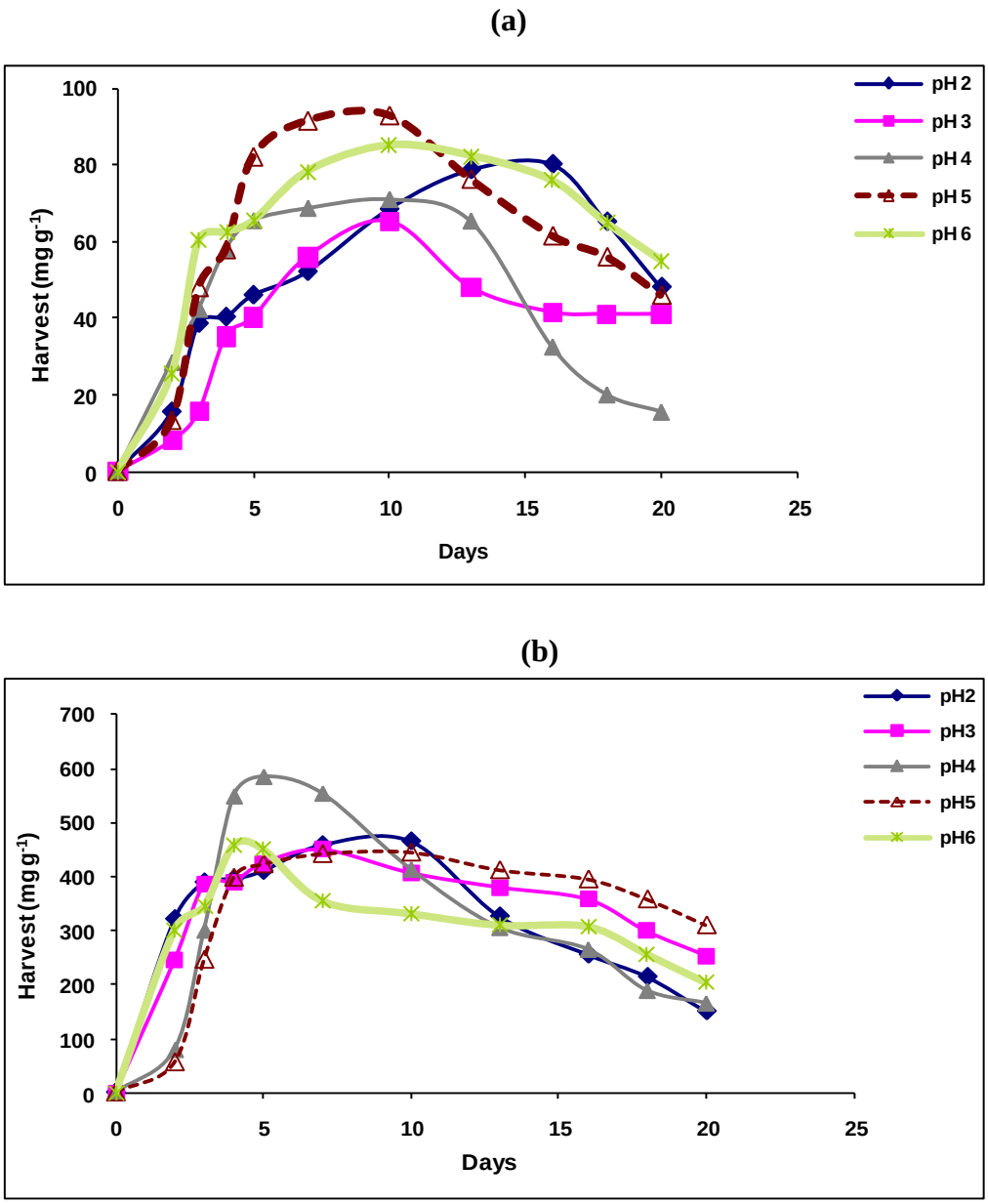

Figure 4.47 Growth curves of (a) *P. simplicissimum* in liquid medium (b) *P.simplicissimum* in liquid medium and supported on bentonite

The pH of most of the polluted tailings in the Witwatersrand is around 4, meaning that *P. simplicissimum* may grow in these tailings since they contain materials like silica and some metals which might constitute nutrient sources for the fungal biomass. In fact, the culture conditions of the fungus strongly affect the chemical composition of the fungal wall and this may in turn affect biosorptive properties. The presence of toxic metals in the growth medium can also alter the cell wall composition, sometimes resulting in the production of melanins and increased metal-binding capacity (Hughes and Poole, 1989).

4.5.2.2 Characteristics of the biomass

i) Physical properties and elemental composition of bentonite-P. simplicissimum

The surface area, cation exchange capacity and elemental composition of the bentonite (natural as well as modified *P. simplicissimum*) are given in Table 4.40.

Table 4.40 Physical properties and elemental composition of natural and functionalised bentonite with *P. simplicissimum*

	Surface area	***CEC***	***C***	***H***	***N***	***S***
	m^2/g	meq/100g	%	%	%	%
Natural-bentonite	73.82	73.80	0.555	1.748	n.d	n.d
Bentonite- *P. simplicissimum*	19.62	65.24	0.785	2.192	0.276	0.031

n.d – not detected

An increase in carbon and hydrogen amount was observed in the biomass compared to the percentage obtained in the natural bentonite. Nitrogen and sulphur were analysed in the biomass, indicating the presence of compounds released by the fungi, e.g. polysaccharides, proteins and amino acids as proven by the IR spectra. These compounds contribute to the increase in the percentage of C, H, N as well as sulphur in the modified bentonite. The cationic exchange capacity of the functionalised bentonite decreased as observed in Table 4.40. This could probably indicate a reaction between cations in bentonite and functional groups present on the fungal biomass surface. This revealed the ion-exchanger character of the biomass.

ii) Zeta potential of P. simplicissimum immobilized on bentonite and zeolite

The zeta potential plots for zeolite/bentonite-*P. simplicissimum* are shown in Figure 4.48. The graphs show the presence of negative charge at the surface of the biomass for pH 2 to 8. The point of zero charge was depicted between pH 3 to 4 and the surface became more negative at pH 6.

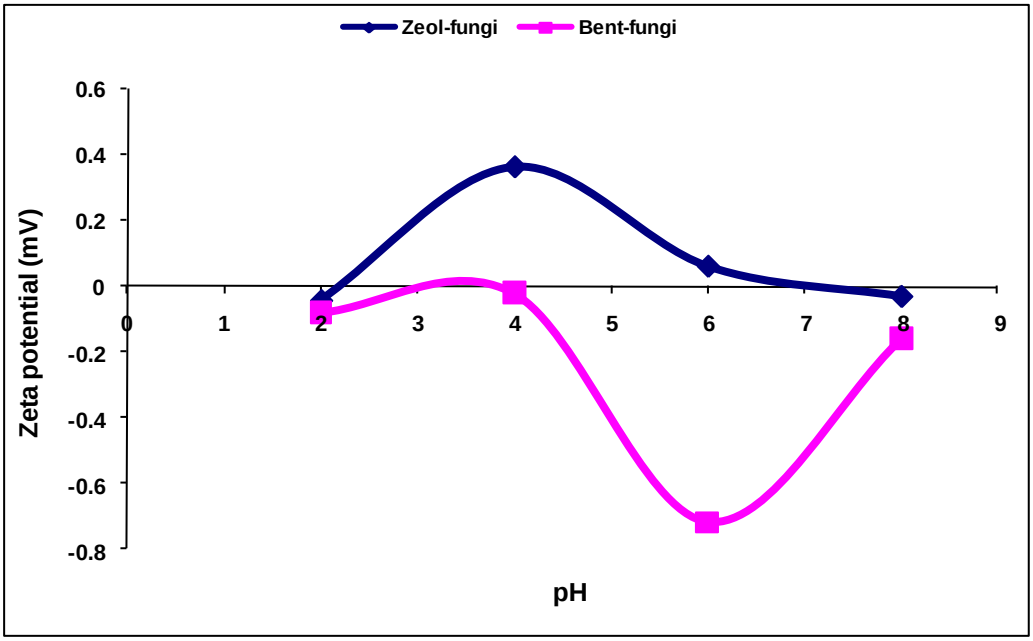

Figure 4.48 Zeta potential plots for bentonite-*P. simplicissimum* and zeolite-*P. simplicissimum*

Compared to the non-functionalised zeolite surface, more negatively charged surfaces were observed between the pH 4 to 8. The changes to the sign of the zeta potential of functionalised bentonite could be related to the presence of functional groups such as –NH, COO-, SH and OH on the surface of the sorbent.

iii) FTIR spectral analysis

The FTIR spectra of bentonite-fungal in the range of 400−4000 cm^{-1} were taken to confirm the presence of functional groups that are usually responsible for the biosorption process and are presented in Figure 4.49.

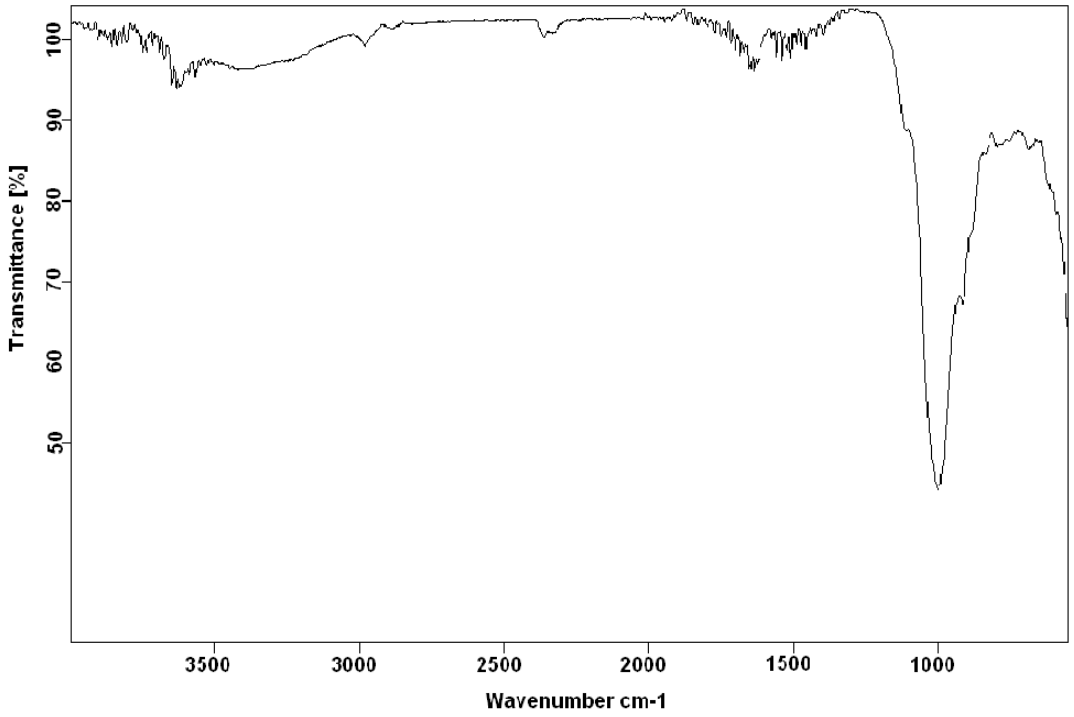

Figure 4.49 FTIR spectra of bentonite-*P. simplicissimum*

The FTIR spectrum showed the characteristic peaks that were demonstrated for the main functional groups of the cell wall for the metals. The spectra disclosed biosorbent heterogeneity though different characteristic peaks of amino, carboxylic, thiol, hydroxyl and carbonyl groups. The major groups categorized according to C-O, C=O, P=O, N-H, C-N, -CH. Table 4.41 presents the FTIR absorption bands and corresponding possible groups that have potential to interact with metal ions.

Table 4.41 FTIR absorption bands and corresponding possible groups observed on the bentonite-*P. simplicissimum* fungal biomass

Wavenumber, cm^{-1}	***Vibration type***
3420	Carboxyl/OH stretch and N-H stretch
2980	Phenolic/carboxylic, S-H
2362	-CH stretch
1635	C= chelate , stretching amide I band
1521	C= chelate, stretching amide I band
1418	Amide II band, OH bands
1247	Symmetric bending of CH_3 of the acetyl moiety, PO_4^{3-} stretch
1064	COO^-
1000	Si-O-Si stretching
914	Al^{3+} binding OH deformation
797	C-H defromation
687	OH bend

4.5.2.3 Sorption studies of metals on Bentonite-P. simplicissimum (active or living) in batch mode

The biosorption of heavy metals (Cu, Co, Cr, Fe, Hg, Ni, Zn and U) in synthetic solution was investigated in immobilized living and heat-killed *P. simplicissimum.* The effects of pH, metal ions concentration (isotherms), the contact time (kinetics) and temperature were assessed. The results obtained for single and multi-component systems are given in the following sections.

4.5.2.3.1 Sorption capacities, pH and isotherms of adsorption

i) Effect of pH

As seen in the previous studies, the solution pH influences the solution chemistry of the metals, the activity of functional groups (carboxylate, phosphate, thiol and amino groups) on the cell wall as well as the competition of metallic ions for the binding site. Figure 4.50

shows the effects of the initial pH on the biosorption of Cu, Co, Cr, Fe, Hg, Ni, Zn and U in single-metal aqueous solutions.

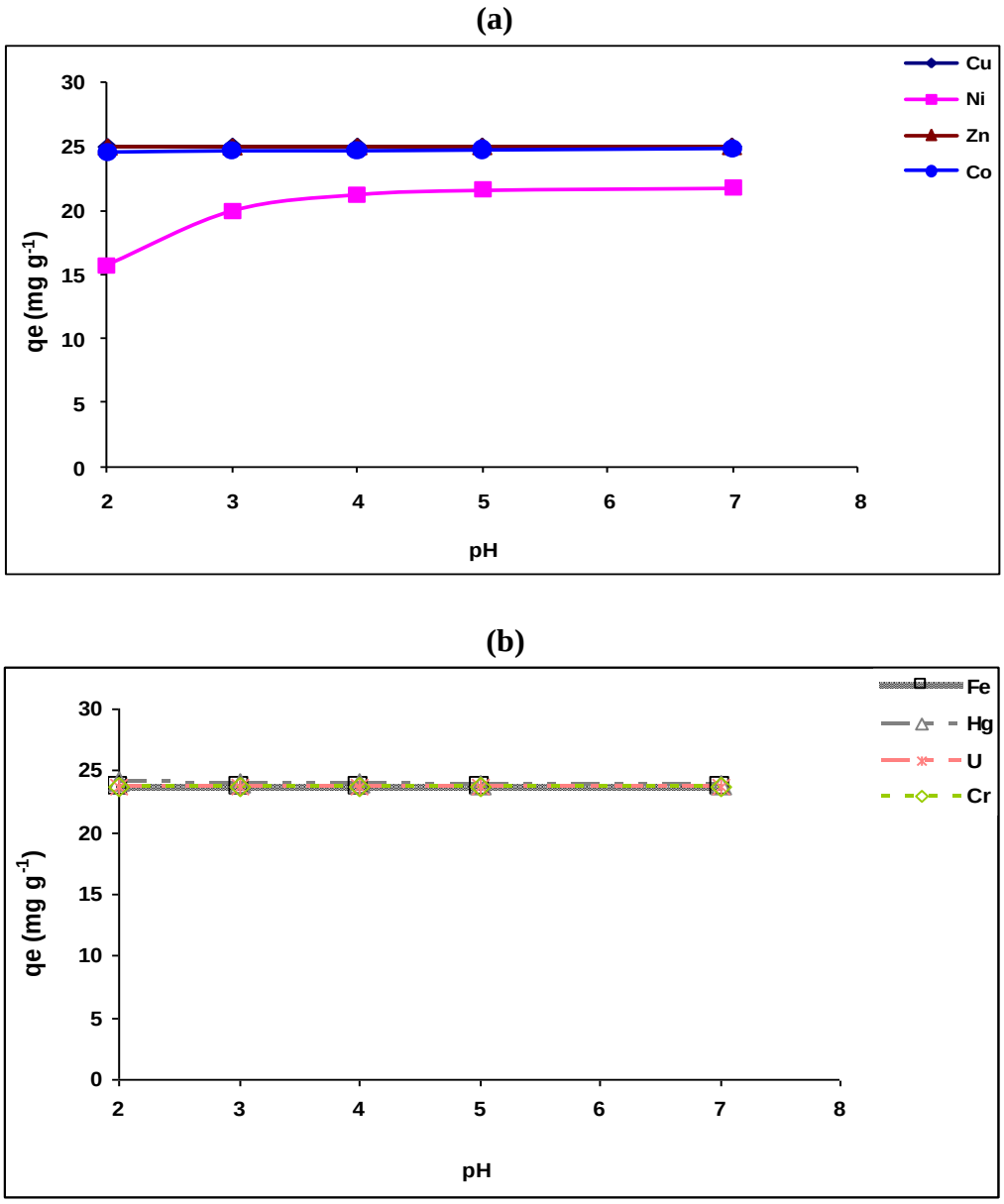

Figure 4.50 Effect of initial pH on adsorption of (a) Cu, Ni, Zn and Co (b) Cr, Fe, Hg and U onto bentonite-*P. simplicissimum* (active) in single component solution (C_i = 100 mg L^{-1}, Temp = 298.15±1^{o}K, agitation rate = 150 rpm, agitation time = 12h)

Maximum biosorption capacity was obtained around pH 4 for Ni. For the rest of the metals, the maximum biosorption capacity (25 mg g^{-1}) was constant for the all ranges of pH studied (2 to 7). The functional groups found on the cell wall of the fungi revealed by FTIR spectra (Figure 4.48) play a major role in the biosorption process.

Comparing the results with those obtained by Yun-guo (2008), it can be observed that immobilized biomass of *P. simplicissimum* was more effective than freely suspended biomass for the metals studied with a possible contribution to sorption by the immobilization matrix (Yun-guo *et al.,* 2008). Yun-guo Liu found that the maximum biosorption capacities of *P. simplicissimum* were very low at low pH due to competition by protons for the binding sites. The studies done by Xiao-ming on copper and lead adsorption on *P. simplicissimum* immobilized within loofa sponge showed low adsorption capacity of Cu and Pb at low pH for the same reasons given above (Xiao-ming *et al*., 2008).

In this study, the values of zeta potential obtained for bentonite-*P. simplicissimum* were negative at low pH, implying that negative charges on the biosorbent surface cause the high adsorption capacity even at low pH values.

Figure 4.51 illustrates the effects of pH on the biosorption capacity of bentonite-*P. simplicissimum* in multi-ion solutions. A maximum adsorption capacity (25 mg g^{-1}) was observed for the pH range studied. Contrary to the single-ion system, the adsorption capacity of Ni was maximum at low pH in the multi-ion system.

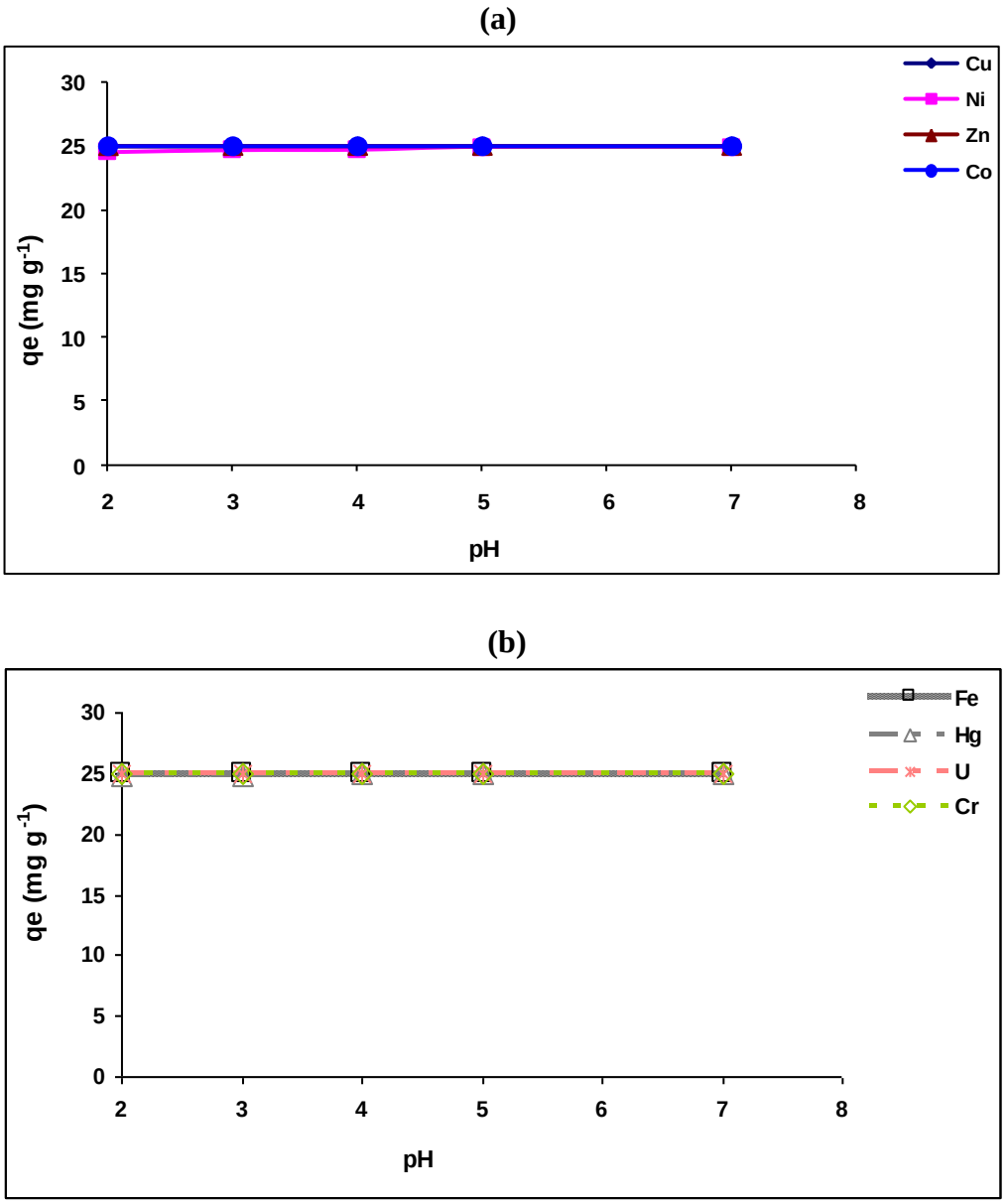

Figure 4.51 Effect of initial pH on adsorption of (a) Cu, Ni, Zn and Co (b) Cr, Fe, Hg and U onto bentonite-*P.simplicissimum* (active) in multi-component solutions (C_i = 100 mg L^{-1}, Temp = 298.15±1^oK, agitation rate = 150 rpm, agitation time = 12 h)

Gadd (2000) explained that cell-bound $HUO_2PO_4^{2-}$ facilitated Ni adsorption by intercalative ion exchange into the polycrystalline lattice. It is well known that uranium forms a strong complex with phosphates. This functional group is depicted in the biomass (FTIR spectra).

ii) Effect of initial metal ion concentration

The influence of initial metal ion concentration was investigated and the plots of initial concentration versus adsorption capacity at pH 3 are shown in Figure 4.52 for the single-ion system.

(a)

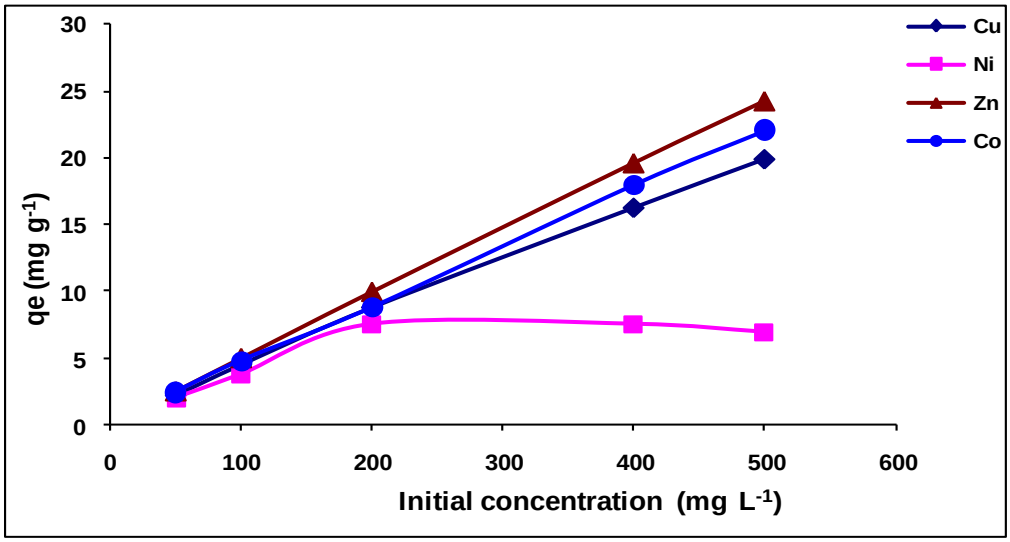

(b)

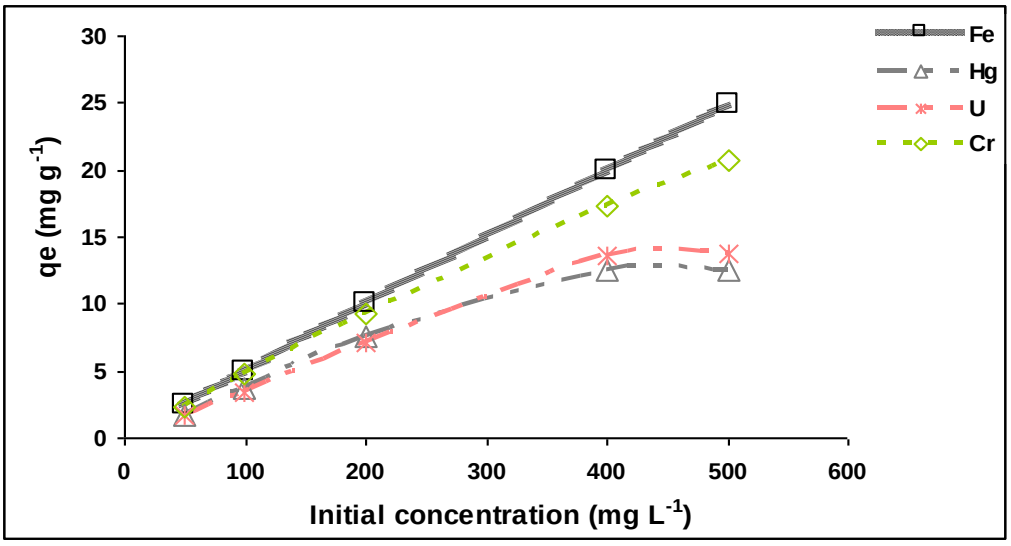

Figure 4.52 Effect of concentration on the adsorption of (a) Cu, Ni, Zn, Co and (b) Cr, Fe, Hg and U in single component solutions onto bentonite-*P. simplicissimum* (active)(pH = 3, Temp = 298.15±1^{o}K, agitation rate = 150 rpm, agitation time = 12 h)

Figure 4.52 shows that all the curves have the same trend. The biosorption of Cu, Ni, Zn, Co, Fe, Hg, Cr and U increased with increasing initial metal concentration. Even though the trend was the same for all the metal ions, high biosorption capacities were observed for zinc and iron compared to other metals.

A low uptake of Ni, Hg and U was observed with a saturation point. For these metals, the uptake decreases until an initial concentration of 200 mg L^{-1} for Ni and Hg; 400 mg L^{-1} for U, most probably because of xenobiotic effects.

The effect of initial metal ion concentration on the biosorption of Cu, Ni, Zn, Co, Fe, Hg, Cr and U on bentonite-*P.simplicissimum* in a multi-ion system is illustrated in Figure 4.53. The adsorption capacity increases linearly with an increase in initial metal ion concentration. The uptake of Ni, Hg and U did not reach the saturation point as seen in the single-ion system. The xenobiotic effect seemed to be inhibited by the presence of competing ions. This phenomenon has not yet been fully understood, but synergistic effects are likely to be playing an important role in reducing the xenobiotic effects.

The main chemical groups in biomass which are able to take part in biosorption are electronegative groups such as the hydroxyl or sulfhydryl groups, anionic groups such as carboxyl or phosphate groups and nitrogen-containing group such as amino groups. Carboxyl and phosphate groups are considered to be important binding sites for metal ions. Nonetheless, the interior of the cell also contains many components which bind metals so that treatments which permeabilize the cell, such as grinding increase the uptake of metals. The thee-dimensional structure of binding sites also appears to be significant as ionic radius affected the biosorption of ions by *P. simplicissimum* (Wang and Chen, 2006; 2009).

In fact, the application of surface complexation modelling or a linear programming approach to specific chemical and electrostatic interactions occurring at the solution-cell-wall interface can also be applied to biosorption phenomena (Wang and Chen, 2009, Prescott *et al.*, 2002). Chemisorption is enhanced when phosphates are produced biologically. The produced phosphate precipitates metals as phosphates and this is effective for a range of metals as well as radionuclides. A mixture of accumulative and chemisorptive mechanisms contributes to the overall process (Gadd, 2000; Lyod and Lovley, 2001).

(a)

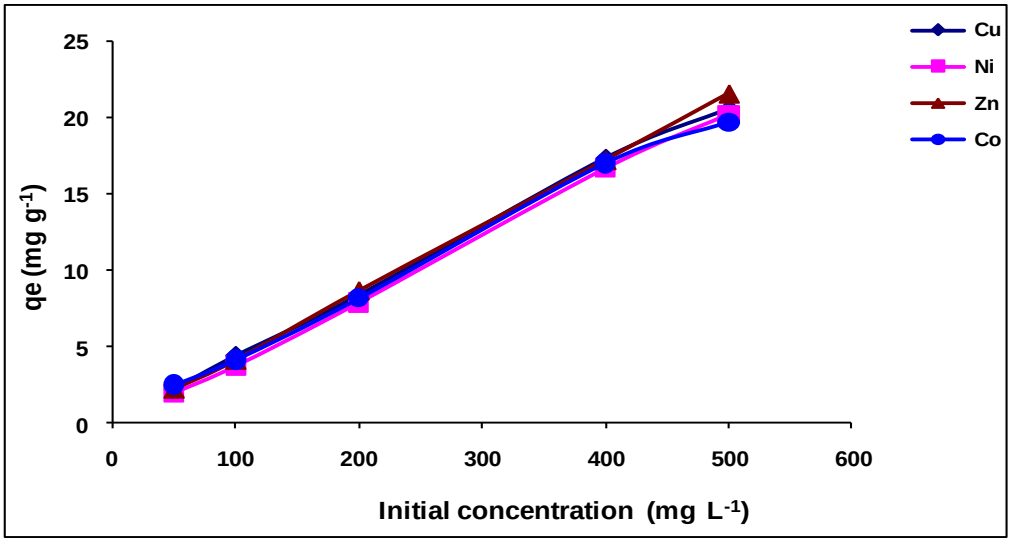

(b)

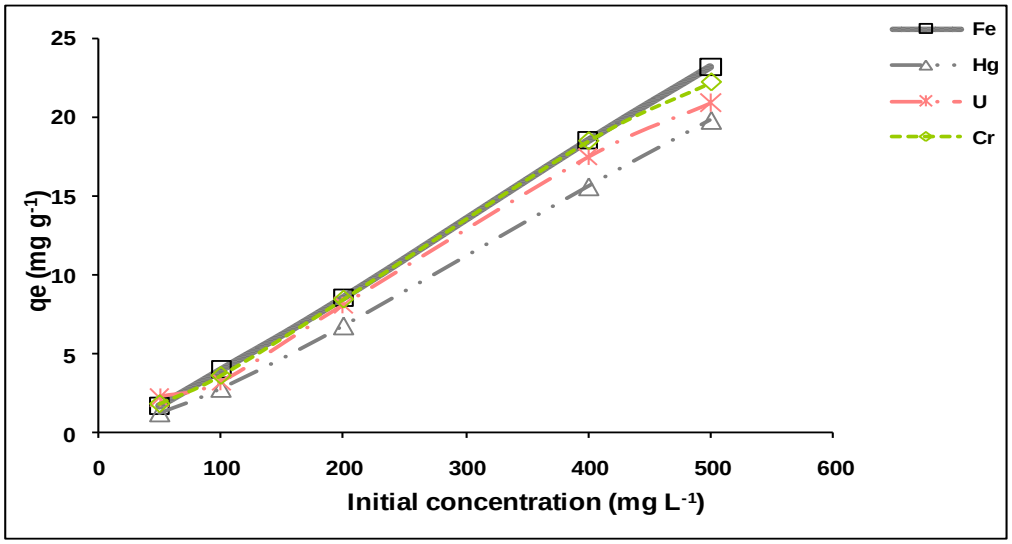

Figure 4.53 Effect of concentration on the adsorption of (a) Cu, Ni, Zn, Co and (b) Cr, Fe, Hg and U in multi component solutions onto bentonite-*P.simplicissimum* (active) (pH = 3, Temp = 298.15±1^{o}K, agitation rate = 150 rpm, agitation time = 12 h)

iii) The isotherms of adsorption for metal ions on bentonite-P. simplicissimum

Biosorption isotherms of Cu, Cr, Co, Fe, Hg, Ni, Zn and U by living biomass of *P. simplicissimum* immobilized on bentonite are shown in Tables 4.42 and 4.43 in a single-metal systems and multi-component systems, respectively.

The adsorption constants of Langmuir, Freundlich, D-R and coefficients partition models and their correlation coefficients (r) were calculated.

Table 4.42 Parameters of Langmuir, Freundlich, D-R and distribution coefficient models for the adsorption of metals on bentonite-*P. simplicissimum* in a single metal system

Langmuir Isotherms	***Fe***	***Cu***	***Co***	***Hg***	***Ni***	***Zn***	***U***	***Cr***
A	0.008	0.089	0.046	0.167	0.166	0.007	0.234	0.053
B	1.733	2.381	2.397	3.195	2.037	2.431	8.245	2.223
b	2184	26.63	52.23	19.16	12.31	335.9	35.19	41.68
qm (mol/kg)	0.577	0.419	0.402	0.313	0.491	0.412	0.121	0.449
ΔGo (kJ/mol)	-19.06	-8.136	-9.805	-7.319	-6.221	-14.42	-8.827	-9.247
Δq (%)	75.97	75.96	76.01	75.91	75.94	76.06	75.93	76.04
r	0.610	0.967	0.966	0.745	0.845	0.994	0.726	0.995
Freundlich Isotherms	***Fe***	***Cu***	***Co***	***Hg***	***Ni***	***Zn***	***U***	***Cr***
A	0.132	0.139	0.151	0.109	0.141	0.146	0.097	0.153
B	0.177	0.319	0.283	0.438	0.354	0.230	0.471	0.277
K_f	1.356	1.377	1.416	1.286	1.384	1.401	1.252	1.423
n	5.652	3.126	3.532	2.282	2.825	4.341	2.124	3.609
ΔGo (kJ/mol)	-14.01	-7.749	-8.755	-5.658	-7.004	-10.76	-5.266	-8.947
Δq (%)	70.79	58.11	49.97	69.20	52.82	65.89	46.75	47.37
r	0.988	0.984	0.994	0.996	0.998	0.960	0.996	0.992
D-R Isotherms	***Fe***	***Cu***	***Co***	***Hg***	***Ni***	***Zn***	***U***	***Cr***
A	0.322	0.229	0.206	0.220	0.237	0.269	0.051	0.184
B	-0.002	-0.006	-0.005	-0.008	-0.007	-0.003	-0.009	-0.005
Xm (mol/kg)	1.380	1.258	1.229	1.246	1.267	1.308	1.051	1.202
Es (kJ/mol)	14.65	8.927	10.02	7.748	8.133	12.09	7.619	10.12
Δq (%)	45.30	22.71	15.48	26.61	19.09	32.66	7.814	13.45
r	0.916	0.990	0.995	0.998	0.995	0.969	0.997	0.997
K_d	***Fe***	***Cu***	***Co***	***Hg***	***Ni***	***Zn***	***U***	***Cr***
A	7.122	4.103	4.814	2.880	3.310	6.622	3.036	4.952
B	2534	1099	1431	5432	944.1	5647	2996	635.1
ΔGo (kJ/mol)	-17.66	-10.17	-11.93	-7.139	-8.207	-16.42	-7.526	-12.27
Kdo	1238	60.48	123.2	17.81	27.41	751.5	20.82	141.4
Δq (%)	85.42	71.14	67.19	83.15	72.49	78.81	71.62	70.41
r	0.564	0.950	0.952	0.764	0.820	0.969	0.713	0.962

The correlation coefficients show that the biosorption process is better defined by the Freundlich and D-R isotherms with r > 0.950. In addition, the adsorption of Cu, Co, Zn and Cr is described by the Langmuir and partition coefficient isotherms. Biosorption of the former occurs in monolayer or multilayer coverage on a heterogenous surface. The values of *n* (2.124 – 5.652) indicate that the process is beneficial; the values of $1/n < 1$ assuming that metals are bound though weak free energies.

The biosorption process was spontaneous; Gibb's free energies calculated from the Freundlich model were negative for all the metals analyzed. The values of the mean free energy (Es) of biosorption range from 8 to 16 kJ mol^{-1}, confirming an ion exchange mechanism. With respect to the distribution coefficient, the sequence is as follows: Fe > Zn > Cr > Co > Cu > Ni > U > Hg. The uptake capacity, q_{max} (mol kg^{-1}), calculated from the Langmuir isotherm decreased in this sequence: Fe >Ni > Cr > Cu > Zn > Co > Hg > U. The uptake depends on the affinity of the metal towards the binding sites and also depends on the nature and the amount of functional groups present on the surface of the biosorbent.

The main ligands found in the cell wall of fungi in general are (Talaro and Talaro, 2002):

a. Hydroxyl (ROH) Carbohydrates, alcohols
b. Carboxyl (RCOOH) Fatty acids, proteins
c. Amino (RCH_2NH_2) Proteins, nucleic acids
d. Ester (RCOOR) Lipids
e. Sulfhydryl (RCH_2SH) Cysteine (amino acid), proteins
f. Carbonyl, terminal end (RCOH) Aldehydes, polysaccharides
g. Carbonyl, internal ($RCOCH_3$) Ketones, polysaccharides
h. Phosphate (ROH_2PO_3) DNA, RNA, ATP

Metal biosorption by biomass mainly depends on the components on the cell, especially though cell surface and the spatial structure of the cell wall. According to the Hard and Soft Acid Base Principle, hard ions, such as Cr^{3+}, UO_2^{2+} could form stable bonds with OH^-, HPO_4^{2-}, CO_3^{2+}, $R–COO^-$ and =C=O, which are oxygen-containing ligands. In contrast to hard ions, soft ions such as Hg^{2+} form strong bonds with $R–S^-$, $–SH^-$, NH_2^- and imidazole, which are groups containing nitrogen and sulfur atoms. Borderline or intermediate metal ions such as $Fe^{3+,}$ Cu^{2+}, Ni^{2+}, Zn^{2+} and Co^{2+} could bind the thee types of ligands with different

preferences. Hard ions mainly show ionic nature of binding, whereas soft ions binding exhibit a more covalent degree (Nieboer and Richardson, 1980; Pearson, 1963; Remacle, 1990

Various polysaccharides exist in fungi cell walls; they have been proved to play a very important role in metal binding. Some functional groups have been found to bind metal ions, especially the carboxylic groups. Other components include proteins, lipids, and pigments. This diversity is reflected by the presence of a range of distinct potential metal complexation sites, e.g., carboxylate, phosphate, sulfhydryl, and amine groups.

As a consequence, the Irving-Williams series [Fe(II) < Co(II) < Ni(II) < Cu(II) > Zn(II)] derived from the stability constants of transition metals with N donor ligands and often referred to in relation to metal adsorption to micro-organisms may not strictly apply to surfaces rich in oxygen-containing ligands, where more stable bonds form with hard ions (Shumate and Strandberg, 1985; Remacle, 1990).

The surface heterogeneity of the fungal cell wall in addition to both ionic and covalent bonding of the metal ions, correlates with the known chemically multi-phasic nature of the wall and indicates the presence of a range of distinct potential binding sites. Carboxylate and phosphate moieties have been proposed as the major functional groups responsible for metal adsorption in denatured fungal biomass (Tobin *et al*., 1990). However, these are hard (oxygen-containing) ligands, and it is unlikely that they alone could account for the large degree of covalent bonding reported here. The degree of covalency in metal-cell wall interactions is known to be much greater in live than in dead fungi (Avery *et al.*, 1992) and it is probable that here, covalent bonding to intact cells was a consequence of metal complexation with the additional soft amine and sulfhydryl ligands that are active on the cell surfaces of live microorganism.

The present results indicate that the complex characteristics of microbial metal uptake correlate well with, and can be accounted for by, considerations based on the hard and soft principle. In addition to relating the nature of bonding and strength of interaction of individual metal ions to the various types of functional group present in cell walls, broader application of the hard and soft principle is relevant to the availability to micro-organisms of both potentially toxic and biologically essential ions in complex ligand-containing media.

To describe two or multi-metal ions biosorption system, various extended Langmuir models (also called competitive Langmuir model) or Freundlich type models have been developed (Aksu *et al*., 1997; Chong and Volesky, 1995; Pagnanelli *et al*., 2002; Volesky, 2003). It was

not relevant to use these empirical models here since they hardly reflect the sorption mechanism.

Table 4.43 Parameters of Langmuir, Freundlich and D-R and distribution coefficient models for the adsorption of metals on bentonite-*P. simplicissimum* in multi-ion system

Langmuir Isotherms	***Fe***	***Cu***	***Co***	***Hg***	***Ni***	***Zn***	***U***	***Cr***
A	0.104	0.084	0.087	0.282	0.129	0.084	0.127	0.118
B	-0.299	2.002	2.619	-5.074	1.151	1.518	9.381	0.255
b	2.853	23.79	30.22	17.99	8.935	18.16	74.03	2.157
qm (mol/kg)	3.340	0.499	0.382	0.197	0.868	0.658	0.106	3.922
ΔGo (kJ/mol)	-7.852	-7.856	-8.449	-5.236	-5.429	-7.186	-10.67	-1.906
Δq (%)	75.92	65.94	76.01	58.97	75.92	75.99	75.96	75.92
r	0.917	0.775	0.722	0.976	0.587	0.865	0.594	0.659
Freundlich Isotherms	***Fe***	***Cu***	***Co***	***Hg***	***Ni***	***Zn***	***U***	***Cr***
A	0.071	0.141	-0.013	0.108	0.139	0.136	0.078	0.091
B	0.284	0.318	0.229	0.469	0.336	0.319	0.414	0.294
K_f	1.179	1.384	0.969	1.284	1.377	1.368	1.198	1.235
n	3.511	3.138	4.356	2.131	2.978	3.133	2.415	3.395
ΔGo (kJ/mol)	-8.704	-7.778	-10.79	-5.281	-7.382	-7.766	-5.988	-8.417
Δq (%)	34.89	59.39	55.72	4.056	9.286	6.651	71.99	13.66
r	0.975	0.991	0.836	0.993	0.986	0.984	0.823	0.979
D-R Isotherms	***Fe***	***Cu***	***Co***	***Hg***	***Ni***	***Zn***	***U***	***Cr***
A	0.294	0.282	-0.767	0.336	0.347	0.317	-0.042	0.335
B	-0.006	-0.006	-0.002	-0.009	-0.007	-0.006	-0.007	-0.008
Xm (mol/kg)	1.342	1.325	0.464	1.399	1.416	1.373	0.959	1.399
Es (kJ/mol)	8.819	8.836	15.27	7.220	8.207	8.730	8.500	8.562
Δq (%)	55.52	24.01	84.59	56.47	34.96	33.52	78.79	24.68
r	0.976	0.991	0.801	0.990	0.981	0.977	0.809	0.981
K_d	***Fe***	***Cu***	***Co***	***Hg***	***Ni***	***Zn***	***U***	***Cr***
A	0.875	3.839	5.639	1.549	3.009	3.424	3.119	2.014
B	9949	1825	-187.5	8446	2058	3010	9560	5006
ΔGo (kJ/mol)	-2.168	-9.514	-13.98	-3.841	-7.461	-8.489	-7.731	-4.993
Kdo	2.397	46.43	28.13	47.09	20.28	30.71	22.61	7.493
Δq (%)	72.17	89.32	45.95	64.73	92.31	78.75	81.28	60.87
r	0.941	0.775	0.960	0.989	0.594	0.463	0.392	0.609

4.5.2.3.2 Effect of contact time and kinetic of adsorption

i) Effect of contact time

The effects of contact time on Cu, Co, Cr, Fe, Hg, Ni, Zn and U uptake capacity by *P. simplicissimum* immobilized on bentonite are given in Figures 4.54 and 4.55 for single-ion and multi-ion systems, respectively. The graphs show that the biosorption capacity increased with

increasing contact time and a large amount of metal ions was adsorbed in the first 30 min. Equilibrium was reached after which no more metal ions were adsorbed. As observed in the previous experiments, the adsorption capacities of Ni, Hg and U were less than those for other metals for the reasons explained in the previously.

(a)

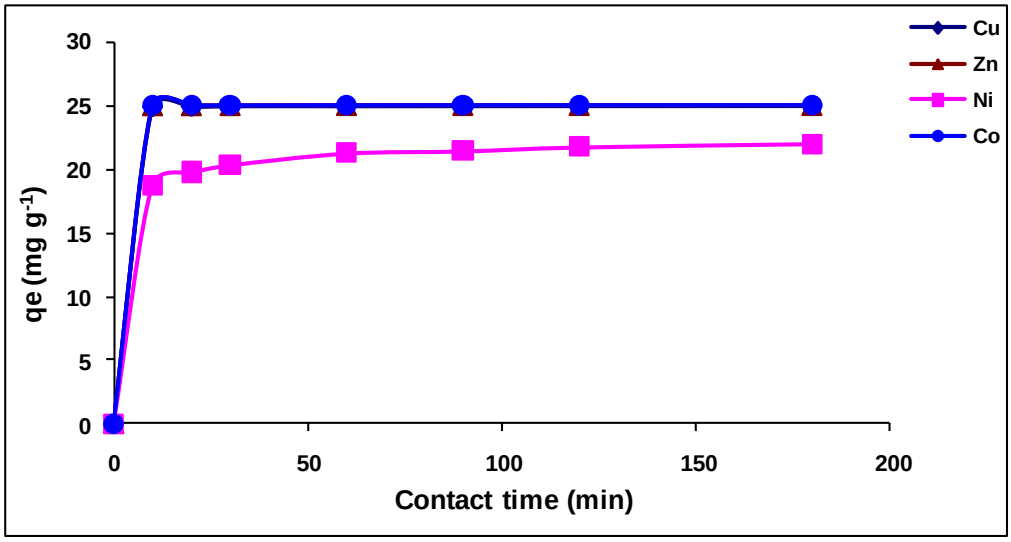

(b)

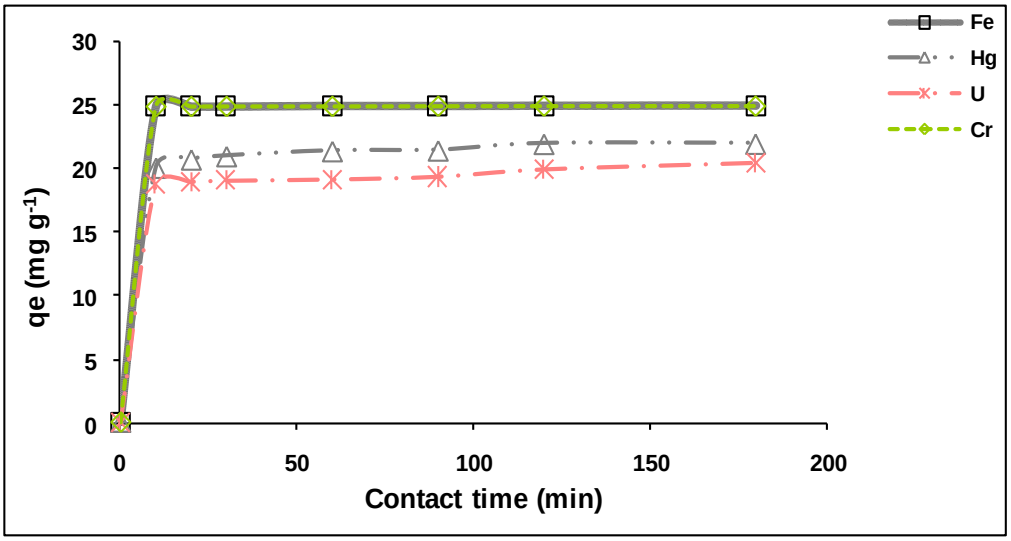

Figure 4.54 Effect of contact time on the adsorption of (a) Cu, Ni, Zn, Co and (b) Cr, Fe, Hg and U on bentonite-*P. simplicissimum* (active) in single component solutions (pH = 3, C*i* = 100 mg L^{-1}, Temp = 298.15±1^{o}K, agitation rate = 150 rpm)

Biosorption from multi-metal ions solution was investigated using a medium containing 100 mg L^{-1} of each metal ion. The results of the multi-component system are given in Figure 4.55. A similar trend was obtained as for the single-metal system regarding the mechanism, that is, fast adsorption during the first 30 minutes followed by a slow down. Maximum adsorption capacity was observed for all the metals. Seemingly, the presence of certain ions enhanced the adsorption efficiency of Ni, Hg and U. The results clearly showed that the combined action of multiple ions was synergistic. A contrary phenomenon was observed when these metals were adsorbed on the non-immobilized *P. simplicissimum.* Further investigation was performed and findings are given in the following section.

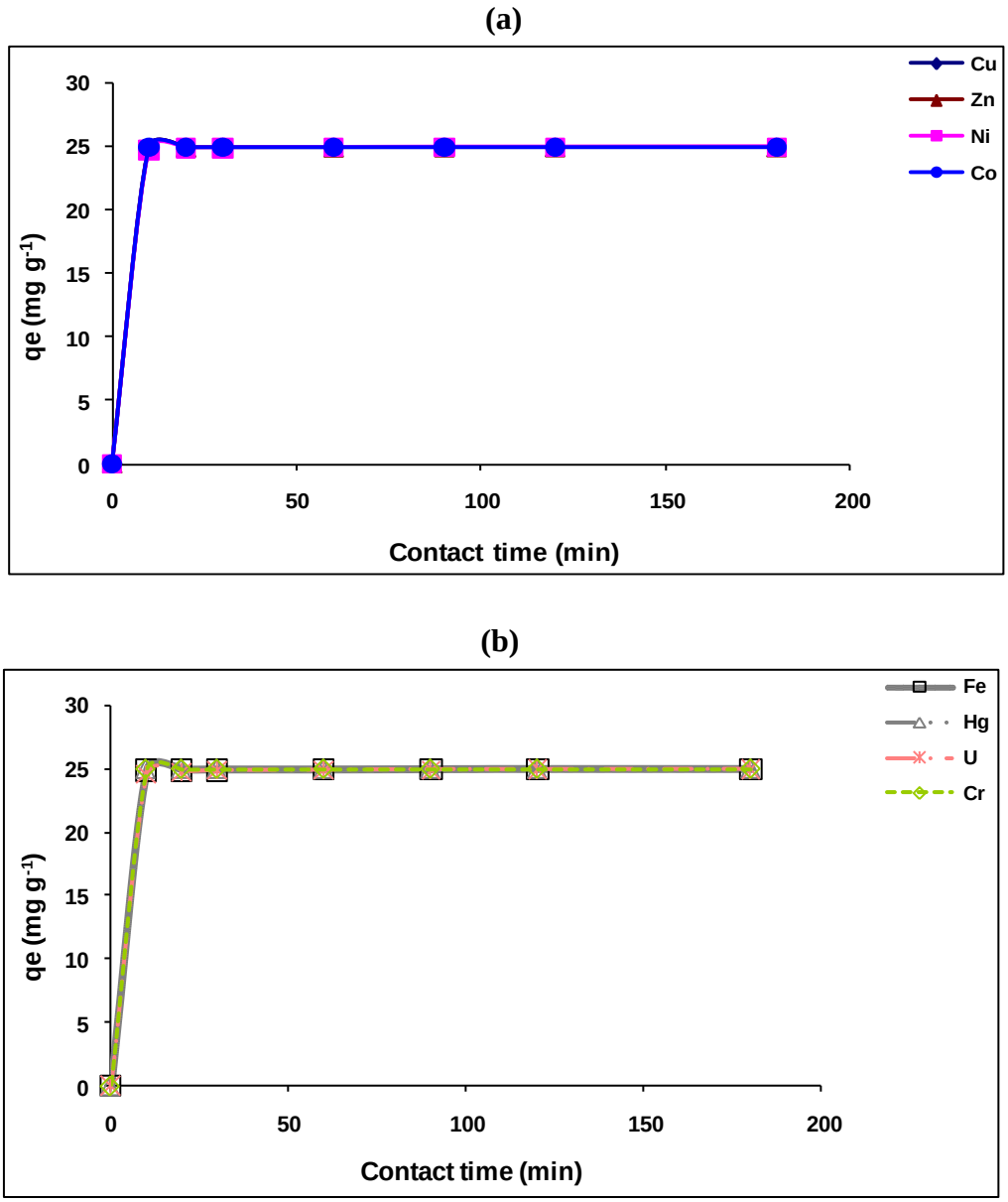

Figure 4.55 Effect of contact time on the adsorption of (a) Cu, Ni, Zn, Co, (b) Cr, Fe, Hg and U on bentonite-*P. simplicissimum* (active) in multi-ion solutions (C_i = 100 L^{-1}, Temp = 298.15±1^oK, agitation rate = 150 rpm)

ii) Kinetics of metal adsorption on bentonite-P. simplicissimum (in single- and multi-components systems)

With respect to the kinetic modelling of Cu, Co, Cr, Fe, Hg, Ni, Zn and U biosorption, the pseudo first-order, pseudo second-order, Elovich , intraparticle diffusion and the film

diffusion models were used to fit the experimental data. The kinetic constants are presented in Table 4.44. In most cases, the pseudo-second order model predicts the behaviour over the whole time adsorption and is in agreement with chemisorption mechanism being the controlling step, except for nickel, mercury and uranium.

Table 4.44 Kinetic constants for the adsorption of metal ions on bentonite-*P. simplicissimum* in single-ion system

Pseudo-first order								
	Fe	***Cu***	***Co***	***Hg***	***Ni***	***Zn***	***U***	***Cr***
A	-2.578	-2.912	-3.253	-2.201	-1.670	-3.381	-2.068	-2.691
B	-0.005	-0.008	-0.009	-0.009	-0.004	-0.011	-0.003	-0.011
q_e (mol/kg)	0.003	0.001	0.001	0.006	0.021	0.004	0.009	0.002
K_1	0.019	0.018	0.020	0.020	0.009	0.025	0.007	0.025
Δq (%)	90.41	91.43	92.08	21.17	60.61	92.15	77.05	90.89
r	0.748	0.764	0.744	0.991	0.904	0.797	0.929	0.810
Pseudo – second order								
	Fe	***Cu***	***Co***	***Hg***	***Ni***	***Zn***	***U***	***Cr***
A	7.434	4.535	1.279	1872	2214	0.932	-1209	2.934
B	11.20	12.73	11.79	76.94	27.79	13.09	105.3	10.43
q_e (mol/kg)	0.089	0.079	0.085	0.013	0.036	0.076	0.009	0.096
K_2	16.88	35.72	108.7	0.316	0.348	184.1	0.917	37.06
Δq (%)	0.242	0.412	0.039	92.28	88.02	0.07	41.04	0.116
r	1.000	1.000	0.999	0.715	0.875	1.000	0.755	1.000
Elovich model								
	Fe	***Cu***	***Co***	***Hg***	***Ni***	***Zn***	***U***	***Cr***
A	0.013	0.012	0.013	-0.001	-0.009	0.012	-0.004	0.015
B	0.015	0.014	0.015	0.002	0.005	0.013	0.001	0.017
b	64.52	73.13	67.72	630.7	193.6	75.18	787.8	59.95
a	0.037	0.033	0.036	0.001	0.002	0.032	0.003	0.040
Δq (%)	16.33	16.41	16.71	33.47	71.61	16.72	10.79	16.59
r	0.965	0.729	0.879	0.964	0.874	0.809	0.981	0.956
Intraparticle diffusion model								
	Fe	***Cu***	***Co***	***Hg***	***Ni***	***Zn***	***U***	***Cr***
A	0.035	0.031	0.034	0.001	-0.011	0.030	-0.005	0.038
B	0.005	0.004	0.001	0.001	0.002	0.004	0.001	0.005
Id	0.035	0.031	0.034	-0.001	-0.011	0.030	-0.005	0.038
Kp	0.005	0.004	0.004	0.001	0.002	0.004	0.001	0.005
Δq (%)	29.40	29.39	31.29	22.59	70.64	29.29	90.74	29.32
r	0.830	0.735	0.823	0.962	0.729	0.883	0.791	0.725
Film diffusion								
	Fe	***Cu***	***Co***	***Hg***	***Ni***	***Zn***	***U***	***Cr***
A	-1.426	-1.513	-1.731	-1.345	-0.624	-2.065	-0.433	-1.928
B	-0.012	-0.014	-0.018	0.002	0.003	-0.018	0.001	-0.014
If	-1.426	-1.513	-1.731	-1.345	-0.624	-2.065	-0.434	-1.928
Kf	0.012	0.014	0.017	0.001	0.001	0.018	-0.001	0.014
Δq (%)	47.11	48.97	50.44	6.037	21.06	46.13	24.38	42.88
r	0.783	0.663	0.743	0.991	0.962	0.796	0.929	0.810

The adsorption of uranium is well described by the Elovich model whereas; the experimental data for mercury fitted well the pseudo-first order, elovich, intraparticle diffusion and film diffusion models. The adsorption of nickel followed the film diffusion model.

The rate constants of pseudo-second order (k_2) were found to be higher than those calculated for the pseudo-first order. Zn had the highest rate constant (184.1 mg min^{-1}) while Hg had the lowest (0.715 mg min^{-1}). The rate constants (k_2) decreased in the sequence: Zn > Co > Cr > Cu > Fe > U > Ni > Hg. Besides, the Elovich coefficients *a* and *b*, were calculated and the values of *a* did not follow the same sequence as that for the for the rate constants (k_2), except for uranium, nickel and mercury. The initial rates (K_p) calculated from the intraparticle diffusion kinetic model range between 1.10^{-3} and 5.10^{-3} mol kg^{-1} $min^{0.5}$. These initial rates decreased in the order of: Fe ~ Cr > Cu ~ Zn ~ Co > Ni > U ~ Hg^{2+}. Contrary to natural bentonite, the boundary layer thickness between the bulk solution and the adsorbent particle increases with the initial rate.

The kinetic constants for the biosorption in multi-ion system are listed in Table 4.45. The results showed that biosorption of metal ions from a multi-metal solution followed the pseudo-second order kinetic for all the metal ions studied. The correlation coefficients for the pseudo-second order were close to unity for most cases. Biosorption of Fe, Zn, Hg and Cr could be described by the Elovich model as well with r > 0.950, implying a chemisorption mechanism.

Table 4.45 Kinetic constants for the adsorption of metal ions on bentonite-*P. simplicissimum* in multi-ion system

Pseudo-first order								
	Fe	***Cu***	***Co***	***Hg***	***Ni***	***Zn***	***U***	***Cr***
A	-2.622	-3.517	-3.458	-3.998	-2.513	-2.958	-3.078	-3.070
B	-0.008	-0.012	-0.009	-0.005	-0.007	-0.009	-0.007	-0.010
q_e (mol/kg)	0.002	0.0.005	0.001	0.002	0.003	0.001	0.001	0.001
K_1	0.019	0.027	0.020	0.021	0.016	0.021	0.017	0.023
Δq (%)	90.57	92.27	92.27	92.27	90.01	91.48	89.64	91.89
r	0.761	0.704	0.671	0.743	0.696	0.731	0.754	0.709
Pseudo – second order								
	Fe	***Cu***	***Co***	***Hg***	***Ni***	***Zn***	***U***	***Cr***
A	5.762	0.496	0.761	2.953	11.99	3.115	67.84	1.239
B	11.18	12.72	11.79	40.13	11.79	13.08	47.82	10.41
q_e (mol/kg)	0.089	0.079	0.085	0.025	0.085	0.076	0.021	0.096
K_2	21.69	325.67	182.6	545.3	11.61	54.94	33.71	87.49
Δq (%)	0.149	0.032	0.09	0.009	0.625	0.045	1.511	0.038
r	1.000	1.000	1.000	1.000	1.000	0.998	1.000	1.000
Elovich model								
	Fe	***Cu***	***Co***	***Hg***	***Ni***	***Zn***	***U***	***Cr***
A	0.014	0.012	0.013	0.004	0.012	0.012	0.003	0.015
B	0.016	0.014	0.015	0.004	0.015	0.013	0.004	0.017
b	64.34	73.01	67.72	230.5	67.94	75.19	275.5	59.79
a	0.037	0.033	0.036	0.011	0.034	0.032	0.008	0.041
Δq (%)	16.42	16.76	15.55	16.75	15.85	16.62	15.24	16.70
r	0.951	0.805	0.882	0.959	0.867	0.961	0.773	0.954
Intraparticle diffusion model								
	Fe	***Cu***	***Co***	***Hg***	***Ni***	***Zn***	***U***	***Cr***
A	0.035	0.031	0.034	0.010	0.035	0.030	0.008	0.038
B	0.005	0.004	0.003	0.001	0.005	0.004	0.001	0.005
Id	0.035	0.014	0.034	0.010	0.035	0.060	0.008	0.038
Kp	0.005	0.004	0.003	0.001	0.005	0.004	0.001	0.005
Δq (%)	29.37	29.28	28.35	26.29	29.56	29.32	29.75	29.30
r	0.728	0.722	0.732	0.732	0.840	0.724	0.754	0.723
Film diffusion								
	Fe	***Cu***	***Co***	***Hg***	***Ni***	***Zn***	***U***	***Cr***
A	-1.560	-2.187	-1.747	-1.800	-1.270	-1.709	-1.356	-1.862
B	-0.013	-0.020	-0.019	-0.019	-0.011	-0.015	-0.010	-0.017
If	-1.559	-2.187	-1.747	-1.799	-1.271	-1.709	-1.356	-1.862
Kf	0.013	0.019	0.019	0.018	0.011	0.015	0.010	0.017
Δq (%)	45.73	46.11	53.51	50.87	48.33	46.41	45.25	46.79
r	0.761	0.731	0.607	0.642	0.696	0.731	0.754	0.791

4.5.2.3.3 Effect of temperature and thermodynamic parameters

i) Effect of temperature

The biosorption of metals on *P. simplicissimum* immobilized on bentonite was investigated at temperatures varying from 25 to 60 ^{o}C in single- and multi-metal ion systems. It was shown that the uptake amount of all metal ions increased with increasing temperature (Figure 4.56),

except for Cu and Fe. Biosorption of Cu and Fe was not affected by the variation of temperature. A similar trend was observed for the biosorption of the metals studied in a multi-metal system. Quintelas *et al*. (2009) observed a similar trend for the study performed on the adsorption of Cr, Cd, Fe and Ni on an *Escherichia coli* biofilm supported on zeolite.

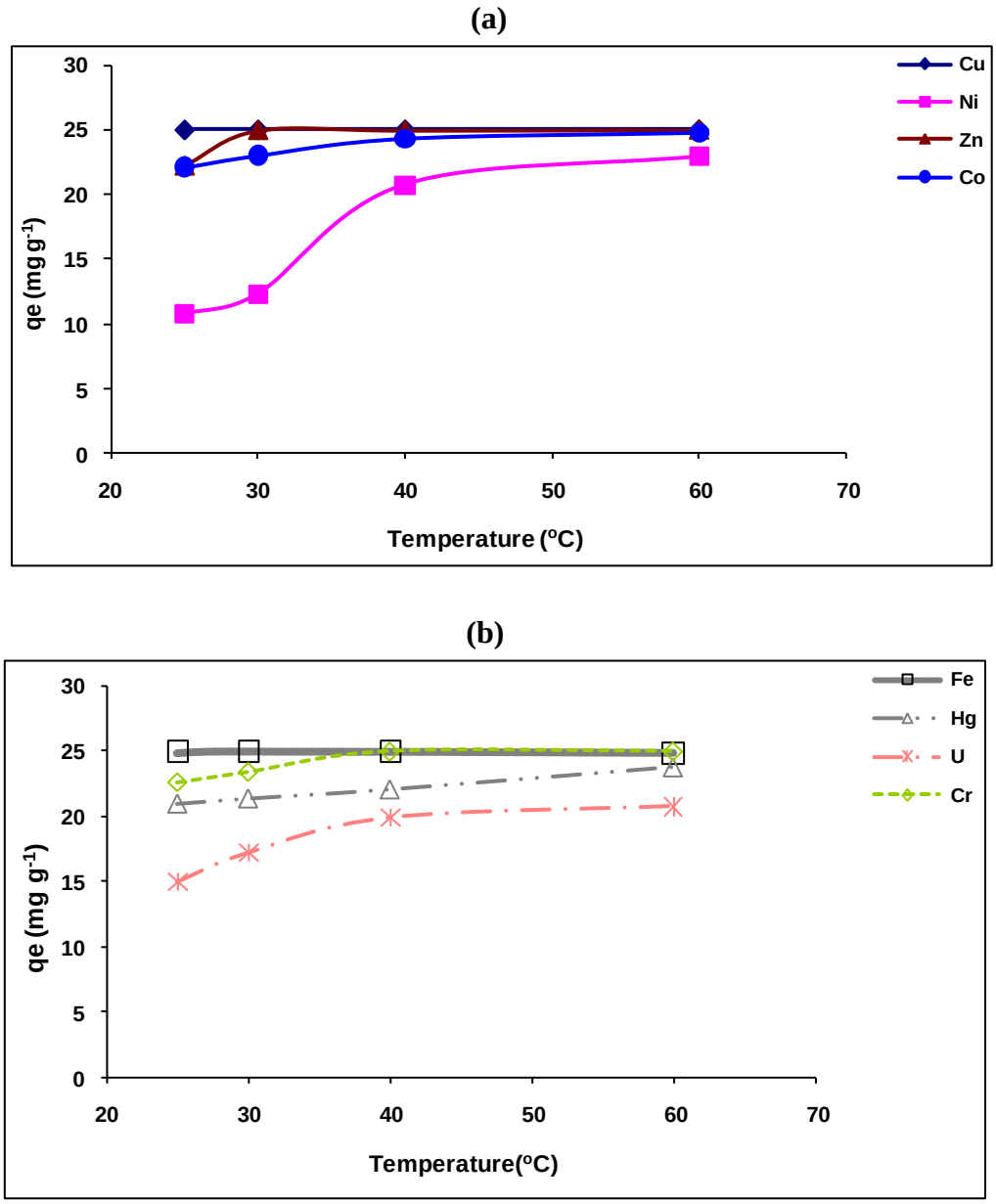

Figure 4.56 Effect of temperature on adsorption of heavy metals onto bentonite-*P.simplicissimum* (active) in single component solutions (pH = 3, Ci = 100 mg L^{-1}, agitation rate = 150 rpm, contact time = 12 h)

The biosorption of Cr, Zn, Ni, Hg, Co and U was endothermic; these results were confirmed by the positive values of enthalpy change. The sorption of these ions may involve not only physical but also chemical sorption. This effect may be caused by the increase of active sites due to bond rupture at higher temperatures (Waswar, 2010; Malkoc and Nuhoglu, 2005).

Figure 4.57 showed that the adsorption capacity of metal ions in multi-metals system was not affected by the temperature. A small increase of adsorption capacity of Ni was observed from 25 to 40 ^{o}C.

(a)

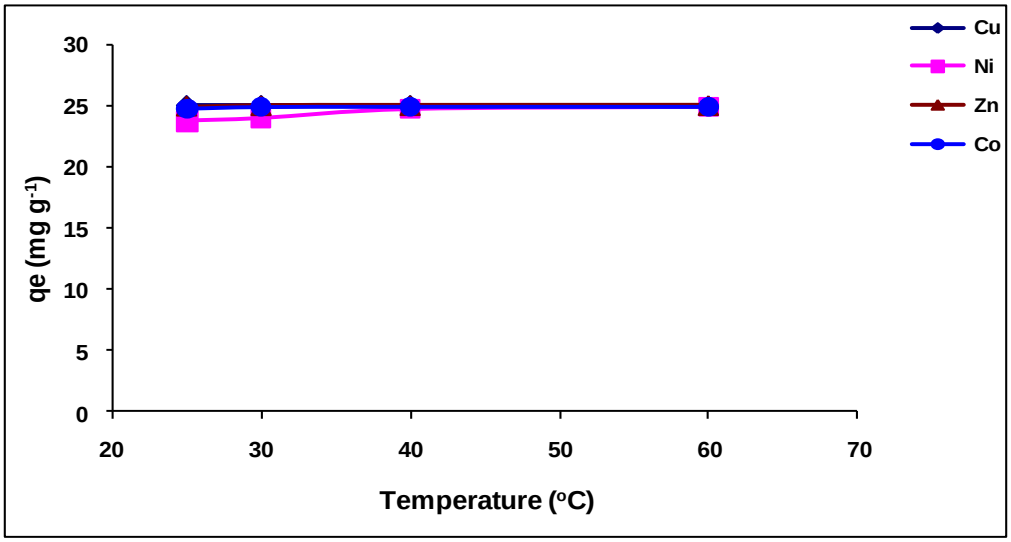

(b)

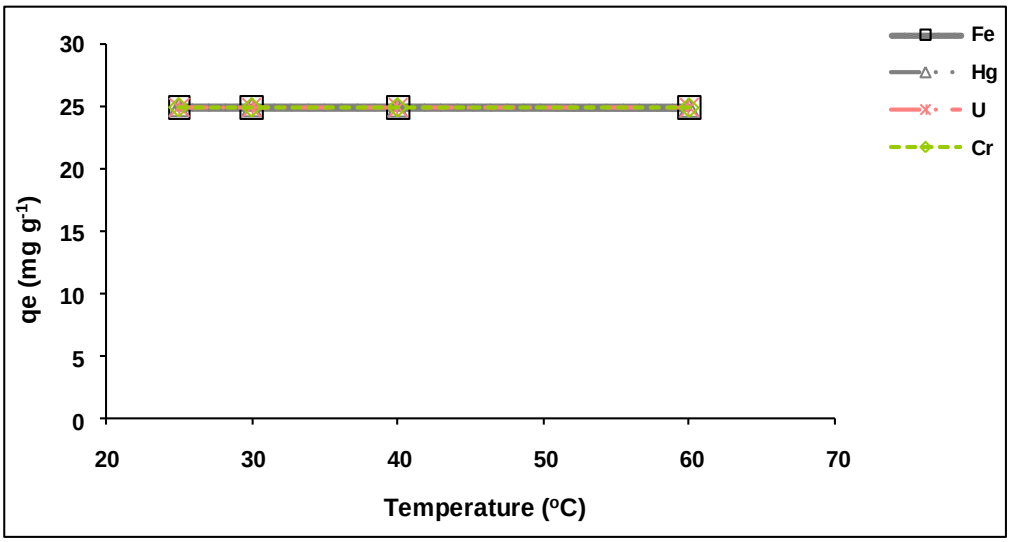

Figure 4.57 Effect of temperature on adsorption of heavy metals onto bentonite-*P. simplicissimum* (active) in multi component solutions (pH = 3, C_i = 100 mg L^{-1}, agitation rate = 150 rpm, contact time = 12 h)

ii) Thermodynamic parameters

Thermodynamic parameters such as Gibbs free energy change (ΔG^0), enthalpy change (ΔH^o) and entropy change (ΔS^o) can be estimated using equilibrium constants changing with

temperature. The calculated values in single-metal systems as well as in multi-metal systems are presented in Tables 4.46 and 4.47, respectively.

The negative values of activation energy (E_a) obtained from the Arrhenius equation (3.34) showed that the adsorption occurs at low binding sites. The adsorption of Fe was a chemisorption process wit Ea > 40 kJ mol^{-1} and the process was exothermic with a decrease in degree of freedom as the calculated value of entropy was negative.

Table 4.46 Thermodynamic parameters of metal ions adsorption on bentonite-*P. simplicissimum* in single-ion system

	Ea	ΔH^o	ΔS^o	ΔG^o			
	kJ mol^{-1}	kJ mol^{-1}	J(K.mol)$^{-1}$	kJ mol^{-1}			
				298.15 ^oK	**303.15** ^oK	**313.15** ^oK	**333.15** ^oK
Cu	-18.53	110.6	0.275	-16.89	-17.10	-17.96	-18.84
Ni	-62.93	375.6	1.110	-0.705	-0.083	-3.916	-5.906
Zn	-111.8	667.4	1.953	-5.172	-14.83	-15.59	-16.92
Co	-59.40	354.5	1.030	-5.022	-6.046	-8.748	-11.26
Fe	54.08	-322.8	-1.008	-18.76	-16.74	-15.45	-13.08
Hg	-30.29	180.8	0.521	-4.102	-4.402	-5.003	-7.284
U	-27.84	166.2	0.487	-0.997	-1.953	-3.351	-3.922
Cr	-94.32	562.9	1.643	-5.529	-6.597	-14.77	-15.44

The negative ΔG^o values of metal ions studied at various temperatures proved that the adsorption processes were spontaneous, and the values of ΔG^o (Table 4.46) increased with an increase in temperature.

The positive value of ΔH^o showed the endothermic nature of biosorption. The positive values of ΔS^o suggested increased randomness at the solid/solution interface during the biosorption of metal ions on bentonite - *P. simplicissimum.*

In multi-metal systems (Table 4.47), the values of Ea calculated from the Arrhenius were negative for Ni, Zn and Co. The results showed Ea < 40 kJ mol^{-1} for Hg and U suggesting a physisorption process. Activation energies values obtained for Cu, Fe and Cr were higher than > 40 kJ mol^{-1} implying a chemisorption process. Contrary to the results for the single-metal system, the adsorption was exothermic with negative values of enthalpy except Co, Ni and Zn for which the process was endothermic. The Gibbs free energy for these metals increased with increasing temperature. For the rest of the metal ions, ΔG^o decreased with

increase of temperature. The negative values of ΔG^o indicated that the adsorption process was spontaneous. The values of entropy of reaction were positive for Co, Ni and Zn, increasing the randomness of the degrees of freedom. This could explain the negative values of activation energy obtained for these metals. The rate of adsorption given in Table 4.48, showed a decrease with increasing temperature for cobalt, nickel and zinc. The opposite phenomenon was observed for the rest of the metal ions, that is, an increase of adsorption rate with the increase of temperature.

Table 4.47 Thermodynamic parameters of metal ions adsorption on bentonite-*P.simplicissimum* in multi-metal system

	Ea kJ mol^{-1}	ΔH^o kJ mol^{-1}	ΔS^o J$(K.mol)^{-1}$	ΔG^o kJ mol^{-1}			
				298.15 ^oK	**303.15** ^oK	**313.15** ^oK	**333.15** ^oK
Cu	75.16	-448.6	-1.391	-22.73	-22.83	-21.39	-14.84
Ni	-76.49	456.5	1.325	-7.234	-7.746	-11.38	-15.27
Zn	-55.23	329.6	0.926	-15.44	-18.78	-20.58	-21.24
Co	-42.83	255.6	0.721	-10.94	-14.25	-15.34	-15.44
Fe	63.25	-377.5	-1.187	-24.65	-22.46	-21.27	-18.01
Hg	36.80	-219.6	-0.704	-18.70	-17.13	-15.79	-14.83
U	39.53	-236.0	-0.759	-21.16	-20.56	-19.68	-17.01
Cr	76.61	-457.3	-1.423	-24.87	-21.67	-20.54	-16.82

The rate of adsorption at different temperature was calculated and listed in Tables 4.48 and 4.49 for single-metal as well as multi-metal systems.

Table 4.48 The reaction rate of the adsorption of metal ions on bentonite-*P.simplicissimum* in single-metal system

Rx rate (h^{-1})				
	298.15 ^oK	**303.15** ^oK	**313.15** ^oK	**333.15** ^oK
Cu	0.568	0.575	0.604	0.633
Ni	0.047	0.056	0.147	0.206
Zn	0.184	0.499	0.524	0.569
Co	0.179	0.210	0.296	0.379
Fe	0.631	0.563	0.519	0.440
Hg	0.152	0.161	0.179	0.249
U	0.076	0.097	0.132	0.147
Cr	0.194	0.227	0.497	0.519

In the adsorption of a single metal, the rate of adsorption increases with the increase of temperature. This may be attributed to the enlargement of pore size and/or activation of the adsorbent surface. A decrease of the reaction rate was obtained for adsorption of Fe, probably due to the exothermic nature of the process.

Table 4.49 presents the rate of adsorption of metal on bentonite-*P. simplicissimum* at different temperatures in multi-metal systems.

Table 4.49 The reaction rate of the adsorption of metal ions onto bentonite-*P.simplicissimum*

Rx rate (h^{-1})				
	298.15 ^{o}K	**303.15 ^{o}K**	**313.15 ^{o}K**	**333.15 ^{o}K**
Cu	0.764	0.768	0.719	0.499
Ni	0.248	0.264	0.383	0.514
Zn	0.519	0.631	0.692	0.714
Co	0.369	0.479	0.516	0.519
Fe	0.829	0.755	0.715	0.605
Hg	0.629	0.576	0.531	0.499
U	0.711	0.691	0.662	0.572
Cr	0.836	0.728	0.691	0.565

The results show two trends. The first was a decrease of adsorption rate with the increase of temperature observed for Ni, Zn, Fe, Hg, Cr and U. This could be explained by the exothermic nature of the process given by a negative enthalpy. Increases of temperature will disfavour metal adsorption. On the other hand, the adsorption rates of Cu and Co increase with an increase of temperature.

4.5.2.4 Sorption of metals on bentonite-P. simplicissimum (inactive or heat-killed) in batch mode

A comparative study was done between bentonite-*P. simplicissimum* (living) and the bentonite-*P. simplicissimum* (inactive or heat-killed). The effects of pH, initial metal concentration, contact time and temperature were investigated in single-metal as well as

multi-metal systems. Similarities and differences are assessed in the following section for each parameter.

4.5.2.4.1 Sorption capacities, pH and isotherms

i) Effect of pH

The adsorption capacities of Cu, Co, Cr, Fe, Hg, Ni, Zn and U on bentonite-*P.simplicissimum* (inactive) are presented in Figure 4.58.

High adsorption efficiency was observed for the heat-killed fungi immobilized on bentonite, 2 times higher in magnitude than the adsorption of metal onto the bentonite-living *P. simplicissimum* system. The difference could be due to the amount of available functional groups or binding sites on the surface of the biomass. The adsorption of metals on living fungi was greatly influenced by the metabolism which does not occur when the biomass is inactive. Some authors (Leitão, 2009; Pócsi, 2011; Wang and Chen, 2009; Vijayaraghavan and Yun, 2008) confirm that when the metabolism stops, compounds from the intracellular appear on the surface of the biomass, causing a large surface area as consequence. This makes the inactive fungi more efficient in terms of metal binding. Besides, the xenobiotic effect is eliminated in that case.

The adsorption capacities were constant for Co, Zn and Fe and maximum adsorption capacities were observed at around pH 5 for Ni, Cu, Cr, Hg and U. Good adsorption was obtained even at low pH (< 3), as seen before, the presence of acidic functional groups like carboxyl, phosphoryl and amino groups on the surface of the biomass are directly responsible for the reactivity of fungal cells.

The increases of adsorption capacity observed around pH 5 for most of the cases could be due to the dissociation of most of the functional groups present on the biomass surface. The sequestration of metals in solution depends on the dissociation of the functional groups, which is higher at high pH.

(a)

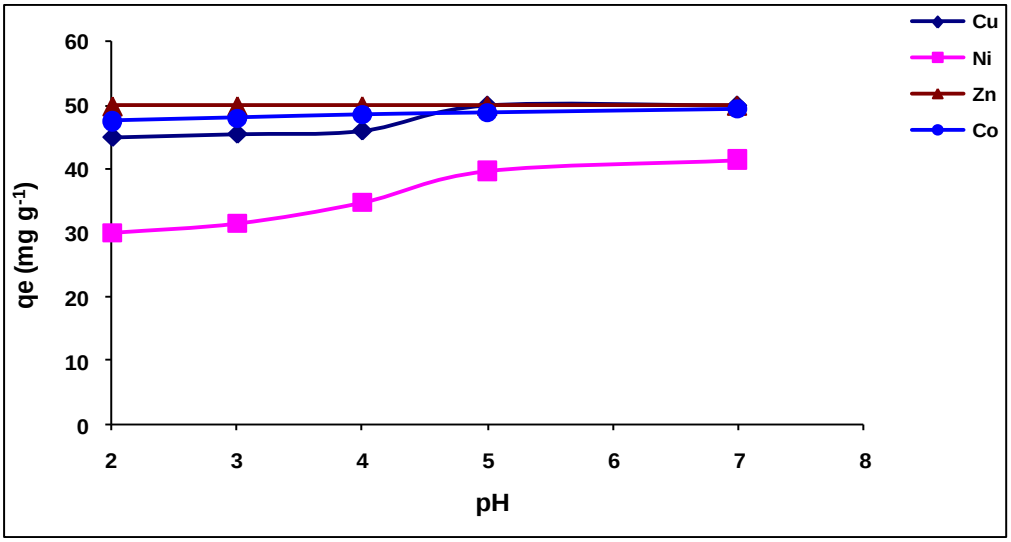

(b)

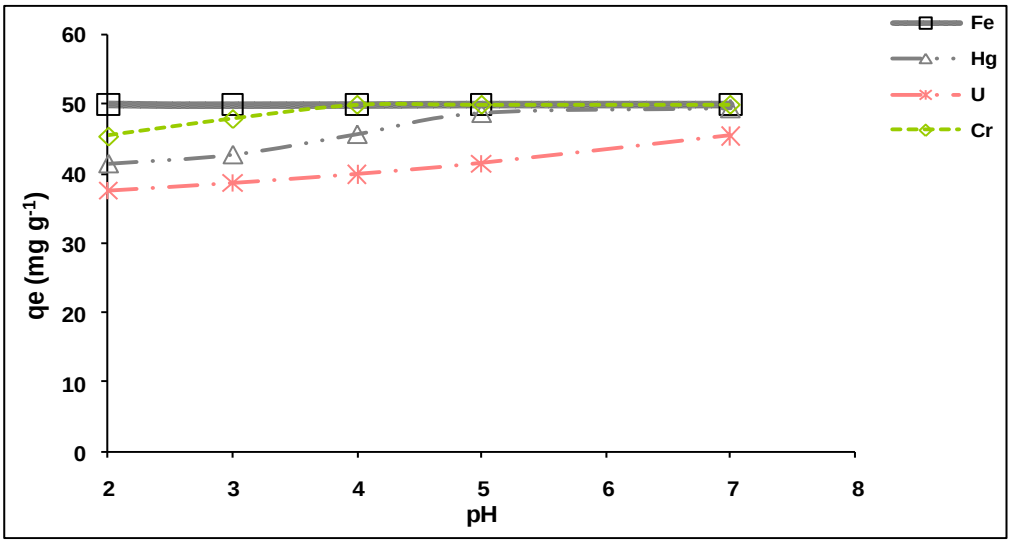

Figure 4.58 Effect of initial pH on adsorption of (a) Cu, Ni, Zn, Co and (b) Fe, Hg, Cr and U onto bentonite-*P. simplicissimum* (inactive) in single component solutions (C_i = 100 mg L^{-1}, Temp = 298.15±1^oK, agitation rate = 150 rpm, agitation time = 12 h)

The results illustrated in Figure 4.59 for the adsorption of metal ions from the multi-ion solutions showed a constant adsorption capacity for the pH range studied (2 -7). As explained in the previously, the presence of functional groups with lone pairs of electrons constitute a proton shuttle and the change in pH does not affect the adsorption of metals. A

slight increase of adsorption capacity was observed for Ni at pH 5. It can be assumed that at this pH, nickel forms hydroxyl species in aqueous solution. With the presence of different functional groups at the surface of the biomass, as proven by FTIR analysis, further investigations are needed to determine the nickel species formed at such conditions.

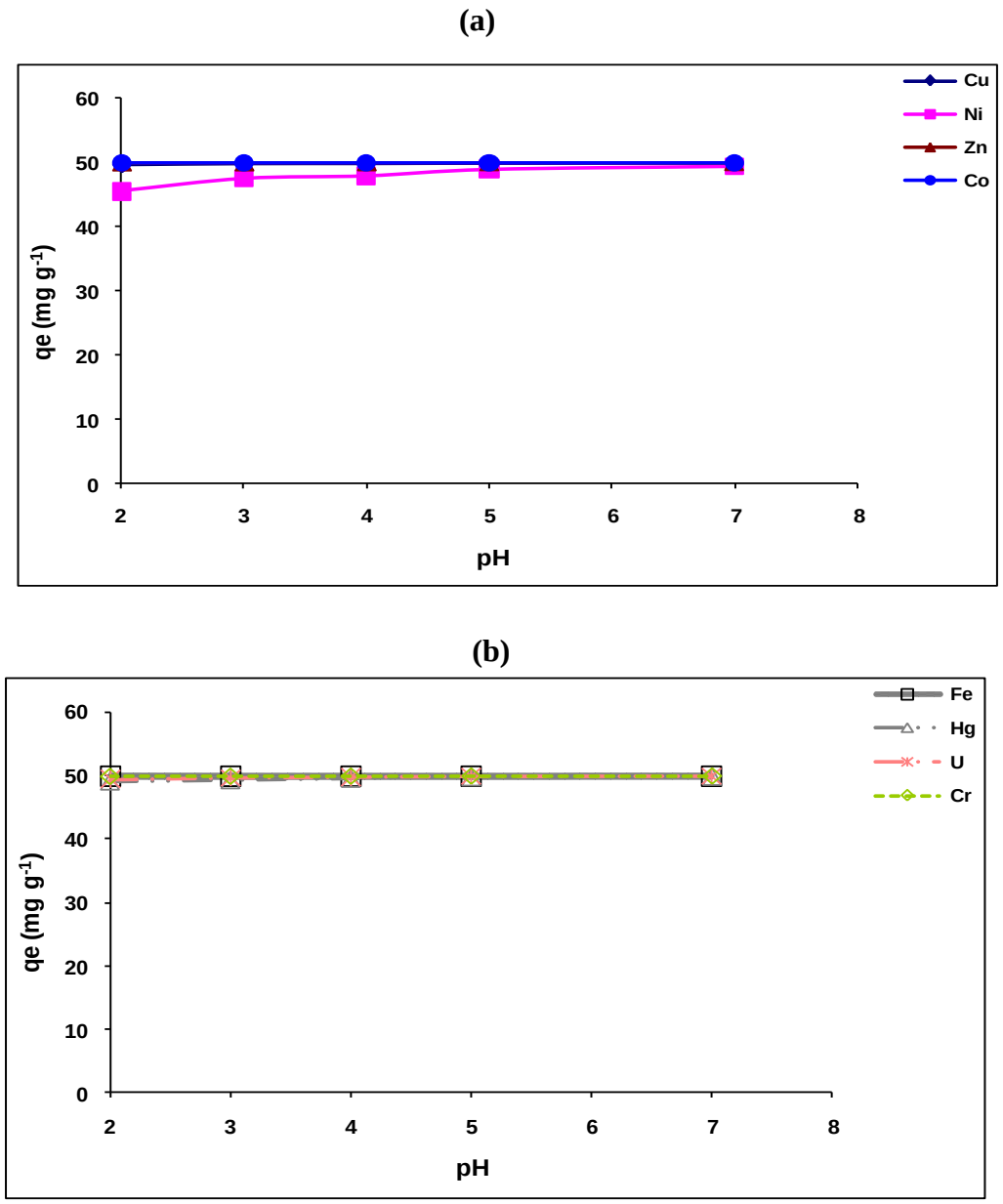

Figure 4.59 Effect of initial pH on adsorption of (a) Cu, Ni, Zn, Co and (b) Fe, Hg, Cr and U onto bentonite-*P. simplicissimum* (inactive) in multi-component solutions (C_i = 100 mg L^{-1}, Temp = 298.15±1^oK, agitation rate = 150 rpm, agitation time = 12 h)

ii) Effect of initial metal ions concentration

Equilibrium sorption isotherms of Cu, Ni, Zn, Co, Fe, Hg, U and Cr by bentonite-*P.simplicissimum* (inactive) with no pH control are shown in Figure 4.60.

(a)

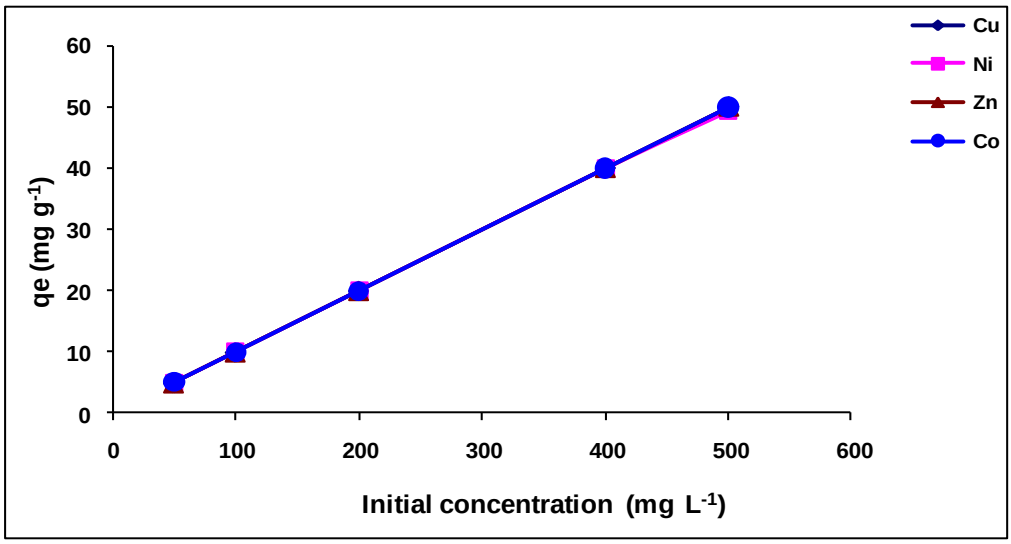

(b)

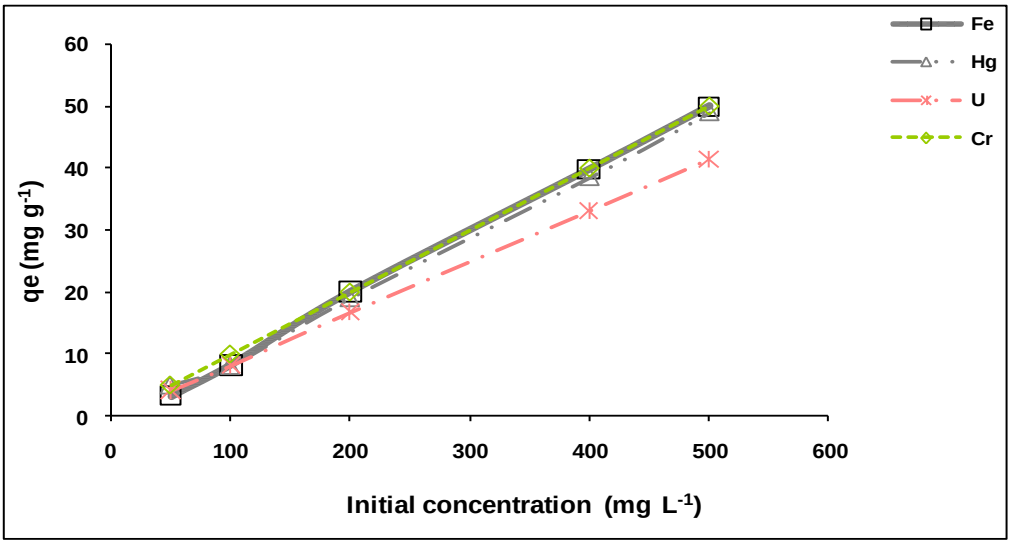

Figure 4.60 Effect of concentration on the adsorption of (a) Cu, Ni, Zn, Co and (b) Fe, Hg, Cr and Uonto bentonite-*P. simplicissimum* (inactive) (in single-metal solutions (pH 3, Temp = 298.15±1^{o}K, agitation rate = 150 rpm, agitation time = 12 h)

Biosorption isotherms represent the equilibrium distribution of metals between the aqueous and solid phases, when the concentration increases. Adsorption capacities increased when the initial concentration increased as long as binding sites were not saturated. The results illustrated in Figure 4.60 showed that the binding sites were not saturated for a concentration up to 500 mg L^{-1}. Further experiments are needed to determine the saturation concentration for the metals. Higher adsorption capacities were obtained compared to those obtained for the living biosorbent. These results show that metal accumulation by the novel biosorbent could be by a chemical, equilibrated and saturatable mechanism.

The biosorption of metal ions onto bentonite-*P. simplicissimum* in a multi-metal system followed a similar trend as for the single-metal system and the results are presented in Figure 4.61.

(a)

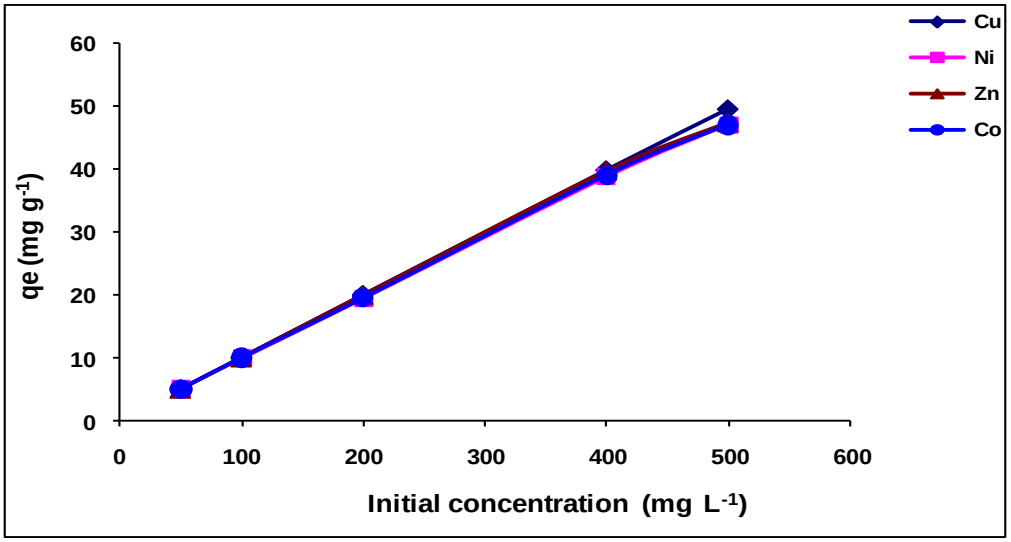

(b)

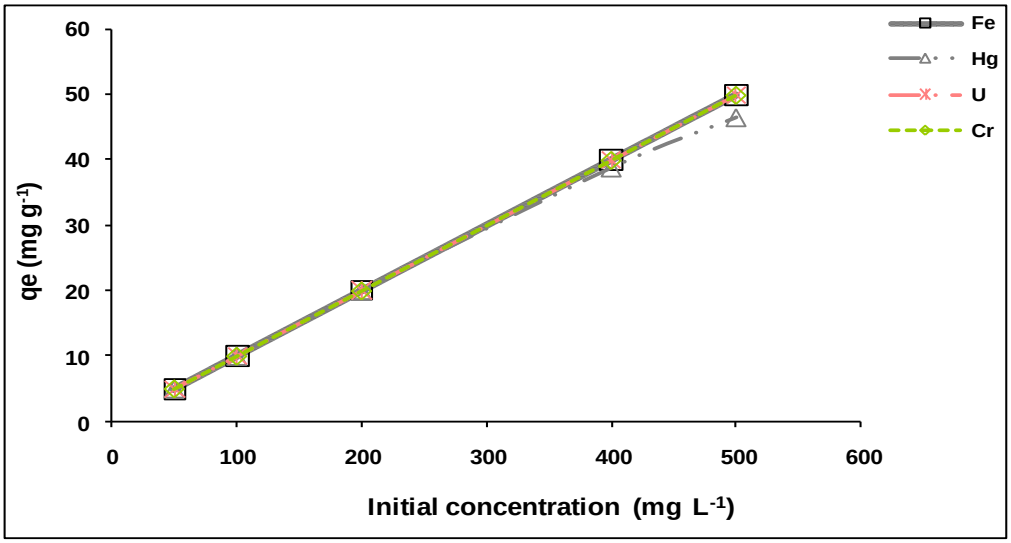

Figure 4.61 Effect of concentration on the adsorption of (a) Cu, Ni, Zn, Co and (b) Fe, Hg, Cr and U onto bentonite-*P. simplicissimum* (inactive) in multi-component solutions (pH 3, Temp = 298.15±1^{o}K, agitation rate = 150 rpm, agitation time = 12 h)

The presence of competing ions did not affect the adsorption efficiency of the biomass for the metals studied; a synergic effect was rather observed, mainly for the adsorption of uranium and nickel. This differed from observations in a study performed by Ting *et al.* (2008) on the adsorption of metal ions on non-immobilized *P. simplicissimum* which showed that the

combined action of multiple ions was antagonistic, due to competition for adsorption sites on the cell surfaces and/or the screening effect by the competing metal ions.

The immobilisation of fungi on bentonite increased the adsorption efficiency and also due to various metal-binding sites added to the ion-exchange possibility, reduced the competition for metal ions. The selection of metal ions for a given binding site depends strongly on the HSAB principle as explained before.

The adsorption isotherms were described using the Langmuir, Freundlich, D-R and distribution coefficient models. The calculated constants and the different parameters in single- and multi-metal systems are listed in Tables 4.50 and 4.51, respectively. Biosorption of Fe and Co is described by the four isotherms mentioned above with correlation coefficients, r > 0.970. Except for nickel, all the metal ions are well described by the Freundlich isotherm. The experimental data for most of the metal ions fitted well the D-R isotherm, except for mercury and nickel. Biosorption of Ni followed the Langmuir and distribution coefficient isotherms. At this stage, we assume that biosorption is a complex process with various mechanisms. The assumptions on which the Langmuir model is based are:

- Metal ions are chemically adsorbed at a fixed number of well defined sites
- Each site can hold one sorbate ion
- All sites are energetically equivalent
- There is no interaction between ions adsorbed on neighbouring sites

None of the metals studied followed strictly the Langmuir isotherm; thus proving the complexity of the process.

Based on the maximum amount adsorbed (q_{max}/ mol kg^{-1}) calculated from the Langmuir isotherm (Table 4.50), the decreasing sequence of uptake values is: Cu > Zn > Cr > Ni > Fe > Co > U > Hg.

The values of *1/n*, less than unity were obtained mostly for the immobilized biomass. The values of the apparent energy (Es) calculated from the D-R isotherm depicts a physisorption process (8 < Es < 16 kJ mol^{-1}), except for the adsorption of chomium with Es of 18.24 kJ mol^{-1}. The distribution coefficient values were in the decreasing order of: Ni > Fe > Cr>> Co > Zn > Cu > Hg > U. K_{do} values were high for Ni, Fe and Cr, implying strong bonds.

Table 4.50 Parameters of the Langmuir, Freundlich and D-R models for the adsorption of metals on the bentonite-*P. simplicissimum* (inactive) in a single metal system

Langmuir Isotherms	***Fe***	***Cu***	***Co***	***Hg***	***Ni***	***Zn***	***U***	***Cr***
A	0.012	0.005	0.012	0.025	0.002	0.004	0.105	0.0004
B	2.259	0.007	2.385	9.254	2.166	0.474	5.516	0.867
b	192.3	0.164	202.9	368.7	890.3	1201	52.49	2161
qm (mol/kg)	0.443	6.091	0.419	0.108	0.462	2.108	0.181	1.152
ΔGo (kJ/mol)	-13.03	-13.32	-13.17	-14.65	-16.84	-17.58	-9.817	-24.74
Δq (%)	60.63	75.91	76.06	75.98	14.77	75.91	75.92	75.91
r	0.982	0.613	0.982	0.672	0.989	0.693	0.439	0.657
Freundlich Isotherms	***Fe***	***Cu***	***Co***	***Hg***	***Ni***	***Zn***	***U***	***Cr***
A	0.157	0.062	0.155	0.081	0.124	0.0695	0.104	0.078
B	0.233	0.171	0.237	0.327	0.193	0.165	0.419	0.129
K_f	1.439	1.155	1.430	1.024	1.330	1.174	1.270	1.198
n	4.289	5.877	4.226	3.056	5.190	6.044	2.386	7.711
ΔGo (kJ/mol)	-10.63	-14.57	-10.47	-7.577	-12.86	-14.98	-5.916	-19.11
Δq (%)	11.16	10.35	28.55	35.61	81.42	29.9	9.03	5.689
r	0.974	0.966	0.974	0.936	0.867	0.973	0.999	0.978
D-R Isotherms	***Fe***	***Cu***	***Co***	***Hg***	***Ni***	***Zn***	***U***	***Cr***
A	0.273	0.249	0.259	-0.124	0.294	0.275	0.165	0.308
B	-0.004	-0.002	-0.004	-0.005	-0.002	-0.002	-0.007	-0.002
Xm (mol/kg)	1.314	1.283	1.296	0.883	1.343	1.317	1.179	1.362
Es (kJ/mol)	11.75	14.57	11.72	10.50	13.58	15.13	8.224	18.24
Δq (%)	26.22	29.46	25.57	72.22	53.37	18.81	18.18	25.70
r	0.982	0.969	0.982	0.823	0.889	0.976	0.998	0.975
K_d	***Fe***	***Cu***	***Co***	***Hg***	***Ni***	***Zn***	***U***	***Cr***
A	7.122	5.057	6.194	4.277	7.849	5.868	3.351	7.100
B	2534	9898	3478	3721	6025	1673	8071	1414
ΔGo (kJ/mol)	-17.65	-12.54	-15.36	-10.60	-19.46	-14.54	-8.308	-17.61
Kdo	1238	157.2	490.2	71.99	2564	353.7	28.55	1212
Δq (%)	70.79	55.21	39.77	63.39	69.91	65.01	77.57	81.81
r	0.990	0.648	0.990	0.513	0.960	0.658	0.425	0.698

In the multi-metal system (Table 4.51), the biosorption of Cu, Co, Hg, Ni, Zn and U followed the Langmuir, Freundlich and D-R isotherms. In general, the Freundlich isotherm described the biosorption of all the metal ions with r > 0.950. The sequence of the maximum amount of metal adsorbed by bentonite-inactive *P. simplicissimum* is: Fe > Cr > Cu > Co > Ni > Zn > U > Hg. The selectivity depends on factors such as: the chemical properties of each metal (e.g. valence, atomic weight, and ionic radius), properties of the biomass (e.g. structure, functional groups, surface area) (Sari *et al*., 2007). The free energy of adsorption obtained from the D-R isotherm ranged from 12.75 to 16.25 kJ mol^{-1}, that is, the energy range for the ion exchange mechanism. A similar trend was observed for the living fungi. The *1/n* values were less than

unity, confirming the feasibility of the process. The decreasing sequence of the distribution coefficients is: Zn > Ni > Co > U > Cr > Fe > Cu > Co. K_{do} values were 100 times more than those obtained with the living *P. simplicissimum* immobilized on bentonite.

Table 4.51 Parameters of the Langmuir, Freundlich and D-R models for the adsorption of metals on the bentonite-*P. simplicissimum* (inactive) in multi-metal system

Langmuir Isotherms	***Fe***	***Cu***	***Co***	***Hg***	***Ni***	***Zn***	***U***	***Cr***
A	0.008	0.003	0.014	0.012	0.009	0.006	0.004	0.003
B	1.369	2.049	2.238	8.649	2.521	2.722	8.473	1.443
b	1557	711.9	159.2	746	258.2	437.9	2232	4426
qm (mol/kg)	0.730	0.488	0.447	0.116	0.396	0.367	0.118	0.693
ΔGo (kJ/mol)	-18.22	-16.28	-12.57	-16.39	-13.77	-15.07	-24.82	-20.81
Δq (%)	75.97	34.46	76.05	27.31	26.04	40.62	76.02	75.96
r	0.655	0.974	0.972	0.998	0.996	0.999	0.974	0.796
Freundlich Isotherms	***Fe***	***Cu***	***Co***	***Hg***	***Ni***	***Zn***	***U***	***Cr***
A	0.073	0.133	0.156	0.027	0.124	0.131	0.102	0.110
B	0.163	0.208	0.242	0.257	0.193	0.196	0.244	0.157
K_f	1.183	1.358	1.432	1.065	1.331	1.353	1.266	1.290
n	6.121	4.803	4.135	3.890	5.173	5.100	4.088	6.375
ΔGo (kJ/mol)	-15.17	-11.91	55.15	-9.644	-12.82	-12.64	-10.13	-15.80
Δq (%)	17.16	77.97	0.977	9.639	24.37	30.63	64.30	37.51
r	0.986	0.958		0.995	0.988	0.973	0.978	0.969
D-R Isotherms	***Fe***	***Cu***	***Co***	***Hg***	***Ni***	***Zn***	***U***	***Cr***
A	0.203	0.349	0.239	-0.645	-0.189	-0.128	0.187	0.366
B	-0.002	-0.003	-0.004	-0.002	-0.002	-0.002	-0.003	-0.002
Xm (mol/kg)	1.226	1.417	1.271	0.525	0.828	0.880	1.205	1.442
Es (kJ/mol)	15.12	12.75	11.55	14.64	16.29	15.97	13.67	15.46
Δq (%)	81.21	44.67	22.24	35.12	18.32	22.73	26.83	32.56
r	0.782	0.967	0.981	0.997	0.984	0.973	0.982	0.955
K_d	***Fe***	***Cu***	***Co***	***Hg***	***Ni***	***Zn***	***U***	***Cr***
A	7.464	6.988	6.103	8.142	8.481	8.637	8.365	8.267
B	2385	2727	2480	-9531	-3812	-4441	1128	3867
ΔGo (kJ/mol)	-18.50	-17.32	-15.13	-20.18	-21.03	-21.41	-20.74	-20.49
Kdo	1744	1084	447.2	3436	4826	5637	4294	3890
Δq (%)	78.49	33.88	82.58	70.12	71.96	70.74	32.81	56.49
r	0.521	0.944	0.900	0.829	0.831	0.780	0.970	0.743

4.5.2.4.2 Effect of contact time and kinetics of adsorption

i) Effect of contact time

The effects of contact time on Cu, Co, Cr, Fe, Hg, Ni, Zn and U uptake capacity by inactive *P. simplicissimum* immobilized on bentonite are illustrated in Figures 4.62 and 4.63 for single-metal and multi-component systems, respectively.

Figure 4.62 showed a similar trend to that observed previously, that is, with 2 steps characterizing the biosorption process: a fast one with 99 % of metals adsorbed within the 30 first minutes and then a slow one when the equilibrium was reached.

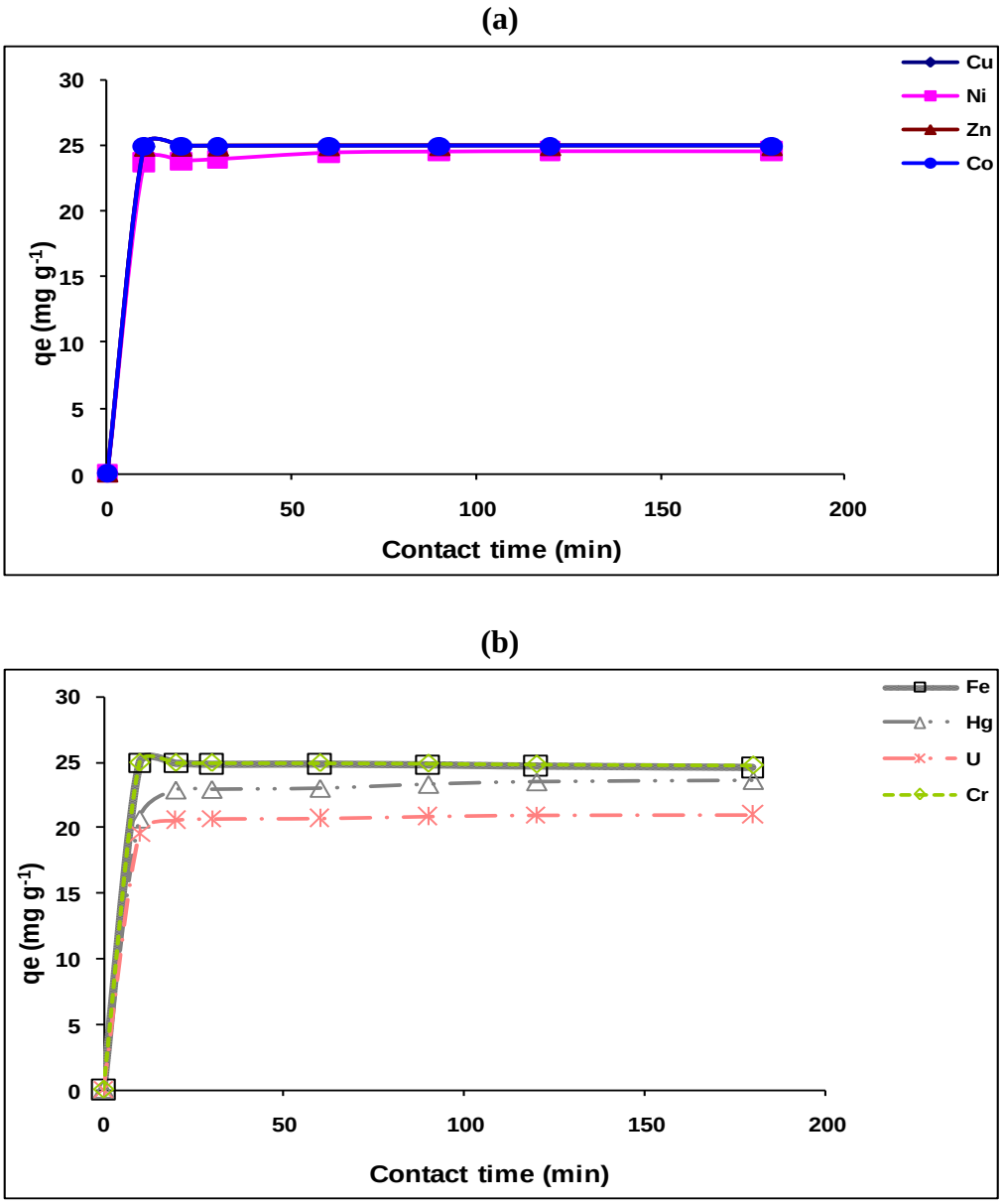

Figure 4.62 Effect of contact time on the adsorption of (a) Cu, Ni, Zn, Co and (b) Fe, Hg, Cr and U onto bentonite-*P. simplicissimum* in single component solutions (pH 3, Temp = 298.15±1^{o}K, agitation rate = 150 rpm, agitation time = 12 h)

As observed for the living fungi, the biosorption of Ni, Hg and U was lower than that for other metal ions. As explained, the adsorption depends on the chemistry of the metal in

aqueous solution as well as the amount and nature of functional groups present on the biomass surface.

The biosorption of Cu, Ni, Zn, Co, Fe, Hg, Cr and U on bentonite-*P.simplicissimum* (inactive) with respect to the contact time is illustrated in Figure 4.63. The results showed the same trend as for the biosorption of metal ions in living fungi immobilized on bentonite. The increase in adsorption capacity for Ni, Hg and U could be due to some synergistic effect.

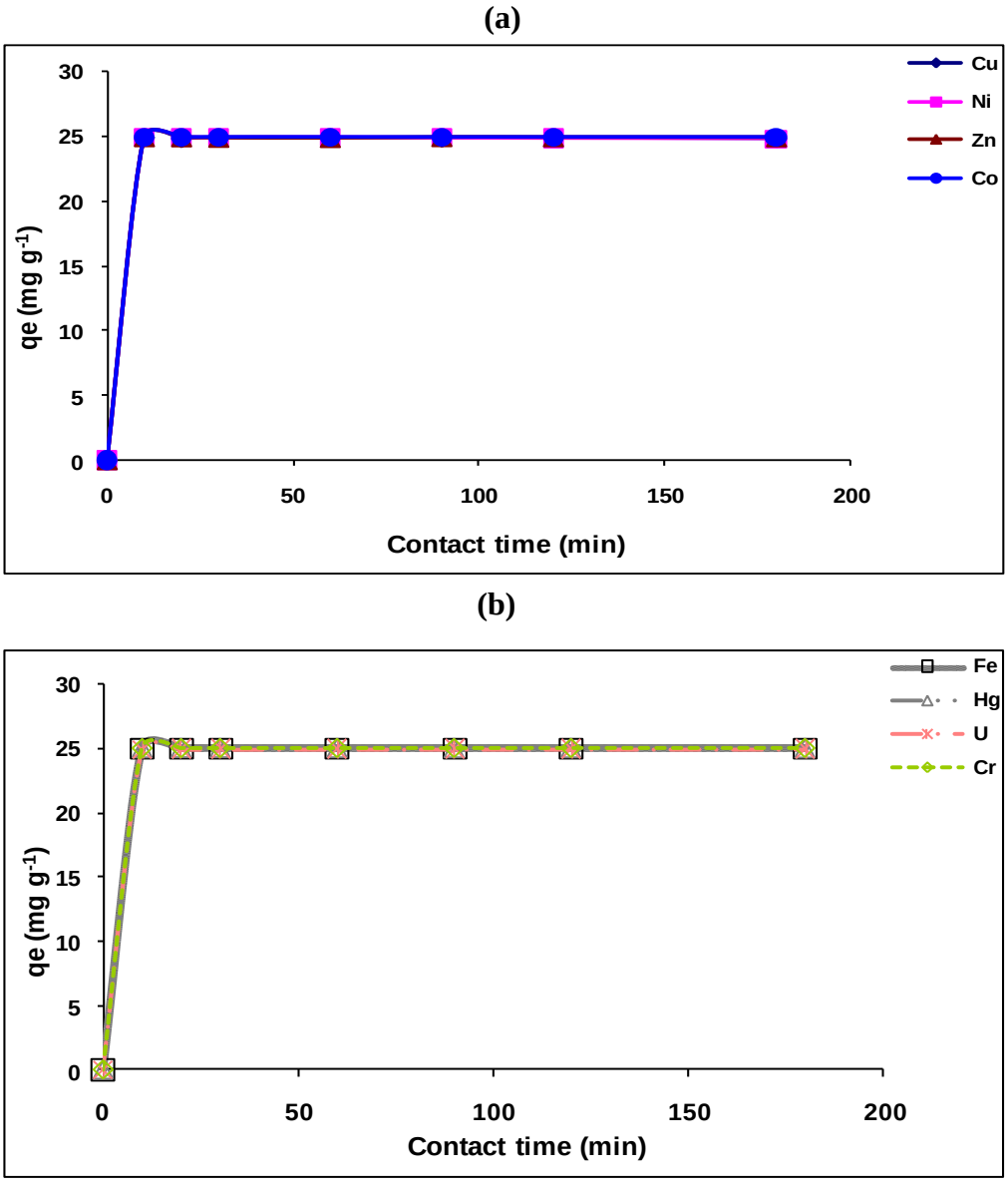

Figure 4.63 Effect of contact time on the adsorption of (a) Cu, Ni, Zn, Co and Fe, Hg, Cr and U onto bentonite-*P.simplicissimum* in multi component solutions (pH 3, Temp = 298.15±1^{o}K, agitation rate = 150 rpm, agitation time = 12 h)

ii) Kinetic modelling of metal ions adsorption on bentonite-P. simplicissimum (inactive) in single- and multi-component systems

Batch kinetic data was fitted to the models by non-linear regression analysis using software Stastistica (Release 5.0) and Excel. Tables 4.52 and 4.53 present the rate constants, amount adsorbed and statistical parameters calculated for the kinetic models used to analyse the experimental data.

Table 4.52 Kinetic constants for the adsorption of metal ions on bentonite-*P. simplicissimum* (inactive) in single-metal systems

Pseudo-first order								
	Fe	***Cu***	***Co***	***Hg***	***Ni***	***Zn***	***U***	***Cr***
A	-2.107	-3.662	-2.884	-2.286	-1.738	-2.640	-2.857	-2.326
B	-0.007	-0.010	-0.007	-0.006	-0.008	-0.013	-0.004	-0.008
q_e (mol/kg)	0.008	0.003	0.001	0.005	0.018	0.002	0.001	0.005
K_1	0.017	0.023	0.017	0.014	0.019	0.031	0.009	0.018
Δq (%)	86.09	92.37	91.47	65.86	74.06	90.09	74.92	88.94
r	0.852	0.819	0.655	0.921	0.954	0.886	0.884	0.783
Pseudo – second order								
	Fe	***Cu***	***Co***	***Hg***	***Ni***	***Zn***	***U***	***Cr***
A	26.19	0.464	4.304	2189	98.32	4.065	1330	12.12
B	11.26	12.71	11.82	52.34	12.67	13.07	238.5	14.46
q_e (mol/kg)	0.089	0.079	0.085	0.019	0.079	0.076	0.004	0.096
K_2	4.837	348.1	32.43	1.251	1.632	42.05	42.75	9.024
Δq (%)	0.519	0.023	0.187	50.06	3.673	0.175	13.87	0.385
r	1.000	1.000	1.000	0.984	0.999	1.000	0.978	1.000
Elovich model								
	Fe	***Cu***	***Co***	***Hg***	***Ni***	***Zn***	***U***	***Cr***
A	0.012	0.012	0.013	-0.001	0.007	0.012	-0.001	0.014
B	0.015	0.014	0.015	0.003	0.013	0.013	0.001	0.017
b	65.30	72.99	67.96	323.8	75.16	75.17	1475	60.33
a	0.034	0.034	0.036	0.003	0.023	0.032	0.001	0.038
Δq (%)	14.98	16.77	16.59	69.99	11.24	16.52	71.11	15.79
r	0.959	0.808	0.990	0.787	0.900	0.892	0.815	0.963
Intraparticle diffusion model								
	Fe	***Cu***	***Co***	***Hg***	***Ni***	***Zn***	***U***	***Cr***
A	0.032	0.031	0.034	0.002	0.023	0.030	-0.001	0.036
B	0.005	0.004	0.004	0.001	0.004	0.004	0.004	0.005
Id	0.032	0.031	0.034	0.002	0.023	0.030	-0.001	0.036
Kp	0.005	0.004	0.004	0.001	0.004	0.004	0.004	0.005
Δq (%)	29.76	29.28	29.33	60.58	30.94	29.34	74.41	29.56
r	0.756	0.722	0.724	0.875	0.828	0.727	0.753	0.741
Film diffusion								
	Fe	***Cu***	***Co***	***Hg***	***Ni***	***Zn***	***U***	***Cr***
A	-1.297	-1.943	-1.412	-0.994	-1.340	-2.328	-0.621	-1.388
B	-0.008	-0.021	-0.014	-0.003	-0.005	-0.013	-0.001	-0.010
If	-1.297	-1.943	-1.412	-0.994	-1.339	-2.327	-0.621	-1.388
Kf	0.008	0.021	0.014	0.003	0.005	0.013	0.001	0.011
Δq (%)	44.01	52.06	51.06	45.08	40.46	40.08	94.37	45.31
r	0.852	0.619	0.655	0.951	0.953	0.886	0.883	0.783

The pseudo second-order described best the kinetics of adsorption for most of the metal ions studied with a correlation coefficient close to unity. The difference with the living biomass was that adsorption of uranium and mercury on living fungi was not described by the pseudo second-order. The amount of metal ions adsorbed q_e (mol kg^{-1}) and the rate constant K_2 (mg min^{-1}) were higher for the pseudo second-order model compared to those obtained for the pseudo first-order model. A similar trend was observed in the adsorption of metals in living biomass immobilized on bentonite.

The kinetics of the adsorption of mercury and nickel on dead biomass were also described by the film diffusion model as observed for the living biomass. The results showed that the kinetics of Fe, Co and Cr adsorption on dead biomass followed the Elovich models as well. On the other hand, the adsorption of Hg followed the film diffusion kinetic model.

In multi-metal system, the different kinetic constants and parameters for the biosorption of metal ions on bentonite-*P.simplicissimum* (inactive) are presented in Table 4.53. The results show that the process followed the pseudo-second order model with $r > 0.985$ for all the metal ions studied like for the immobilized living biomass. The Elovich model also describes the kinetics of most of the metal ions except for Fe^{3+} and Zn^{2+}. In general, the rate constants calculated from the pseudo-second order model were higher than those obtained for the living biomass. Cu and Zn gave higher rate constant for the living biomass, whereas, in the inactive fungi, Fe exhibits the highest rate constant.

Table 4.53 Kinetic constants for the adsorption of metal ions on bentonite-*P. simplicissimum)* inactive in multi-metal systems

Pseudo-first order								
	Fe	***Cu***	***Co***	***Hg***	***Ni***	***Zn***	***U***	***Cr***
A	-3.970	-2.642	-3.472	-3.796	-2.563	-2.783	-3.861	-3.377
B	-0.012	-0.007	-0.010	-0.007	-0.008	-0.009	-0.009	-0.009
q_e (mol/kg)	0.003	0.002	0.001	0.001	0.003	0.002	0.003	0.002
K_1	0.027	0.016	0.022	0.016	0.017	0.021	0.021	0.022
Δq (%)	92.49	90.49	92.27	92.12	90.21	90.93	92.08	92.25
r	0.633	0.708	0.647	0.576	0.746	0.756	0.679	0.638
Pseudo – second order								
	Fe	***Cu***	***Co***	***Hg***	***Ni***	***Zn***	***U***	***Cr***
A	0.112	9.624	0.611	7.657	8.831	5.135	6.441	0.625
B	11.17	12.78	11.79	40.21	11.84	13.09	47.67	10.41
q_e (mol/kg)	0.089	0.078	0.085	0.025	0.085	0.076	0.021	0.096
K_2	1114	16.98	227.2	211.09	15.87	33.35	352.8	173.2
Δq (%)	0.002	0.305	0.010	0.069	0.211	0.196	0.044	0.015
r	0.996	0.995	0.997	0.998	0.986	1.000	0.998	1.000
Elovich model								
	Fe	***Cu***	***Co***	***Hg***	***Ni***	***Zn***	***U***	***Cr***
A	0.014	0.012	0.013	0.004	0.013	0.012	0.003	0.015
B	0.016	0.014	0.015	0.004	0.015	0.013	0.004	0.017
b	64.14	73.65	67.68	231.1	68.21	75.25	273.8	59.76
a	0.038	0.032	0.036	0.011	0.035	0.032	0.009	0.041
Δq (%)	16.79	16.27	16.77	15.69	16.26	16.45	16.69	16.76
r	0.910	0.954	0.957	0.951	0.960	0.874	0.971	0.951
Intraparticle diffusion model								
	Fe	***Cu***	***Co***	***Hg***	***Ni***	***Zn***	***U***	***Cr***
A	0.036	0.031	0.034	0.010	0.033	0.030	0.008	0.038
B	0.005	0.004	0.004	0.001	0.004	0.004	0.001	0.005
Id	0.036	0.031	0.034	0.010	0.033	0.030	0.008	0.038
Kp	0.005	0.004	0.004	0.001	0.004	0.004	0.001	0.005
Δq (%)	29.27	29.42	29.23	29.31	29.42	29.37	29.30	29.28
r	0.721	0.731	0.722	0.723	0.731	0.728	0.723	0.722
Film diffusion								
	Fe	***Cu***	***Co***	***Hg***	***Ni***	***Zn***	***U***	***Cr***
A	-2.286	-1.335	-1.901	-1.422	-1.405	-1.667	-1.764	-1.841
B	-0.024	-0.012	-0.019	-0.017	-0.012	-0.013	-0.017	-0.019
If	-2.286	-1.335	-1.900	-1.422	-1.405	-1.666	-1.764	-1.841
Kf	0.024	0.012	0.019	0.016	0.012	0.013	0.017	0.019
Δq (%)	51.14	48.47	50.53	55.96	46.91	45.23	48.35	51.19
r	0.633	0.708	0.647	0.578	0.746	0.756	0.679	0.640

4.5.2.4.3 Effect of temperature and thermodynamic parameters

i) Effect of contact time

Experiments were conducted at four different temperatures (25, 30, 40 and 60^{o}C) in single-metal and multi-metal systems. The results illustrated in Figure 4.64 showed that the biosorption of Cu, Zn, Co, Cr and Fe was not affected by temperature.

(a)

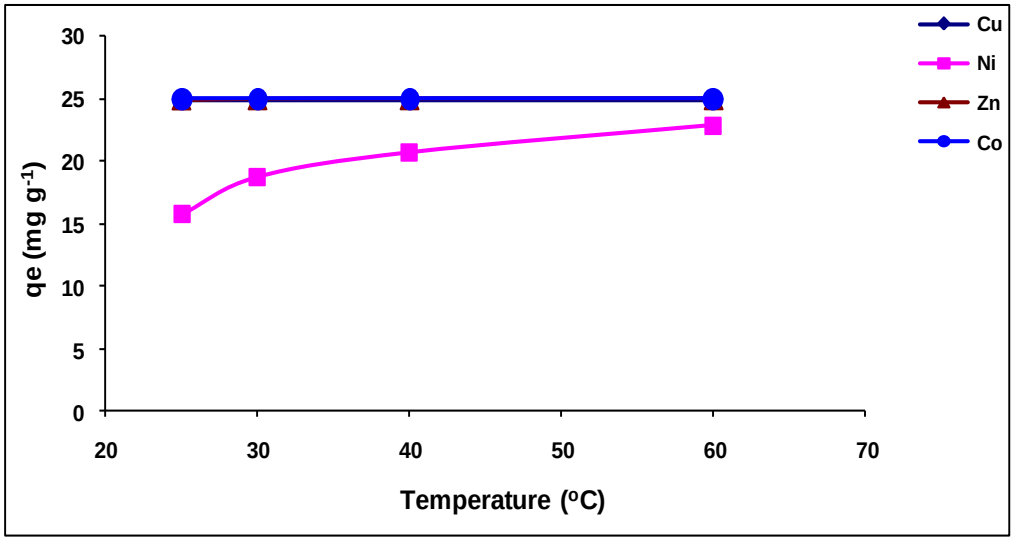

(b)

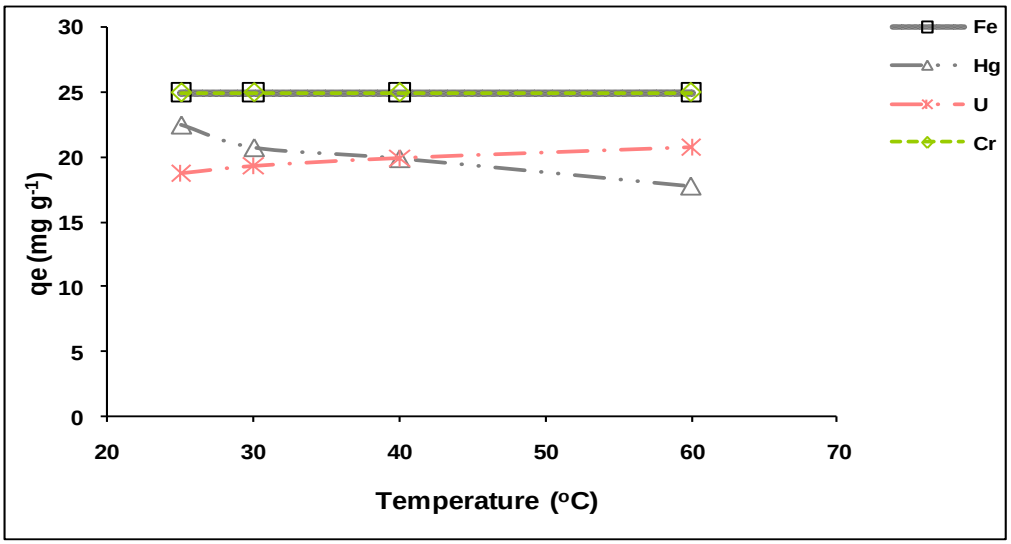

Figure 4.64 Effect of temperature on the adsorption of (a) Cu, Ni, Zn, Co and (b) Fe, Hg, Cr and U onto bentonite-*P.simplicissimum* (inactive) in single component solutions (pH = 3, C_i = 100 mg L^{-1}, Temp = 298.15±1°K, agitation rate = 150 rpm)

The adsorption capacities were constant though the temperature changes. An increase in the uptake of Ni and U was observed at 40°C. Besides, the uptake of mercury on bentonite-inactive *P. simplicissimum* decreased with an increase of temperature. This phenomenon was not observed for the adsorption performed on living biomass.

In the multi-metal system (Figure 4.65), the maximum adsorption capacities were not affected by the change of temperature. Similar results were obtained for the living biomass.

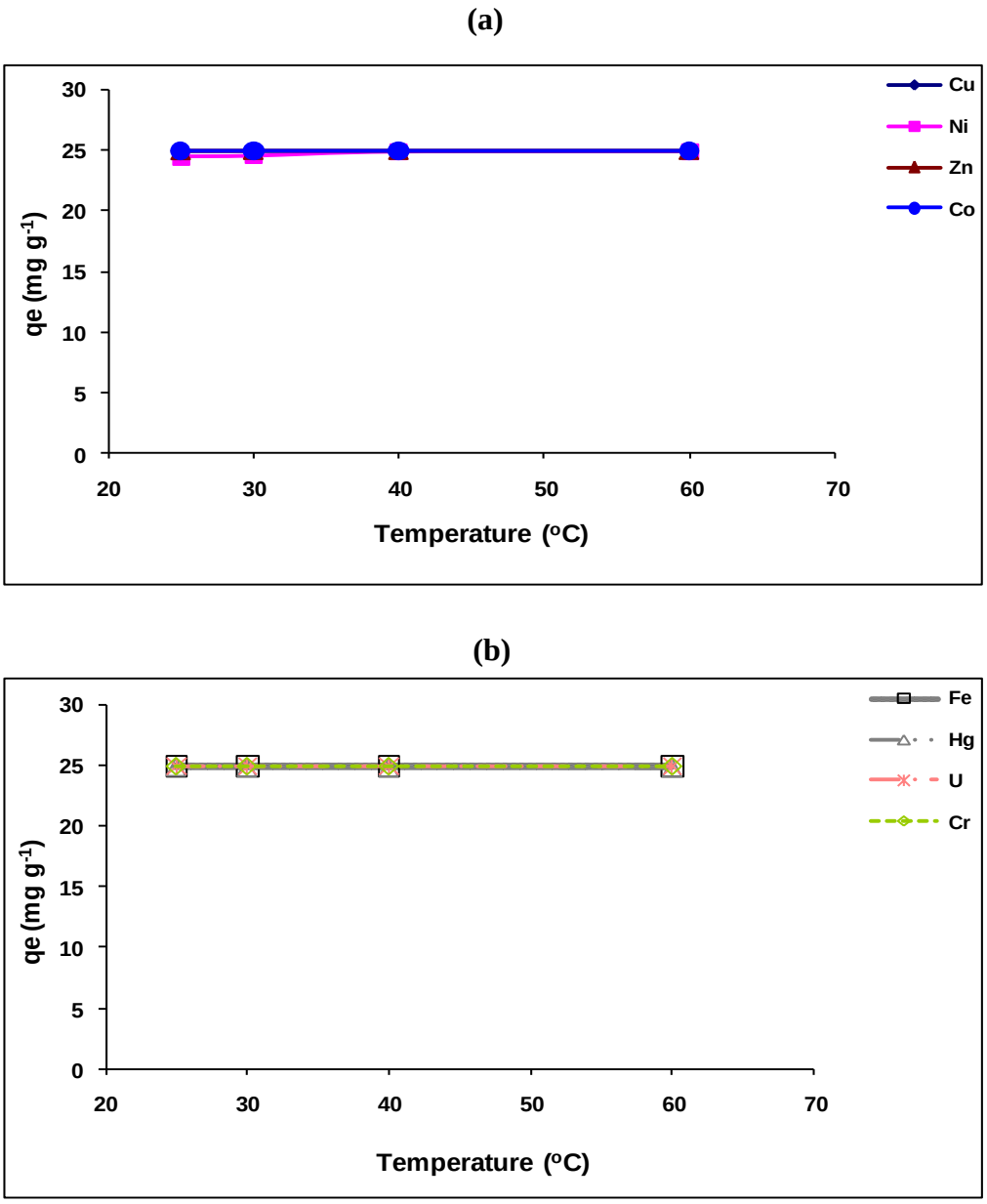

Figure 4.65 Effect of temperature on the adsorption of (a) Cu, Ni, Zn, Co and (b) Fe, Hg, Cr and U onto bentonite-*P.simplicissimum (inactive)* in multi-component solutions (pH = 3, C_i = 100 mg L^{-1}, Temp = 298.15±1^oK, agitation rate = 150 rpm)

ii) Thermodynamic parameters

Thermodynamic parameters, i.e. activation energy E_a, enthalpy (heat of adsorption) ΔH^o, entropy change ΔS^o and the free energy ΔG^o for the biosorption of Cu, Co, Cr, Hg, Fe, Ni, Zn and U in single-metal and multi-metal systems were calculated and the results are presented in Tables 4.54 and 4.55.

Table 4.54 Thermodynamic parameters of metal ions adsorption on bentonite-*P. simplicissimum* (inactive) in single-metal system

	Ea	**ΔH^o**	**ΔS^o**	**ΔG^o**			
	kJ mol^{-1}	kJ mol^{-1}	J$(K.mol)^{-1}$	kJ mol^{-1}			
				298.15 ^oK	**303.15** ^oK	**313.15** ^oK	**333.15** ^oK
Cu	-25.23	150.6	0.509	-16.46	-16.66	-18.22	-19.11
Ni	-43.74	261.0	0.801	-1.319	-2.729	-3.909	-5.914
Zn	-32.50	194.0	0.647	-18.19	-20.19	-21.06	-21.60
Co	-25.34	151.2	0.522	-19.98	-21.09	-21.60	-22.64
Fe	-17.70	105.6	0.379	-18.80	-19.38	-20.04	-20.66
Hg	-30.74	-183.5	-0.544	-5.447	-3.923	-3.366	-2.217
U	-11.29	67.39	0.214	-2.723	-3.023	-3.375	-3.909
Cr	-32.77	195.6	0.647	-16.57	-17.55	-18.76	-20.01

The results show that biosorption of metal ions on inactive biomass is an endothermic process, except for Hg, for which a negative value of enthalpy was obtained. The exothermic nature of the mercury adsorption was proven by the decrease of mercury uptake when the temperature increases. The negative values of activation energies suggest that the biosorption occurs at low energy binding sites. The values of free energy ΔG^o for these processes become more negative with increasing temperature which indicates the spontaneity of the process. As observed for the living biomass, positive values of entropy suggest an increase of randomness except for mercury with a negative value of entropy, suggesting a decrease in the degrees of freedom.

Biosorption of metal ions from a multi-metal system occurs at low binding sites as seen in Table 4.55 with negative values of activation energy, except for Fe, Hg and U, with positive values of activation energy. A similar phenomenon was observed for the biosorption on living biomass, except for chomium with a very low activation energy compared to the Ea

values obtained for the living biomass where a chemisorption process was depicted. The process was endothermic for Cu, Ni, Zn, Co and Cr with a positive heat of adsorption.

Table 4.55 Thermodynamic parameters of metal ions adsorption on bentonite-*P. simplicissimum* (inactive) in multi-metal system

	Ea	**ΔH^o**	**ΔS^o**	**ΔG^o**			
	kJ mol^{-1}	kJ mol^{-1}	J$(K.mol)^{-1}$	kJ mol^{-1}			
				298.15 ^oK	**303.15** ^oK	**313.15** ^oK	**333.15** ^oK
Cu	-26.31	157.0	0.541	-20.56	-21.06	-21.52	-23.32
Ni	-45.39	270.9	0.856	-9.585	-9.890	-13.66	-14.35
Zn	-45.69	272.7	0.883	-16.80	-20.56	-21.06	-21.60
Co	-18.88	112.7	0.405	-20.31	-21.06	-21.24	-22.30
Fe	30.33	-181.0	-0.485	-22.73	-21.40	-20.24	-19.55
Hg	15.94	-95.12	-0.246	-14.84	-13.70	-13.66	-13.16
U	66.76	-398.5	-1.143	-24.55	-22.93	-20.56	-17.54
Cr	-14.31	85.38	0.321	-20.04	-21.06	-21.24	-21.54

The negative values of entropy obtained for Fe, Hg and U show a decrease in the degrees of freedom of the metal ions which gives rise to a negative entropy change. These results implied that the metals are stabilised on the solid surface since the decrease in the degrees of freedom is attributed to immobilization of metal ions. Positive entropy values were obtained for Cu, Ni, Zn, Co and Cr, a trend similar to that observed for the living biomass.

The values of free energy for these processes were negative, confirming the spontaneous nature of the processes. The positive values of entropy change for Cu, Ni, Zn, Co and Cr suggested an increase of randomness at the interface of biomass and metal solution during the adsorption of metals.

The rate of reaction increased with an increase of temperature except for Fe, Hg and U as seen in Table 4.56.

Table 4.56 Rate of adsorption in a single-metal system at different temperatures

Rx rate (h^{-1})				
	298.15 ^{o}K	**303.15** ^{o}K	**313.15** ^{o}K	**333.15** ^{o}K
Cu	0.691	0.708	0.723	0.784
Ni	0.324	0.334	0.460	0.483
Zn	0.565	0.691	0.708	0.726
Co	0.683	0.708	0.714	0.750
Fe	0.764	0.719	0.681	0.657
Hg	0.499	0.461	0.460	0.443
U	0.825	0.771	0.691	0.590
Cr	0.674	0.708	0.714	0.724

The rate of the biosorption shown in Table 4.57 increases with increasing temperature, but an opposite trend was observed for Fe, Hg and U. This could be explained by the exothermic character of the process.

Table 4.57 Rate of adsorption in a multi-metal system at different temperatures

Rx rate (h^{-1})				
	298.15 ^{o}**K**	**303.15** ^{o}**K**	**313.15** ^{o}**K**	**333.15** ^{o}**K**
Cu	0.554	0.560	0.613	0.643
Ni	0.083	0.116	0.147	0.206
Zn	0.612	0.679	0.708	0.726
Co	0.672	0.709	0.726	0.761
Fe	0.632	0.652	0.674	0.695
Hg	0.192	0.147	0.132	0.103
U	0.116	0.123	0.132	0.147
Cr	0.557	0.590	0.631	0.673

4.5.2.4.4 Metal biosorption as a function of culture age

In order to see the effect of culture age on heavy metal adsorption, a biosorption study of heavy metals onto heat-killed *P. simplicissimum* immobilized on bentonite was performed with respect to the growth days in multi-metal solutions. The solution contains 100 mg L^{-1} of each metal ion, the pH, the temperature and agitation time were fixed at 3, 25^{o}C and 12 h, respectively. The results obtained after 2, 5 and 20 days of growth are shown in Figure 4.66.

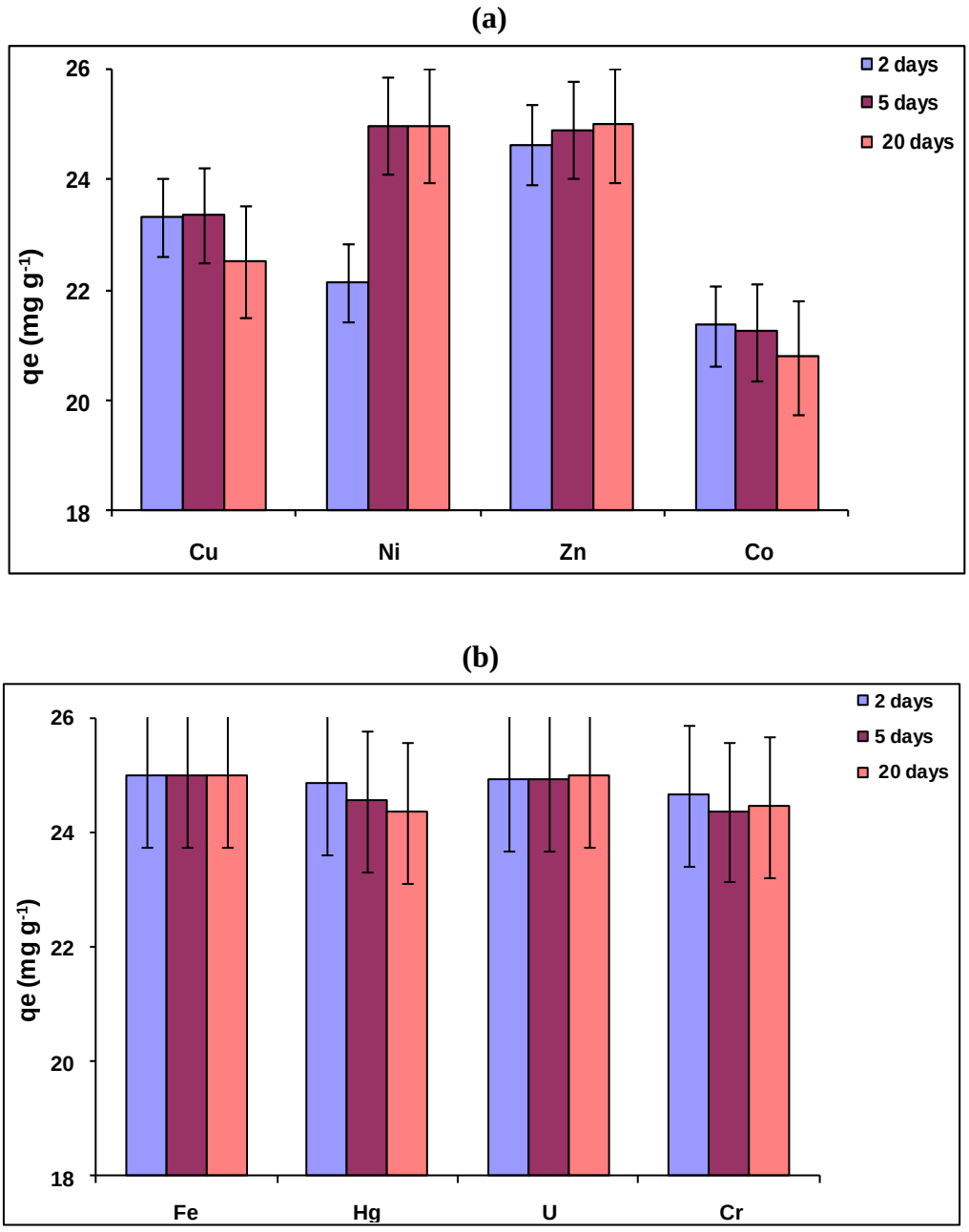

Figure 4.66 Effect of growth days of the biomass on the adsorption of metals (a) Cu, Ni, Zn and Co (b) Fe, Hg, U and Cr

The results show that a maximum adsorption capacity was obtained for metal ions adsorbed on biomass harvested after two days of culturing, except for nickel. The uptake of mercury, copper and cobalt was less for the biomass harvested after 20 days. This is due to the decrease of compounds containing functional groups reponsible for binding these metals. Maximum uptake of nickel was obtained with the biomass obtained after 5 and 20 days.

Biosorption of zinc, uranium and iron was maximal using the biomass grown after 2, 5 and 20 days respectively.

Experiments on the effect of biomass dose as well as the regeneration of the biomass were performed using zeolite. Since a similar trend was observed for bentonite, the results were given only for zeolite and are presented in the coming section.

4.5.3 Zeolite-*P. simplicissimum*

4.5.3.1 Growth curve of P. simplicissimum

The growth rate of the fungal culture in natural zeolite as a function of the number of days and medium pH was assessed. As for the natural bentonite, optimum growth conditions were determined and the plots are presented in Figure 4.67.

A similar trend was obtained as that observed for the *Penicillium* grown on natural bentonite since their mineral compositions are not different. The biomass harvested at pH 4 after 5 days of growth on natural zeolite was 10-fold higher than that obtained with the fungal biomass grown without matrix. A decrease of biomass was observed after 10 days of growth due to the decrease of nutrients in the medium. These results are confirmed later by FTIR analysis.

(a)

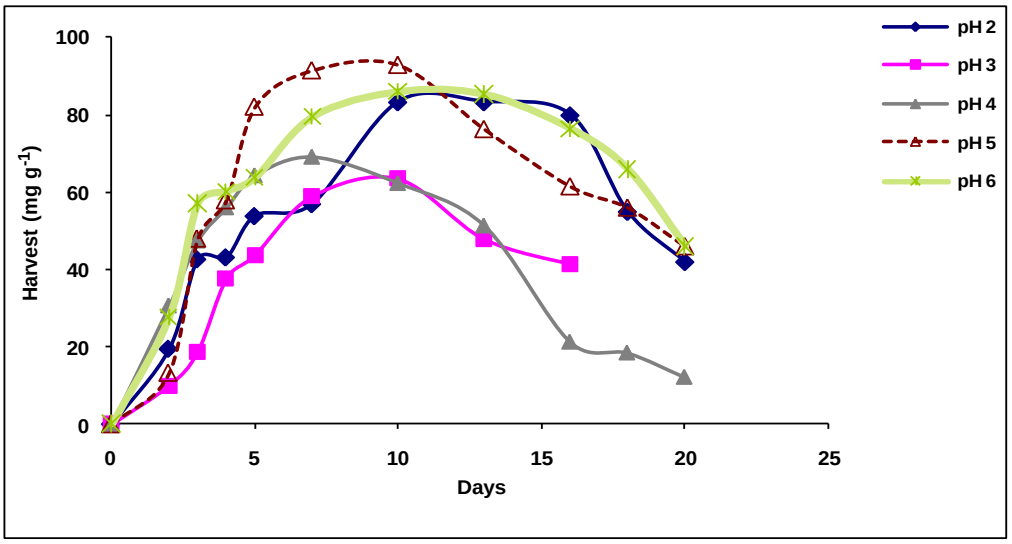

(b)

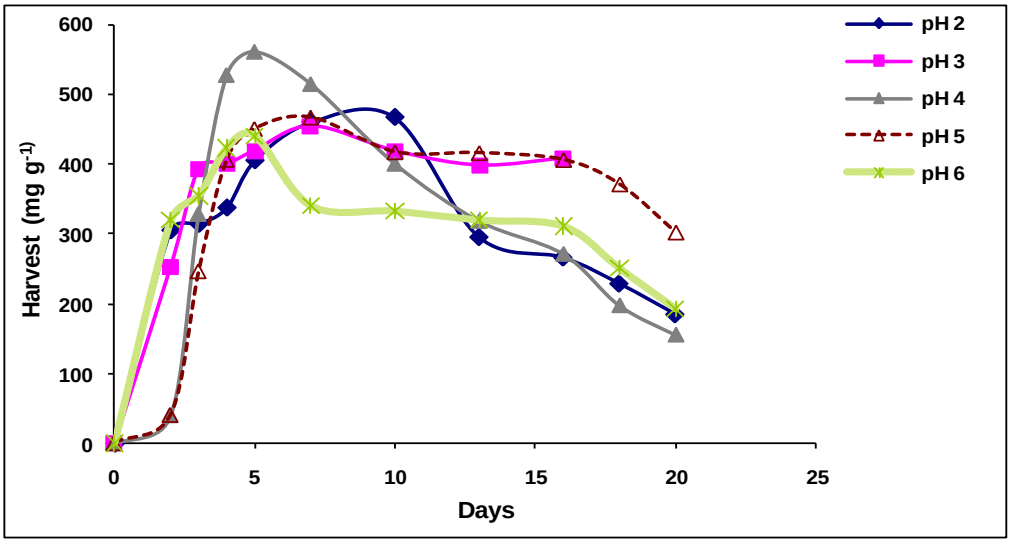

Figure 4.67 Growth curves for (a) *P. simplicissimum* in liquid medium

(b) *P. simplicissimum* in liquid medium supported on zeolite

4.5.3.2 Characteristics of the biomass

i) Physical properties and elemental composition of zeolite-P. simplicissimum

The elemental composition of natural zeolite as well as zeolite-*P.simplicissimum* is presented in Table 4.58.

Table 4.58 *Elemental* composition of natural zeolite and zeolite-*P. simplicissimum*

	Surface area	***CEC***	***C***	***H***	***N***	***S***
	m^2/g	meq/100g	%	%	%	%
Natural-zeolite	0.692	82.50	0.388	2.295	n.d	n.d
Zeolite- *P. simplicissimum*	0.386	61.06	0.578	2.361	0.254	0.035

n.d-not detected

The % of C was high in the biomass; these results confirm the presence of organic compounds released by the fungi as revealed with the IR spectra.

ii) Zeta potential of P. simplicissimum immobilized on zeolite

The plot of zeta potential for zeolite-*P. simplicissimum* is shown in Figure 4.48. The PZC was obtained at pH 2 and 7. A positive surface charge was obtained between pH 2 and 7. A negative charge was obtained below pH 2 and above pH 7.

iii) FTIR spectral analysis

The infrared spectra of the biomass pointed to more compounds released after 10 days of inoculation and confirmed the presence of functional groups with lone pairs of electrons that are available to bind to the positive divalent metal ions. These include: hydroxyl, carbonyl, carboxyl, amine, imidazole, phosphate groups as seen in Figure 4.68.

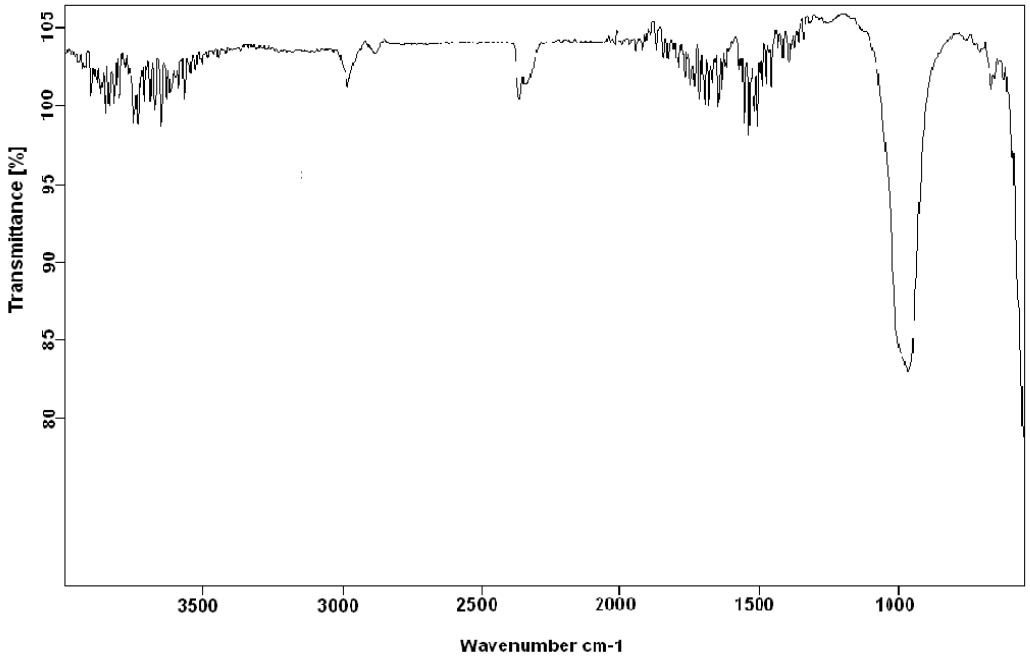

Figure 4.68 FTIR for zeolite-*P.simplicissimum*

Table 4.59 presents the functional groups such as carboxyl (COOH), amid ($-NH_2$), phosphate (PO_4^{-3}) and hydroxyl (-OH) that can interact with metal ions.

Table 4.59 FTIR absorption bands and corresponding possible groups observed on the zeolite-P. *simplicissimum* fungal biomass

Wavenumber, cm^{-1}	***Vibration type***
3666	Carboxyl/OH stretch and N-H stretch
2982	Phenolic/carboxylic, S-H
2359	-CH stretch
1716	C= chelate , stretching amide I band
1507	C= chelate, stretching amide I band
	Amide II band, OH bands
966	Si-O-Si stretching
797	C-H bending
687	OH bend

4.5.3.3 Sorption studies of metals on Zeolite-P. simplicissimum (active or living) in batch mode

The biosorption of Cu, Co, Cr, Fe, Hg, Ni, Zn and U on the active as well as inactive form of zeolite- *P. simplicissimum* was investigated. The pH, effect of metal concentration (isotherms), the contact time (kinetics) and the temperature were assessed. The results obtained for the active form in a single- and multi-systems are given in the following sections.

4.5.3.3.1 Sorption capacities, pH and isotherms of adsorption

i) Effect of pH

The effect of pH on the biosorption of heavy metal ions on zeolite-*P.simplicissimum* in a single ion system are shown in Figure 4.69.

As explained previously, the presence of functional groups such as carboxylate, phosphate, amino and thiol groups on the surface of the biomass are responsible for binding the metals. A maximum adsorption capacity was obtained for Cu, Zn, Co, Fe and Hg for all regimes of pH studied (pH 2 to 7). Although a positive surface charge was measured at this pH range, this did not affect the biosorption of metal ions. The ion exchange process could explain the high amount of metal ions adsorbed in such conditions.

A maximum amount of nickel was adsorbed at pH 3 and then a decrease of adsorption capacity was observed at pH 4 to 7. This phenomenon could be an adsorption followed by desorption at high pH due to breakdown of weak bonds. The uptake of uranium and chomium increased with the increase of pH, at pH 4 and 5, respectively.

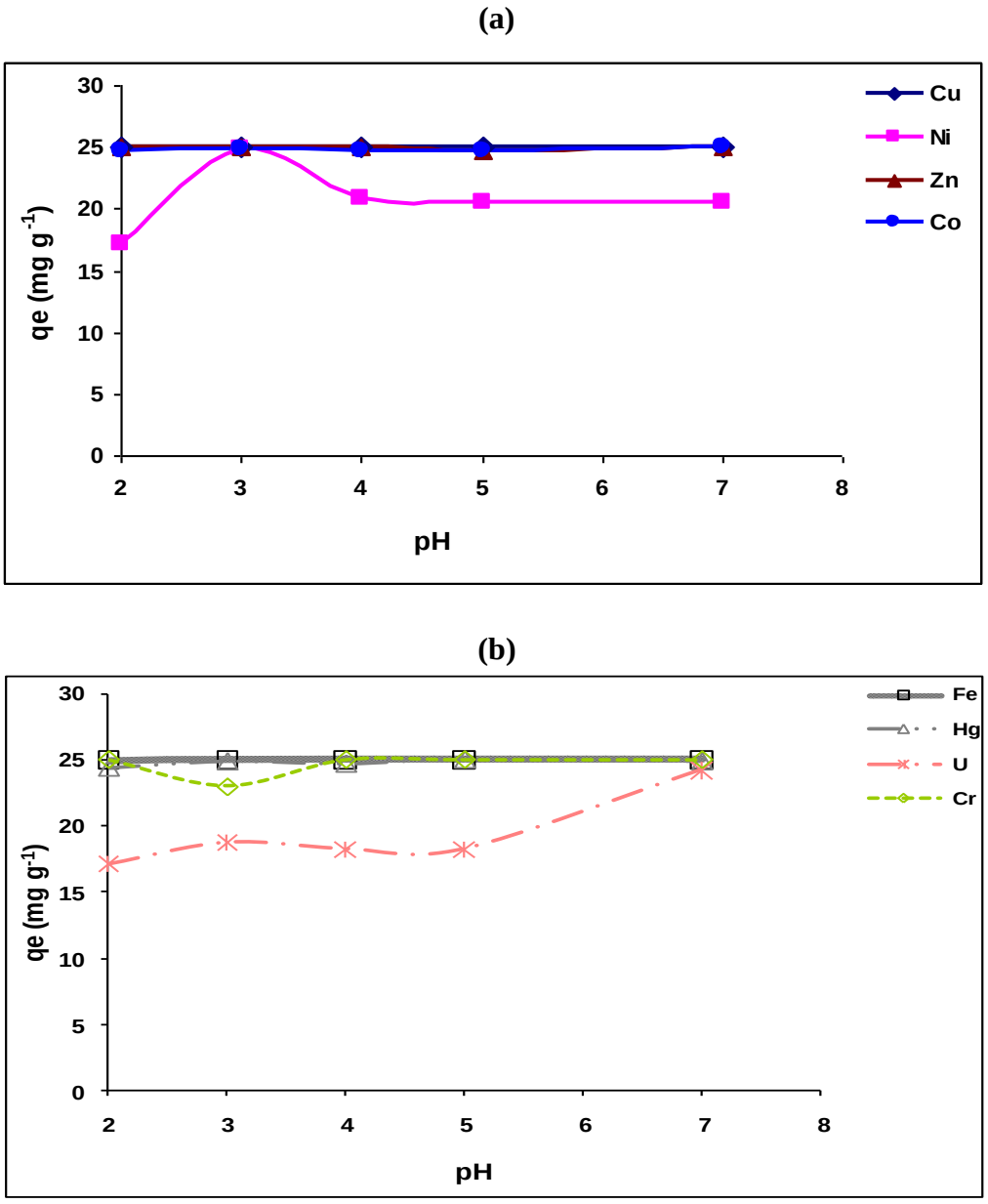

Figure 4.69 Effect of initial pH on adsorption of (a) Cu, Co, Ni and Zn (b) Cr, Fe, Hg and U onto zeolite-*P. simplicissimum* (active) in single component solution (C_i = 100 mg L^{-1}, Temp = 298.15±1^{o}K, agitation rate = 150 rpm, agitation time = 12 h)

The effect of pH on the biosorption capacity of heavy metal ions on zeolite-*P.simplicissimum* in a multi-metal system are illustrated in Figure 4.70. As for the bentonite-*P.simplicissimum*, the uptake of metal ions studied was maximal for all the ranges of pH studied. The synergistic effect was also observed in such a system.

(a)

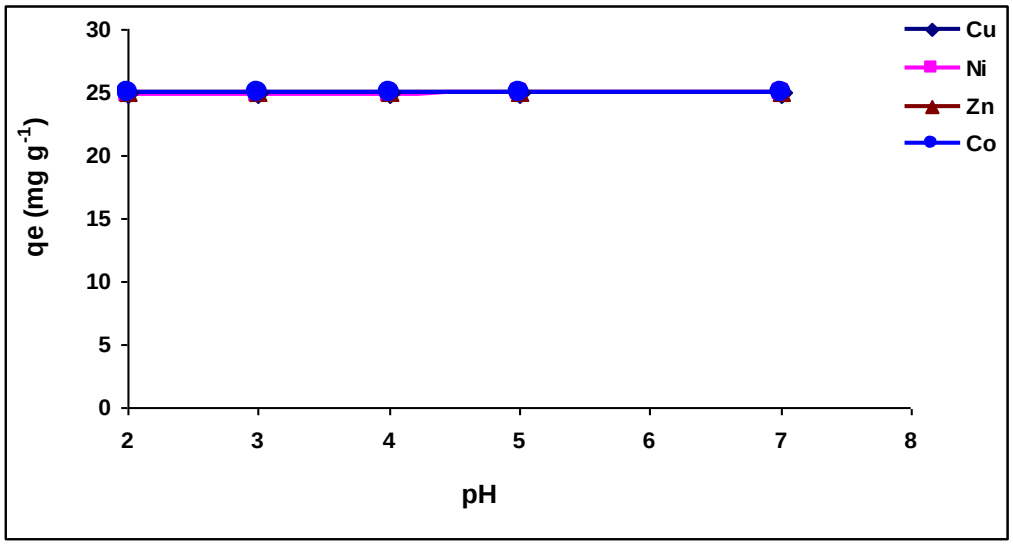

(b)

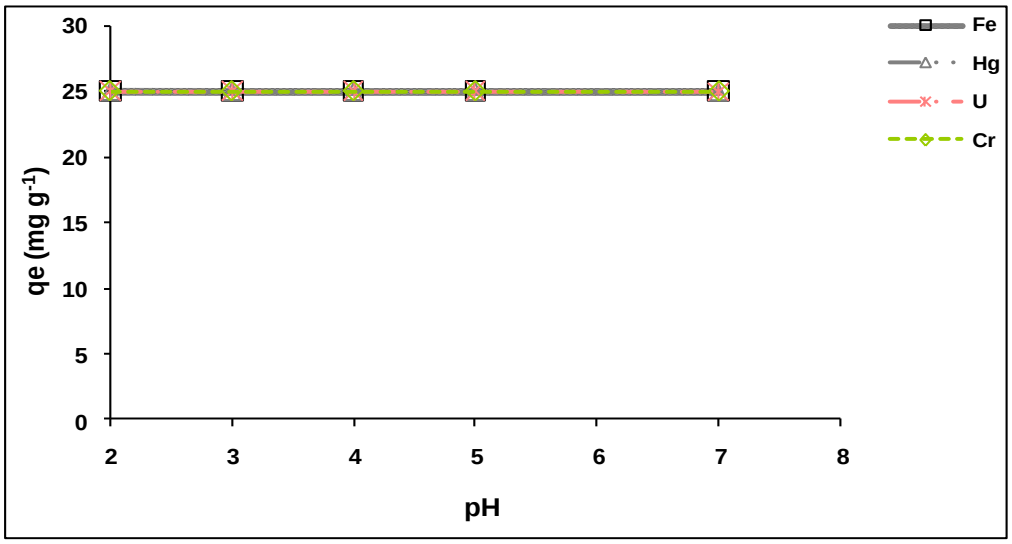

Figure 4.70 Effect of initial pH on adsorption of (a) Cu, Co, Ni and Zn (b) Cr, Fe, Hg and U zeolite-*P.simplicissimum* (active) in multi component solution (C_i = 100 mg L^{-1}, Temp = 298.15±1^oK, agitation rate = 150 rpm, agitation time = 12 h)

ii) Effect of initial metal ion concentration

The plots of initial concentration metal ion concentration versus adsorption capacity in single-metal solutions are given in Figure 4.71.

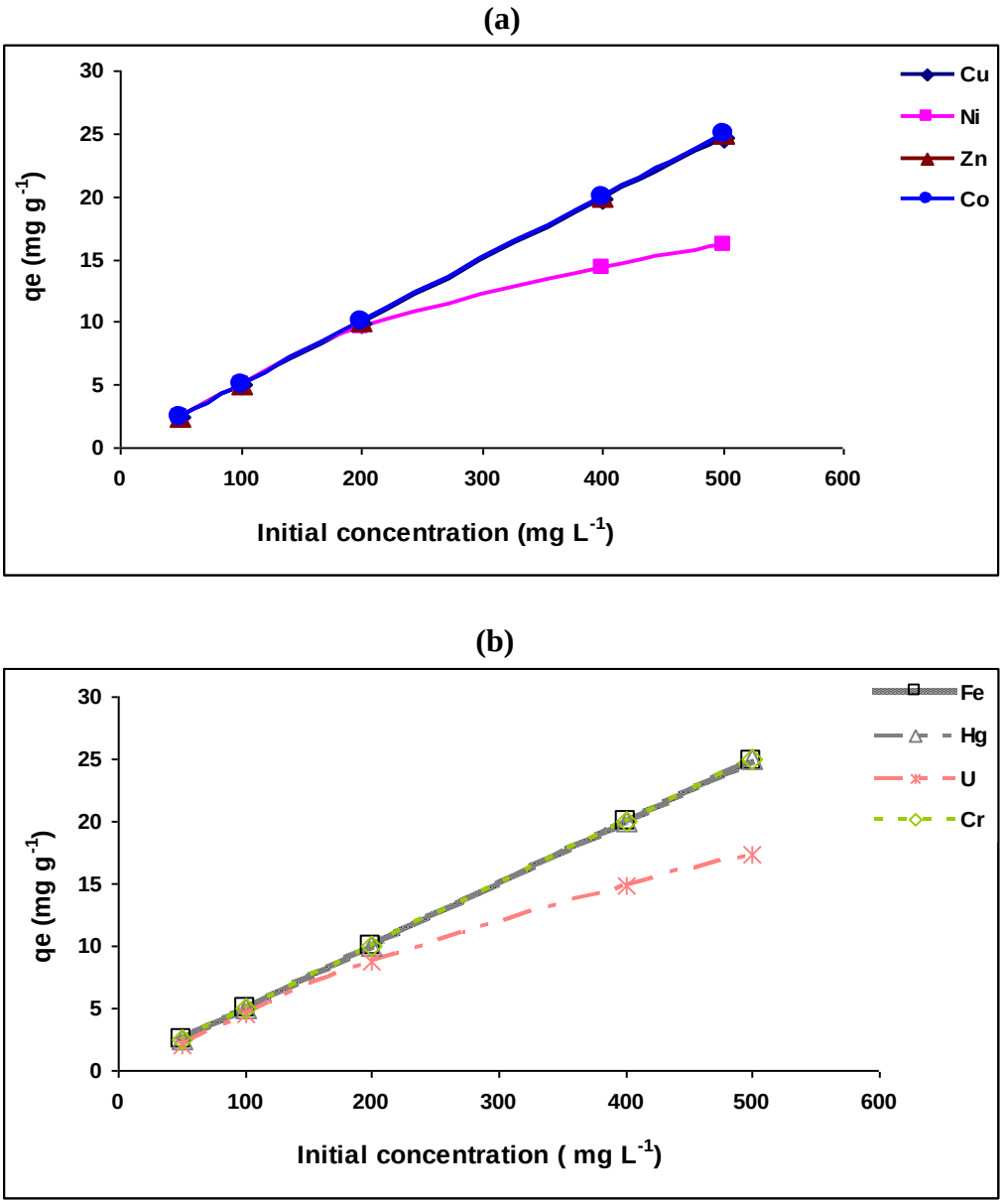

Figure 4.71 Effect of initial concentration on adsorption of (a) Cu, Co, Ni and Zn (b) Cr, Fe, Hg and U onto zeolite-*P*. *simplicissimum* (active) in single component solution (pH = 3, C_i = 100 mg L^{-1}, Temp = 298.15±1^{o}K, agitation rate = 150 rpm, agitation time = 12 h)

In general, linear curves were observed for most of the cases, meaning an increase of metal uptake with an increase of initial metal concentration. A decrease of adsorption capacity was seen for Ni and U up to an initial concentration of 200 mg L^{-1} for both metals, due probably to the xenobiotic effect as explained previously.

The results obtained for the plots of initial concentration metal ions versus adsorption capacity for multi-metal solutions are shown in Figure 4.72.

(a)

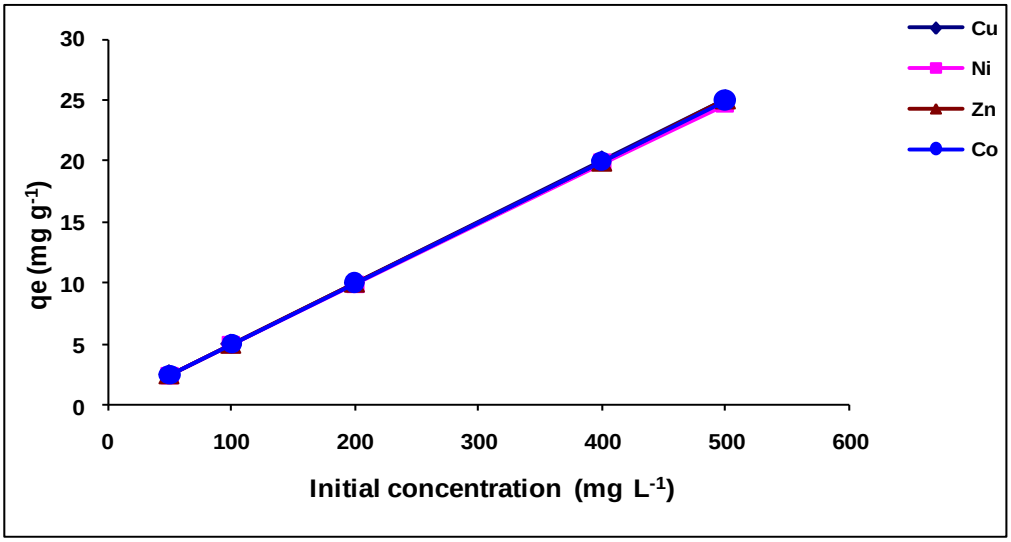

(b)

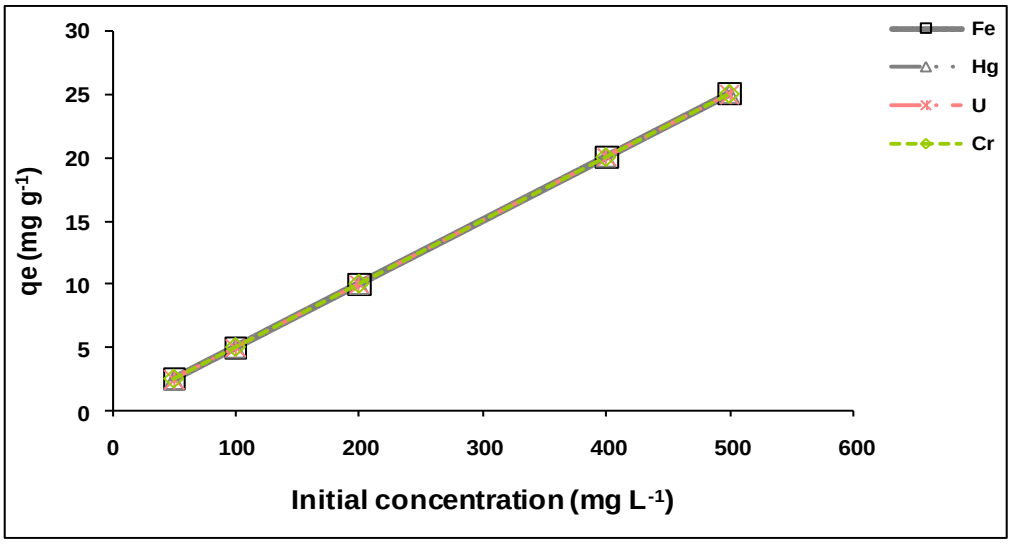

Figure 4.72 Effect of initial concentration on adsorption of (a) Cu, Co, Ni and Zn (b) Cr, Fe, Hg and U onto zeolite-*P. simplicissimum* (active) in multi component solution (pH = 3, C_i = 100 mg L^{-1}, Temp = 298.15±1^{o}K, agitation rate = 150 rpm, agitation time = 12 h)

The uptake of metal ions in such a system increased linearly with an increase of metal ions concentration. The presence of competiting ions inhibits the xenobiotic effect observed for Ni and U in a single-ion solution. Further explanations were given in section 4.5.2.3.

iii) The isotherms of adsorption for metal ions on zeolite-P. simplicissimum (living)

The biosorption constants for the Langmuir, Freundlich, D-R and partition coefficient models as well the correlation coefficient were calculated for a single-metal and multi-metal systems are given in Tables 4.60 and 4.61, respectively.

Table 4.60 Parameters of Langmuir, Freundlich and D-R and correlation coefficient for the adsorption of metals on zeolite-*P. simplicissimum* (active) in a single metal system

Langmuir Isotherms	***Fe***	***Cu***	***Co***	***Hg***	***Ni***	***Zn***	***U***	***Cr***
A	0.012	0.007	0.004	0.025	0.002	0.001	2.115	4.015
B	2.259	0.315	0.952	9.254	2.166	0.474	80.13	0.868
b	192.3	404.2	2154	368.7	890.3	1201	37.88	2162
qm (mol/kg)	0.443	3.174	1.051	0.108	0.462	2.108	0.013	1.152
ΔGo (kJ/mol)	-13.04	-14.88	-19.03	-14.65	-16.84	-15.58	-9.009	-24.74
Δq (%)	76.06	75.91	75.29	75.98	76.15	75.92	76.06	75.91
r	0.982	0.554	0.668	0.672	0.989	0.690	0.609	0.659
Freundlich Isotherms	***Fe***	***Cu***	***Co***	***Hg***	***Ni***	***Zn***	***U***	***Cr***
A	0.158	0.058	0.064	0.081	0.124	0.069	-0.008	0.078
B	0.233	0.169	0.158	0.327	0.193	0.165	0.628	0.129
K_f	1.439	1.143	1.159	1.204	1.330	1.174	0.981	1.198
n	4.289	5.910	6.314	3.056	5.190	6.044	1.592	7.711
ΔGo (kJ/mol)	-10.63	-14.65	-15.65	-7.577	-12.87	-14.98	-3.946	-19.11
Δq (%)	60.12	111.4	107.1	61.03	81.41	42.99	80.72	56.81
r	0.974	0.877	0.839	0.956	0.867	0.973	0.669	0.978
D-R Isotherms	***Fe***	***Cu***	***Co***	***Hg***	***Ni***	***Zn***	***U***	***Cr***
A	0.273	0.229	0.244	-0.123	0.295	0.275	-0.531	0.309
B	-0.004	-0.002	0.002	-0.005	-0.003	-0.002	-0.115	-0.002
Xm (mol/kg)	1.314	1.258	1.277	0.883	1.343	1.317	0.588	1.362
Es (kJ/mol)	11.75	14.65	15.42	10.50	13.58	15.13	6.542	18.24
Δq (%)	26.22	95.16	87.44	72.22	52.38	61.88	50.14	75.26
r	0.982	0.857	0.847	0.983	0.889	0.976	0.685	0.976
K_d	***Fe***	***Cu***	***Co***	***Hg***	***Ni***	***Zn***	***U***	***Cr***
A	6.195	5.089	7.018	4.277	7.849	5.868	2.163	7.102
B	3296	9815	8653	3720	6025	1673	204.9	1414
ΔGo (kJ/mol)	-15.36	-12.62	-17.39	-10.60	-19.45	-14.55	-5.364	-17.61
Kdo	490.2	162.3	1117	71.99	2564	353.7	8.705	1212
Δq (%)	70.79	114.3	96.68	63.39	82.69	81.99	91.64	81.52
r	0.990	0.508	0.552	0.632	0.961	0.658	0.623	0.698

The high coefficients of correlation values ($R^2 > 0.95$) for most of the studied metals except Ni suggested that the Freundlich isotherm provides a good model of the adsorption process for the metal ions studied. The calculated values of *n* range from 1.592 to7.711 with the values of 1/n < 1, suggesting that the metal binding is characterized by weak free energies. The biosorption of Fe was described by all the models used to fit the experimental data as well; numerous mechanisms contribute to the adsorption of Fe on the zeolite-*P.simplicissimum* as seen before. The biosorption data of Ni fitted well the Langmuir isotherm assuming that the uptake of nickel occurs on a homogenous surface by monolayer adsorption without any interaction between adsorbed ions. The distribution coefficient could as well describe the Ni biosorption with a correlation coefficient > 0.950.

The maximum amount of metal ions adsorbed (q_m) on zeolite-*P.simplicissimum* (active) obtained from the Langmuir isotherm decreased in the following order: Cu > Zn > Cr > Co > Ni > Fe >Hg > U. The free energy of adsorption calculated from the D-R isotherm was in the range of values of the ion exchange mechanism (8 – 16 kJ mol^{-1}), except for U and Cr with an adsorption free energy of 6.542 and 18.14 kJ mol^{-1}, respectively. The distribution coefficient decreased in the following: Ni, Cr, Co, Fe, Zn, Cu, Hg and U.

In the multi-metal system (Table 4.61), the biosorption of Fe, Co, Zn and Cr followed the D-R isotherm; assuming that the adsorption occurs on heterogeneous surface energy.

The experimental data of Co and Zn fitted well the Langmuir isotherm, whereas, Fe and Cr were described better by the Freundlich isotherm. These results prove that the biosorption of metal ions on *P.simplicissimum* (active) immobilized on zeolite occurs though different mechanisms. The uptake of metal ions on zeolite-*P simplicissimum* (active) followed the sequence: Ni > Cu > Cr > Fe > U > Co > Zn > Hg. The values of K_{do} were very high for Co (74363), Zn (22301), Cr (18335) and Fe (8465) compared to those obtained for Ni (229.8), Cu (13.01), Hg (10.99) and U (44.15).

Table 4.61 Parameters of Langmuir, Freundlich and D-R and correlation coefficient models for the adsorption of metals on zeolite-*P. simplicissimum* (active) in multi-metal systems

Langmuir Isotherms	***Fe***	***Cu***	***Co***	***Hg***	***Ni***	***Zn***	***U***	***Cr***
A	0.003	0.001	0.001	0.001	0.006	0.001	0.001	0.001
B	1.749	1.325	2.337	4.188	0.899	2.863	1.974	1.357
b	47586	22932	18993	6438	142.8	2871	3298	62002
qm (mol/kg)	0.572	0.755	0.427	0.239	1.112	0.349	0.507	0.736
ΔGo (kJ/mol)	-26.69	-24.89	-24.42	-21.74	-12.29	-19.73	-20.08	-27.35
Δq (%)	70.96	75.94	16.28	75.94	75.93	76.24	75.92	75.95
r	0.705	0.757	0.998	0.738	0.823	0.989	0.731	0.781
Freundlich Isotherms	***Fe***	***Cu***	***Co***	***Hg***	***Ni***	***Zn***	***U***	***Cr***
A	0.111	0.027	0.154	0.029	0.094	0.141	0.039	0.093
B	0.137	0.133	0.149	0.229	0.208	0.173	0.240	0.127
K_f	1.290	1.065	1.429	1.070	4.795	1.384	1.095	1.239
n	7.263	7.496	6.679	4.362	1.242	5.791	4.165	7.863
ΔGo (kJ/mol)	-18.01	-18.58	-16.56	-10.81	-11.89	-14.35	-10.32	-19.49
Δq (%)	17.73	85.22	65.49	83.95	12.89	53.18	107.2	97.56
r	0.974	0.930	0.948	0.885	0.891	0.958	0.908	0.968
D-R Isotherms	***Fe***	***Cu***	***Co***	***Hg***	***Ni***	***Zn***	***U***	***Cr***
A	0.339	0.119	0.238	0.123	0.317	0.053	0.157	0.345
B	-0.002	-0.002	-0.001	-0.003	-0.003	-0.002	-0.003	-0.001
Xm (mol/kg)	1.403	1.127	1.269	1.131	1.373	1.055	1.170	1.421
Es (kJ/mol)	18.18	18.36	18.55	13.49	11.98	17.16	13.26	18.79
Δq (%)	34.43	52.24	35.88	89.79	59.01	29.74	87.76	70.43
r	0.980	0.931	0.955	0.887	0.897	0.968	0.911	0.973
K_d	***Fe***	***Cu***	***Co***	***Hg***	***Ni***	***Zn***	***U***	***Cr***
A	9.044	2.566	11.21	2.392	5.437	10.02	3.787	9.816
B	786402	364969	3477	786892	39273	-22365	736737	968719
ΔGo (kJ/mol)	-22.42	-6.361	-27.81	-5.931	-13.48	-24.82	-9.389	-24.33
Kdo	8465	13.01	74363	10.94	229.8	22301	44.15	18335
Δq (%)	89.13	95.81	80.45	74.96	87.33	74.87	95.61	105.7
r	0.735	0.837	0.887	0.726	0.717	0.984	0.676	0.695

4.5.3.3.2 Effect of contact time and kinetics of adsorption

i) Effect of contact time

The effect of contact time on the uptake capacity of Cu, Co, Cr, Fe, Hg, Ni, Zn and U by active *P. simplicissimum* immobilized on zeolite is illustrated in Figure 4.73 and 4.74 for single-metal and multi-metal systems, respectively. The results in Figure 4.73 show that the biosorption consisted of two phases, namely: a primary rapid phase followed by a second slow phase as was seen in the previous cases. The rapid phase lasted approximately 30

minutes and accounted for the major part in the total metal biosorption. The equilibrium was reached straight after the first stage and maximum biosorption was reached. The maximum amount of uranium adsorbed was less compared to the maximum amount for the other metals.

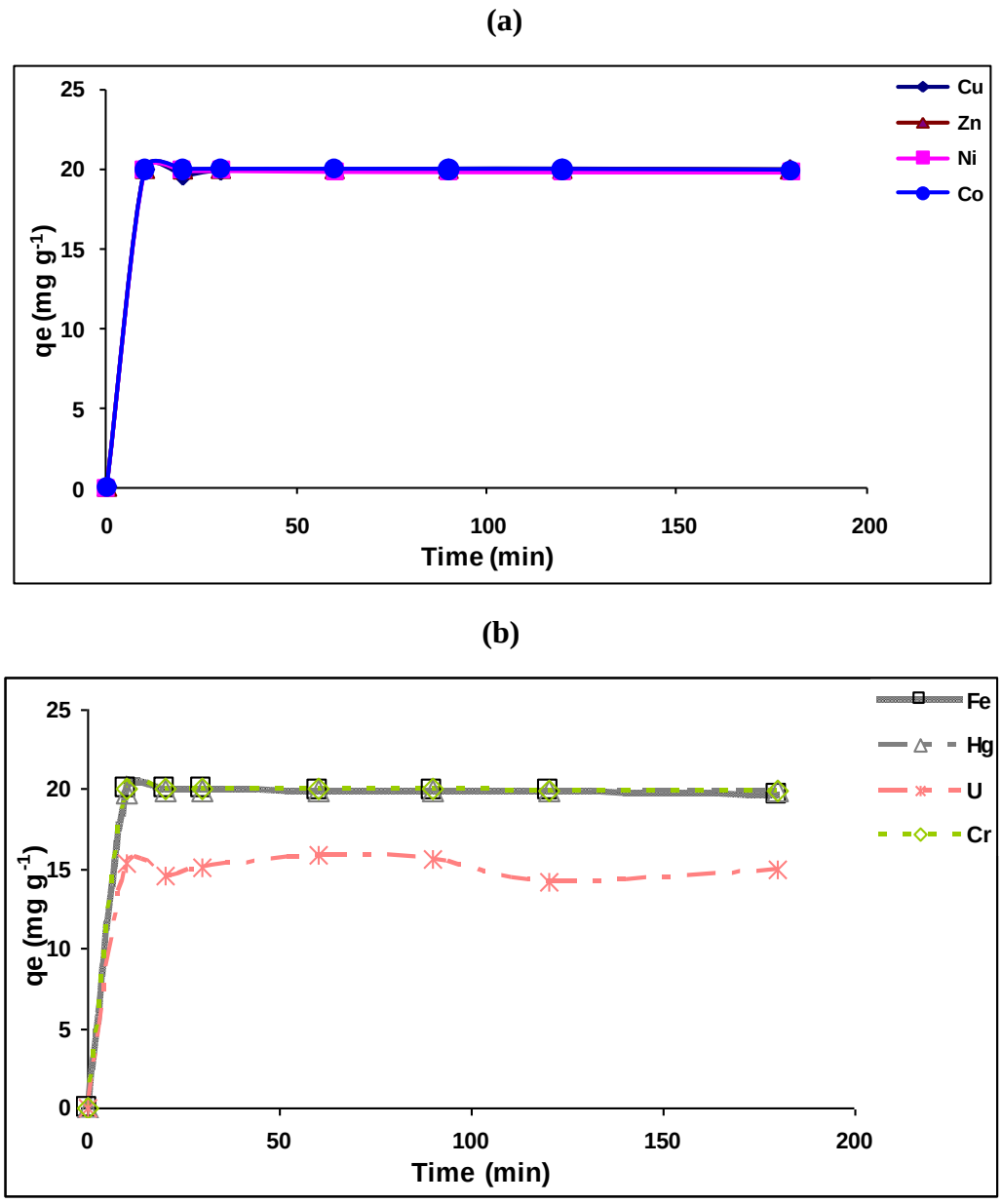

Figure 4.73 Effect of contact time on the adsorption of (a) Cu, Ni, Zn and Co (b) Cr, Fe, Hg, U on zeolite-*P. simplicissimum* (active) in single component solutions (pH = 3, C_i = 100 mg L^{-1}, Temp = 298.15±1^oK, agitation rate = 150 rpm)

The effect of contact time on the biosorption of metal ions on zeolite-*P.simplicissimum* (active) in a multi-metal system is shown in Figure 4.74. The trend is similar to that seen in a single-metal system: a rapid phase with the maximum uptake of metals followed by a slow phase where equilibrium was reached. In the multi-metal system, the uptake of uranium increased and this phenomenon has been explained in the previous study.

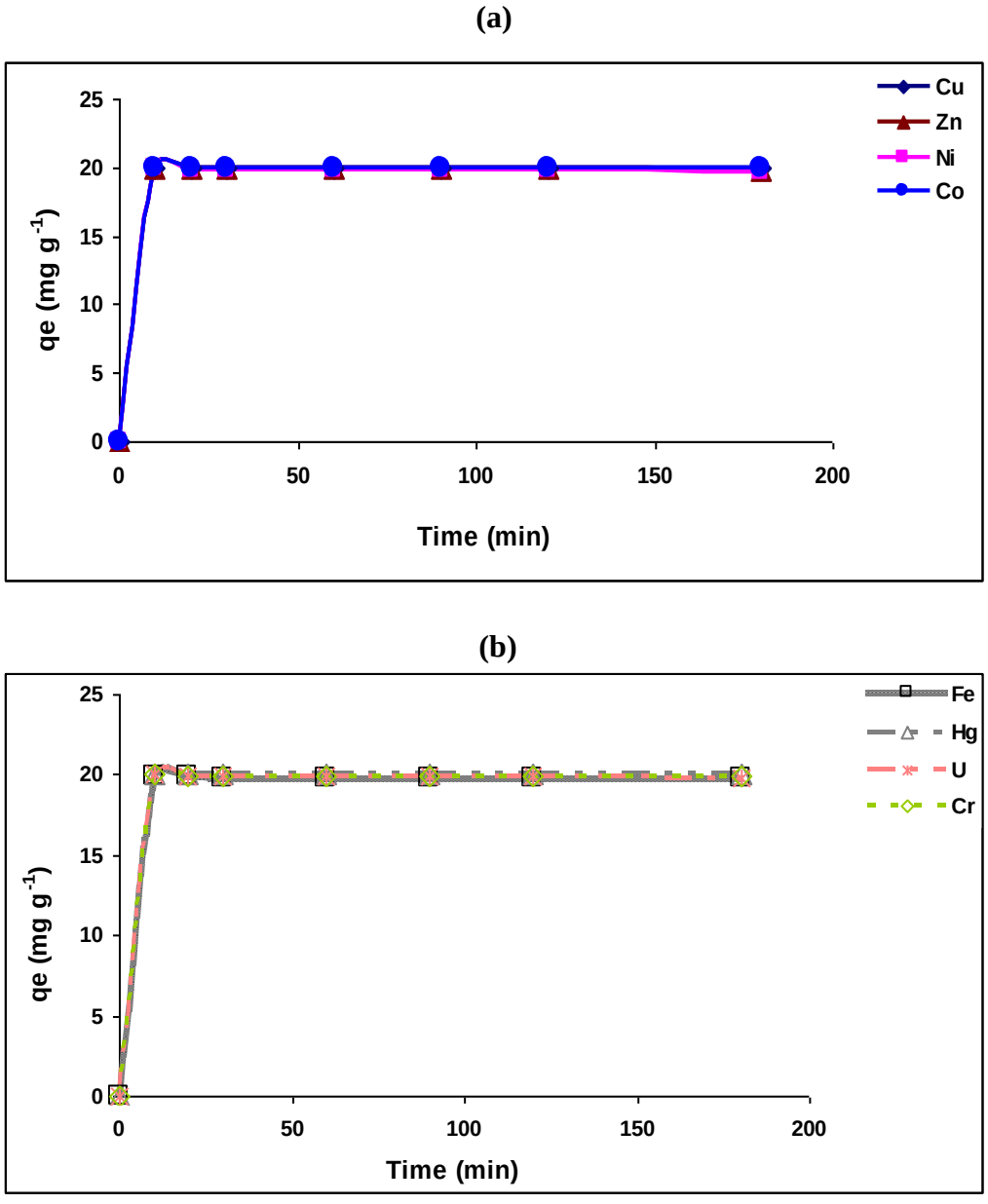

Figure 4.74 Effect of contact time on the adsorption of (a) Cu, Ni, Zn and Co (b) Cr, Fe, Hg and U on zeolite-*P. simplicissimum* (active) in multi- component solutions (pH = 3, C_i = 100 mg L^{-1}, Temp = 298.15±1^oK, agitation rate = 150 rpm)

ii) Kinetic modelling of metal ions adsorption on zeolite-P. simplicissimum (in single- and multi-component systems)

Batch kinetic data was fitted to the models by regression analysis using Software Statistica (Release 5.0) and Excel. The constants and parameters calculated for the single-ion and multi-ion systems are listed in Tables 4.62 and 4.63.

Table 4.62 Kinetic constants for the adsorption of metal ions on zeolite-*P. simplicissimum* (active) (in single-metal system)

Pseudo-first order								
	Fe	***Cu***	***Co***	***Hg***	***Ni***	***Zn***	***U***	***Cr***
A	-2.821	-2.772	-3.409	-4.086	-2.870	-3.431	-2.833	-3.618
B	-0.013	-0.007	-0.012	-0.014	-0.010	-0.010	-0.006	-0.010
q_e (mol/kg)	0.002	0.002	0.001	0.001	0.001	0.002	0.001	0.001
K_1	0.029	0.017	0.027	0.033	0.023	0.024	0.014	0.023
Δq (%)	91.19	91.30	92.21	92.31	91.34	92.20	86.35	92.39
r	0.809	0.652	0.721	0.744	0.770	0.684	0.846	0.625
Pseudo – second order								
	Fe	***Cu***	***Co***	***Hg***	***Ni***	***Zn***	***U***	***Cr***
A	2.530	4.262	0.546	2.976	2.775	0.810	247.7	0.306
B	11.17	10.42	11.79	40.18	11.78	13.09	59.87	10.39
q_e (mol/kg)	0.089	0.096	0.085	0.025	0.085	0.076	0.0167	0.096
K_2	49.32	25.46	254.6	542.6	50.05	211.5	14.47	353.6
Δq (%)	0.481	0.328	0.056	0.266	0.126	0.031	0.956	0.018
r	1.000	1.000	1.000	1.000	1.000	1.000	1.000	1.000
Elovich model								
	Fe	***Cu***	***Co***	***Hg***	***Ni***	***Zn***	***U***	***Cr***
A	0.014	0.015	0.013	0.004	0.013	0.012	0.002	0.015
B	0.016	0.017	0.015	0.004	0.015	0.013	0.003	0.017
b	64.14	59.88	67.71	230.6	67.74	75.16	350.4	59.71
a	0.037	0.040	0.036	0.011	0.036	0.033	0.006	0.041
Δq (%)	16.45	16.39	16.75	16.65	16.65	16.75	13.87	16.78
r	0.714	0.773	0.775	0.634	0.966	0.888	0.965	0.802
Intraparticle diffusion model								
	Fe	***Cu***	***Co***	***Hg***	***Ni***	***Zn***	***U***	***Cr***
A	0.035	0.038	0.034	0.010	0.034	0.031	0.006	0.038
B	0.005	0.005	0.004	0.001	0.004	0.004	0.001	0.005
Id	0.035	0.038	0.034	0.010	0.034	0.031	0.006	0.038
Kp	0.005	0.005	0.004	0.001	0.004	0.004	0.001	0.005
Δq (%)	29.38	29.40	29.29	29.32	29.31	29.28	30.08	29.27
r	0.729	0.729	0.722	0.725	0.724	0.722	0.774	0.721
Film diffusion								
	Fe	***Cu***	***Co***	***Hg***	***Ni***	***Zn***	***U***	***Cr***
A	-2.251	-1.433	-2.229	-2.636	-1.852	-2.002	-1.080	-2.013
B	-0.015	-0.014	-0.019	-0.020	-0.015	-0.019	-0.007	-0.021
If	-2.251	-1.433	-2.229	-2.636	-1.852	-2.002	-1.080	-2.013
Kf	0.015	0.014	0.019	0.020	0.015	0.018	0.007	0.021
Δq (%)	41.29	49.90	44.97	41.97	44.40	47.53	45.23	51.59
r	0.809	0.652	0.721	0.744	0.771	0.684	0.846	0.625

The pseudo 2nd order model fits better the biosorption kinetics of all the metal ions with a correlation coefficient equal to unity, suggesting a chemisorption mechanism. The calculated values of q_e (mol kg^{-1}) from the pseudo-2nd order were higher than those obtained for the pseudo-1st order. The biosorption of Ni and U can be described by the Elovich model as well ($r > 0.950$). The calculated rate constants (k_2) were found to be higher than (k_1) and decreased in the sequence: Hg > Cr > Co > Zn > Ni > Fe > Cu > U. The Elovich constant, *b*, related to the surface coverage was higher for U and Hg.

A similar trend was observed in a multi-metal system (Table 4.63). The pseudo 2nd order fits the experimental data with a correlation coefficient equal to 1. In addition, the biosorption of Fe, Cu, Zn and U from a multi-metal solution is also described by the Elovich kinetic model with $r > 0.950$, implying a chemisorption mechanism.

Table 4.63 Kinetic constants for the adsorption of metal ions on zeolite-*P.simplicissimum* (active) (in multi-metal system)

Pseudo-first order								
	Fe	***Cu***	***Co***	***Hg***	***Ni***	***Zn***	***U***	***Cr***
A	-2.997	-3.529	-3.975	-4.736	-3.156	-3.332	-3.938	-2.976
B	-0.006	-0.008	-0.014	-0.012	-0.012	-0.007	-0.007	-0.006
q_e (mol/kg)	0.001	0.001	0.001	0.002	0.001	0.001	0.001	0.001
K_1	0.014	0.018	0.033	0.028	0.028	0.016	0.015	0.014
Δq (%)	91.80	92.36	92.48	92.52	91.91	92.15	92.19	91.83
r	0.562	0.550	0.693	0.636	0.747	0.553	0.553	0.551
Pseudo – second order								
	Fe	***Cu***	***Co***	***Hg***	***Ni***	***Zn***	***U***	***Cr***
A	3.673	0.731	0.107	0.281	1.328	1.980	8.673	3.488
B	11.23	12.72	11.79	40.12	11.86	13.11	47.75	10.41
q_e (mol/kg)	0.089	0.078	0.085	0.025	0.084	0.076	0.021	0.096
K_2	34.36	221.3	1301	5726	105.8	86.87	262.8	31.02
Δq (%)	0.167	0.033	0.009	0.004	0.233	0.073	0.096	0.252
r	1.000	1.000	1.000	1.000	1.000	1.000	1.000	1.000
Elovich model								
	Fe	***Cu***	***Co***	***Hg***	***Ni***	***Zn***	***U***	***Cr***
A	0.014	0.012	0.013	0.004	0.013	0.012	0.003	0.015
B	0.015	0.014	0.015	0.004	0.015	0.013	0.004	0.017
b	64.61	73.02	67.67	230.3	68.07	75.34	274.4	58.84
a	0.038	0.034	0.036	0.011	0.036	0.032	0.009	0.041
Δq (%)	16.64	16.78	16.79	16.79	16.63	16.73	16.71	16.67
r	0.964	0.990	0.823	0.842	0.713	0.955	0.970	0.949
Intraparticle diffusion model								
	Fe	***Cu***	***Co***	***Hg***	***Ni***	***Zn***	***U***	***Cr***
A	0.035	0.038	0.034	0.010	0.033	0.030	0.008	0.038
B	0.005	0.005	0.004	0.001	0.004	0.004	0.001	0.005
Id	0.035	0.038	0.034	0.010	0.033	0.030	0.008	0.038
Kp	0.005	0.005	0.004	0.001	0.004	0.004	0.001	0.005
Δq (%)	29.33	29.28	29.27	29.21	29.32	29.29	29.30	29.32
r	0.723	0.721	0.721	0.723	0.725	0.722	0.722	0.722
Film diffusion								
	Fe	***Cu***	***Co***	***Hg***	***Ni***	***Zn***	***U***	***Cr***
A	-1.269	-1.640	-2.690	-2.402	-2.205	-1.428	-1.386	-1.249
B	-0.015	-0.020	-0.024	-0.025	-0.017	-0.017	0.017	-0.015
If	-1.269	-1.639	-2.689	-2.402	-2.205	-1.428	-1.386	-1.249
Kf	0.015	0.021	0.024	0.025	0.017	0.017	0.017	0.015
Δq (%)	57.09	59.29	44.94	50.56	43.25	58.22	58.15	58.09
r	0.562	0.551	0.693	0.636	0.747	0.553	0.553	0.551

4.5.3.3.3 Effect of temperature and thermodynamic parameters on adsorption of metals on zeolite-P. simplicissimum

i) Effect of temperature

The biosorption of metal ions on zeolite-*P.simplicissimum* (active) was studied at temperatures between 25 and 60^{o}C in a single-metal as well as in multi-metal systems. The results are given in Figure 4.75 and 4.76, respectively.

The plots demonstrate that the increase of temperature did not influence the uptake of Cu, Zn and Fe. The biosorption of Ni on zeolite-*P. simplicissimum* (active) was the most affected by the increase of temperature. The adsorption capacity of Ni increases from 30 to 40^{o}C and remains constant up to 60^{o}C. The biosorption capacities of Zn, Co and Hg were slightly affected by the increases of temperature. The uptake of uranium decreases with an increase of temperature. A similar observation was made by Olmez *et al*., (2004) while studying the effect of temperature on the adsorption of uranium on zeolite.

The finding revealed that room temperature was the most suitable for maximum uranium adsorption on zeolite and the distribution coefficient values decreased with the increase of temperature.

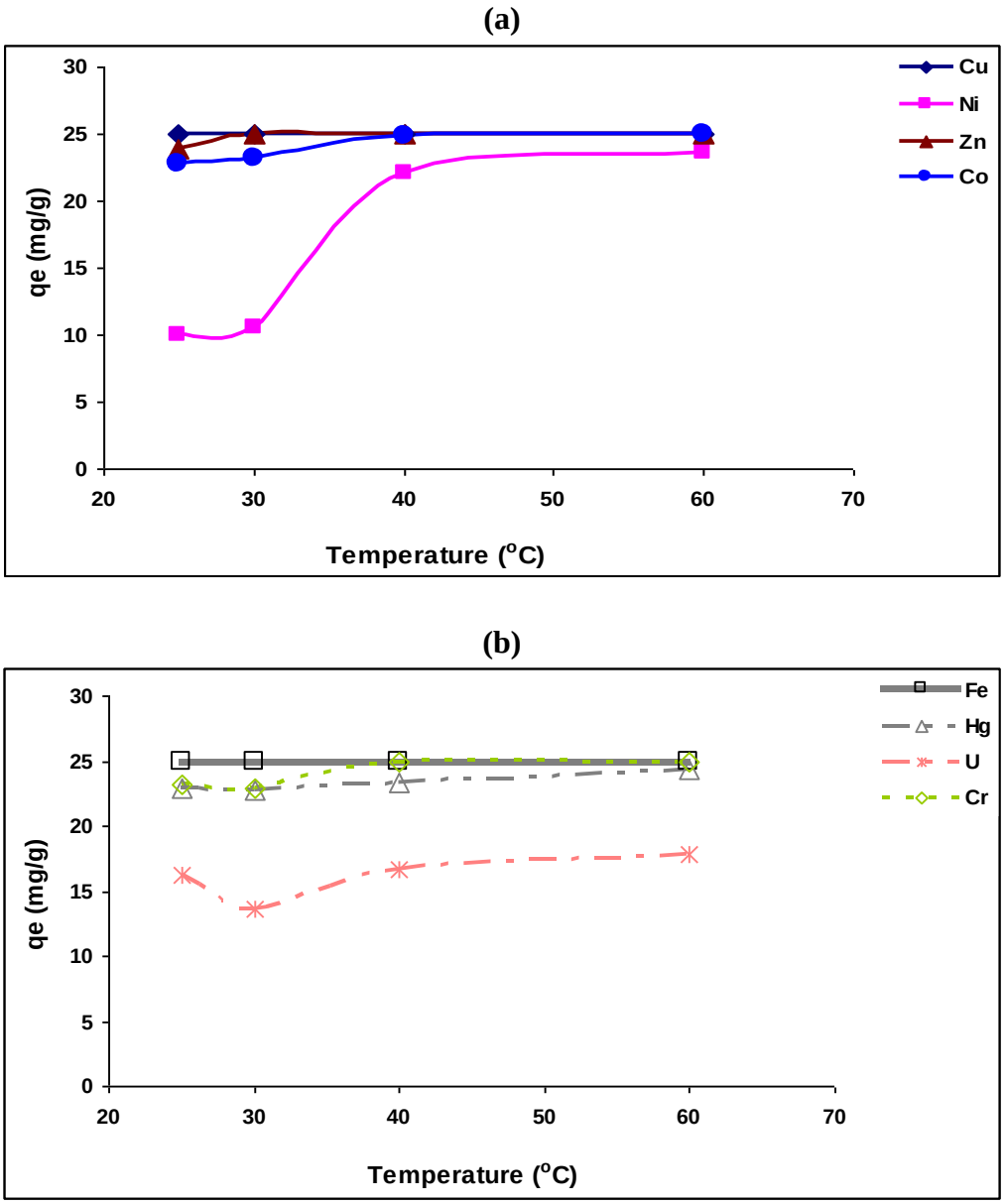

Figure 4.75 Effect of temperature on adsorption of (a) Cu, Ni, Zn and Co (b) Cr, Fe, Hg and U onto zeolite-*P.simplicissimum* (active) in single component solutions (pH = 3, C_i = 100 mg L^{-1}, pH 3, agitation rate = 150 rpm, contact time = 12 h)

In a multi-ion system as shown in Figure 4.76, q_e was constant at each temperature. The increases of temperature had no effect on the biosorption of metal-ions from a multi-metal solution. This trend was also observed for *P. simplicissimum* immobilized on bentonite.

(a)

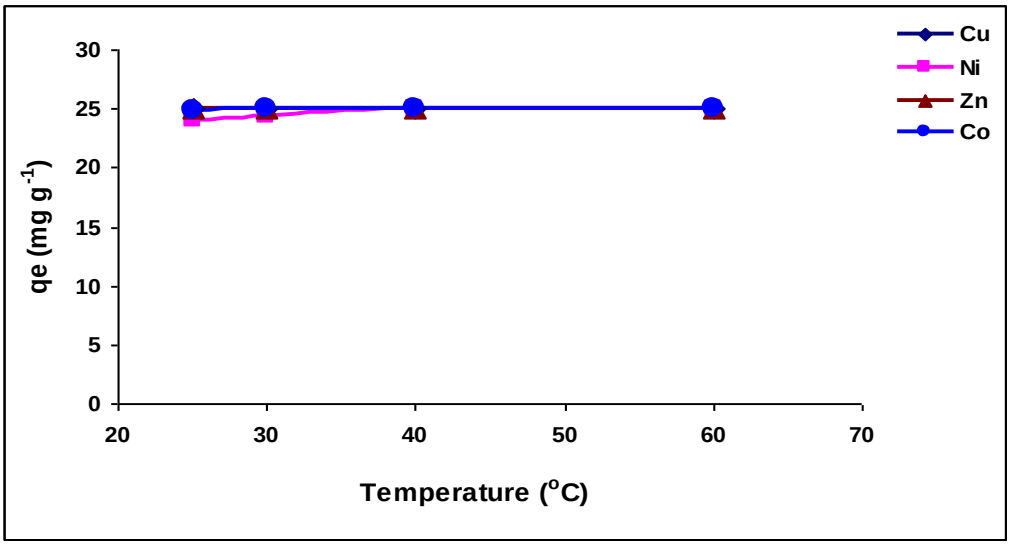

(b)

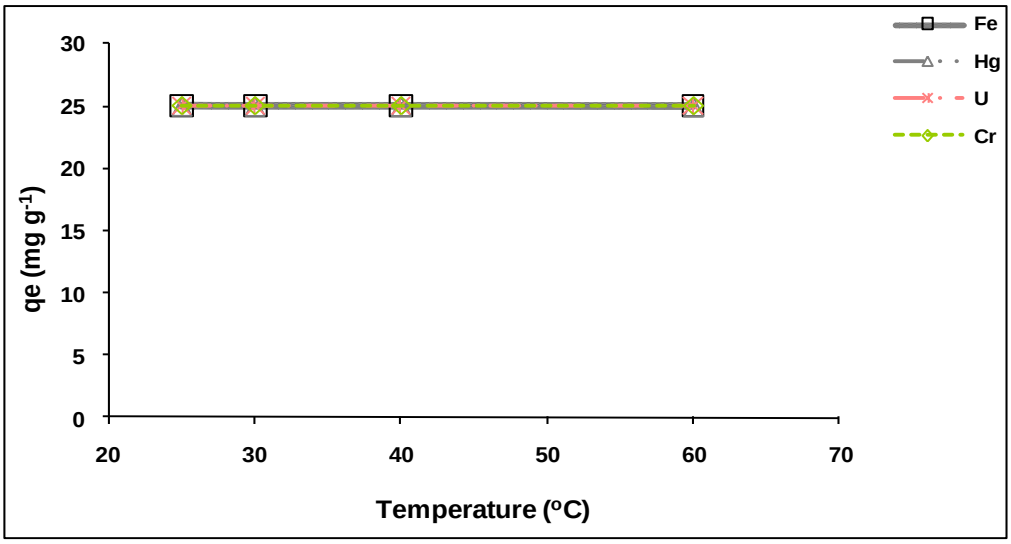

Figure 4.76 Effect of temperature on adsorption of (a) Cu, Cr, Ni, Zn, Co and (b) Cr, Fe, Hg, U onto zeolite-*P.simplicissimum* (active) in multi-ion solutions (pH = 3, C_i = 100 mg L^{-1}, pH 3, agitation rate = 150 rpm, contact time = 12 h)

ii) Thermodynamic parameters

Thermodynamic parameters were determined at different temperatures and the results are tabulated in Tables 4.64 and 4.65 for single-metal as well as multi-metal systems, respectively.

Table 4.64 Thermodynamic parameters of metal ions adsorption on zeolite-*P. simplicissimum* (active) in single-ion system

	Ea	**Δ *H*^{o}**	**Δ *S*^{o}**			**Δ *G*^{o}**	
	kJ mol^{-1}	kJ mol^{-1}	J(K mol)$^{-1}$			kJ mol^{-1}	
				298.15 ^{o}K	**303.15** ^{o}K	**313.15** ^{o}K	**333.15** ^{o}K
Cu	17.49	-104.4	-0.255	-19.11	-19.32	-17.09	-19.31
Ni	-75.83	452.4	1.381	1.009	0.794	-5.202	-7.771
Zn	-111.3	675.7	2.093	-7.549	-19.66	-19.47	-21.73
Co	-120.4	718.9	2.220	-5.827	-6.346	-12.75	-20.65
Fe	109.9	-651.1	-1.904	-26.58	-21.65	-22.25	-16.89
Hg	-27.91	166.6	0.530	-6.000	-5.770	-6.898	-9.981
U	-6.424	38.32	0.122	-1.549	-0.437	-1.834	-2.485
Cr	-80.57	-370.1	-1.061	-6.382	-6.022	-22.79	-16.59

In a single-metal system, the values of activation energy were negative for most of the metals, except for Cu and Fe. The biosorption occurs at low binding sites as explained before. The biosorption of Cu with Ea < 40 kJ mol^{-1} suggested a physisorption process whereas chemisorption was observed for Fe with Ea > 40 kJ mol^{-1}. The process was exothermic for Cu, Fe and Cr, with negative values of enthalpy change. For the rest of the metals, the process was endothermic. Biosorption of uranium decreased with an increase of temperature, although a positive value of enthalpy was obtained, even though the value was very low.

The standard free energy changes were negative for all the metals studied, suggesting a spontaneous process. The positive value of entropy showed the increased randomness at the solid–liquid interface during the adsorption process and also suggested that the process was entropy driven. The negative values of entropy for Fe, Cu and Cr suggested a decrease of degrees of freedom.

The thermodynamic parameters calculated for the biosorption of metals on zeolite-*P. simplicissimum* (active) in a multi-metal system are given in Table 4.65. Unlike in the single-ion system, the biosorption of Hg, Cu and U with values of Ea < 40 kJ mol^{-1} was a physisorption whereas Fe and Cr followed a chemisorption process with Ea > 40 kJ mol^{-1}. Biosorption of Ni, Zn and Co occurred at low energy binding sites with negative values of Ea. The process was exothermic for Cu, Fe, Hg, U and Cr with negative enthalpy changes. A decrease of degrees of freedom was observed with these metals; in fact the entropy changes were negative. In general, the standard free energy was negative, meaning that the process was spontaneous.

Table 4.65 Thermodynamic parameters of metal ions adsorption on zeolite-*P. simplicissimum* (active) in a multi-metal system

	Ea	**Δ *H*^{o}**	**Δ *S*^{o}**			**Δ *G*^{o}**	
	kJ mol^{-1}	kJ mol^{-1}	J(K mol)$^{-1}$			kJ mol^{-1}	
				298.15 ^{o}K	**303.15** ^{o}K	**313.15** ^{o}K	**333.15** ^{o}K
Cu	33.17	-198.4	-0.525	-24.55	-25.17	-24.63	-23.54
Ni	-153.5	916.3	2.831	-7.968	-9.533	-16.14	-26.93
Zn	-41.13	245.5	0.821	-20.66	-22.63	-24.08	-27.91
Co	-121.6	726.1	2.265	-12.73	-17.08	-27.92	-28.49
Fe	97.38	-593.3	-1.718	-29.09	-29.02	-22.85	-20.84
Hg	23.67	-141.3	-0.374	-17.54	-17.31	-16.97	-16.82
U	37.67	-224.7	-0.615	-21.6	-24.26	-20.71	-19.72
Cr	62.07	-370.1	-1.044	-26.37	-23.21	-23.68	-22.19

The rate of metal biosorption at different temperature was calculated and presented in Tables 4.66 and 4.67 for single-metal as well as multi-metal systems, respectively. In single-metal systems, the rate of adsorption increased with the increase of temperature, except for Cu for which a decrease of the adsorption rate with an increase of temperature.

Table 4.66 The reaction rate of the adsorption of metal ions on zeolite-*P. simplicissimum* (active) (in single-metal solutions)

Rx rate (h^{-1})				
	298.15 ^{o}K	**303.15** ^{o}K	**313.15** ^{o}K	**333.15** ^{o}K
Cu	0.643	0.639	0.581	0.547
Ni	0.042	0.046	0.177	0.239
Zn	0.258	0.623	0.649	0.654
Co	0.203	0.261	0.409	0.621
Fe	0.894	0.716	0.712	0.508
Hg	0.209	0.199	0.226	0.302
U	0.087	0.065	0.092	0.103
Cr	0.206	0.221	0.429	0.799

Table 4.67 presents the rate of adsorption of metal-ions on bentonite-*P. simplicissimum* at different temperatures in a multi-metal system.

Table 4.67 The reaction rate of the adsorption of metal ions on zeolite-*P. simplicissimum* (active) (in multi-metal solutions)

Rx rate (h^{-1})				
	298.15 ^{o}K	**303.15** ^{o}K	**313.15** ^{o}K	**333.15** ^{o}K
Cu	0.825	0.832	0.788	0.708
Ni	0.271	0.317	0.516	0.810
Zn	0.694	0.748	0.771	0.839
Co	0.428	0.565	0.894	0.857
Fe	0.978	0.959	0.731	0.627
Hg	0.589	0.572	0.543	0.506
U	0.802	0.726	0.662	0.593
Cr	0.886	0.767	0.758	0.667

The adsorption rate of Cr, U, Cu, Hg and Fe decreased with increases of temperature. Besides, the adsorption rate of Ni, Zn and Co increased with increasing temperature.

4.5.3.4 Sorption studies of metals on Zeolite-P. simplicissimum (inactive or heat-killed) in batch mode

Biosorption studies were also performed on the inactive zeolite-*P.simplicissimum*. As for the previous studies, the effects of pH, initial metal concentration, contact time and temperature were investigated in a single-ion as well as multi-ion systems. The similarities and differences found with the active form of zeolite-*P.simplicissimum* are discussed in the following section.

4.5.3.4.1 Sorption capacities, pH, isotherms of adsorption

i) Effect of pH

The effects of pH on the biosorption of Cu, Co, Cr, Fe, Hg, Ni, Zn and U by zeolite- *P. simplicissimum* (inactive) are presented in Figures 4.77 and 4.78 in single-ion as well as multi-ion systems, respectively. The adsorption capacities were higher in the inactive form of zeolite-*P.simplicissimum*. Further explanations have been given in section 4.5.2.4, since a similar trend was observed for the bentonite-*P. simplicissimum* (inactive). The adsorption capacity was constant for the all regime of pH. The presence of various functional groups

(electron donors) for instance: carboxyl, amino, imidazole, phosphate as seen in the IR spectra could be available for characteristic bonding with cations and such bond formation could be accompanied by displacement of protons depending on the pH.

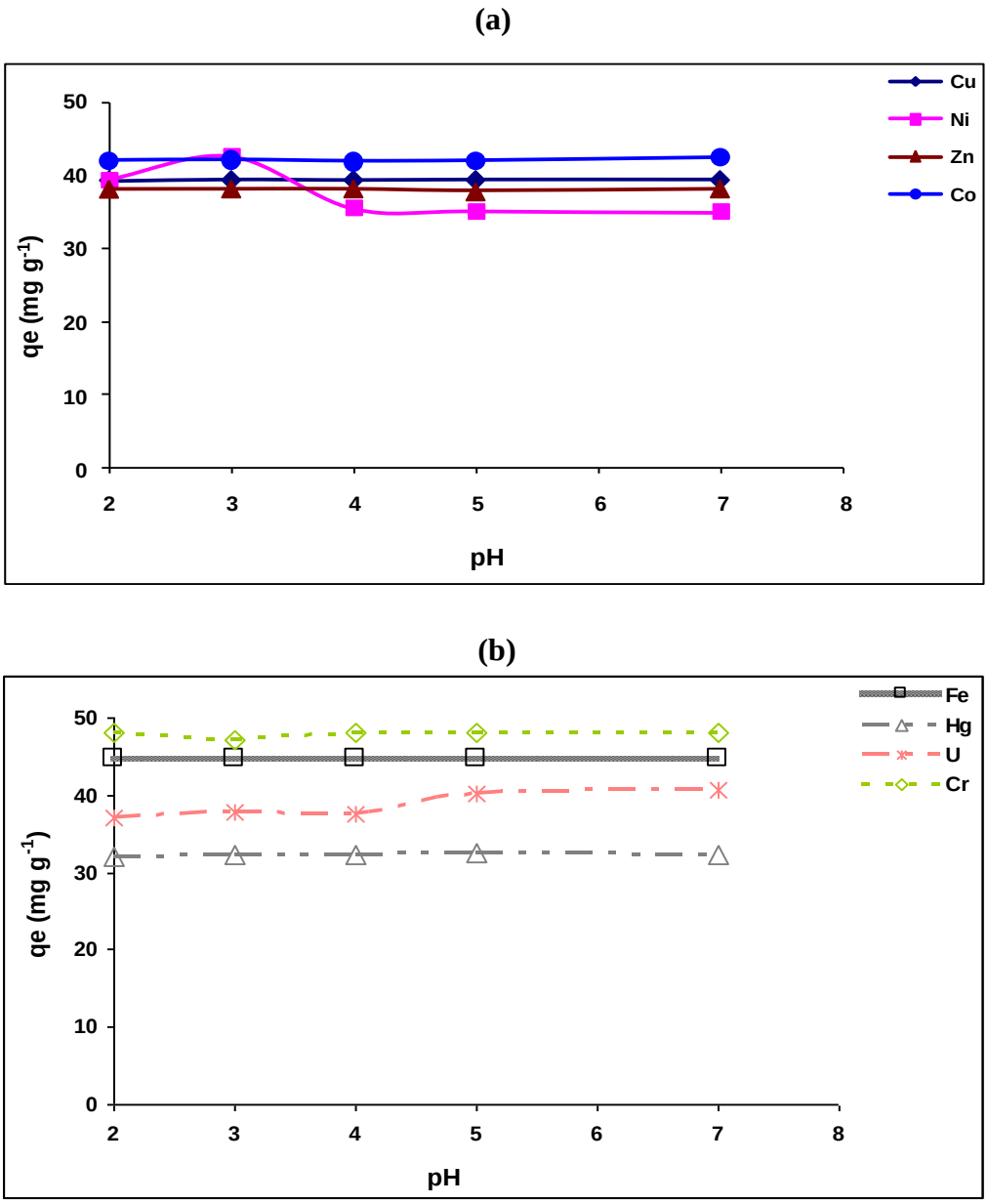

Figure 4.77 Effect of initial pH on adsorption of (a) Cu, Cr, Ni, Zn and Co (b) Cr, Fe, Hg and U onto zeolite-*P. simplicissimum* (inactive) in single component solutions (C_i = 100 mg L^{-1}, Temp = 298.15±1^oK, agitation rate = 150 rpm, agitation time = 12 h)

Metal ions could also be electrostatically bonded to unprotonated carboxyl and sulphate.

The biosorption of Ni presented a unique trend, namely an increase of adsorption capacity

with a maximum adsorption capacity (q_e) reached at pH 3, followed by a decrease at pH 4. This could be due to desorption if Ni forms weak bonds with the functional groups. This assumption needs further experiments to be confirmed. The uptake of U and Hg was lower compared to that for other metals.

Biosorption of metal ions by zeolite-*P. simplicissimum* (inactive) in a multi-ion system is shown in Figure 4.78.

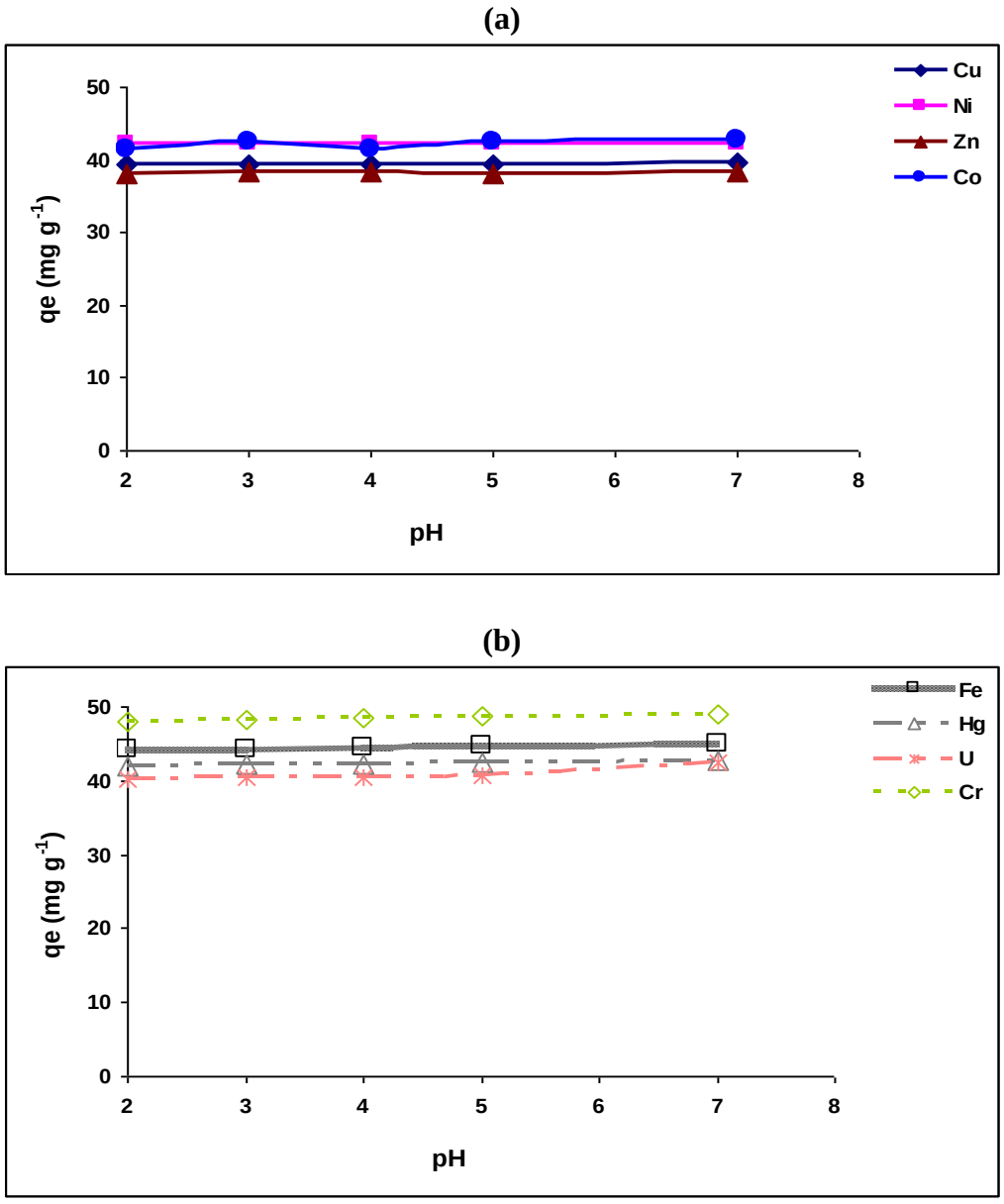

Figure 4.78 Effect of initial pH on adsorption of (a) Cu, Ni, Zn, Co and (b) Cr, Fe, Hg and U onto zeolite-*P. simplicissimum* (inactive) in multi-component solutions (C_i = 100 mg L^{-1}, Temp = 298.15±1^oK, agitation rate = 150 rpm, agitation time = 12 h)

A similar trend was observed with a constant maximum adsorption capacity for all the studied pH regimes and an increase of the uptake of uranium and mercury. The synergistic effect on metal uptake was also observed in this case.

ii) Effect of initial metal concentration

The plots of adsorption capacity versus initial metal ion concentration illustrated in Figure 4.79 show a linear increase of adsorption capacity with an increase of metal concentration. Biosorption of metal ions by zeolite-*P. simplicissimum* (inactive) did not reach the saturation point up to an initial concentration of 500 mg L^{-1}. The same observation was made for the biosorption of metal ions on bentonite-*P.simplicissimum* (inactive). As such, the explanations given in that section are also valid in this case. The saturation point was observed for the biosorption of uranium at a concentration of 400 mg L^{-1}. The amount of functional groups (such as phosphate) responsible for uranium binding should be considered as one of the limiting factors for uranium adsorption since the xenobiotic effect does not exist for the inactive fungi.

(a)

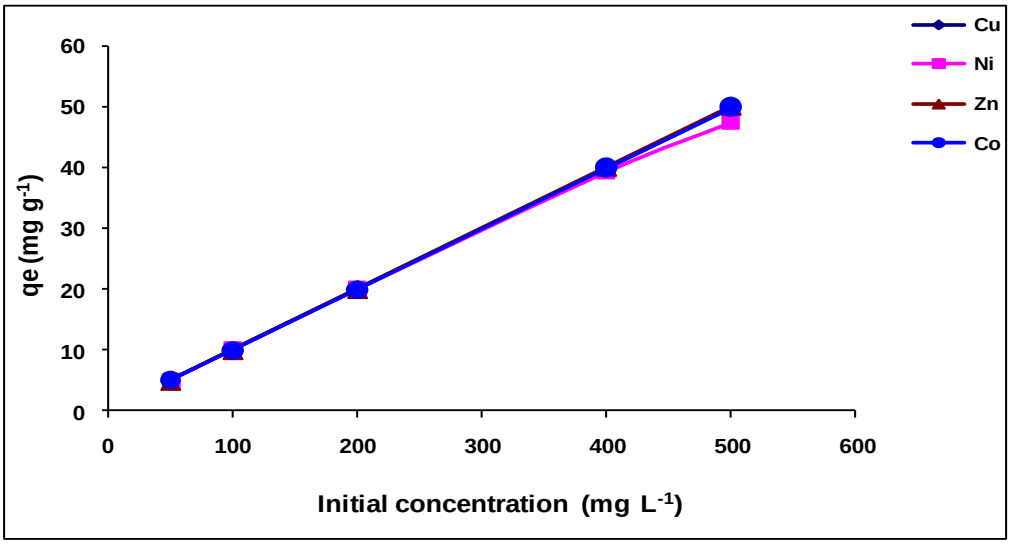

(b)

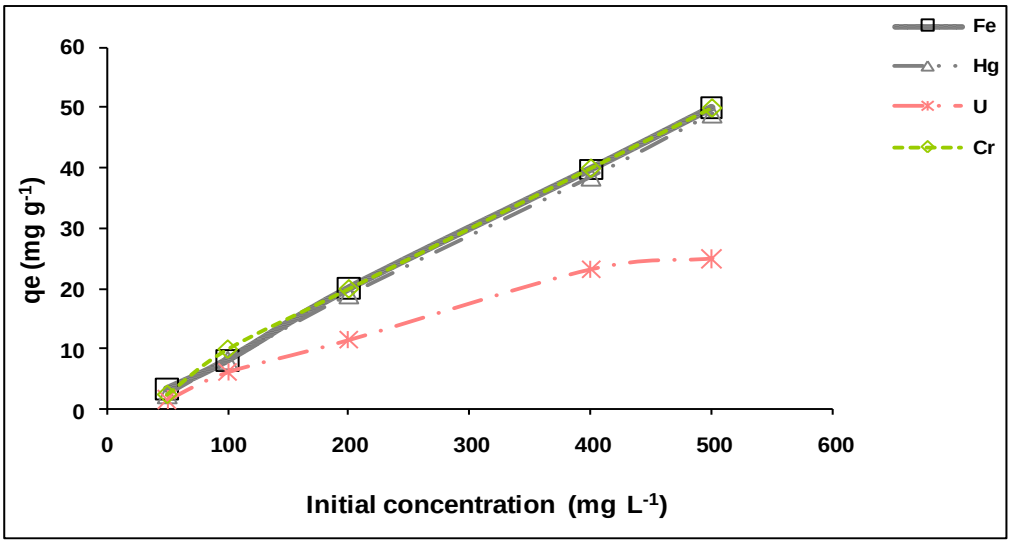

Figure 4.79 Effect of initial concentration on adsorption of (a) Cu, Ni, Zn and Co (b) Cr, Fe, Hg and U onto zeolite-*P.simplicissimum* (inactive) in single-ion solutions (pH = 3, C_i = 100 mg L^{-1}, Temp = 298.15±1^oK, agitation rate = 150 rpm, agitation time = 12 h)

In a multi-metal system, the biosorption of uranium on zeolite-*P. simplicissimum* (inactive) increased as seen in Figure 4.80. A similar trend was seen in the previous studies with the presence of other metals favouring the adsorption of uranium as proven by the results obtained in section 4.5.2.4.

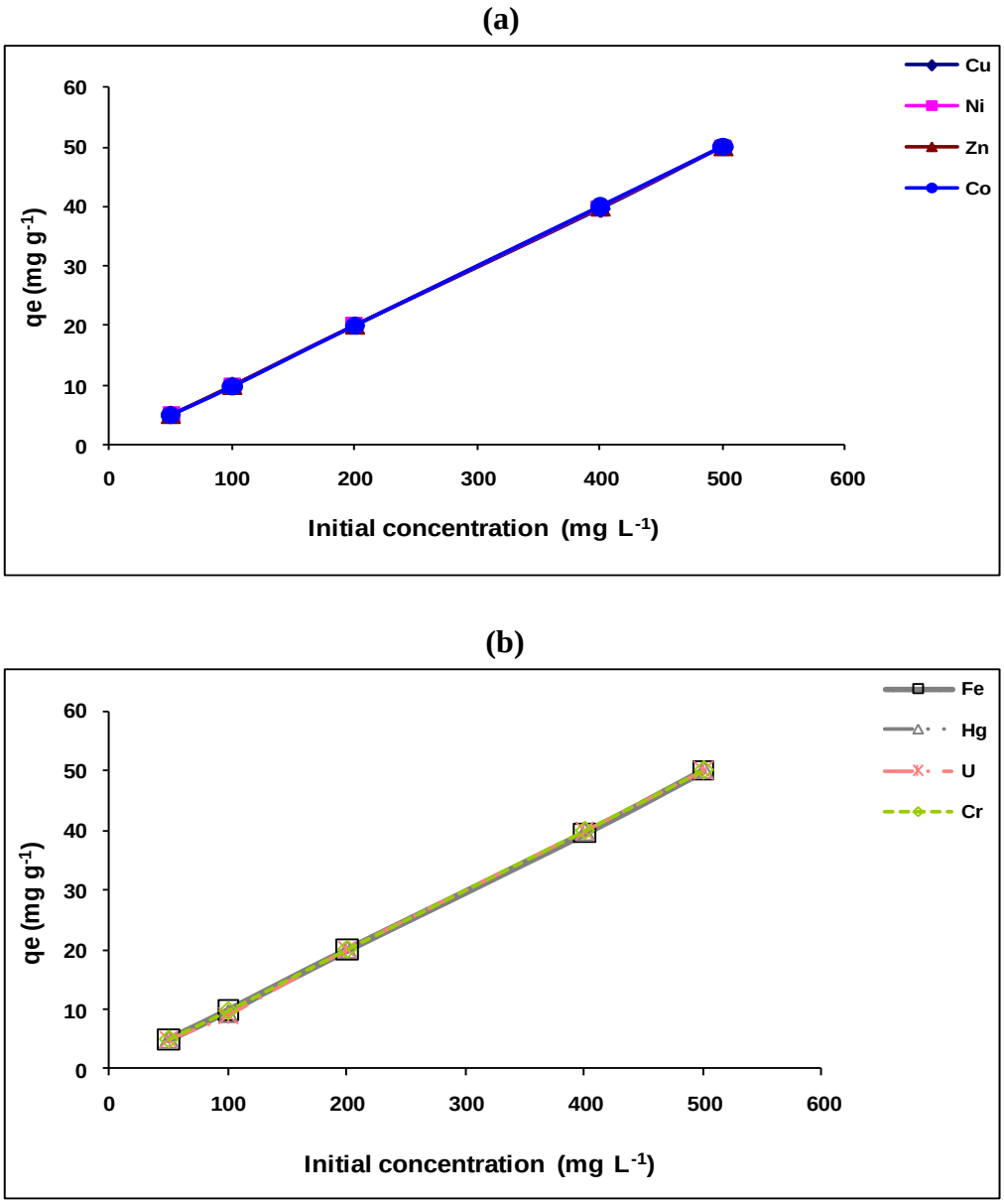

Figure 4.80 Effect of initial concentration on adsorption of (a) Cu, Ni, Zn and Co (b) Cr, Fe, Hg and U onto zeolite-*P. simplicissimum* (inactive) in multi-component solutions (pH = 3, C_i = 100 mg L^{-1}, Temp = 298.15±1 ^{o}K, agitation rate = 150 rpm, agitation time = 12 h)

iii) Isotherms of adsorption of metals on zeolite-P. simplicissimum (inactive)

Biosorption isotherms were determined using four different models: Langmuir, Freundlich, D-R and distribution coefficient. The calculated constants as well as the correlation

coefficient for the single-ion and multi-ion systems are listed in Tables 4.68 and 4.69, respectively.

Table 4.68 Parameters of Langmuir, Freundlich and D-R models for the adsorption of metals on the zeolite-*P. simplicissimum* (inactive) in a single metal system

Langmuir Isotherms	***Fe***	***Cu***	***Co***	***Hg***	***Ni***	***Zn***	***U***	***Cr***
A	0.012	0.007	0.004	0.025	0.002	0.004	0.371	0.005
B	2.259	0.164	0.952	9.254	2.166	0.474	12.61	0.868
b	192.3	215.3	2154	368.7	890.3	1201	33.97	2162
qm (mol/kg)	0.443	6.090	1.051	0.108	0.462	2.108	0.079	1.152
ΔGo (kJ/mol)	-13.03	-13.32	-19.03	-14.65	-16.84	-17.58	-8.739	-24.74
Δq (%)	76.06	75.91	65.93	75.99	14.77	75.91	59.52	75.92
r	0.982	0.613	0.668	0.672	0.989	0.693	0.927	0.656
Freundlich Isotherms	***Fe***	***Cu***	***Co***	***Hg***	***Ni***	***Zn***	***U***	***Cr***
A	0.158	0.062	0.064	0.081	0.124	0.069	0.081	0.078
B	0.233	0.171	0.158	0.327	0.193	0.165	0.502	0.129
K_f	1.439	1.155	1.159	1.204	1.330	1.174	1.202	1.198
n	4.289	5.877	6.314	3.056	5.190	6.044	1.992	7.711
ΔGo (kJ/mol)	-10.63	-14.57	-15.65	-7.577	-12.86	-14.98	-4.938	-19.12
Δq (%)	11.63	11.03	70.21	61.03	71.42	10.43	34.51	10.56
r	0.974	0.956	0.958	0.996	0.867	0.973	0.994	0.978
D-R Isotherms	***Fe***	***Cu***	***Co***	***Hg***	***Ni***	***Zn***	***U***	***Cr***
A	0.273	0.249	0.244	-0.124	0.295	0.275	-0.094	0.309
B	-0.004	-0.002	-0.003	-0.004	-0.003	-0.003	-0.009	-0.002
Xm (mol/kg)	1.314	1.283	1.277	0.883	1.343	1.317	0.910	1.362
Es (kJ/mol)	11.75	14.57	15.42	10.49	13.59	15.13	7.377	18.24
Δq (%)	26.22	32.98	87.44	72.22	52.38	61.88	11.67	52.57
r	0.982	0.959	0.847	0.823	0.889	0.976	0.996	0.975
K_d	***Fe***	***Cu***	***Co***	***Hg***	***Ni***	***Zn***	***U***	***Cr***
A	6.194	5.057	7.018	4.277	7.849	5.868	2.888	7.102
B	3296	98988	8653	3720	6025	1673	1609	1415
ΔGo (kJ/mol)	-15.36	-12.54	-17.39	-10.61	-19.46	-14.55	-7.160	-17.61
Kdo	490.2	157.2	1117	71.99	2564	353.7	17.97	1212
Δq (%)	70.79	35.52	49.68	63.39	26.99	65.2	68.16	81.81
r	0.990	0.648	0.552	0.536	0.960	0.658	0.937	0.698

In general, the Freundlich model better described the biosorption of metal ions studied with r < 0.950, except for Ni. The biosorption of Ni is well described by the Langmuir and the distribution coefficient models. The biosorption of Fe could be described by the Langmuir, D-R and the distribution coefficient as well.

The maximum amount (q_m/mol kg^{-1}) of metal calculated from the Langmuir isotherm decreases in the order: Cu >> Zn > Cr > Co >> Ni > Fe > Hg > U. The magnitude of the exponent *n* gives an indication on the favourability of adsorption. To recap, values of *n* in the

range 2− 10 represent good, 1− 2 moderately difficult, and less than 1 poor adsorption characteristics (Treybal, 1981). For most of the cases, the biosorption was good with $2.992 \leq n \leq 7.711$. In Table 4.68, it can be seen that the Freundlich constant, $K_{f,}$ which represents the adsorption capacity of heavy metals was of the same magnitude for all the metals. All the Es (free energy of adsorption) values from D-R model were between 8 and 16 kJ mol^{-1}, which may correspond to a chemical ion-exchange mechanism, except for Cr with Es = 18.24 kJ mol^{-1}. The values of q_{max} obtained from the Langmuir isotherm were quite different to the X_{max} derived from the D-R, except for Co and Cr. This may be attributed to the different assumptions considered in the formulation of the isotherms. The differences were also reported in other studies (Kumar *et al*., 2009; Tan *et al*., 2007; Fan *et al*., 2008). The distribution coefficient values were higher for Ni, Cr and Co and the sequence decreased in the order: Ni > Cr > Co >> Fe > Zn > Cu > Hg > U.

Table 4.69 presents the isothermic constants as well as the correlation coefficients for metal ions adsorbed on zeolite-*P. simplicissimum* (inactive) in a multi-metal system. Based on the correlation coefficient (r > 0.950), the Freundlich isotherm fits well the experimental data for the metals studied except for uranium, suggesting that the heterogeneity of the surface. None of the isotherms listed in Table 4.69 described the uranium biosorption. The Langmuir isotherm gave a good fit for the adsorption of Zn and Cr with r > 0.990. The biosorption of these metal ions could occur in monolayer coverage on finite sites. The fit for the D-R model was also good for the metals studied except for Hg and U. According to q_{max} from the Langmuir model, biosorption on zeolite-*P. simplicissimum* in a multi-metal system is produced following the sequence: Cu > Hg > Fe > Ni > Co > Cr > Zn > U. The numerical values of sorption energy (Es) were in the range 13 to 16 kJ mol^{-1} for Fe, Hg, Ni and U suggesting a chemical adsorption. On the other hand, Es values were in the range 17 to 20 kJ mol^{-1} for Cu, Co, Zn and Cr. The adsorption process was good according to the *n* values (4 – 8) from the Freundlich model. K_{do} values were in the following order: Cr > Zn > Co > > Fe > Ni > U >> Cu > Hg.

Table 4.69 Parameters of Langmuir, Freundlich and D-R models for the adsorption of metals on the zeolite-*P. simplicissimum* (inactive) in a multi-metal system

Langmuir Isotherms	***Fe***	***Cu***	***Co***	***Hg***	***Ni***	***Zn***	***U***	***Cr***
A	0.008	0.002	0.012	0.007	0.001	0.002	0.006	0.002
B	0.757	0.406	1.663	0.439	0.792	2.617	4.071	2.118
b	945.1	3188	1465	633.2	906.8	1657	6146	1311
qm (mol/kg)	1.320	2461	0.601	2.275	1.263	0.382	0.246	0.472
ΔGo (kJ/mol)	-16.98	-19.99	-29.48	-15.99	-16.88	-24.11	-21.62	-23.50
Δq (%)	75.91	75.93	75.94	75.92	75.92	76.19	75.93	76.23
r	0.533	0.648	0.468	0.776	0.825	0.995	0.767	0.993
Freundlich Isotherms	***Fe***	***Cu***	***Co***	***Hg***	***Ni***	***Zn***	***U***	***Cr***
A	0.082	0.039	0.062	0.043	0.079	0.152	0.046	0.163
B	0.167	0.143	0.123	0.234	0.171	0.162	0.244	0.148
K_f	1.209	1.093	1.155	1.104	1.199	1.420	1.113	1.456
n	5.974	6.975	8.114	4.275	5.845	6.169	4.104	6.775
ΔGo (kJ/mol)	-14.81	-17.29	-20.11	-10.59	-14.49	-15.29	-10.17	-16.79
Δq (%)	9.449	18.34	10.28	23.11	61.54	64.01	104.1	62.59
r	0.959	0.992	0.988	0.983	0.951	0.969	0.830	0.954
D-R Isotherms	***Fe***	***Cu***	***Co***	***Hg***	***Ni***	***Zn***	***U***	***Cr***
A	0.314	0.164	0.248	0.172	0.302	0.272	0.169	0.275
B	-0.003	-0.002	-0.002	-0.003	0.002	-0.017	-0.003	-0.002
Xm (mol/kg)	1.369	1.179	1.282	1.188	1.353	1.313	1.184	1.316
Es (kJ/mol)	14.47	17.14	19.74	13.26	14.32	17.25	13.12	18.34
Δq (%)	35.85	10.18	80.23	48.98	73.94	29.85	82.79	30.41
r	0.961	0.963	0.984	0.940	0.952	0.977	0.836	0.964
K_d	***Fe***	***Cu***	***Co***	***Hg***	***Ni***	***Zn***	***U***	***Cr***
A	5.904	4.133	7.087	3.867	5.588	10.41	5.469	10.87
B	5415	1130	7921	5139	5844	1461	40190	2811
ΔGo (kJ/mol)	-14.63	-10.25	-17.56	-9.586	-13.85	-25.81	-13.56	-26.95
Kdo	366.5	62.41	1196	47.81	267.4	3313	237.3	5257
Δq (%)	81.51	63.55	59.14	42.17	86.03	80.52	77.15	77.47
r	0.448	0.732	0.852	0.772	0.882	0.947	0.608	0.946

4.5.3.4.2 Effect of contact time and kinetics of adsorption of metals on zeolite-P. simplicissimum

i) Effect of contact time

The effect of contact time was studied using a constant concentration of metal ions solution at room temperature. The sorption of metal ions onto zeolite-*P.simplicissimum* (inactive) in a single-ion and multi-ion system as a function of time in the range 0–180 min was studied. The plots of adsorption capacity versus contact time for a single-ion as well as multi-ion

systems are presented in Figure 4.81 and 4.82, respectively. As seen in the previous studies, the biosorption capacity increased with an increase of contact time and a maximum amount of metal ions was adsorbed in the first 30 minutes. This step was fast and the equilibrium was reached just after no more metal ions were adsorbed.

(a)

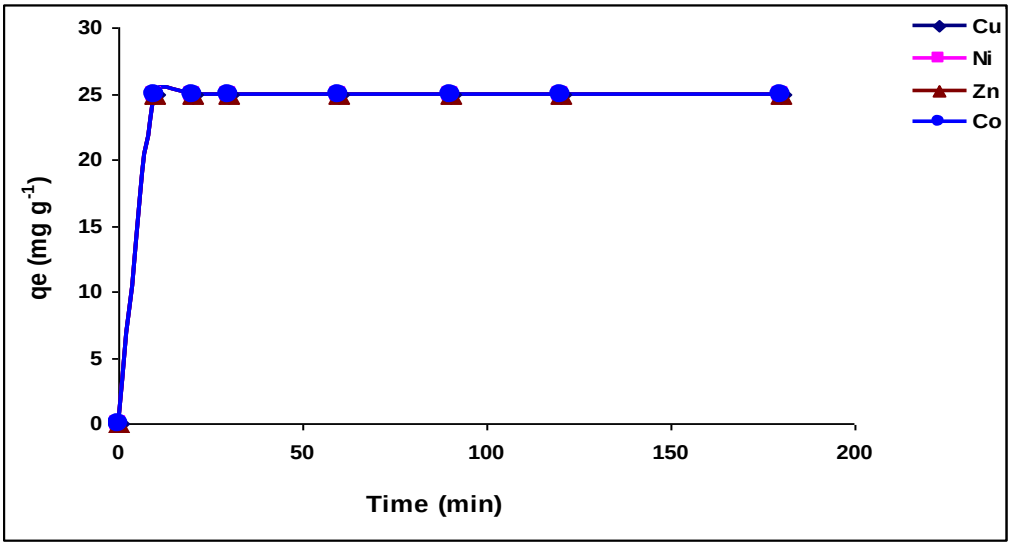

(b)

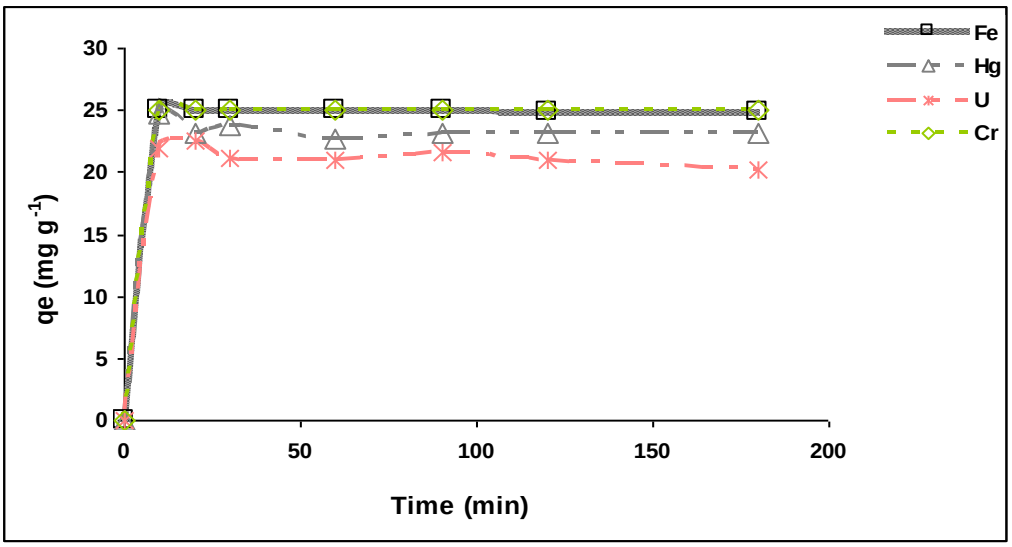

Figure 4.81 Effect of contact time on the adsorption of (a) Cu, Ni, Zn and Co (b) Cr, Fe, Hg and U in single component solutions onto zeolite-*P. simplicissimum* (pH 3, Temp = 298.15±1^{o}K, agitation rate = 150 rpm, agitation time = 12 h)

In Figure 4.82, a similar trend was observed for the biosorption of metal ions from multi-ion solutions. The metal uptake increased with increasing contact time and the maximum adsorption capacity was reached after 30 minutes. An increase in adsorption capacity of U and Hg was observed, due probably to the synergistic effect.

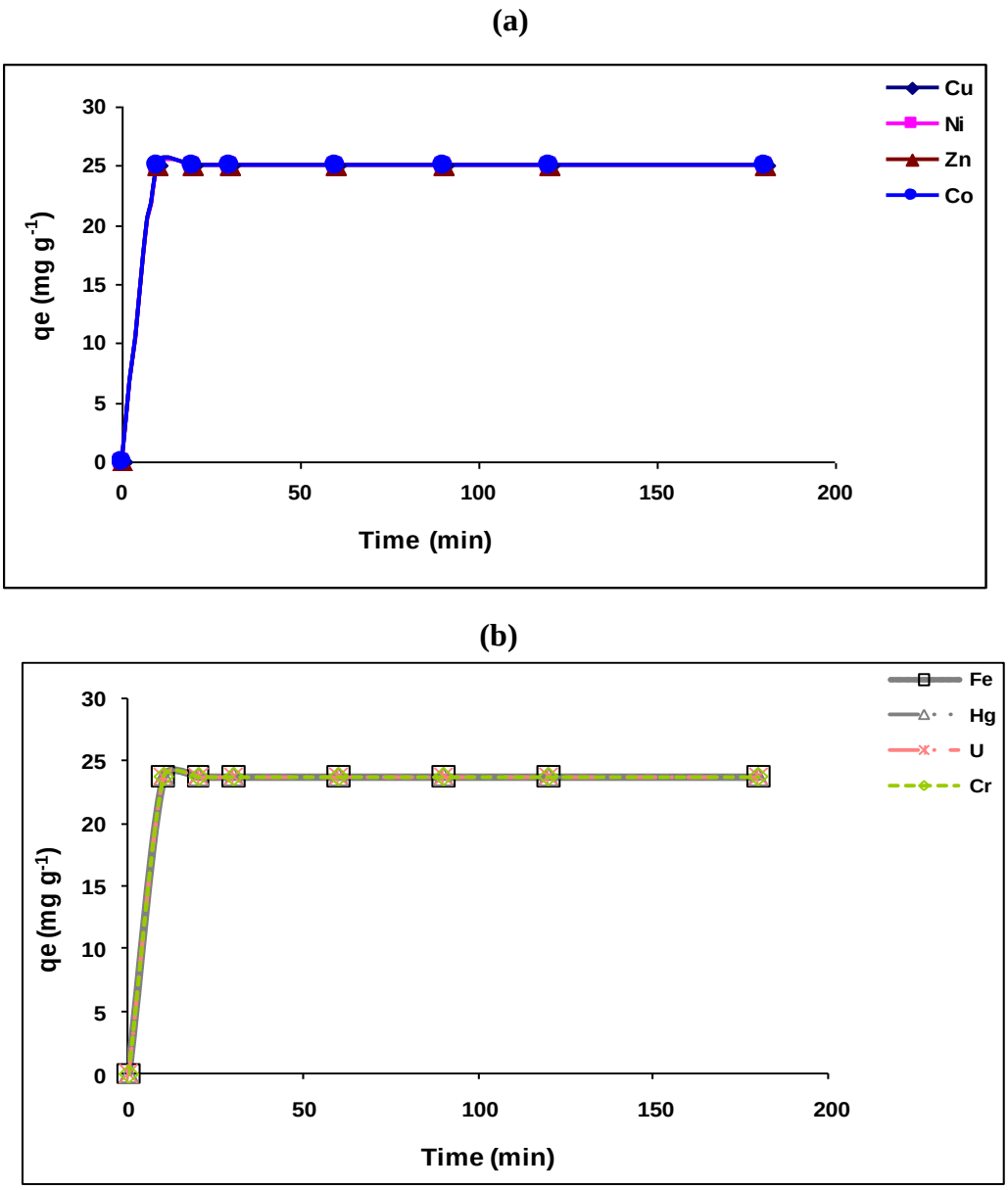

Figure 4.82 Effect of contact time on the adsorption of (a) Cu, Ni, Zn, Co (b) Cr, Fe, Hg and U in multi-component solutions onto zeolite-*P. simplicissimum* (pH = 3, Temp = 298.15±1^{o}K, agitation rate = 150 rpm, agitation time = 12 h)

ii) Kinetic modelling of metal ions adsorption on zeolite-P. simplicissimum (inactive)

The experimental data have been analysed using these kinetic models: the pseudo1st and 2nd-order, Elovich, intraparticle and film diffusion models. The rate constants, different parameters and the correlation coefficients calculated for the single-ion and multi-ion systems are presented in Tables 4.70 and 4.71, respectively.

Table 4.70 Kinetic constants for the adsorption of metal ions on zeolite-*P. simplicissimum* (inactive) in a single-metal system

Pseudo-first order								
	Fe	***Cu***	***Co***	***Hg***	***Ni***	***Zn***	***U***	***Cr***
A	-1.964	-2.870	-3.994	-1.845	-3.515	-4.071	-1.997	-2.382
B	-0.045	-0.026	0.021	-0.007	-0.049	-0.040	-0.007	-0.031
q_e (mol/kg)	0.011	0.001	0.001	0.014	0.002	0.002	0.010	0.004
K_1	0.104	0.060	-0.047	0.015	0.114	0.093	0.017	0.071
Δq (%)	87.43	91.92	96.26	75.05	92.43	92.54	44.73	90.87
r	0.924	0.631	0.630	0.805	0.714	0.614	0.959	0.767
Pseudo – second order								
	Fe	***Cu***	***Co***	***Hg***	***Ni***	***Zn***	***U***	***Cr***
A	0.704	0.185	0.072	201.9	0.032	0.004	2609	0.337
B	5.592	6.376	5.899	22.77	5.869	6.539	40.88	5.201
q_e (mol/kg)	0.179	0.157	0.169	0.044	0.171	0.153	0.024	0.192
K_2	44.44	219.7	485.3	2.568	1075	10493	0.641	80.28
Δq (%)	0.177	0.037	0.019	11.01	0.048	0.008	36.74	0.053
r	1.000	1.000	1.000	0.973	1.000	1.000	0.535	1.000
Elovich model								
	Fe	***Cu***	***Co***	***Hg***	***Ni***	***Zn***	***U***	***Cr***
A	0.032	0.028	0.031	0.002	0.031	0.028	-0.003	0.035
B	0.040	0.035	0.038	0.009	0.038	0.034	0.004	0.043
b	25.18	28.69	26.54	113.1	26.39	29.41	275.9	23.41
a	0.088	0.079	0.085	0.011	0.086	0.077	0.002	0.096
Δq (%)	17.54	17.79	17.83	11.59	17.82	17.85	88.67	17.69
r	0.979	0.975	0.958	0.854	0.720	0.992	0.946	0.979
Intraparticle diffusion model								
	Fe	***Cu***	***Co***	***Hg***	***Ni***	***Zn***	***U***	***Cr***
A	0.067	0.060	0.065	0.009	0.065	0.058	-0.001	0.073
B	0.016	0.014	0.015	0.003	0.015	0.014	0.002	0.017
Id	0.067	0.060	0.065	0.009	0.065	0.058	-0.001	0.073
Kp	0.016	0.014	0.015	0.003	0.015	0.014	0.002	0.017
Δq (%)	29.83	29.76	29.75	33.92	29.75	29.74	66.56	18.28
r	0.744	0.738	0.737	0.863	0.724	0.737	0.956	0.740
Film diffusion								
	Fe	***Cu***	***Co***	***Hg***	***Ni***	***Zn***	***U***	***Cr***
A	-3.913	-1.492	2.940	0.390	-3.427	-2.225	0.041	1.987
B	-0.023	-0.073	-0.142	-0.020	-0.091	-0.119	-0.006	-0.106
If	-3.913	-1.492	2.940	0.391	-3.426	-2.225	0.041	1.987
Kf	0.022	0.073	0.142	0.021	0.091	0.119	0.006	0.106
Δq (%)	38.69	86.48	85.65	133.5	45.48	153.3	180.4	65.41
r	0.924	0.631	0.631	0.692	0.714	0.613	0.892	0.733

The pseudo 2nd-order fits better the adsorption kinetics of metal ions on zeolite-*P. simplicissimum* with r ~ 1 for the metals studied, except for uranium. The biosorption kinetics of uranium followed the pseudo 1st order as well as the intraparticle diffusion models. The experimental data for Fe, Cu, Co, Zn and Cr fitted well the Elovich kinetic model with r > 0.950. The calculated rate constants k_2 were higher than k_1.

The results presented in Table 4.71 for the biosorption of metal ions from a multi-ion solution show that the pseudo 2nd-order fits better the kinetics of adsorption for all the metals studied with r = 1. The kinetics of adsorption could as well be described by the Elovich model except for Ni and U.

Table 4.71 Kinetic constants for the adsorption of metal ions on zeolite-*P. simplicissimum* (inactive) in a multi-ion system

Pseudo-first order								
	Fe	***Cu***	***Co***	***Hg***	***Ni***	***Zn***	***U***	***Cr***
A	-5.425	-3.379	-5.240	-3.313	-2.568	-3.468	-3.603	-5.284
B	0.026	-0.043	0.026	-0.025	-0.051	-0.037	-0.029	0.055
q_e (mol/kg)	0.001	0.001	0.001	0.001	0.003	0.001	0.001	0.002
K_1	-0.059	0.100	-0.059	0.057	0.118	0.085	0.068	-0.126
Δq (%)	93.05	92.36	93.37	91.84	91.22	92.40	92.11	88.37
r	0.643	0.725	0.624	0.638	0.864	0.663	0.657	0.824
Pseudo – second order								
	Fe	***Cu***	***Co***	***Hg***	***Ni***	***Zn***	***U***	***Cr***
A	0.002	0.022	0.003	0.903	0.155	0.024	0.517	0.001
B	5.585	6.356	5.893	20.11	5.869	6.540	23.81	5.199
q_e (mol/kg)	0.179	0.157	0.169	0.049	0.170	0.153	0.042	0.192
K_2	18235	1825	10834	447.8	221.6	1802	1096	20727
Δq (%)	0.003	0.005	0.008	0.039	0.159	0.003	0.056	0.004
r	1.000	1.000	1.000	1.000	1.000	1.000	1.000	1.000
Elovich model								
	Fe	***Cu***	***Co***	***Hg***	***Ni***	***Zn***	***U***	***Cr***
A	0.033	0.029	0.031	0.009	0.031	0.028	0.008	0.035
B	0.040	0.035	0.038	0.011	0.038	0.034	0.009	0.043
b	25.12	28.59	26.51	90.51	26.39	29.42	107.1	23.38
a	0.090	0.079	0.085	0.025	0.085	0.077	0.021	0.097
Δq (%)	17.85	17.85	17.85	17.60	17.74	17.85	17.79	17.85
r	0.966	0.972	0.966	0.954	0.781	0.991	0.842	0.962
Intraparticle diffusion model								
	Fe	***Cu***	***Co***	***Hg***	***Ni***	***Zn***	***U***	***Cr***
A	0.068	0.060	0.065	0.019	0.064	0.058	0.016	0.073
B	0.016	0.014	0.015	0.004	0.015	0.014	0.004	0.017
Id	0.068	0.060	0.065	0.019	0.064	0.058	0.016	0.073
Kp	0.016	0.014	0.015	0.004	0.015	0.014	0.004	0.017
Δq (%)	29.64	29.74	29.74	29.77	29.77	29.74	29.76	18.35
r	0.717	0.737	0.735	0.739	0.740	0.737	0.738	0.735
Film diffusion								
	Fe	***Cu***	***Co***	***Hg***	***Ni***	***Zn***	***U***	***Cr***
A	4.360	-2.920	4.217	2.266	-4.186	-2.253	2.441	6.905
B	-0.213	-0.086	-0.203	-0.114	-0.046	-0.094	-0.127	-0.225
If	4.359	-2.920	4.217	2.266	-4.186	-2.253	2.441	6.901
Kf	0.213	0.086	0.203	0.114	0.046	0.094	0.127	0.225
Δq (%)	98.52	49.40	85.21	65.23	39.64	77.82	85.63	95.31
r	0.643	0.725	0.624	0.676	0.864	0.663	0.709	0.824

4.5.3.4.3 Effect of temperature and thermodynamic parameters

i) Effect of temperature

The effects of temperature on the biosorption of metals on zeolite-*P. simplicissimum* (inactive) for single-ion as well as multi-ion systems are presented in Figures 4.83 and 4.84, respectively.

(a)

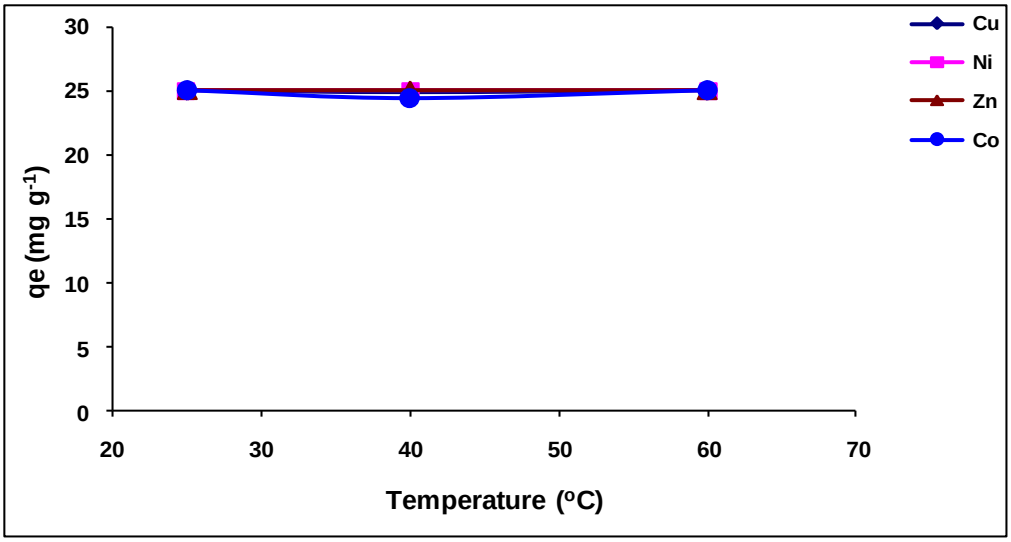

(b)

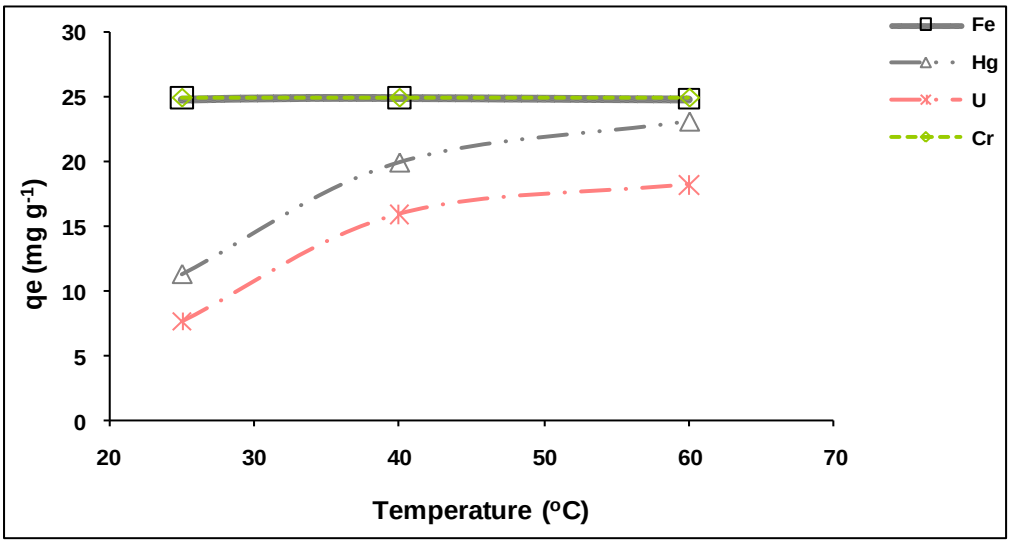

Figure 4.83 Effect of temperature on the adsorption of (a) Cu, Ni, Zn and Co (b) Cr, Fe, Hg and U zeolite-*P.simplicissimum* in single component solutions (pH = 3, C_i = 100 mg L^{-1}, Temp = 298.15±1°K, agitation rate = 150 rpm).

The plots of adsorption capacity versus temperature in Figure 4.83 showed that the biosorption of Cu, Ni, Zn, Co, Fe and Cr was not affected by temperature. The uptake of Hg and U increased with increasing temperature.

The results in Figure 4.84 for the biosorption of metal ions in a multi-ion system show that the maximum adsorption capacity was constant with increasing temperature for all the metals studied.

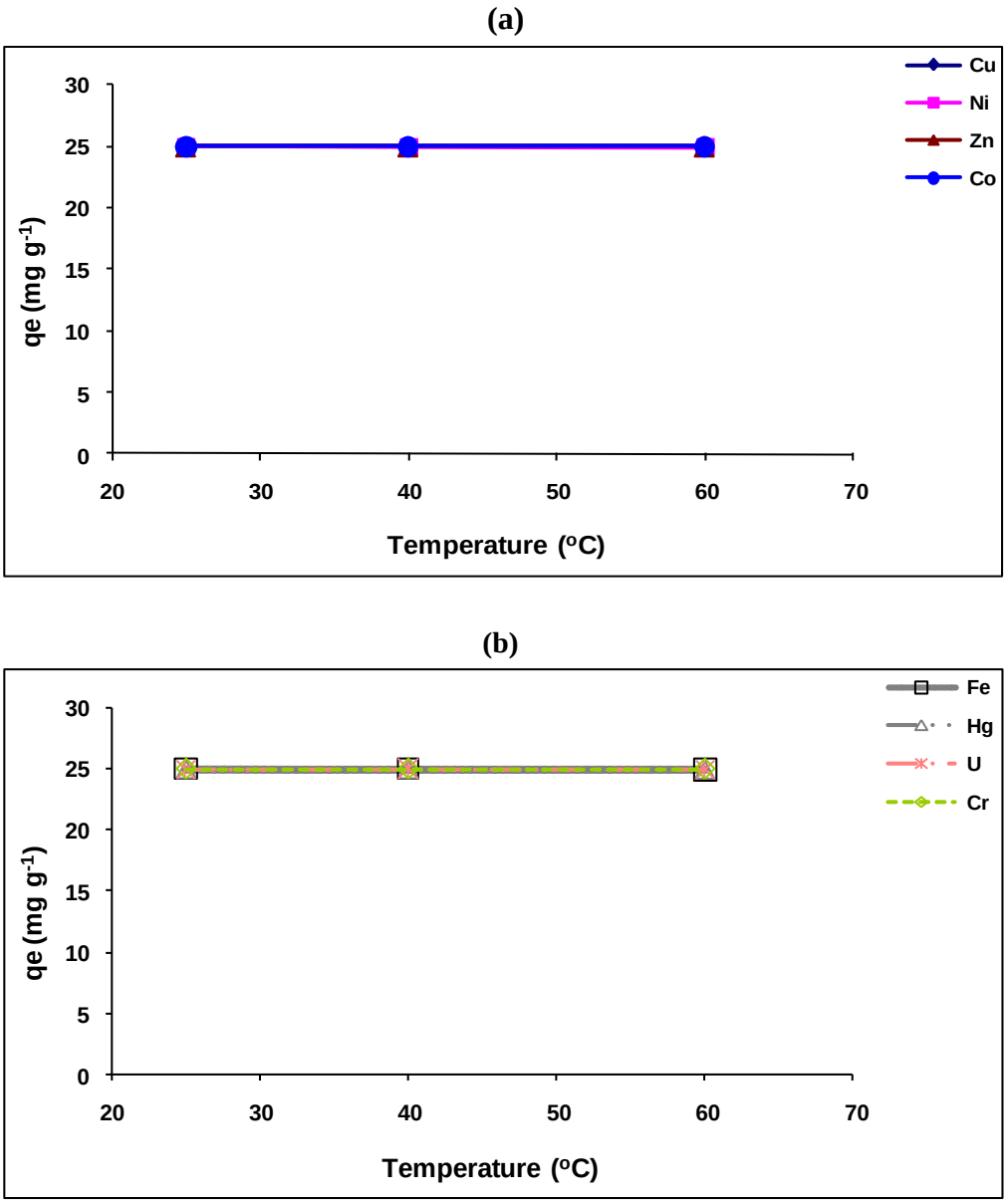

Figure 4.84 Effect of temperature on the adsorption of (a) Cu, Ni, Zn and Co (b) Cr, Fe, Hg and U onto zeolite-*P.simplicissimum* in multi- component solutions (pH = 3, C_i = 100 mg L^{-1}, Temp = 298.15±1°K, agitation rate = 150 rpm)

ii) Thermodynamic parameters

Tables 4.72 and 4.73 present the thermodynamic parameters , i.e. activation energy Ea, enthalpy (heat of adsorption) ΔH^o, entropy change ΔS^o and the free energy ΔG^o for the biosorption of Cu, Co, Cr, Hg, Fe, Ni, Zn and U in single-ion and multi-ion systems.

Table 4.72 Thermodynamic parameters of metal ions adsorption on zeolite-*P.simplicissimum* (inactive) in single-ion systems

	Ea	**Δ *H°***	**Δ *S°***	**Δ *G°***			
	kJ mol^{-1}	kJ mol^{-1}	J(K $mol)^{-1}$	kJ mol^{-1}			
				298.15 ^{o}K	**303.15** ^{o}K	**313.15** ^{o}K	**333.15** ^{o}K
Cu	-1.338	-7.986	0.045	-20.04	-18.35	-14.37	-23.08
Ni	-64.18	118.2	0.406	-16.86	-16.54	-16.30	-16.97
Zn	3.637	72.56	0.279	-19.02	-20.45	-21.22	-20.34
Co	82.64	61.80	0.249	-19.51	-15.46	-9.81	-21.11
Fe	10.35	493.2	1.524	-21.28	-21.95	-22.31	-14.65
Hg	-42.62	-383.0	-1.129	0.460	-1.256	-3.593	-7.007
U	12.16	-254.4	-0.755	1.983	-1.258	-1.464	-2.735
Cr	19.80	21.71	0.152	-25.75	-26.55	-27.29	-29.04

The negative activation energy obtained for Cu, Ni and Hg indicates that the adsorption occurs in binding sites with low energy. Biosorption of Zn, Fe, U and Cr occur though physisorption with activation energy values ranging from 3 to 20 kJ mol^{-1}. E_a for Co was greater than 40 kJ mol^{-1}, showing a chemisorption process.

The values of ΔH^o were found to be negative for Cu, Hg and U, implying the exothermic nature of the process in contrast to the endothermic process for the rest of the metals for which positive enthalpy changes were observed. The positive value of ΔS^o for most of the cases shows the increasing randomness at the solid-liquid interface during the biosorption, except for Hg and U with negative values of entropy changes indicating the decrease in the degrees of freedom. The positive value of entropy also suggested that the process was entropy-driven and not enthalpy-driven. The negative adsorption standard free energy changes (ΔG^o) at all temperatures indicated that the adsorption reactions were generally spontaneous processes.

The thermodynamic parameters obtained for the adsorption of heavy metals on zeolite-*P. simplicissimum* in a multi-ion system are listed in Table 4.73.

Table 4.73 Thermodynamic parameters of metal ions adsorption on zeolite-*P.simplicissimum* (inactive) in a multi-ion system

	Ea	**Δ *H*^{o}**	**Δ *S*^{o}**	**Δ *G*^{o}**			
	kJ mol^{-1}	kJ mol^{-1}	J(K mol)$^{-1}$	kJ mol^{-1}			
				298.15 ^{o}K	**303.15** ^{o}K	**313.15** ^{o}K	**333.15** ^{o}K
Cu	44.59	168.5	0.584	-25.56	-26.02	-26.95	-27.93
Ni	49.07	984.5	3.006	-31.76	-22.54	-17.18	-16.98
Zn	56.04	401.1	1.278	-28.41	-29.04	-29.62	-29.97
Co	86.25	138.1	0.506	-29.11	-28.65	-27.49	-20.59
Fe	125.4	669.5	2.079	-31.76	-31.56	-31.31	-23.18
Hg	-35.19	164.8	0.546	-17.91	-18.23	-18.49	-19.25
U	86.50	279.1	0.903	-23.69	-24.12	-26.64	-27.63
Cr	129.9	432.1	1.369	-28.41	-28.95	-29.01	-29.72

It is well known that these parameters can evaluate the orientation and feasibility of the physicochemical adsorptive reaction (Li *et al*., 2005). The activation energy values were positive in general, except for Hg with negative activation energy. In most cases, the biosorption occurs though chemisorption with an E_a > 40 kJ mol^{-1}. The positive values of enthalpy changes (ΔH^o) suggest an endothermic adsorption of metals on zeolite-*P. simplicissimum* in a multi-ion system. One possible explanation could be the fact that the metal ions studied are well solvated in water. In order for these ions to adsorb, they are to some extent denuded of their hydration sheath. This dehydration process of ions requires energy (i.e. Ni has a dehydration energy of 2106 kJ mol^{-1}). The implicit assumption here is that after adsorption the environment of the metal ions is less aqueous than it was in the solution state.

In Table 4.73, the negative values of standard free energy changes (ΔG^o) confirm the feasibility of the process and the spontaneous nature of sorption. The positive value of entropy showed the increased randomness at the solid-liquid interface during the adsorption process, and also reflects the affinity of adsorbent for the heavy metals studied. The decrease of Gibbs free energy ($\Delta G\circ$) with increasing temperature for Co and Ni indicated higher adsorption at higher temperature.

The rate of adsorption calculated for the biosorption of metal ions from single-ion solutions are given in Table 4.74. The rate of adsorption decreased with increasing temperature, except for U and Hg.

Table 4.74 Rate of adsorption in single-metal systems at different temperatures

Rx rate (h^{-1})				
	298.15 ^{o}K	**303.15** ^{o}K	**313.15** ^{o}K	**333.15** ^{o}K
Cu	0.690	0.652	0.465	0.460
Ni	0.580	0.558	0.522	0.511
Zn	0.655	0.640	0.629	0.612
Co	0.672	0.635	0.366	0.335
Fe	0.733	0.721	0.714	0.441
Hg	0.050	0.115	0.134	0.217
U	0.030	0.058	0.084	0.109
Cr	0.886	0.880	0.874	0.872

As observed in the previous study, the rate of adsorption (Table 4.75) decreased with an increase in temperature for all the metal ions studied.

Table 4.75 Rate of adsorption in a multi-ion system at different temperatures

Rx rate (h^{-1})				
	298.15 ^{o}K	**303.15** ^{o}K	**313.15** ^{o}K	**333.15** ^{o}K
Cu	0.880	0.875	0.862	0.780
Ni	1.094	0.896	0.550	0.511
Zn	0.978	0.965	0.959	0.741
Co	1.002	0.980	0.920	0.880
Fe	1.094	1.055	1.002	0.697
Hg	0.617	0.602	0.592	0.519
U	0.856	0.815	0.803	0.651
Cr	0.978	0.950	0.931	0.722

4.5.3.4.4 Metal ions biosorption as a function of culture age

The study of adsorption of heavy metals on heat-killed *P. simplicissimum* immobilized on zeolite was performed with respect to the growth days. The solution contained 100 mg L^{-1} of each metal ion and the pH, temperature and agitation time were fixed at 3, 25^{o}C and 12 h, respectively. The results obtained after 2, 5 and 20 days of growth are illustrated in Figure 4.85.

(a)

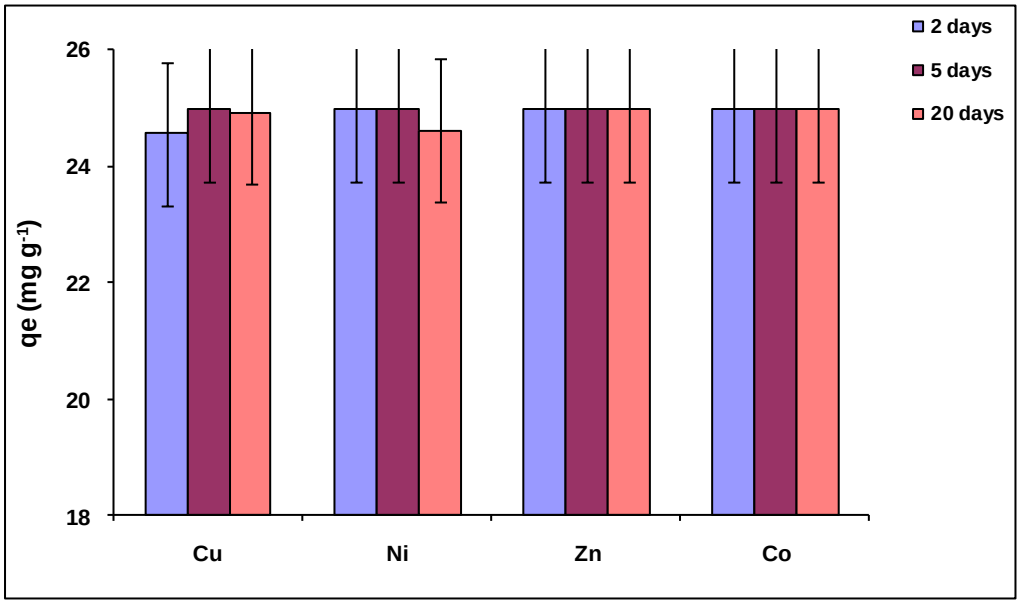

(b)

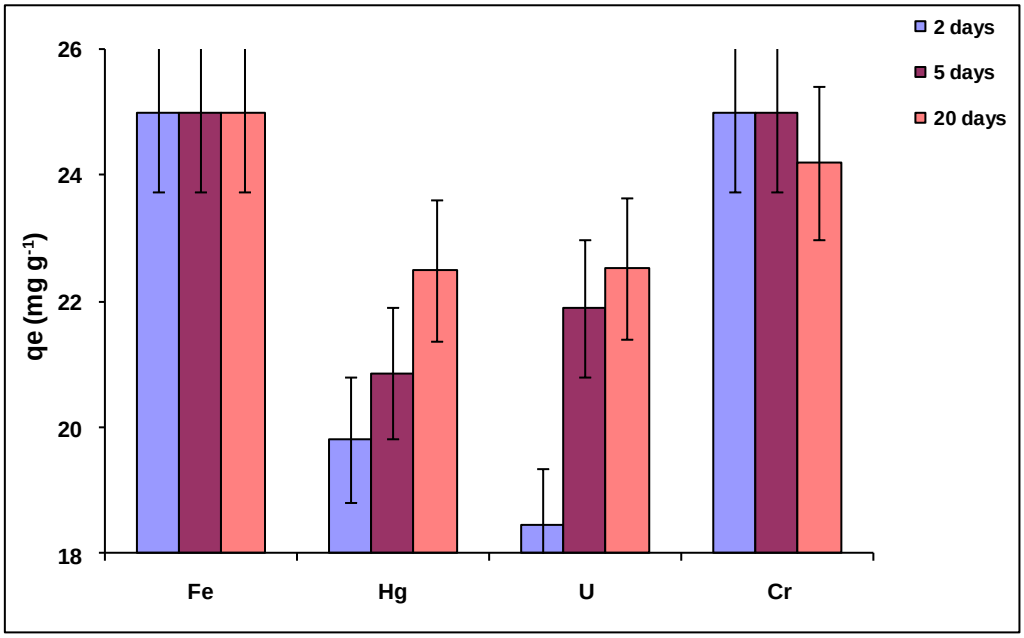

Figure 4.85 (a) and (b) Effect of growth days of the zeolite-*P. simplicissimum* on the adsorption of metal

The graphs indicate a maximum uptake of Ni, Zn, Co, Fe and Cr when adsorbed on biomass harvested after 2 days. The adsorption capacity was constant throughout the growth days for Fe, Zn and Co. The uptake of Hg and U increased with the growth days and a maximum adsorption capacity was obtained with the biomass harvested after 20 days meaning that more

compounds with high affinity to Hg and U were synthesized after 20 days. On the other hand, a decrease in the uptake of Cr and Ni can be seen with the biomass collected after 20 days.

4.5.3.4.5 Adsorption study of uranium in the presence of other metals

The biosorption of uranium on zeolite-*P. simplicissimum* was studied in the presence of Cu, Co, Cr, Hg, Fe, Ni and Zn. The results presented in Figure 4.86 showed that the adsorption capacity of uranium was enhanced by the presence of metal ions in the sequence: Fe > Zn > Cr > Cu > Ni > Hg > Co.

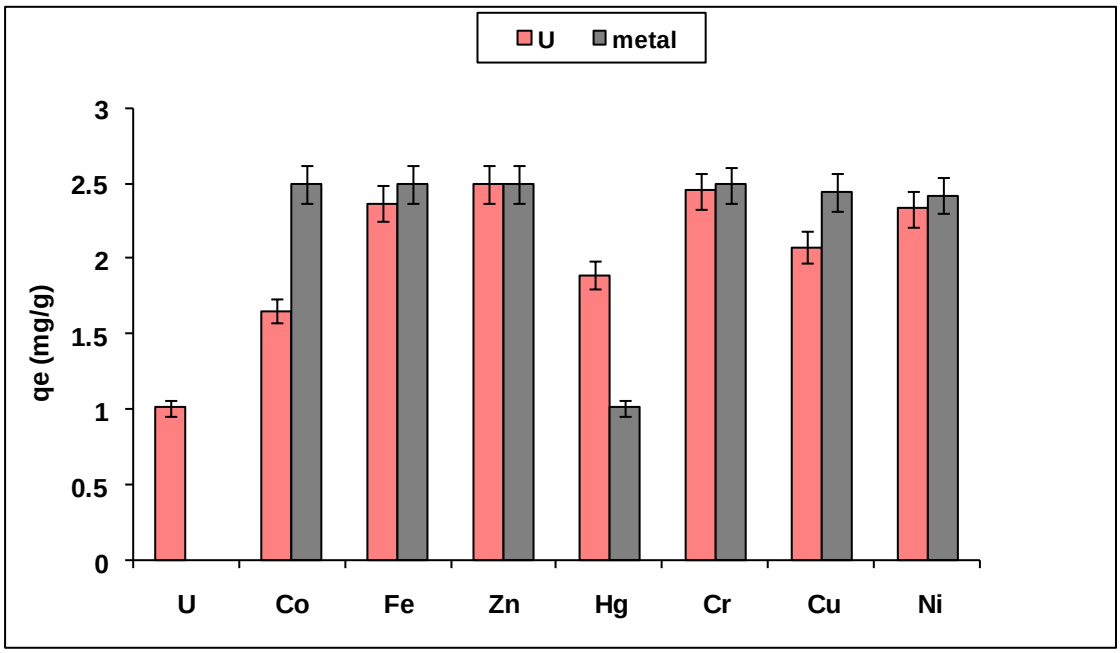

Figure 4.86 Adsorption capacity of U in solution with Cu, Co, Fe, Zn, Hg, Cr and Ni

The adsorption capacity of uranium as a single entity was 1 mg g^{-1}, but increased up to 2.5 mg g^{-1} when uranium was in the presence of Zn or Fe for the same amount of adsorbent. This explains the increase in uptake of uranium in the multi-component system compared to the uptake in the single–component system. This phenomenon (or synergistic effect) was not fully explored and provides an opportunity for further investigation. The strong dependence of adsorption on pH can be explained by changes in the surface charge and uranyl speciation with pH.

4.5.3.4.6 Effect of biosorbent mass on the adsorption capacity

Figure 4.87 presents the adsorption of heavy metal ions at various biosorbent amounts. This experiment showed that metal uptake decreases when the amount of biomass increases. This reduction is attributable to metal shortage in solution.

(a)

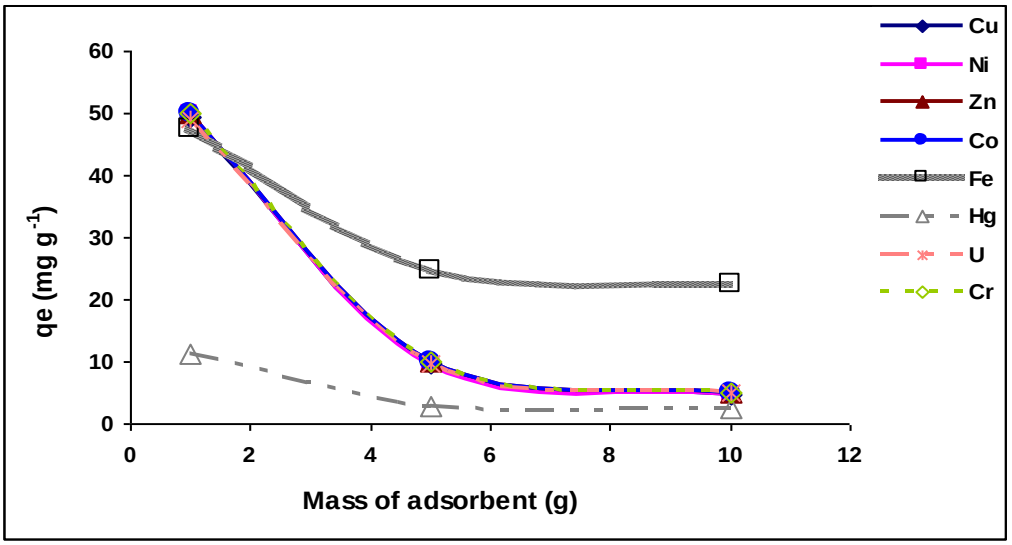

(b)

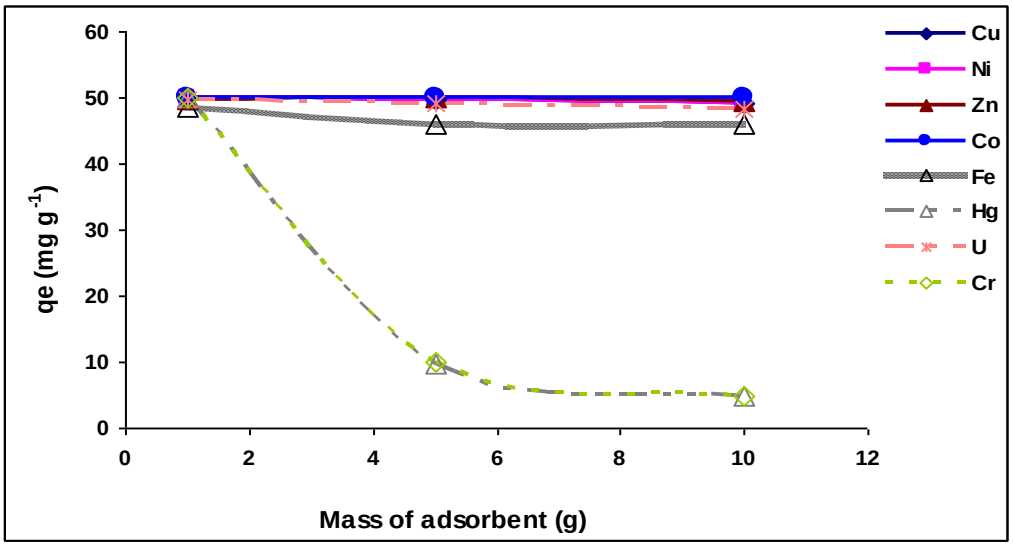

Figures 4.87 Effect of biomass concentration in (a) single ion system (b) multi-ion system (C_i = 100 mg L^{-1})

These results invalidate the hypothesis that electrostatic interaction between cells may be a significant factor in the biomass dependence of metal adsorption (de Rome and Gadd, 1987). Therefore, it is not useful to increase the biomass beyond 1 g to purify a 100 mg L^{-1} single-metal solution. Similar results were obtained by Fourest and Roux (1992).

The metal ions uptake was constant from 1 to 10 g of biosorbent for a 100 mg L^{-1} of metal ions in a multi-component system. A decrease was observed for chomium and mercury. Reduction of the amount of biomass at a given metal concentration enhances the metal/biosorbent ratio, and thus increases metal uptake per gram of biosorbent, as long as the latter is not saturated. An illustration of this behaviour is given by the effect of initial metal ions concentration.

The influence of the biomass on biosorption shows an initial quick decrease followed by a final stability, with increasing biomass dose mainly for the single-ion system. Similar results were obtained by Ting *et al*. (2008). This is could be due to the interference between binding sites and higher biomass dose or insufficiency of metal ions with respect to available binding sites (Rome and Gadd, 1987). This can explain the opposite phenomenon observed for the multi-component system with more metals. The decrease of adsorption capacity was only observed for chomium and mercury. The uptake of U and Hg was lower compared to other metals.

4.5.3.4.7 Regeneration of the biosorbent

Biosorption capability of fungal biomass and its regeneration would have a bearing on its potential as a biosorbent for commercial application. Results for the desorption of metals by different concentrations of HNO_3 (2 mol L^{-1}, 3 mol L^{-1}, 5 mol L^{-1}, and 7 mol L^{-1}) are shown in Figure 4.88.

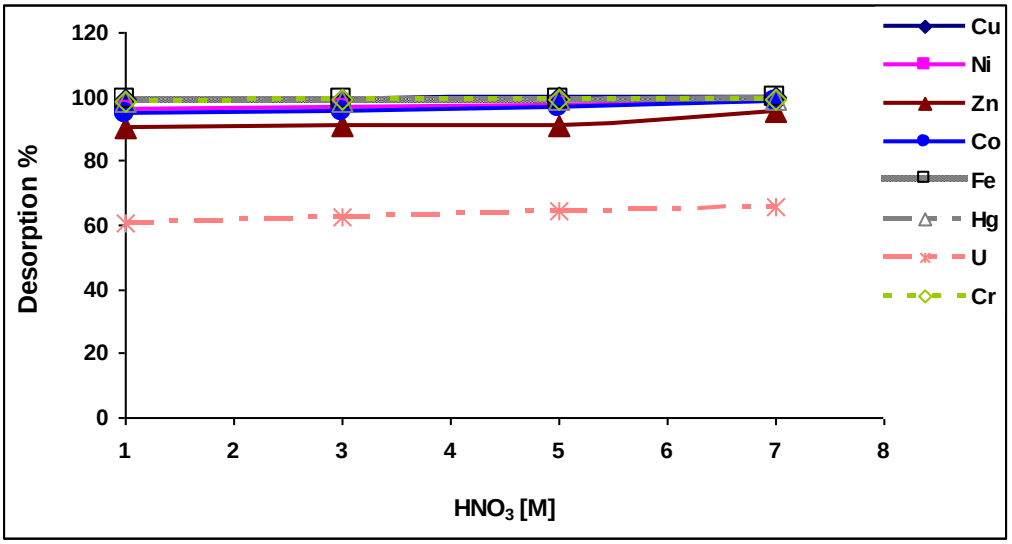

Figure 4.88 Regeneration of the zeolite-*P.simplicissimum* in a multi-ion system

The desorption percentages are given in Figure 4.89. Most of the metal ions were desorbed with 1 mol L^{-1} HNO_3. The capacity of the zeolite-*P.simplicissimum* to adsorb metal ions was determined by repeating the biosorption experiments in five consecutive cycles using 1 mol L^{-1} of HNO_3 as a desorption agent.

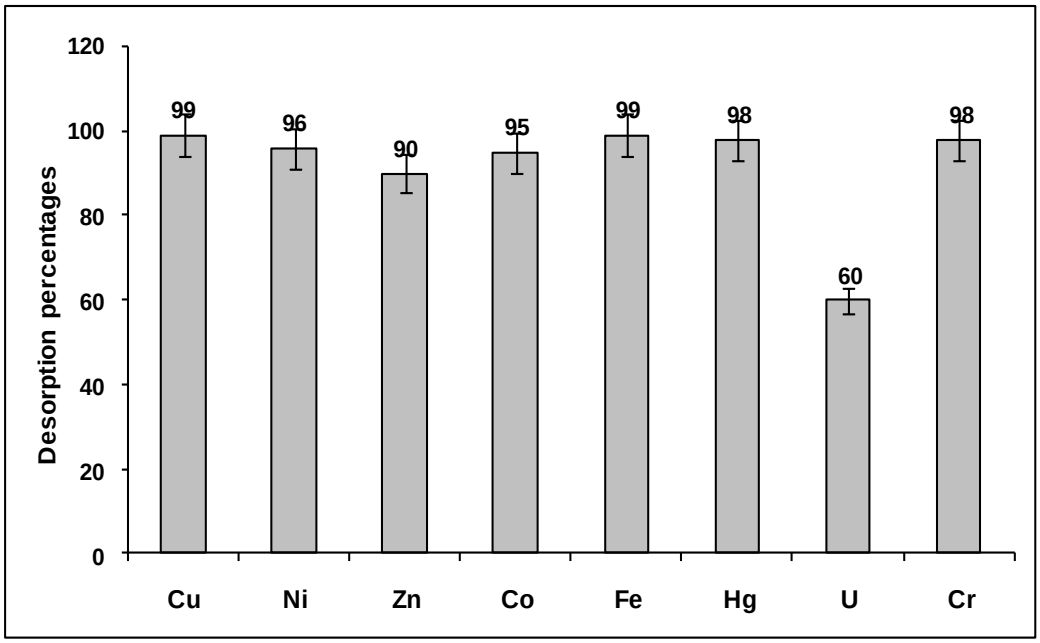

Figure 4.89 Desorption percentages of metal ions

As illustrated in Figure 4.90, the biomass undergoing successive adsorption-desorption processes retained good metal biosorption capacity even after five cycles of adsorption-desorption. The total decrease in biosorption efficiency of zeolite-*P.simplicissimum* after five cycles was ≤ 5% which showed that zeolite-*P.simplicissimum* had good potential to adsorb metal ions repeatedly from aqueous solution.

The results for the desorption of uranium essentially showed an optimum desorption of 60%. Previous studies (Tutu *et al*., 2010) proved the optimum desorption of uranium with 0.8 mol L^{-1} Na_2CO_3. In fact, uranium tends to form strong complexes with carbonates. The regeneration of the biosorbent and adsorption after five cycles gave a good adsorption capacity even for uranium, suggesting a good re-useability potential.

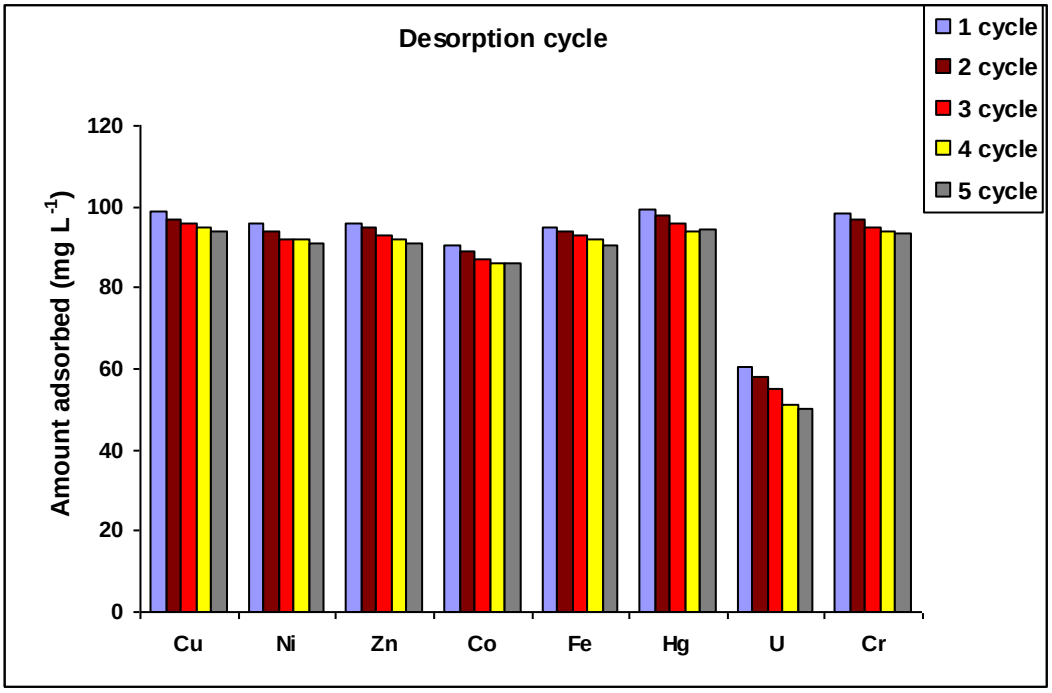

Figure 4.90 Regeneration and re-use of the zeolite-*P.simplicissimum*

4.5.3.4.8 Application of zeolite-P. simplicissimum (inactive) in mine wastewater remediation

The performance of zeolite-*P.simplicissimum* on the removal of heavy metal from mine wastewater samples is presented in Table 4.76.

Table 4.76 Removal of heavy metal ions from wastewater samples by zeolite-*P.simplicissimum* (inactive)

		SW1			*SW2*			*SW3*			*SW4*			*Pit water*		
pH		3.8			7.2			4			5.6			3		
SO_4^{2-} (mg L^{-1})		383.6			19.80			819.4			653.6			1669		
		C_i	C_f	%	C_i	C_f	%	C_i	C_f	%	C_i	C_f	%	C_i	C_f	%
Fe		6.100	0.018	99.7				4.500	0.004		5.800	0.006	99.9	0.600	< DL	99.8
	RSD	0.075	2.014					0.564	4.210		0.352	4.265		0.421	-	
Ni		6.000	0.012	99.8	1.600	0.040	97.5	1.800	0.010	99.4	4.700	0.005	99.9	10.70	0.010	99.9
	RSD	0.704	1.565		2.856	3.562		0.254	5.214		0.754	6.311		0.125	2.655	
Zn		4.300	0.004	99.9	n.a			1.600	0.002	99.9	1.700	0.005	99.7	14.80	0.015	99.9
	RSD	0.875	0.985					0.851	6.201		0.221	5.468		0.524	4.216	
Cr		n.a			n.a			0.300	0.005	98.3	n.a			0.040	0.001	97.5
	RSD							0.477	4.252					3.652	5.624	
Hg		n.a			n.a			n.a			n.a			0.300	0.003	99
	RSD													1.485	4.784	
U		n.a			n.a			n.a			n.a			0.200	< DL	100
	RSD													0.258	-	

C_i - initial metal concentration (mg L^{-1}) ; C_f - final metal concentration (mg L^{-1}); % - Removal %; SW - surface water; RSD - relative standard deviation (n=3); n.a - non analysed

The limit of detection (LOD, mg L^{-1}) and the method quantitation limit (MQL, mg $L^{-}1$) are given below: LOD: Cr - 0.003; Fe - 0.002; Hg - 0.001; Ni - 0.007; Zn - 0.008; U - 0.035; SO_4^{2-} - 0.01 (by ion chomatography). MQL: Cr – 0.010; Fe – 0.007; Hg – 0.003; Ni – 0.023; Zn – 0.027; U – 0.117; SO_4^{2-} - 0.03 (by ion chomatography).

Table 4.77 presents the discharge standards for industrial wastewater as stipulated by the USEPA.

Table 4.77 Discharge standards for industrial wastewater (US EPA, 1996)

pH	6 - 9
Fe	0.3 mg L^{-1}
Ni	0.05mg L^{-1}
Zn	5 mg L^{-1}
Cr	0.01 mg L^{-1}
Hg	0.002 mg L^{-1}

After treatment with the zeolite-fungi, the quality of the effluent complied with the discharge standards for industrial wastewater as stipulated in Table 4.77.

Conclusion

The following conclusions can be drawn from this study:

The growth of *Penicillium simplicissimum* fungal biomass showed a 10-fold increase in biomass when immobilized on bentonite/zeolite at pH 4. Infrared spectra of the biomass confirmed the presence of functional groups with lone pairs of electron that are available to bind to the positively divalent metal ions. These include: hydroxyl, carbonyl, carboxyl, amide, amine, imidazole and phosphate groups. It was pointed that more compounds were released after 10 days of inoculation. The chemical composition of the fungal wall is strongly dependent on the culture conditions and this may affect biosorptive properties.

The bentonite- P.*simplicissimum* was efficient in adsorption of Cu, Ni, Zn, Co, Fe, Hg, Cr and U at low pH, in single as well as multi-ion systems. The maximum adsorption capacities were obtained at pH 2, a strong synergic effect was observed, mostly between uranium and nickel.

High adsorption efficiency was observed for the inactive fungi immobilized on bentonite due to the amount of available functional groups or binding sites on the surface of the biomass.

The adsorption of metal ions on a living was greatly influenced by the metabolism which does not occur when the biomass is inactive.

Interesting is that he presence of competing ions seemed to inhibit the xenobiotic effect of micro-organisms on the toxic metals as uranium and also the adsorption capacities of metals studied was not affected by the presence of competing ions.

The increase of adsorption capacity in the bentonite- P.*simplicissimum* is mainly due to the presence of chemical groups on the cell walls of the micro-organisms in conjugation with the components contains in the interior of the cells. The presence of phosphates enhanced the uptake of uranium.

Biosorption equilibrium data fitted very well to both the Freundlich and D-R models in the single and multi-ion systems. The maximum loading capacity (mol kg^{-1}) followed the order of Fe >Ni > Cr > Cu > Zn > Co > Hg > U. The uptake depends on the affinity of the metal towards the binding sites (depends on the nature and the amount of functional groups present on the surface of the biosorbent). In the multi-ion system, the affinity of metal ions towards the biomass was in the sequence of Hg > Cu > Zn > Co > U > Ni > Cr > Fe.

Ion-exchange was found to be an important process based on free energy value from D–R isotherm for all metal ions.

For all heavy metal ion systems at the different temperature studied, the rate of adsorption was found to follow the pseudo second-order kinetics, except the adsorption of Ni described by the film diffusion model.

The negative activation energies gave an indication that the metals studied prefer to bind to low energy binding sites, therefore adsorption of these metals occurs without an energy barrier which could be a combination of a chemisorption, physisorption or diffusion.

The adsorption of metal ions on bentonite-*P.simplicissimum* was spontaneous and endothermic in the single ion system, whereas the adsorption of Ni, Zn and Co was exothermic in a multi components system.

The results show that a maximum adsorption capacity was observed for metal ions adsorbed on biomass harvest after two days of culture, except for nickel.

The adsorption capacity of uranium increased in the presence of Zn or Fe, this explains increasing in uptake of uranium in the multi-components system. This phenomenon has been not yet fully understood.

99% of metal ions were desorbed with 1 M $HNO_{3,}$ whereas, only 60% of uranium was desorbed. The regeneration of the biosorbent and adsorption after five cycles gave a good adsorption capacity even for uranium, suggesting a multi-layer adsorption**.**
Sodium carbonate solution may be used to remove the uranium. It is well known that carbonate ions have high affinity for the uranyl ion; therefore the energy of formation of uranyl-carbonate complex is greater than that for the uranyl-phosphate complex. Further experiments have to be done with the sodium carbonate to remove the uranium from the biosorbent.

The application of the zeolite-P.*simplicissimum* for the adsorption of heavy metals from industrial effluents was a success with more than 97% of metals removed.

4.5.4 Sorption studies of metals on natural and functionalised bentonite/zeolite with P. simplicissimum (inactive) in column mode

Batch adsorption tests provide information on adsorption equilibrium characteristics and adsorption kinetics, which is important in determining the effectiveness of the adsorbent in removing solutes from solution. However, batch operations are not often economical or available in practice and the data obtained from these is not sufficient to give accurate scale-up data required in the design of industrial adsorption columns. Therefore, column studies have to be performed, whereby the most important parameter to be determined is the column breakthrough curve, which determines the operating life span of the fixed adsorbent bed.
In this section, the breakthrough and exhaustion points are determined for fixed-bed columns packed with natural zeolite/bentonite as well as modified zeolite/bentonite used for the continuous adsorption of heavy metals from their respective multi-component solutions. The system variables or parameters such as solution flow rate and bed height were not investigated in this study, although very important, because of time restraint. The desorption behaviour of biosorbents (cited above) and the performance following regeneration were assessed.

4.5.4.1 Breakthrough curves

The performance of a column adsorption process is described though the concept of the breakthrough curve. Breakthrough point is the time that sorbed species are detected in the column effluent at a given concentration and breakthrough curve is the shape of the concentration–time profile. Breakthrough point and curve are very important characteristics for process design, dynamic response and operation of a biosorption column because they directly affect the feasibility and economics of the sorption phenomena. Besides, in the column studies, the effectiveness of biomass can be evaluated from the breakthrough curve of the effluent concentration (or the concentration–time profile) and a typical S-shaped breakthrough curve is usually observed (Chu, 2004).

The breakthrough curve shows the loading behaviour of metal ions to be adsorbed in a fixed bed and is usually expressed in terms of adsorbed metals concentration (Co = inlet metal concentration, Ce = outlet metal concentration). In this experiment, the breakthrough and exhaustion points were defined as the points when effluent concentrations were about 10% and 90% of the initial feed concentration, respectively (Han *et al*., 2006; Kundu and Gupta,

2005). The normalised concentration is defined as the ratio of effluent metal concentration to inlet metal concentration (*Ce*/*Co*) as a function of time or volume of effluent for a given bed height (Aksu and Gönen, 2004).

The area under the breakthrough curve obtained by integrating the sorbed concentration (Cs – mg L^{-1}) versus the throughput volume (V- L) plot can be used to find the quantity (maximum column capacity) of sorbed metals. The total metals sorbed (q_o mg g^{-1}) in the column for a given feed concentration and flow rate is calculated from equation 4.10.

$$q_o = \int_0^{VT} \frac{(Co-Ce)dV}{m} \qquad (4.10)$$

where: *m* is the mass of the sorbent (g). The capacity value q_o was obtained by graphical integration (Tabakci and Yilmaz, 2008).

4.5.4.2 Column performance

The influent was a synthetic mixed feed of Cu, Co, Cr, Fe, Hg, Ni, Zn and U ions. Figures 4.91 and 4.92 show, respectively, the breakthrough curves obtained with a mixed feed containing the pre-cited ions at 100 mg L^{-1} and feed rate of 2 mL min^{-1} (an average flow rate used in many studies as observed in literature) and pH 3 on natural bentonite as well as on natural zeolite. The effluent samples were collected and metal concentrations analysed. The *Ce/Co* ratio was plotted against time to observe the behaviour of natural zeolite/bentonite as well as modified in column studies.

a. Natural bentonite

The results in Figure 4.91 show that the initial breakthrough points were obtained at almost the same time (30 minutes) for all the metal ions in solution. This suggests that the bentonite exchange sites were readily available and easily accessed by all the metals. However, the exhaustion points (point at which the final effluent concentration was 90% of the initial influent) were different.

(a)

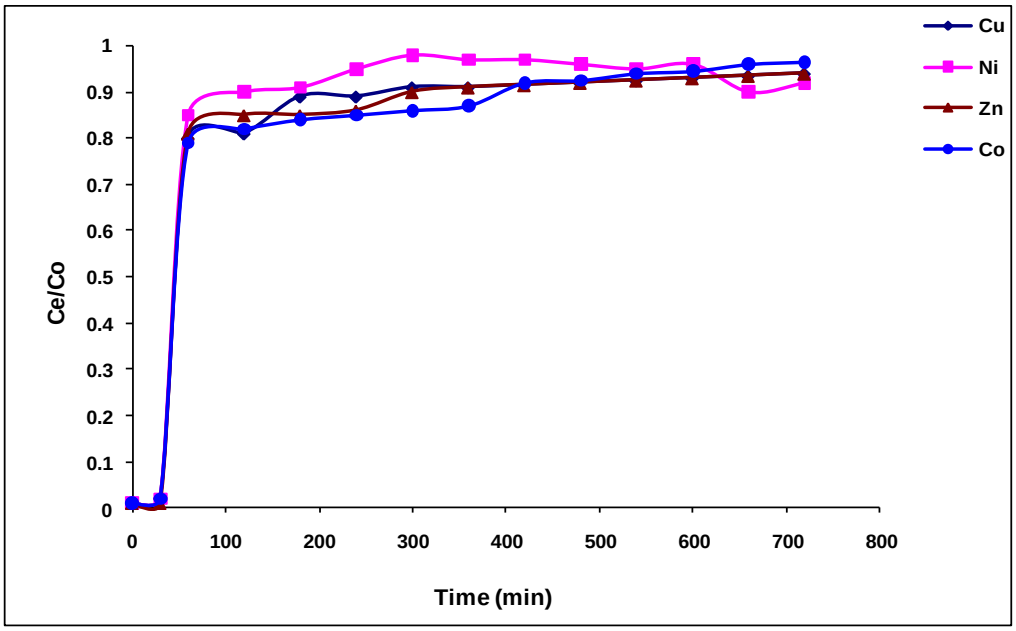

(b)

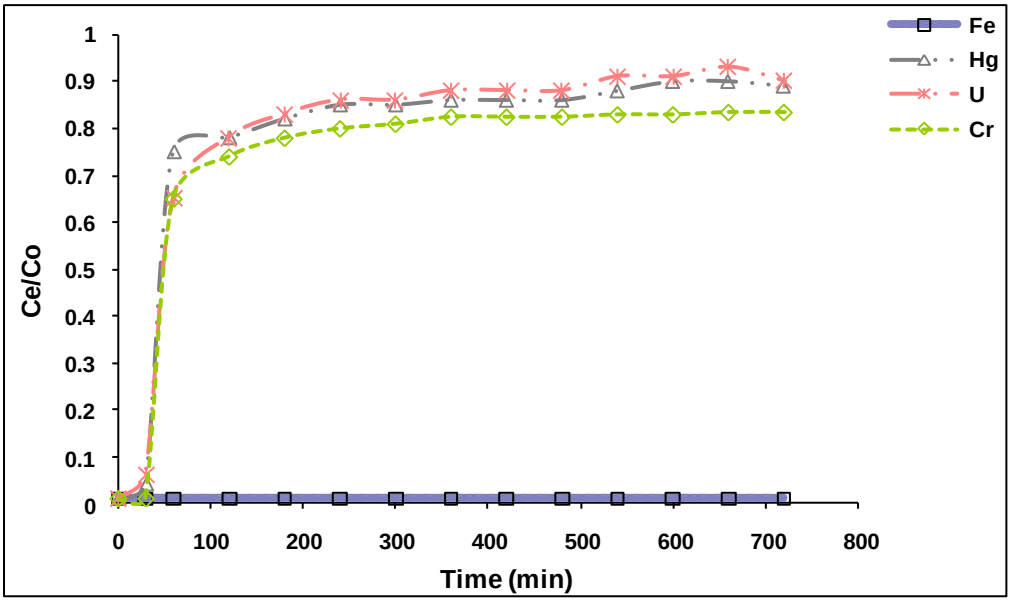

Figure 4.91 Breakthrough curves for biosorption of (a) Cu, Co, Ni and Zn (b) Cr, Hg, Fe and U on natural bentonite (concentration = 100 mg L^{-1}, pH 3 at 2 mL min^{-1})

The exhaustion points were attained at 300 min (5 h) for Cu and Zn, 120 min (2 h) for Ni, 420 min (7 h) for Co, 600 min (10 h) for Hg and U. For the rest of the metal ions (Fe and Cr), the exhaustion point could not be reached, with the effluent concentration below 90% of the influent. We assume that more time is required to reach the saturation point. These results imply that Ni was taken up into the exchange sites at a faster rate than other ions. The

selectivity series (based on the exhaustion time and the ratio *Ce*/*Co*) were in the following order: Ni > Zn, Cu > Co > Hg, U > Fe, Cr. This selectivity order was different from that obtained in the batch experiment, indicating that many factors affect the adsorption of metal ions on bentonite.

b. Natural zeolite

A similar trend was observed for the column adsorption of metal ions by the natural zeolite as shown in Figure 4.92.

The breakthrough time was about 30 minutes for all the metal ions as for the bentonite. The metal ions were preferred by the natural zeolite in the sequence as follows: Ni > Cu > Zn, Co > Hg, U > Cr, Fe. The selectivity series shows high affinity of Fe towards the adsorbent (and Ni exhibits less affinity). This order is more or less the one observed in the batch tests.

(a)

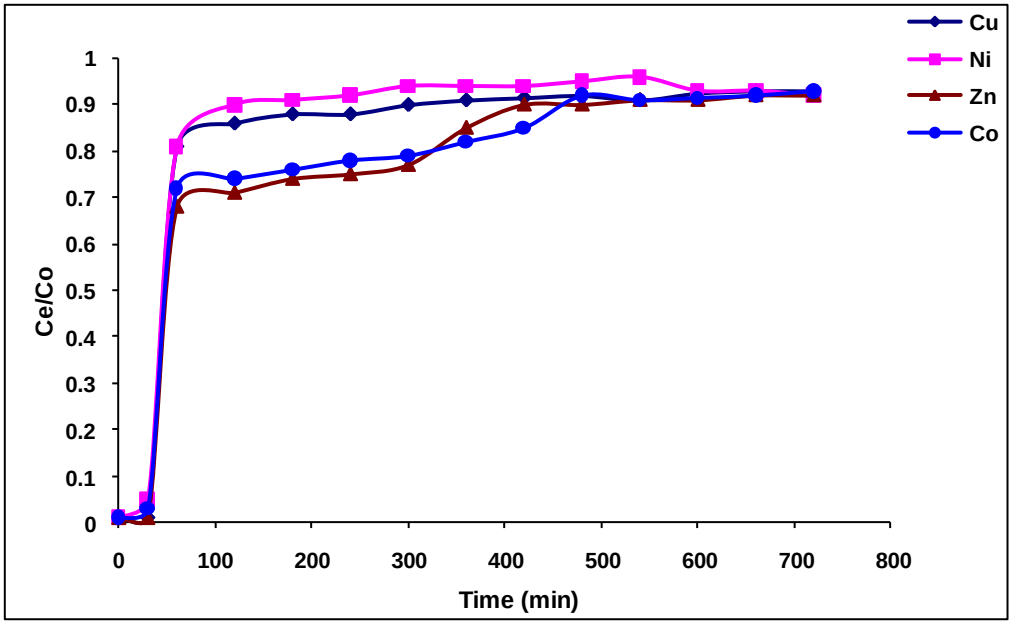

(b)

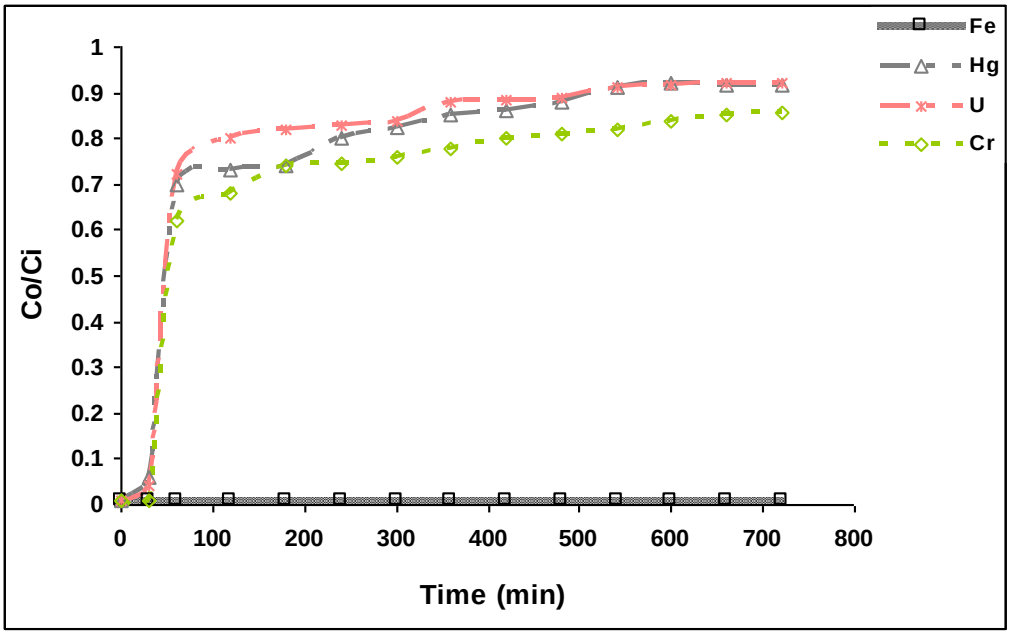

Figure 4.92 Breakthrough curves for the biosorption of Cu, Co, Cr, Hg, Fe, Ni, Zn and U on natural zeolite (concentration = 100 mg L^{-1}, pH 3 at 2 mL min^{-1})

c. Bentonite-*P. simplicissimum*

The breakthrough curves obtained for the biosorption of Cu, Co, Cr, Hg, Fe, Ni, Zn and U (single- and multi-metal) on bentonite modified by P. *simplicissimum* are shown in Figures 4.93 and 4.94.

(a)

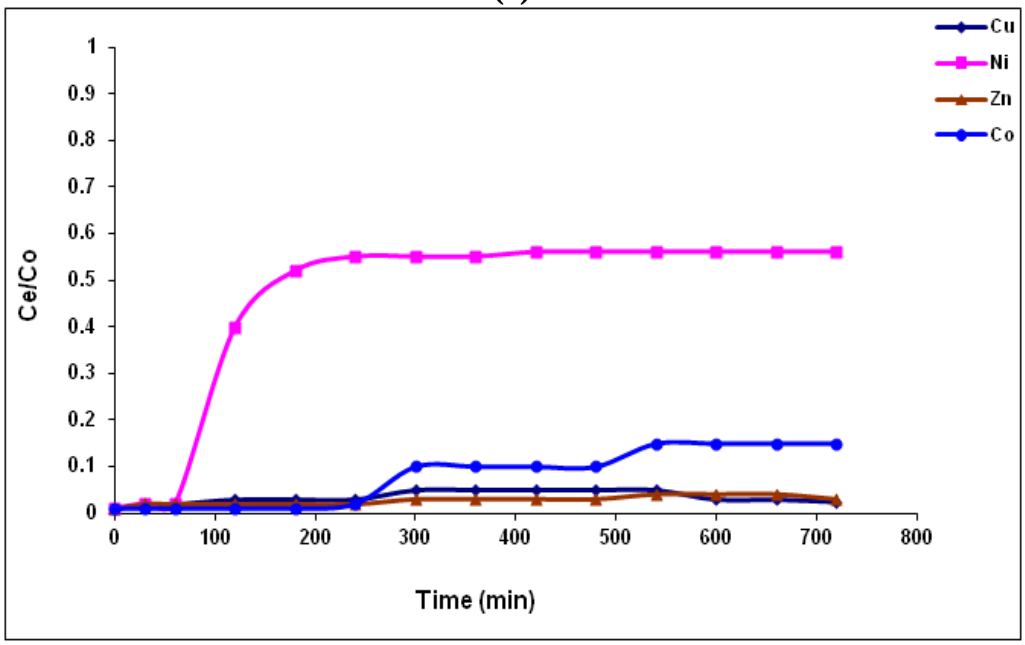

(b)

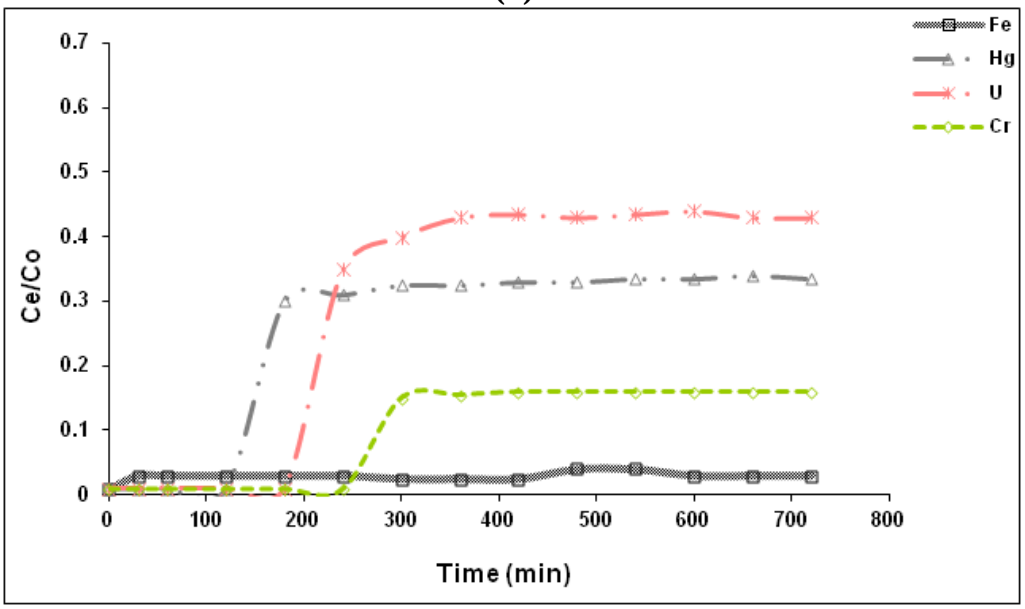

Figure 4.93 Breakthrough curves for the biosorption of (a) Cu, Co, Ni, and Zn (b) Cr, Hg, Fe and U (single-ion solution) on bentonite P. *simplicissimum* (concentration = 100 mg L^{-1}, pH 3 at 2 mL min^{-1})

From these figures, it is clear that the exhaustion points were not reached for all the metal ions in single-ion as well as in multi-ion systems. These results confirm the increases of adsorption efficiency of the biosorbent as observed for the batch tests.
The breakthrough points occurred after 60 min (1 h) for Ni, at 120 min (2 h) for Hg, at 180 min (3 h) for U, at 240 min (4 h) for Cu, Zn, Co, and Cr. The effluent for Fe was obtained after 410 min (6.83 h). The breakthrough time increased with the modification of the bentonite, implying higher affinity of metal ions towards the biosorbent.

In the multi-ion system in Figure 4.94, the breakthrough time was about 120 min for Ni. An increase of the breakthrough time was observed with the presence of other ions.

(a)

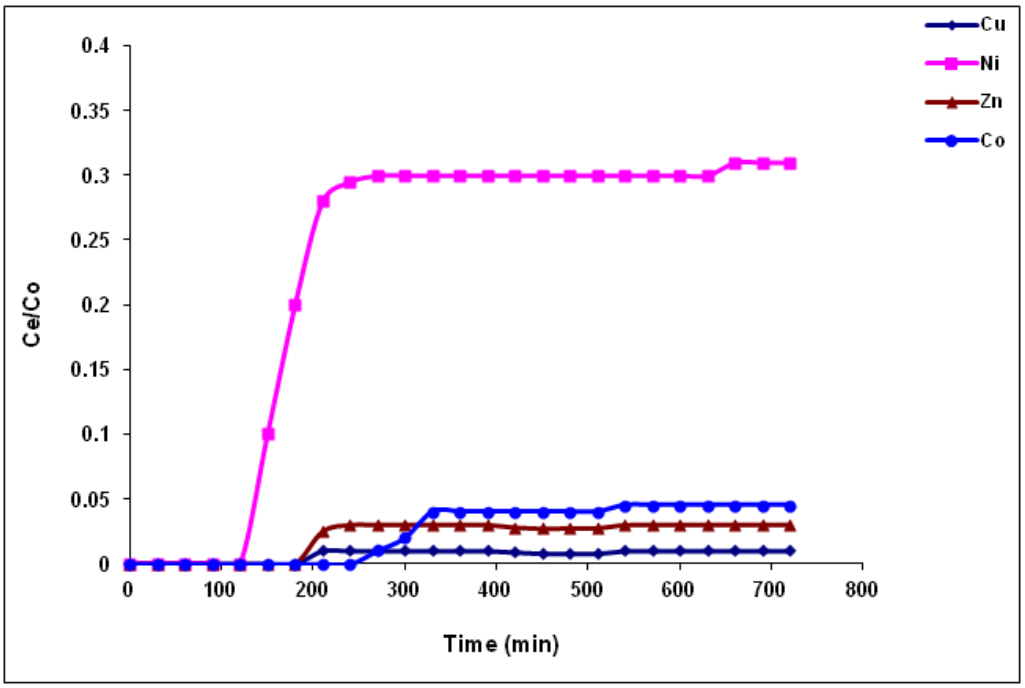

(b)

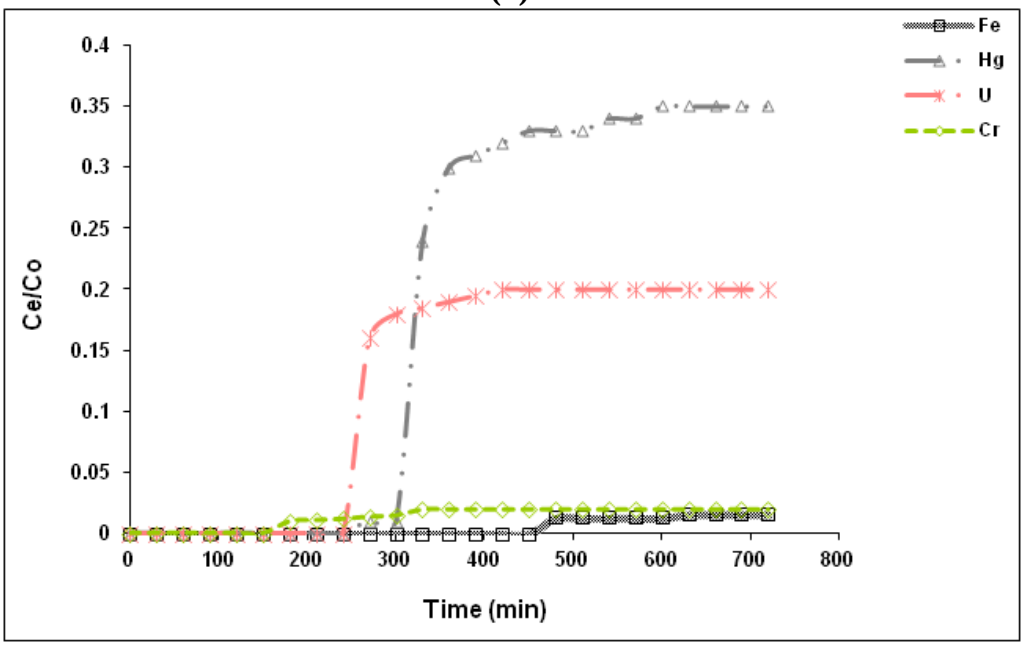

Figure 4.94 Breakthrough curves biosorption of (a) Cu, Co, Ni and Zn (b) Cr, Hg, Fe and U (multi-ion solutions) on bentonite-P. *simplicissimum* (concentration = 100 mg L^{-1}, pH 3 at 2 mL min^{-1})

A similar observation was obtained for Hg and U, with an increase of breakthrough time for 180 min (3 h) for Hg and 60 min (1 h) for U. A different trend was observed for the metals, namely: Zn and Cr, a decrease of breakthrough time from 240 min (4 h) to 180 min (3 h). The breakthrough time did not change for Fe.

d. Zeolite–*P. simplicissimum*

As for the bentonite-P. *simplicissimum*, the breakthrough time for the biosorption of metal ions in single-ion systems for zeolite-P. *simplicissimum* was higher than that obtained for the natural zeolite. The results obtained in Figure 4.95 show an increase of breakthrough time for Cu (120 min), Ni (60 min), Co (360 min), Hg (120 min) and U (180 min). The breakthrough was not obtained for the following metal ions: Zn, Fe and Cr. The exhaustion point was not reached as for the previous cases. The increase of the breakthrough time could be explained by the increase of residence time of the metal ions in the column due to the high affinity for the biosorbent. This high affinity is attributed to the presence of functional groups which bind with the metal ions.

(a)

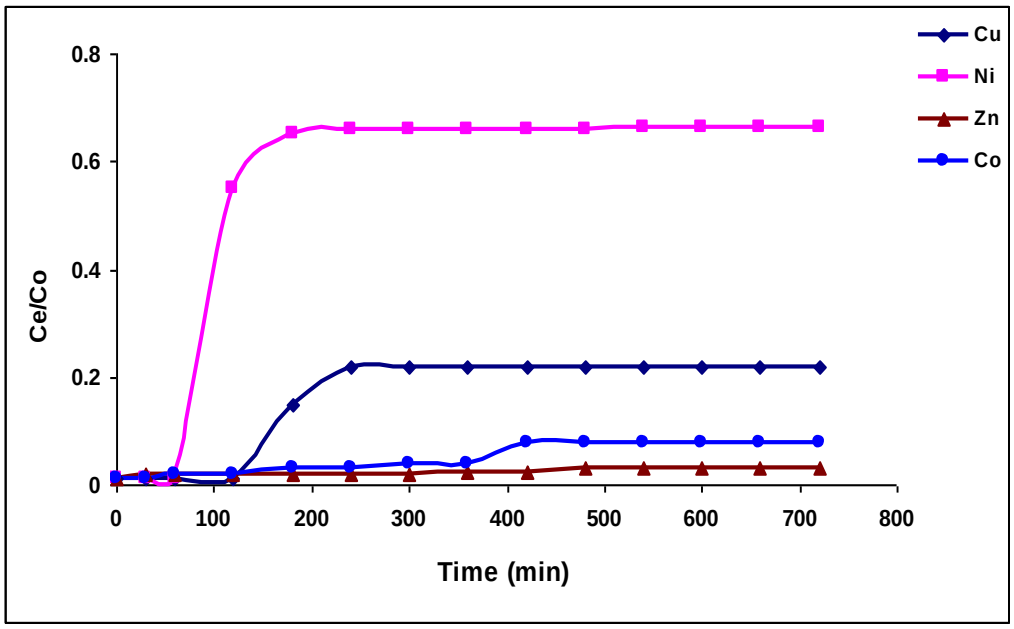

(b)

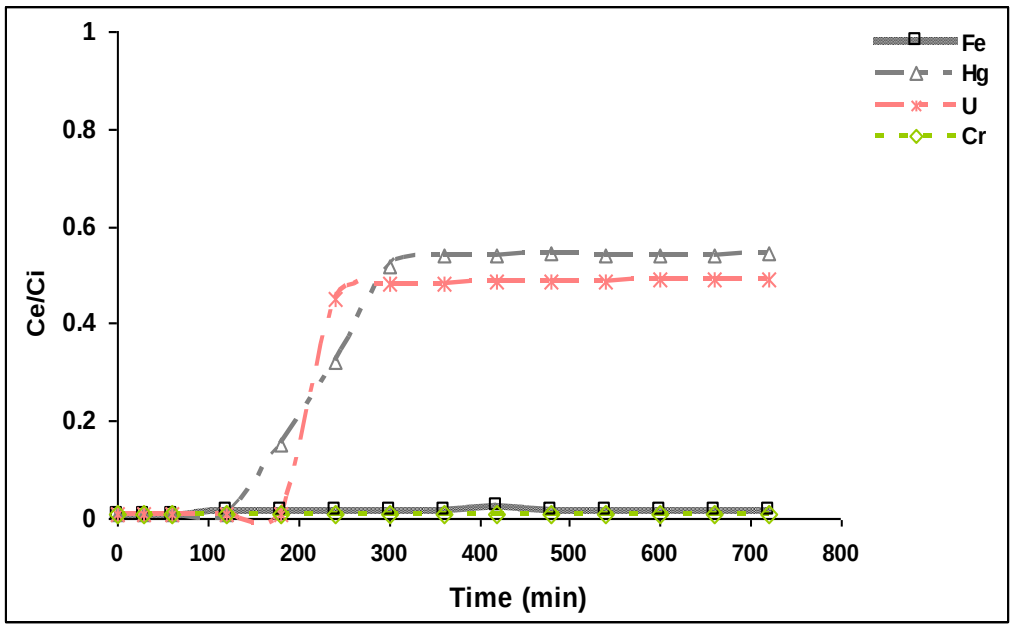

Figure 4.95 Breakthrough curves biosorption of (a) Cu, Co, Ni, and Zn (b) Cr, Hg, Fe and U (single-ion system) zeolite-P.*simplicissimum* (concentration = 100 mg L^{-1}, pH 3 at 2 mL min^{-1})

Figure 4.96 shows the breakthrough curves in a multi-ion system.

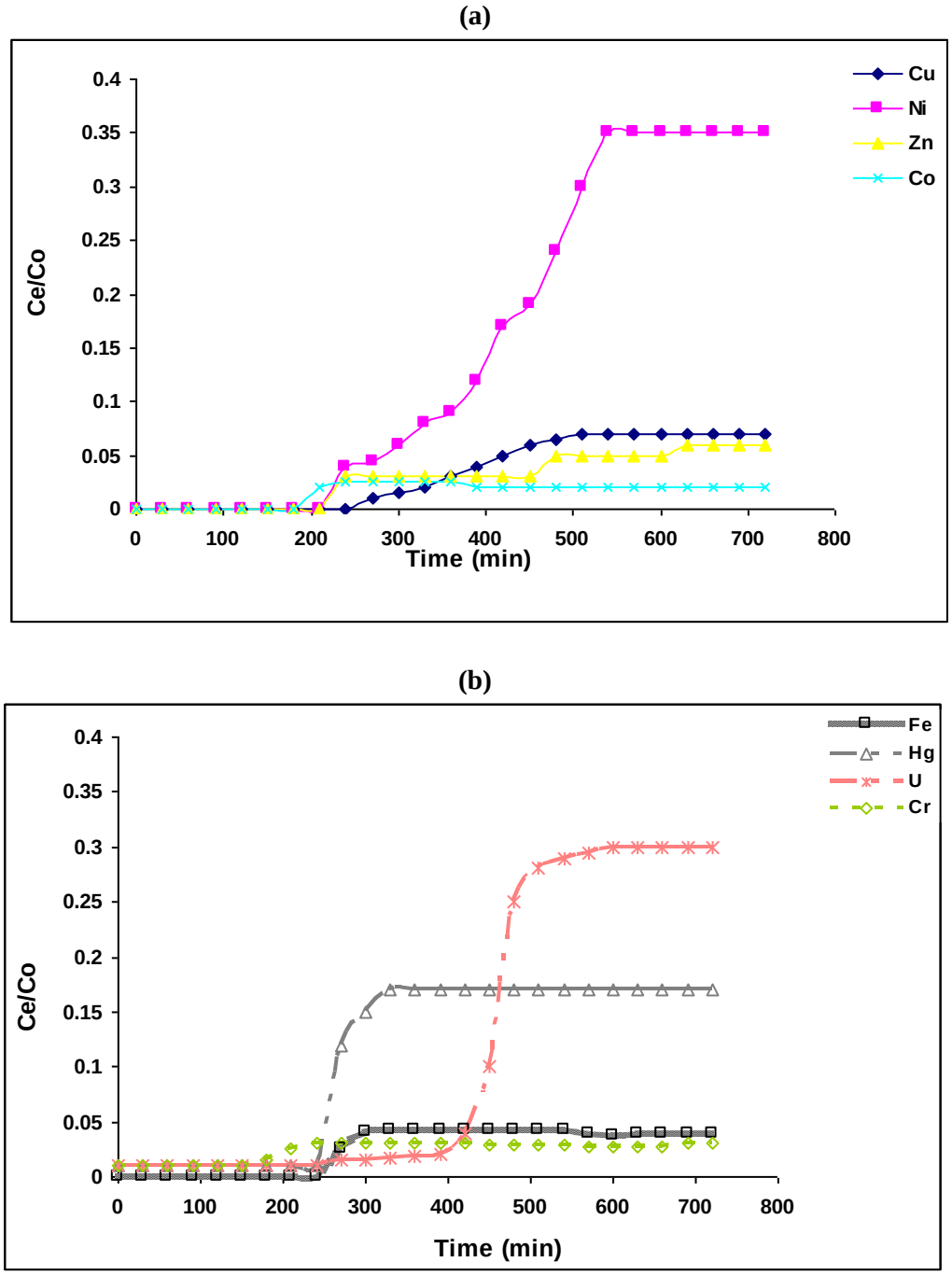

Figure 4.96 Breakthrough curves biosorption of (a) Cu, Co, Ni, and Zn (b) Cr, Hg, Fe and U (multi-ion) on zeolite-P.*simplicissimum* (concentration = 100 mg L^{-1}, pH 3 at 2 mL min^{-1})

An increase in the breakthrough time was obtained for Cu (240 min), Ni (210 min), Hg (230 min) U (400 min). Compared to the adsorption in a single-ion system, a decrease of the

breakthrough time was obtained for Zn (210 min), Fe (240 min), and Cr (150 min). In fact, the breakthrough point was not observed for these metals for a single-ion system.

In order to optimize the efficiency of the column adsorption, a number of factors that affect the behaviour of breakthrough curves have to be assessed and these include the effect of flow rate, adsorbent bed height and dimensions of the adsorption column. These factors will be investigated in a future work.

When the relationship is converted from time scale to volume scale, one can define the breakthrough volume as the function of the plate number of the column (Lövkvist and Jöensson, 1987).

4.5.4.3 Number of theoretical plates

The number of theoretical plates, also known as column efficiency, depends on: column parameters (as diameter, length) and on the physico-chemical properties of the biosorbent. To evaluate the efficiency of the column used in this study, the plate number was calculated from the breakthrough curves for Ni and U desorbed on natural and modified bentonite/zeolite. Since the parameters of the column were constant, only the properties of the biosorbent influence the theoretical plate number. This was calculated using the following equation:

$$N = \frac{V_R(V_R - \sigma_V)}{\sigma_V^2} \qquad (5.11)$$

where: V_R is the retention volume (mL) and σ is the numerical coefficient. Figure 4.97 illustrates these parameters and the number of plates calculated is given in Table 4.78.

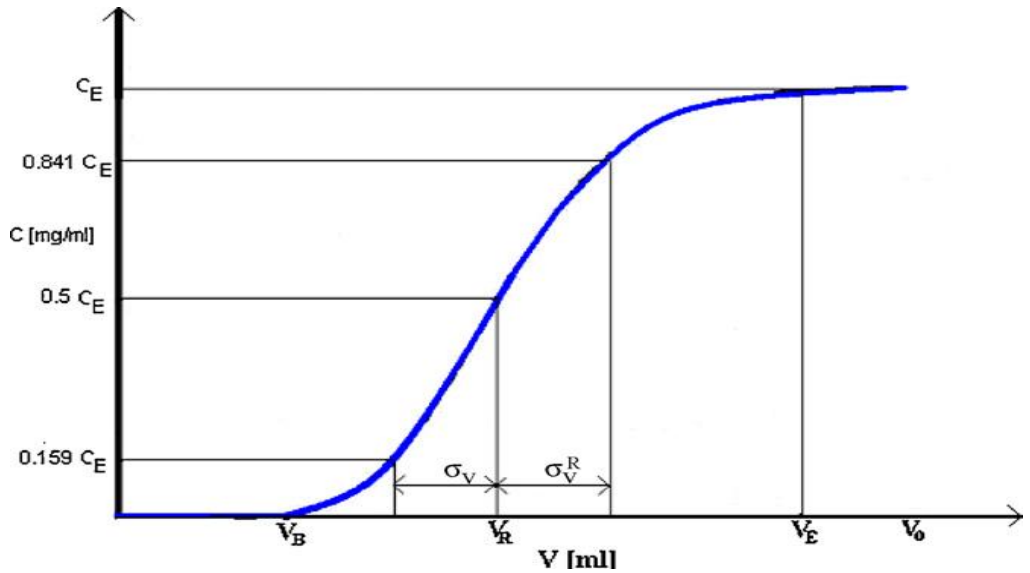

Figure 4.97 Breakthrough curve (Daszkiewicz and Voelkel, 2009)

The adsorption capacity (q_o) of the various adsorbents was calculated for Ni and U according to equation 4.11 and the results are listed in Table 4.78.

Table 4.78 Theoretical number of plates of the column and adsorption capacity of the biosorbents for Ni and U

		Bentonite		
		Natural bentonite	***Bentonite-P.simplicissimum***	
			Single-ion system	***Multi-ion system***
Ni	THPN	6	7	17
	q_o (mg g^{-1})	3.081	21.12	33.12
U	THPN	15	71	83
	q_o (mg g-1)	4.8	37.92	38.40
		Zeolite		
		Natural zeolite	***Zeolite-P.simplicissimum***	
			Single-ion system	***Multi-ion system***
Ni	THPN	6	8	8
	q_o (mg g-1)	3.840	16.08	31.20
U	THPN	10	15	56
	q_o (mg g-1)	2.95	36.48	33.61

THPN= theoretical plate number

The results in Table 4.78 show that the number of theoretical plates was higher in the modified bentonite/zeolite, proof of their efficiency for the adsorption of heavy metals. These results are in agreement with those obtained in the batch experiments where the modified biosorbents were found to be more efficient than the natural entities. These results do not follow the trend seen with the surface area for which some authors confirmed that the large surface area of the sorbent is accompanied by high *N* values while a small surface area corresponds to lower efficiency (Daszkiewicz and Voelkel, 2009). In fact, the surface area for the natural bentonite was higher (73.82 m^2 g^{-1}) than the surface area of bentonite P. *simplicissimum* (19.62 m^2 g^{-1}), for instance. A similar trend was obtained for the zeolite with a surface area of 0.692 m^2 g^{-1} for the natural zeolite and 0.386 m^2 g^{-1} of the zeolite modified with fungi. The efficiency of a biosorbent in column experiments does not depend only on the theoretical plate number but also on other factors such as the flow rate, the nature of the biosorbent and the height of the bed.

Most of the calculated values of the loading capacity in column adsorption were close to those obtained in the batch tests. For instance, the loading capacity of Ni and U given in Table 4.78, where 3.081 mg g^{-1} and 4.800 mg g^{-1} for the natural bentonite. In the batch test, the adsorption capacities for Ni and U were 4.014 mg g^{-1} and 4.498 mg g^{-1}, respectively. For the modified bentonite, the adsorption capacity was about 25 mg $g^{-1}$for both ions, whereas 21.12 mg g^{-1} and 33.12 mg g^{-1} were obtained for Ni and U, respectively.

4.5.4.4 Desorption studies and regeneration of the biosorbent

A good adsorbent, as noted earlier should not only have a high adsorption capacity, but must also exhibit good regeneration for multiple usages (Richardson *et al.,* 2002). One of the aims of regeneration of metal-loaded adsorbent is to reduce the volume of liquid waste, that is, desorption liberates small volumes of concentrated metals solutions, which are more appropriate for conventional metal recovery processes such as electrolysis. Once the column reached exhaustion, the biosorbent was regenerated using 0.1 M HNO_3 at 25 ± 1^{o}C, at a flow of 4 mL min^{-1} for 60 mins, by this time, most of the ions would have been desorbed. The column was finally washed with de-ionized water at 4mL min^{-1} for 10 min before proceeding to the next run. About 3 regeneration cycles were carried out for each experiment and the adsorption efficiencies determined. All experimental analyses were carried out in duplicate and mean values are presented in all the results.

The mass of metal desorbed, m_d, can be calculated from the area below the desorption curve multiplied by the flow rate.

$$m_d = Q_v \int Ct\, dt \qquad (4.12)$$

The desorption efficiency is a ratio of the amount of solute desorbed over the amount adsorbed by the adsorbent (Marandi, 2011):

$$\text{Desorption (\%)} = \frac{m_d}{m_{ads}} \text{ x } 100 \qquad (4.13)$$

The desorption curves of heavy metals from natural as well as modified zeolite/ bentonite are presented in the APPENDICES E, F, G and H. In general, the desorption curves for all the heavy metals show a general increase in the concentration of metal ions initially in the effluent, that is, within the first 20 minutes followed by a decrease at approximately the same rate and then the concentration gradually levels off after 50 minutes.

The amount of heavy metals desorbed from natural zeolite for the 3 cycles and desorption efficiencies are presented in Table 4.79a, b, c, d.

Table 4.79a Calculated desorption efficiencies for the desorption of heavy metals from natural Bentonite in fixed bed columns using 0.1 M HNO_3 at 25ºC; bed height 13 cm, flow rate 4 mL/min; contact time 540 minutes

Heavy metals	*Amount adsorbed from solution, m_{ads} (mg L^{-1})*	*Amount desorbed from biosorbent, m_d (mg L^{-1})*	*Desorption efficiency (%)*
Cu			
Cycle 1	74	70	95
Cycle 2	70	65	93
Cycle 3	71	62	87
Ni			
Cycle 1	8	7	87
Cycle 2	15	12	80
Cycle 3	18	13	72
Zn			
Cycle 1	90	85	94
Cycle 2	95	91	96
Cycle 3	95	90	95
Co			
Cycle 1	69	60	87
Cycle 2	75	65	87
Cycle 3	72	60	83
Fe			
Cycle 1	99	95	94
Cycle 2	96	90	94
Cycle 3	97	90	93
Hg			
Cycle 1	11	10	91
Cycle 2	15	12	80
Cycle 3	12	9	75
U			
Cycle 1	10	4	40
Cycle 2	45	16	36
Cycle 3	38	12	32
Cr			
Cycle 1	30	25	83
Cycle 2	25	20	80
Cycle 3	42	40	95

Table 4.79b Calculated desorption efficiencies for the desorption of heavy metals from natural Zeolite in fixed bed columns using 0.1 M HNO_3 at 25°C; bed height 13 cm, flow rate 4 mL/min; contact time 540 minutes

Heavy metals	*Amount adsorbed from solution, m_{ads} (mg L^{-1})*	*Amount desorbed from biosorbent, m_d (mg L^{-1})*	*Desorption efficiency (%)*
Cu			
Cycle 1	85	82	96
Cycle 2	83	79	95
Cycle 3	80	75	94
Ni			
Cycle 1	8	7	88
Cycle 2	10	9	90
Cycle 3	8	7	88
Zn			
Cycle 1	91	86	95
Cycle 2	92	85	92
Cycle 3	90	82	91
Co			
Cycle 1	69	65	94
Cycle 2	68	60	88
Cycle 3	65	60	92
Fe			
Cycle 1	99	92	93
Cycle 2	97	88	91
Cycle 3	94	84	89
Hg			
Cycle 1	22	20	91
Cycle 2	20	17	85
Cycle 3	15	12	80
U			
Cycle 1	19	15	79
Cycle 2	16	12	75
Cycle 3	12	8	67
Cr			
Cycle 1	65	60	92
Cycle 2	70	64	91
Cycle 3	68	60	88

Table 4.79c Calculated desorption efficiencies for the desorption of heavy metals from Bentonite- *P. simplicissimum* in fixed bed columns using 0.1 M HNO_3 at 25ºC; bed height 13 cm, flow rate 4 mL/min; contact time 540 minutes

Heavy metals	*Amount adsorbed from solution, m_{ads} (mg L^{-1})*	*Amount desorbed from biosorbent, m_d (mg L^{-1})*	*Desorption efficiency (%)*
Cu			
Cycle 1	99	95	96
Cycle 2	98	90	92
Cycle 3	97	89	92
Ni			
Cycle 1	69	65	94
Cycle 2	64	60	91
Cycle 3	62	58	87
Zn			
Cycle 1	97	92	95
Cycle 2	95	88	93
Cycle 3	92	85	92
Co			
Cycle 1	96	91	95
Cycle 2	93	85	91
Cycle 3	90	82	91
Fe			
Cycle 1	98	93	95
Cycle 2	96	90	94
Cycle 3	96	89	93
Hg			
Cycle 1	65	62	95
Cycle 2	62	56	90
Cycle 3	60	52	87
U			
Cycle 1	80	50	63
Cycle 2	78	45	58
Cycle 3	75	40	53
Cr			
Cycle 1	98	90	92
Cycle 2	93	80	86
Cycle 3	90	75	83

Table 4.79d Calculated desorption efficiencies for the desorption of heavy metals from Zeolite-*P. simplicissimum* in fixed bed columns using 0.1 M HNO_3 at 25°C; bed height 13 cm, flow rate 4 mL/min; contact time 540 minutes

Heavy metals	*Amount adsorbed from solution, m_{ads} (mg L^{-1})*	*Amount desorbed from biosorbent, m_d (mg L^{-1})*	*Desorption efficiency (%)*
Cu			
Cycle 1	93	90	97
Cycle 2	90	85	94
Cycle 3	92	85	93
Ni			
Cycle 1	65	62	95
Cycle 2	62	58	94
Cycle 3	60	55	92
Zn			
Cycle 1	94	85	90
Cycle 2	91	80	88
Cycle 3	89	78	88
Co			
Cycle 1	98	96	98
Cycle 2	96	90	94
Cycle 3	93	84	90
Fe			
Cycle 1	96	91	95
Cycle 2	92	84	91
Cycle 3	90	80	89
Hg			
Cycle 1	83	80	96
Cycle 2	80	75	94
Cycle 3	77	71	92
U			
Cycle 1	70	35	50
Cycle 2	65	30	46
Cycle 3	62	28	45
Cr			
Cycle 1	97	91	94
Cycle 2	93	85	91
Cycle 3	91	80	88

Table 4.79 shows that the total adsorption capacity, m_{ads}, of the natural and modified zeolite/ bentonite (after 540 min) was not drastically altered by regeneration. Desorption efficiencies for heavy metals removal were generally high. These could be further improved if optimised for practical applications. Cobalt gave the highest desorption efficiencies and uranium was the less desorbed, probably due to the solvent used. This is similar to the results obtained in batch desorption studies. As seen in the batch tests, the biosorbents investigated gave good adsorption efficiency even after the 3rd regeneration cycle. This is a positive toward the

determination of natural and modified zeolite/bentonite as a potential low cost adsorbent for heavy metal removal.

4.5.4.5 Mathematical models

Adsorption models are used to predict breakthrough curves of adsorption systems and capacity of adsorbent. The Bed Depth Service Time (BDST) model, mass transfer model, Thomas model and Yoon Nelson model are some of popular models used in column study. The BDST model analyses the system within service time. The mass transfer model analyses the behaviour of the system in the mass transfer zone. The mass transfer zone may be considered as a region inside the column in which the sorbate concentration changes from 10% to 90% of its inlet value (Naja and Volesky, 2006). Thomas and Yoon Nelson models analyse the behaviour of the whole breakthrough curve (Ramesh *et al.*, 2011).

In this study, a simple approach (BDST) has been proposed to correlate the service time, t, with the process variables. The original work on the BDST model was carried out by Bohart and Adams (1920) who proposed a relationship between bed depth, Z, and the time taken for breakthrough to occur. The service time, t, is related to process conditions and operating parameters by the following equation:

$$ln\left(\frac{Co}{Ct} - 1\right) = ln(e^{KNoZ/\mu} - 1) - KC_o t \qquad (4.14)$$

The linear relationship between the bed depth and service time can be written as follows (Hutchins, 1974):

$$t = \frac{NoZ}{Co\mu} - \frac{1}{KCo}\ln\left(\frac{Co}{Ce} - 1\right) \qquad (4.15)$$

where: t is the service time at breakthrough point, min; C_o and C_e are the initial metal concentration and effluent solute concentration respectively, mg L^{-1}; u is the linear velocity, cm min^{-1}; K adsorption rate constant, L [(mg min^{-1})]; N_o is the dynamic adsorption capacity, mg L^{-1} and Z column bed depth, cm.

Equation (4.15) shows how the service time and bed depth are correlated with the process parameters and initial solute concentration, solution flow rate and adsorption capacity. This equation can also be written in the form of a straight line:

$$t = mZ - b \quad (4.16)$$

Therefore, the dynamic adsorption capacity (N_o) and the adsorption rate constant (K) can be evaluated from the slope (m) and intercept (b) by plotting t versus Z, that is ($\ln \frac{Co}{Ce} - 1$).

Data collected during laboratory column tests were used to determine the BDST model parameters, namely BDST adsorption capacity (No) and rate constant (K) for Ni and U in multi-components solutions. These parameters are presented in Table 4.80.

Table 4.80 Values of BDST model parameters for the adsorption of Ni and U from multi-component solutions by natural and modified zeolite/bentonite at breakthrough, 12 cm column height and a flow rate of 2 mL min^{-1}

		Bentonite	
		Natural bentonite	***Bentonite-P.simplicissimum***
Ni	N_o *(mg g^{-1})*	1.849	2.302
	K [L(mg min^{-1})]	0.0084	0.0010
	R^2	0.921	0.692
U	N_o *(mg g-1)*	2.639	7.612
	K [L(mg min^{-1})]	0.0013	0.0011
	R^2	0.836	0.583
		Zeolite	
		Natural zeolite	***Zeolite-P.simplicissimum***
Ni	N_o *(mg g^{-1})*	2.814	5.417
	K [L(mg min^{-1})]	0.0029	0.0061
	R^2	0.960	0.893
U	N_o *(mg g^{-1})*	1.897	8.491
	K [L(mg min^{-1})]	0.0017	0.0095
	R^2	0.91	0.821

N_o was calculated with the unit mg L^{-1} and converted to mg g^{-1} by multiplying it with the column bulk density of 0.593 g cm^{-3} and 0.800 g cm^{-3} for bentonite and zeolite, respectively.

The calculated values of the adsorption capacity, N_o, are consistent for Ni and U with the observed values from column operation (Table 4.80) for adsorption on natural zeolite. The BDST model might be used to predict the column adsorption of nickel and uranium on natural zeolite. However, this model is not suitable for describing the adsorption of Ni and U on natural and modified bentonite as well as on zeolite-*P*. *simplicissimum* using the column mode. It is thus suggested that other models such as Thomas and Yoon Nelson models should be used.

Conclusion

The initial breakthrough points were obtained at almost the same time (30 minutes) for all the metal ions in solution for the natural zeolite as well as the natural bentonite. The breakthrough points increased with the modified zeolite/fungi, for instance, the breakthrough occurs after 1h (Ni), 2hrs (Hg), 3hrs (U) and 4 hrs (Cu, Zn, Co and Cr). The difference implies higher affinity of metal ions towards the modified materials.

Most of the calculated values of the loading capacity in column adsorption were close to those obtained in the batch tests.

The total amount of heavy metals adsorbed from solution after about 540 minutes, for the 3 cycles of adsorption-desorption, was more less the same. This indicates that the capacity of adsorbents investigated was not drastically affected by regeneration; neither its efficiency.

Successful design of a column adsorption process requires prediction of the concentration–time profile or breakthrough curve for the effluent. The BDST model was used successfully to fit the experimental data for Ni and U adsorbed on the natural zeolite.

Further studies

Operational conditions such as flow rate and bed height have to be assessed; the results from column studies could be affected by these parameters. Then, the volume treated to the breakpoint and the shape of breakthrough curve for various flow rates and bed depths can be compared.

Different models should be applied to predict the breakthrough curve and the error analysis will be used to compare the better model among them.

4.6 Augmentation of mine water remediation through biofunctionalisation of zeolite and bentonite with alginate extracts and green algae

This section reports results related to: the characterization of the green filamentous algae (*Oedogonium* sp.) from the West Boundary Dam in the West Wits mining complex, Johannesburg (Figure 3.2 and 3.3); the effects of contact time, pH, metals concentration and the study of kinetics as well as thermodynamics of adsorption. The characterization of extracted alginates (mannuronic and guluronic acids) from the green *Oedogonium* sp. algal biomass is presented. The sorption capacity of the novel environmentally-friendly commercial material, namely sodium alginate immobilized on zeolite was assessed. Kinetics and thermodynamic parameters were determined. Sodium alginate was used as proxy to assess the sorption capacity of the natural alginate.

4.6.1 Physical properties and elemental composition of the algal biomass

i) Surface area and elemental composition

The BET surface areas of the algal biomass *Oedogonium* sp. collected in the dam and stream were 1.44 and 1.21 m^2 g^{-1}, respectively. The algal biosorbent subjected to elemental analysis showed a composition consisting of carbon, nitrogen and sulphur as 24.9, 4.12 and 5.85% for *Oedogonium* sp. from the dam and 20.09, 3.05 and 4.36% for the algae from the stream. The % of moisture was 53.07 and 61.57 for *Oedogenium* sp. from the dam and from the stream, respectively.

The results indicate that the algal biomass from the dam exhibited higher surface area as well as higher percentage of C, N and S. The elemental composition could be affected by the nutrients present in the dam and the stream (Borchardt, 1996).

ii) IR spectra of Oedogonium sp.

In order to understand the surface binding mechanism, functional groups present on the biomass were characterized by FTIR. The FTIR spectra of the dried biomass, shown in Figure 4.98, revealed the surface heterogeneity of the biosorbents with evidence of different characteristic peaks with the possible presence of several functional groups such as amino, carboxyl, hydroxyl, phosphate and carbonyl groups.

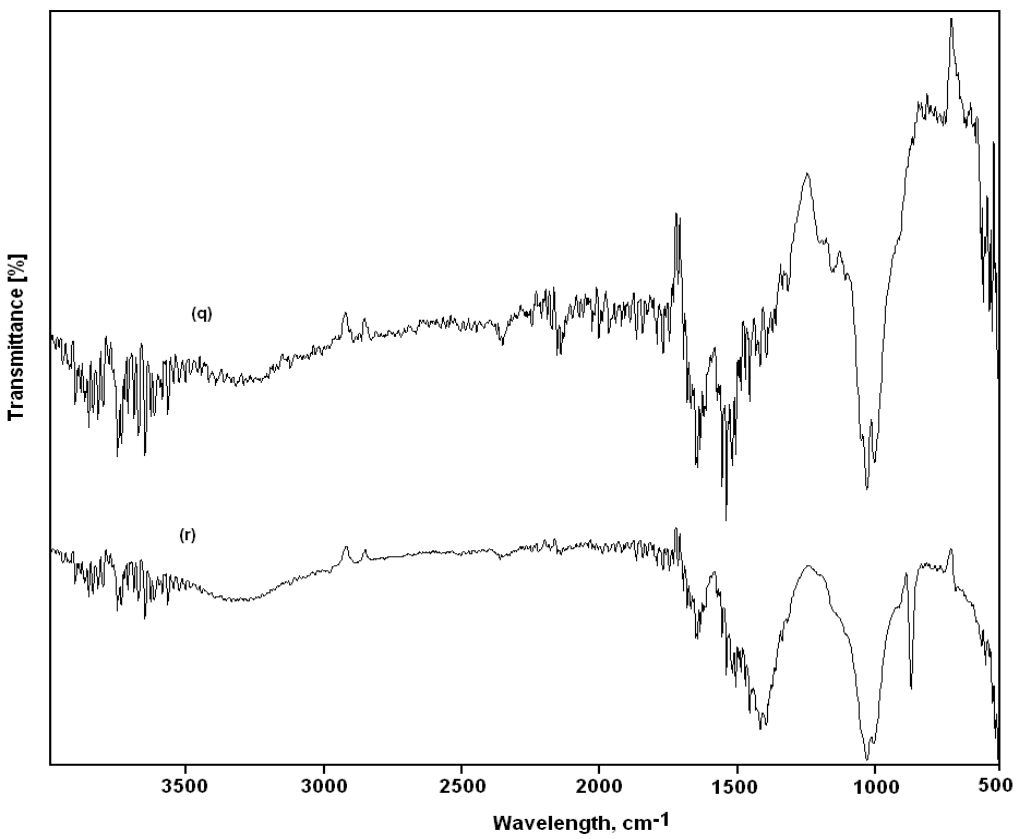

Figure 4.98 FTIR spectra of (q) *Oedogonium* sp. from the stream and (r) *Oedogonium* sp. from the dam

The IR absorption bands and corresponding possible groups able to interact with protons or metal ions are presented in Table 4.81. Several functional groups were found in the structure of *Oedogonium* sp. such as carboxylic acid, hydroxyl, amine and amido groups. The strong bands in the region 3336 cm^{-1} are indicative of the existence of –OH groups of glucose and –NH groups of proteins (Deng and Ting, 2005). The strong absorption peak at 2917–2925 cm^{-1} can be assigned to phenolic/carboxylic stretching and those at 1683–1623 cm^{-1} to C=O chelate stretching of carboxyl groups, respectively (Yee *et al.*, 2004). The absorption peaks at 1646 and 1507 cm^{-1} can be attributed to amide I and amide II bands of protein peptide bonds as suggested by Yee *et al.* (2004). The absorption peak at 1488–1497 cm^{-1} was assigned to the asymmetric bending of the CH_3 of the acetyl moiety. The strong absorption peaks at 1032 cm^{-1} and 1007 cm^{-1} can be assigned to the C–C and –CN stretching vibration of the protein fractions, respectively. Some bands in the finger print region can be attributing to the phosphate groups.

A strong peak was observed at 872 cm^{-1} in the spectrum of the algal from the dam, this peak made the main difference between the two spectra. The analysis of the FTIR spectra showed the presence of ionisable functional groups (i.e. carboxyl, amino, amide and hydroxyl) able to interact with protons or metal ions. The above results give an idea about the presence of functional groups on the algal cell surfaces and on the mechanism of adsorption which is dependent on functional groups especially carboxyl. The spectra show that the structure of algal wall is very complex. The study done by Pearlmutter and Lembi (1980) on P. *Oedogonia* revealed that the outer wall of P. *Oedogonia* contains chitin in addition to N-acetylgalactosamine, protein and phosphosphate whereas the inner wall is the major site of polysaccharide (i.e. glucose, fructose, xylose, mannose) deposition.

Table 4.81 IR adsorption bands for *Oedogonium* sp. from the dam and the river with the corresponding possible groups

Wavenumber (cm^{-1}) Oedogonium from the dam	***Wavenumber (cm^{-1}) Oedogonium from the river***	***Functional groups***
3627-3647	3621-3695	O-H stretching
3342	3352	Carboxylic/OH strech strech and N-H strech
2922-2980	2924	Phenolic/carboxylic
2364		
1623	1661-1634	C=O chelate streching, amide I band, C=C, >C==N
1644	1647-1651	
1506	1418-1575	Amide II band, OH bonds
1032-1055	1032-1005	=C-N< stretching
872		Plane deformation
711-555	555	

4.6.2 Metal analysis

The cold digestion procedure was used to analyse metals in oven-dried algae. The results are given in Table 4.82.

Table 4.82 Results of metals analysed in water and fresh algae from dams and stream

	Dam		***Stream***		***Limit (SAWQG,1996)***
	Oedogonium sp. (mg g^{-1})	Water (mg L^{-1})	*Oedogonium* sp. (mg g^{-1})	Water (mg L^{-1})	(µg L^{-1})
Ag	0.021	0.085	0.018	0.071	
Al	0.660	2.640	0.958	3.340	0-5000
As	0.010	0.041	0.010	0.040	0-100
Au	0.247	0.988	0.231	0.923	
Ca	19.00	141.8	11.50	105.4	
Co	0.355	1.420	0.450	1.800	0-50
Cr	0.251	0.315	0.026	0.102	
Cu	0.029	0.157	0.043	0.179	0-200
Fe	3.725	14.80	7.325	29.30	
Mg	12.60	50.40	6.550	26.20	
Mn	51.55	206.2	47.98	191.9	0-20
Na	1.150	40.00	0.725	49.00	
Ni	0.420	1.680	0.260	0.644	0-200
P	9.850	39.40	11.83	34.20	
Pb	0.014	0.056	0.024	0.091	0-200
Pt	0.001	0.005	0.002	0.009	
Ru	0.025	nd	0.039	nd	
S	38.28	153.1	37.15	148.6	
Se	0.004	nd	0.010	nd	0-20
Si	0.139	0.557	0.046	0.182	
Zn	0.735	2.940	0.923	3.214	0-1000

n.d - not detected; RSD < 5%

The results showed that in general, the concentration of metals analysed were higher in water samples than in filamentous algae. The results point to pollution of the dam and the stream by toxic elements, with concentrations higher than the regulated limit by the Department of Water Affairs (SAWQG, 1996).

4.6.3 Sorption studies of heavy metals on algal biomass

The efficacy of *Oedogonium* sp. in removing heavy metals was investigated in pre-treated and non-pretreated biomass.

4.6.3.1 Effects of pre-treatment on sorption capacity of the biomass

Living biomass of *Oedogonium* sp. was subjected to various pre-treatments, i.e. H_2O (de-ionised), CH_3COOH and $H_2C_2O_4$ with a view to enhance its metal sorption capacity. The adsorption capacities obtained after pre-treatment of the living biomass of *Oedogonium* sp. with selected chemicals are listed in Table 4.83. It is evident that pre-treatment with acetic acid did not substantially increase metal sorption capacity of the biomass. A similar trend was obtained by Gupta (2008) following HCl and HNO_3 treatment; whereas pre-treatment with oxalic acid enhanced the adsorption capacity of the biomass. The increase ranges between 31 to 38%, with the following distribution (%): Fe (39.4), Cu and U (38), Co (36.4), Hg (35.04), Ni (31.32), Zn (30.84), Cr (26.5). This observation agrees with that for Mehta *et al.* (2002) who reported a 39% increase in metal binding capacity following acid pre-treatment.

Table 4.83 Effect of various pre-treatments on metals sorption capacity of *Oedogonium* sp.

		Pre-treated agent	
Metal-ion	***D-H_2O***	***CH_3COOH***	***$H_2C_2O_4$***
	q_e (mg g^{-1})	q_e (mg g^{-1})	q_e (mg g^{-1})
Cu^{2+}	45.22	46.20	62.54
Co^{2+}	44.30	44.85	60.46
Cr^{3+}	46.54	47.52	58.89
Fe^{3+}	50.23	49.31	70.01
Hg^{2+}	35.65	38.45	48.14
Ni^{2+}	38.95	41.26	51.15
Zn^{2+}	42.31	45.23	55.36
UO_2^{2+}	35.44	39.42	48.92

4.6.3.2 Sorption capacity, pH and isotherms

In order to study the biosorption capacity of the *Oedogonium* sp. algal biomass, the samples collected from the dam were used. The effect of pH, metal concentration, contact time, temperature and the algal mass were assessed. The desorption of metals as well as the regeneration of the biomass for re-use were investigated.

i) Effect of pH

As eluded previously, one of the most significant factors influencing heavy metals adsorption is pH. It affects, among others, the degree of functional group dissociation, the form and adsorption of the metals (Banes, 1980). In this study, the effect of pH on the biosorption of Cu, Co, Cr, Fe, Hg, Ni, Zn and U (in single- and multi-component system) on the living biomass was studied in the pH range 2 to 7. Studies could not been carried out in the alkaline range because of hydroxyl metal-complex formation.

As seen in Figure 4.99, the uptake of Cr, Cu, Ni and Zn on *Oedogonium* sp. increases from pH 2-5 and then declined with further increase of pH. This may be caused by an increase in functional group dissociation in this range of pH. As an example, let us consider α-carboxyl groups of amino acids whose pKa is about 2 while that for non α -carboxyl groups pK is about 4. The former are dissociated at pH 3 up to 88.8% but the latter only up to 9%. At pH 4, the groups with pK 2 can be dissociated up to 98% while those with pK 4 by only up to 50%.

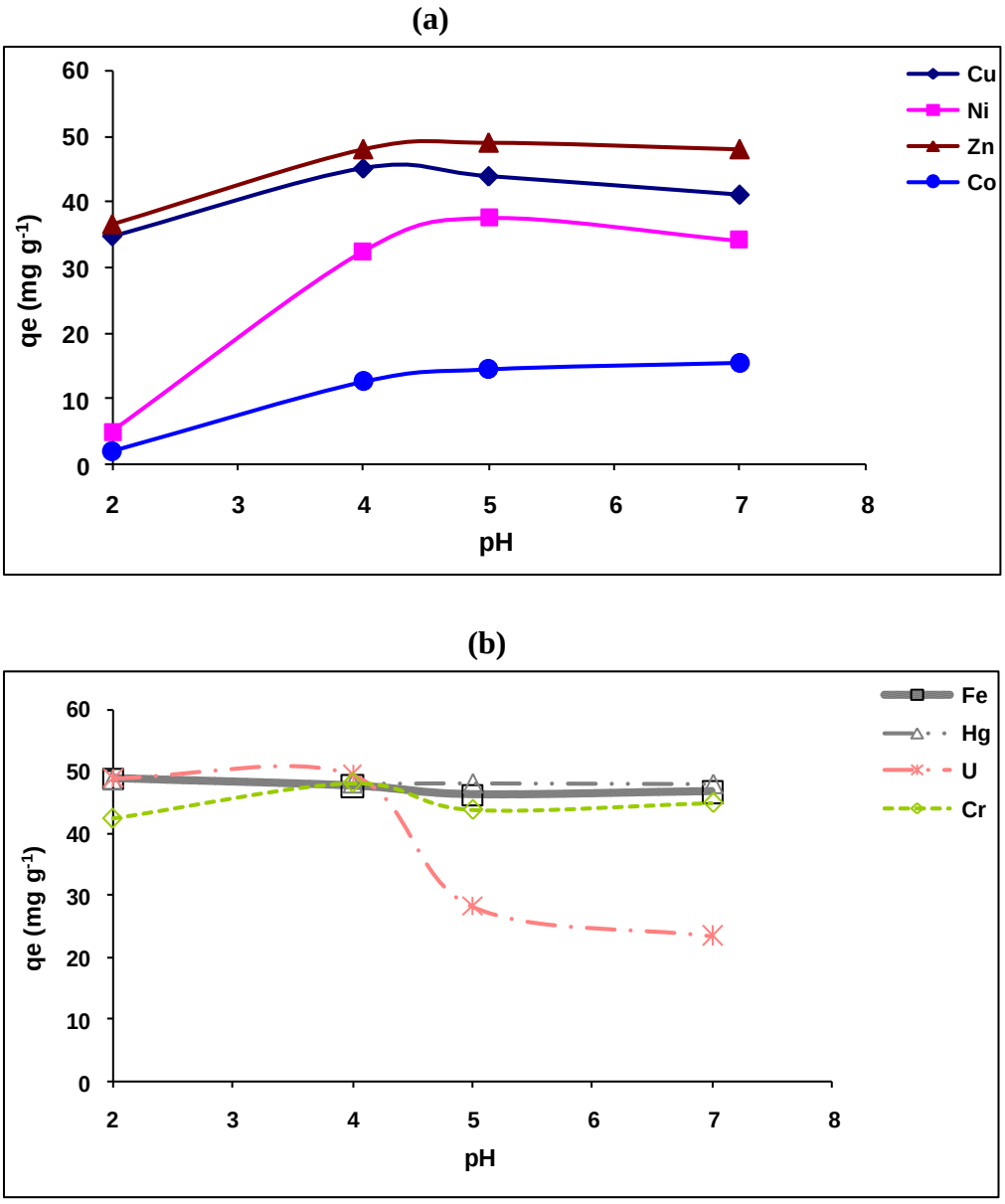

Figure 4.99 Effect of pH on the biosorption of (a) Cu, Co, Ni, Zn (b) Cr, Fe, Hg, U for *Oedogonium* sp. in single-component solutions (C_i = 100 mg L^{-1}, pH = 3, algal mass = 1 g, Temp = 25 ^{o}C)

In the pH area close to the pK value, slight changes in acidity may affect the degree of group dissociation significantly. Thus at pH 6, both carboxyl groups are dissociated by more than 90%. It has been stated that COO^{-} groups play the main part in metal binding through the cell wall of *Oedogonium* sp. It is quite probable they may contribute to the metals binding by algae (Beveridge and Murray, 1980). The adsorption capacity for U decreased drastically above pH 4. While higher pH would imply better adsorption, U tends to form negatively

charged complexes at high pH values (as shown in Figure 4.100). These tend to be repelled at the negative surface of the biomass, thus reducing adsorption significantly.

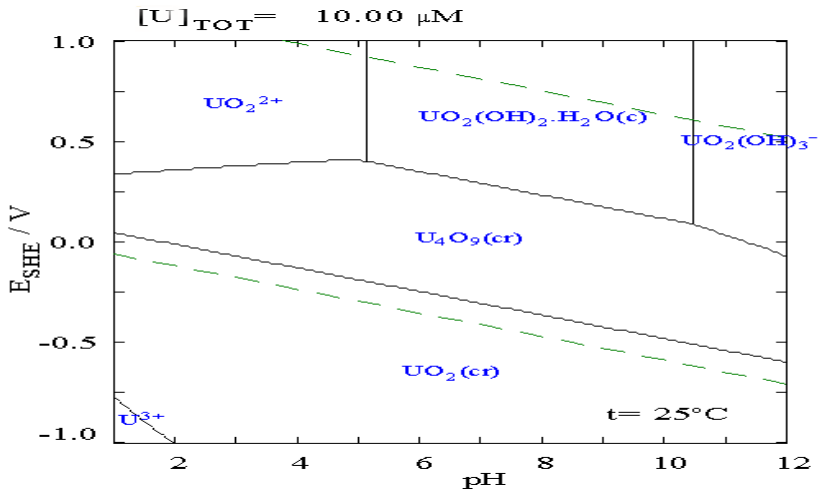

Figure 4.100 Eh-pH diagram for uranium in water at 25°C (Langmuir, 1997)

The adsorption capacities of Hg and Fe were constant for the range of pH studied. In fact, the presence and abundance of functional groups susceptible to bind a specific metal is a major factor on the binding capacity of the biomass as explained in the previous sections. Fe forms hydroxide complexes at pH 2, which is its hydrolysis pH. Thus, precipitation could also contribute to enhance the uptake of iron at low pH.

Solution pH influences both cell surface metal binding sites and metal chemistry in water. At low pH, cell wall ligands were closely associated with the hydronium ions (H_3O^+) and restricted the approach of metal cations as a result of the repulsive force. As the pH is increased, more ligands such as carboxyl, phosphate, imidazole and amino groups would be exposed and carried negative charges with subsequent attraction of metallic ions with positive charge and biosorption onto the cell surface (Aksu, 2001; D'onmez *et al*., 1999).

Different metal ions may have different pH optima due to the different solution chemistry of the species. The initial pH optimum for biosorption is also micro-organism dependent because of different adsorptive sites of different species of micro-organisms. The increase in metal ions biosorption at higher pH values (5–6) may be explained by the ionization of functional groups on the cell surface which serve as the binding sites related to the isoelectric point of the cells. Metal ions have a strong affinity for proteins of the cell wall. At pH values above the isoelectric point, there is a net negative charge on the cell surface and the ionic state of ligands such as carboxyl, phosphoryl, sulfhydryl, hydroxyl, and amino groups will

promote reaction with metal cations. As the pH is lowered, the overall surface charge on the cells will become positive, which will inhibit the approach of positively-charged metal cations.

The decrease in biosorption at higher pH (pH > 5) may also be due to the formation of soluble hydroxylated complexes of the metal ions and their competition with the active sites, and as a consequence, the retention would decrease again.

The effect of pH on the biosorption of Cu, Co, Cr, Fe, Hg, Ni, Zn and U onto the biomass of *Oedogonium sp*. in multi-component solutions is shown in Figure 4.101. The adsorption capacity was constant for all the metal ions, except for Ni. This phenomenon was observed and explained in the previous sections.

(a)

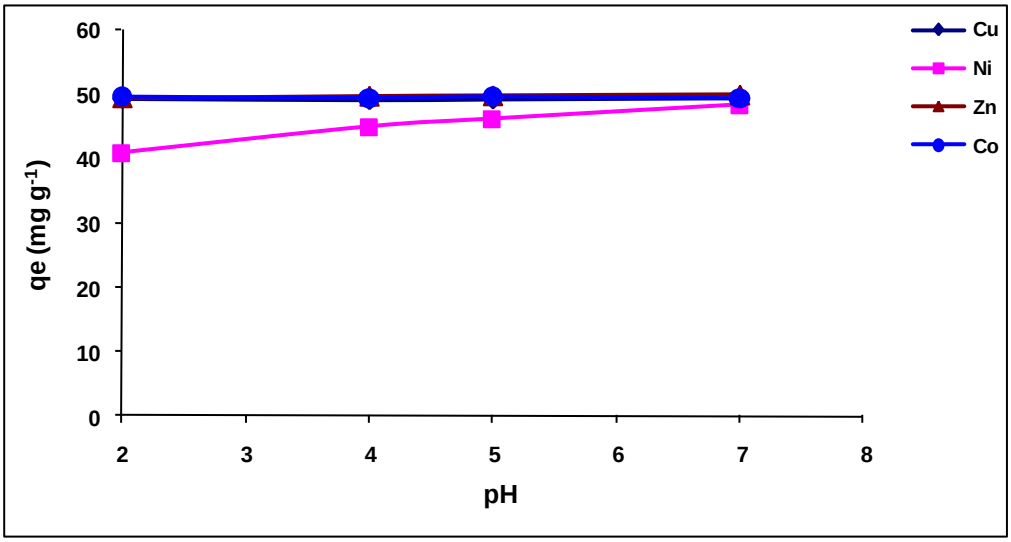

(b)

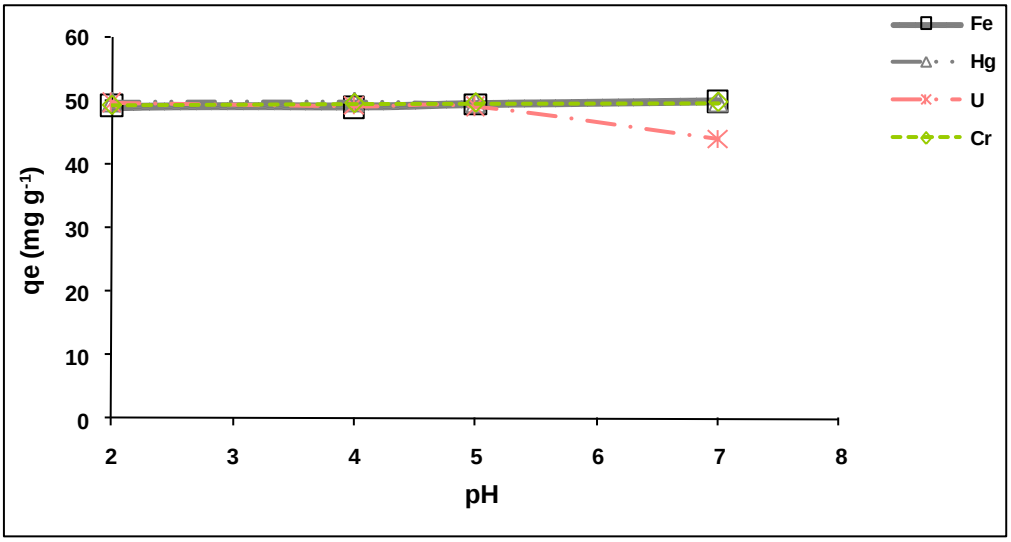

Figure 4.101 Effect of pH on the biosorption of (a) Cu, Co, Ni and Zn (b) Cr, Fe, Hg and U for *Oedogonium* sp. in multi-component solutions (C_i = 100 mg L^{-1}, pH = 3, algal mass = 1 g, Temp = 25 ^oC)

ii) Effect of metal concentration

The plots of initial concentration versus adsorption capacity at pH 3 for the biosorption of Cu, Ni, Zn, Co, Fe, Hg, Cr and U are shown in Figure 4.102 for the single-ion system.

(a)

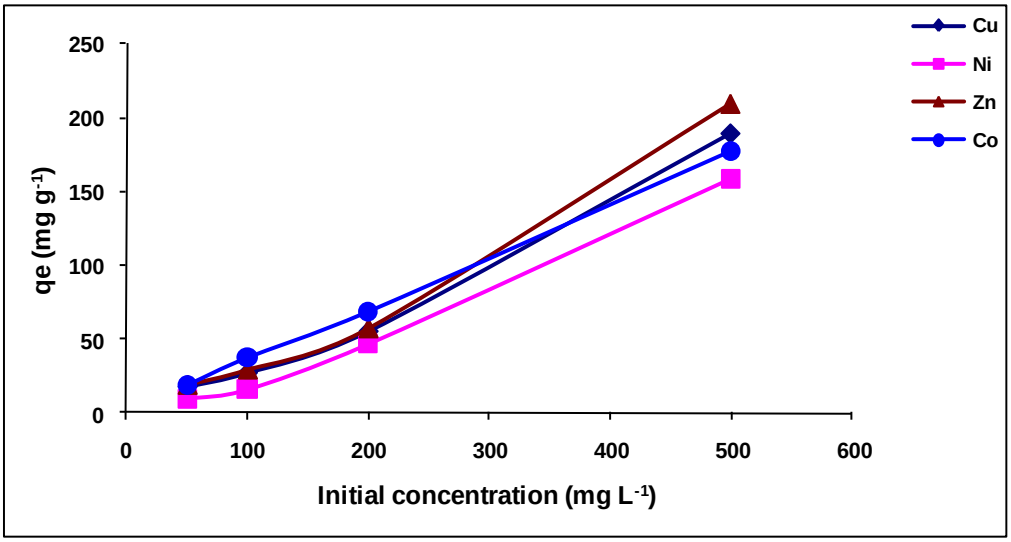

(b)

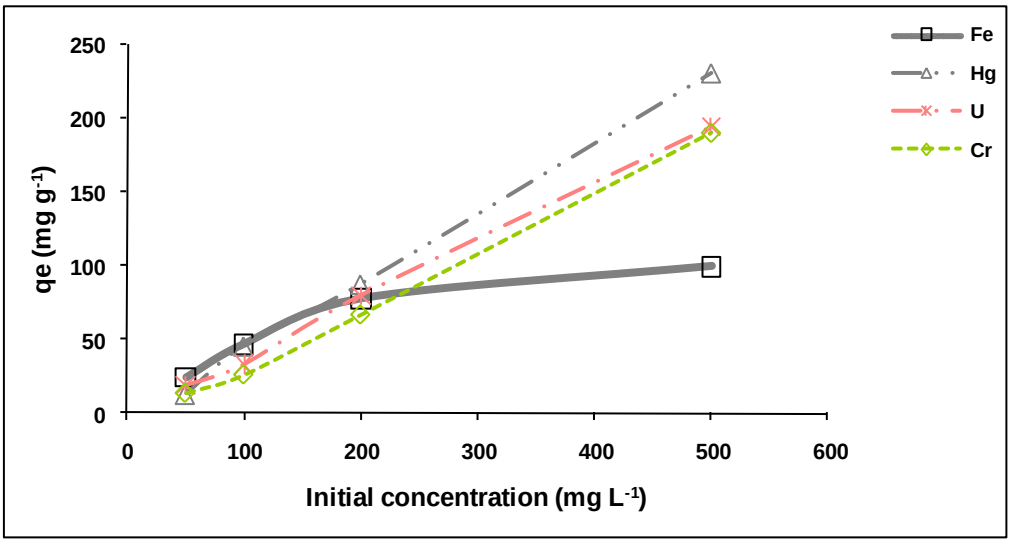

Figure 4.102 Effect of concentration on the biosorption of (a) Cu, Co, Ni, Zn (b) Cr, Fe, Hg, U for *Oedogonium* sp. in single component solutions (C_i = 100 mg L^{-1}, pH = 3, algal mass = 1 g, Temp = 298.15 ^{o}K)

The trend observed was that the biosorption of Fe showed a fairly rapid rise in adsorbed amount with increasing concentration up to saturation (200 mg L^{-1}) characterized by a plateau that is nearly or quite horizontal, assuming monolayer coverage. This observation is in good agreement with the experimental parameters given in Table 4.84.

For the rest of the metals, we can note that the adsorption capacity increases with an increase in metal concentration. The positive curvature indicates that the value of *n* is greater than unity. We can suppose that the adsorption takes place with only one energy level or a set of

energies but very close, assuming that the number of adsorbed molecules per site is finite (Khalfaoui *et al.*, 2003).

The biosorption of Cu, Co, Cr, Fe, Hg, Ni, Zn and U in multi-component solutions are shown in Figure 4.103.

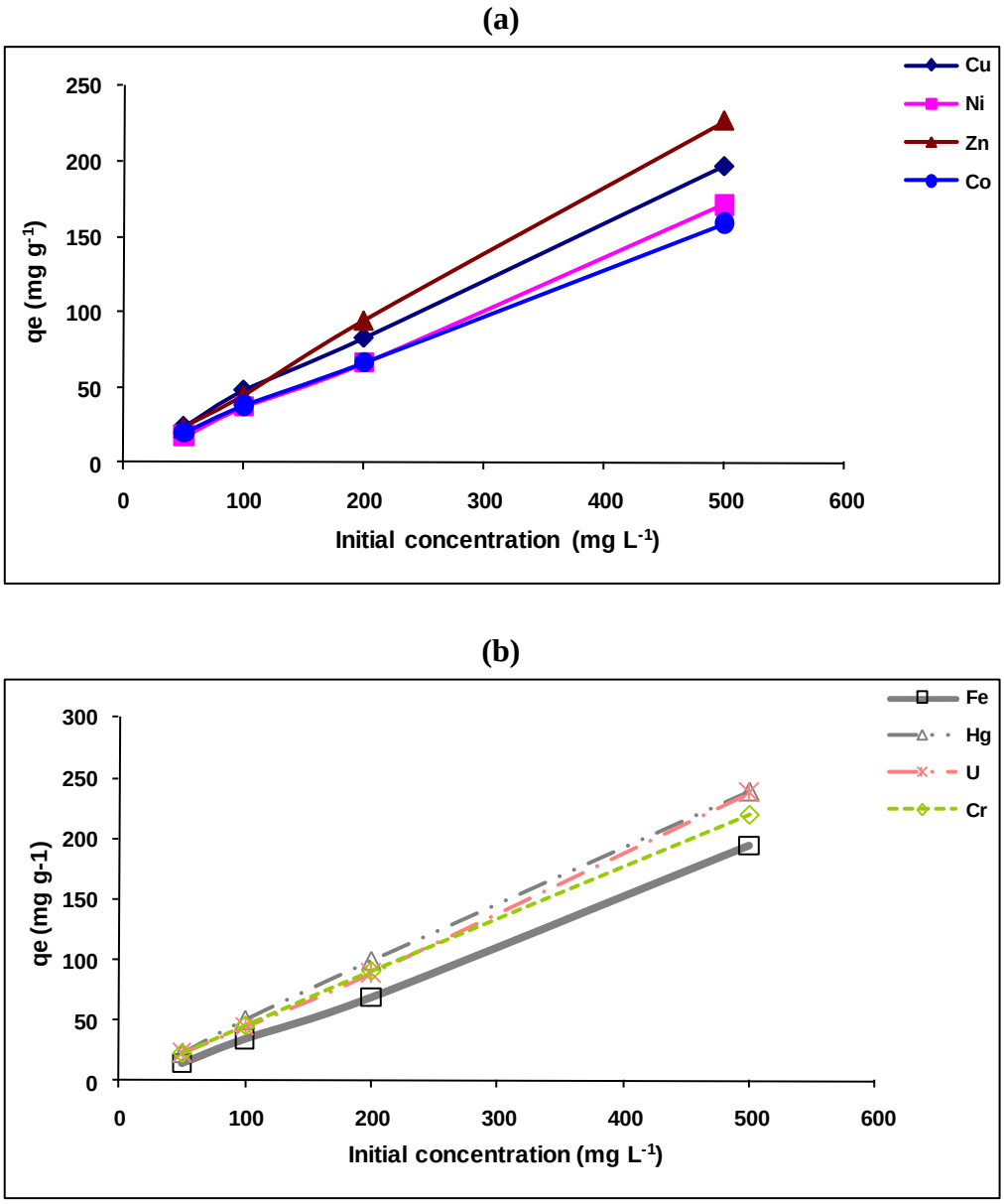

Figure 4.103 Effect of concentration on the biosorption of (a) Cu, Co, Ni and Zn (b) Cr, Fe, Hg and U for *Oedogonium* sp. in multi- component solutions (C_i = 100 mg L^{-1}, pH = 3, algal mass = 1 g, Temp = 298.15^{o}K)

The adsorption capacity for all the metal ions increases linearly with an increase in metal concentration.

iii) Isotherms of metal adsorption on Odoegonium sp.

The experimental results were fitted to the Langmuir and Freundlich and D-R sorption isotherm models. The parameters determined for the biosorption of Cu, Co, Cr, Fe, Hg, Ni, Zn and U (in single-metal solutions) on algal biomass at different initial concentrations are tabulated in Table 4.84.

Table 4.84 Parameters of the Langmuir, Freundlich and D-R models for the adsorption of metals *Oedogonium* sp. in single-ion systems

Langmuir Isotherms	***Fe***	***Cu***	***Co***	***Hg***	***Ni***	***Zn***	***U***	***Cr***
A	0.146	0.183	0.119	0.098	0.423	0.381	0.105	0.191
B	4.269	3.690	2.172	25.69	2.461	8.076	7.396	1.815
b	29.07	20.15	18.21	262.9	5.824	21.17	70.18	9.497
qm (mol/kg)	0.234	0.271	0.460	0.038	0.406	0.124	0.135	0.551
ΔGo (kJ/mol)	-8.353	-7.445	-7.194	-13.81	-4.367	-7.568	-10.54	-5.580
Δq (%)	67.67	67.26	67.24	67.39	67.22	67.50	67.23	67.22
r	0.999	0.560	0.569	0.656	0.833	0.995	0.535	0.877
Freundlich Isotherms	***Fe***	***Cu***	***Co***	***Hg***	***Ni***	***Zn***	***U***	***Cr***
A	0.003	0.050	0.058	0.011	0.064	-0.003	0.041	0.058
B	0.262	0.352	0.321	0.362	0.432	0.375	0.414	0.342
K_f	1.007	1.123	1.143	1.026	1.160	0.993	1.098	1.142
n	3.821	2.835	3.115	2.764	2.312	2.667	2.416	2.929
ΔGo (kJ/mol)	-9.471	-7.029	-7.723	-6.853	-5.731	-6.611	-5.989	-7.260
Δq (%)	13.37	48.67	46.97	69.92	69.46	16.19	52.45	72.75
r	0.962	0.984	0.995	0.995	0.958	0.977	0.959	0.975
D-R Isotherms	***Fe***	***Cu***	***Co***	***Hg***	***Ni***	***Zn***	***U***	***Cr***
A	0.226	0.095	0.122	0.009	0.177	-0.222	0.075	0.185
B	-0.004	-0.008	-0.007	0.006	-0.011	-0.007	-0.007	-0.008
Xm (mol/kg)	0.797	1.102	1.130	1.001	1.194	0.801	1.078	1.204
Es (kJ/mol)	10.90	7.972	8.435	8.882	6.829	8.182	0.218	7.772
Δq (%)	33.22	37.43	21.24	84.66	44.32	46.12	31.42	46.19
r	0.983	0.868	0.992	0.380	0.946	0.936	0.955	0.967
K_d	***Fe***	***Cu***	***Co***	***Hg***	***Ni***	***Zn***	***U***	***Cr***
A	3.878	1.596	2.363	1.405	1.067	2.652	2.171	1.306
B	35.42	2244	1518	3128	1430	172.8	9807	2274
ΔGo (kJ/mol)	-9.613	-3.956	-5.858	-3.485	-2.664	-6.576	-5.381	-3.238
Kdo	48.33	4.933	10.63	4.078	2.906	14.17	8.765	3.692
Δq (%)	71.88	63.61	103.2	102.5	70.65	76.88	108.6	11.10
r	0.915	0.562	0.598	0.353	0.903	0.962	0.341	0.923

Based on the correlation coefficient, the experimental data fits well the Freundlich model with r > 0.950, except for Fe. The biosoption of Cu, Co, Cr, Ni, Zn, U and Hg on the *Oedogonium* sp. biomass occurs on a heterogeneous surface, where different sites could have different energies. The adsorption of iron is well described by the Langmuir isotherm with r =

0.999, this result confirms the shape of the curve observed in Figure 4.103 (a), assuming a monolayer adsorption on homogenous surface, a constant free-energy change (ΔG^o ads) for all the adsorption sites. According to *b* (L mg^{-1}) parameter the affinity of metals on algae cells produced this sequence: Hg > U > Fe > Zn > Cu > Co > Cr > Ni. The D-R isotherm can also describe the biosorption of Fe, Co, U and Cr.

The maximum adsorption (mol kg^{-1}) capacities obtained from the Langmuir isotherm are in the sequence as follow: Cr > Co > Ni > Cu > Fe > U > Zn > Hg. The biosorption of most of the metals was spontaneous (ΔG^o negative) and occurring on heterogenous surface. The values of *n* range from 2.312 to 3.821 with the value of $1/n < 1$, indicating metal binding to sites with weak free energies.

The values of the mean free energy (Es) obtained from the D-R isotherm were less than 16 kJ mol^{-1}, confirming an ion exchange mechanism. With respect to the distribution coefficient, the sequence is in the order: Fe > Zn > Co > U > Cu > Hg > Cr > Ni. The different constants and correlation coefficients for the biosorption of Cu, Co, Cr, Fe, Hg, Ni, Zn and U (in multi-ion system) on *Oedogonium* sp. biomass are listed in Table 4.85. Contrary to the single-ion system, the biosorption of Fe and U was not described by the above isotherm models. Other isotherms could be used to fit the data. The experimental data for the biosorption of Cu, Co, Cr, Hg, Ni and Zn fit well the Freundlich as well as the D-R isotherms, meaning that these metals are bound on heterogeneous surface with ion exchange being the main process; the values of free energy range between 8 and 11 kJ mol^{-1}. The maximum metals uptake as calculated from the Langmuir isotherm is in the order of: Cr > Zn > Ni > Cu > Co > Hg > Fe> U. The affinity of metal ions in the multi-ion system on *Oedogonium* sp. algae cells followed the order: Hg > U > Zn > Fe > Cu > Cr > Ni > Co. As in the single-ion system, Hg and U showed high affinity for the algae cells. The affinity depends strongly on the functional groups present on the cell surface. The values of the distribution coefficient were higher than those obtained in the single-ion system.

Table 4.85 Parameters of the Langmuir, Freundlich and D-R models for the adsorption of metals *Oedogonium* sp. in multi–ion system

Langmuir Isotherms	***Fe***	***Cu***	***Co***	***Hg***	***Ni***	***Zn***	***U***	***Cr***
A	0.125	0.043	0.128	0.009	0.132	0.026	0.028	0.033
B	7.061	2.447	2.558	5.306	2.240	1.789	10.89	1.469
b	56.64	56.72	19.94	562.3	16.98	66.89	383.5	45.05
qm (mol/kg)	0.142	0.409	0.391	0.188	0.446	0.559	0.091	0.681
ΔGo (kJ/mol)	-10.01	-10.01	-7.491	-15.69	-7.021	-10.42	-14.75	-9.438
Δq (%)	67.32	67.40	67.28	67.27	67.24	67.25	67.24	67.25
r	0.310	0.909	0.894	0.996	0.577	0.439	0.594	0.999
Freundlich Isotherms	***Fe***	***Cu***	***Co***	***Hg***	***Ni***	***Zn***	***U***	***Cr***
A	-0.034	0.054	0.053	0.045	0.057	0.054	0.034	0.0625
B	0.254	0.259	0.322	0.298	0.327	0.252	0.344	0.242
K_f	0.924	1.133	1.131	1.110	1.141	1.134	1.083	1.155
n	3.929	3.866	3.108	3.347	3.055	3.969	2.907	4.118
ΔGo (kJ/mol)	-9.739	-9.583	-7.703	-8.296	-7.572	-9.838	-7.207	-10.21
Δq (%)	127.1	35.08	35.80	49.68	47.71	56.43	53.67	55.23
r	0.321	0.965	0.996	0.993	0.991	0.956	0.912	0.998
D-R Isotherms	***Fe***	***Cu***	***Co***	***Hg***	***Ni***	***Zn***	***U***	***Cr***
A	-0.205	0.014	0.064	0.084	0.117	0.142	0.081	0.168
B	-0.004	-0.004	-0.007	-0.004	-0.007	-0.005	-0.006	-0.005
Xm (mol/kg)	0.815	1.014	1.066	1.088	1.124	1.153	1.084	1.183
Es (kJ/mol)	10.17	10.62	8.577	10.62	8.323	10.28	9.428	10.18
Δq (%)	134.5	19.29	11.97	20.44	21.74	34.98	32.31	30.07
r	0.352	0.961	0.992	0.997	0.989	0.954	0.906	1.000
K_d	***Fe***	***Cu***	***Co***	***Hg***	***Ni***	***Zn***	***U***	***Cr***
A	2.392	3.787	2.626	4.139	2.348	3.309	2.042	3.267
B	3621	1382	960.8	3830	1335	6175	5685	3457
ΔGo (kJ/mol)	-5.929	-9.388	-6.511	-10.26	-5.822	-8.203	-5.061	-8.099
Kdo	10.93	44.13	13.83	62.79	10.47	27.36	7.702	26.25
Δq (%)	155.3	77.82	90.49	102.6	99.78	138.5	98.01	22.91
r	0.522	0.855	0.867	0.994	0.591	0.747	0.731	0.998

4.6.3.3 Effect of contact time and kinetics of adsorption

i) Effect of contact time

The plot of adsorption capacity of biomass in contact with each metal solution (in single-ion solution) with respect to the residence time is given in Figure 4.104.

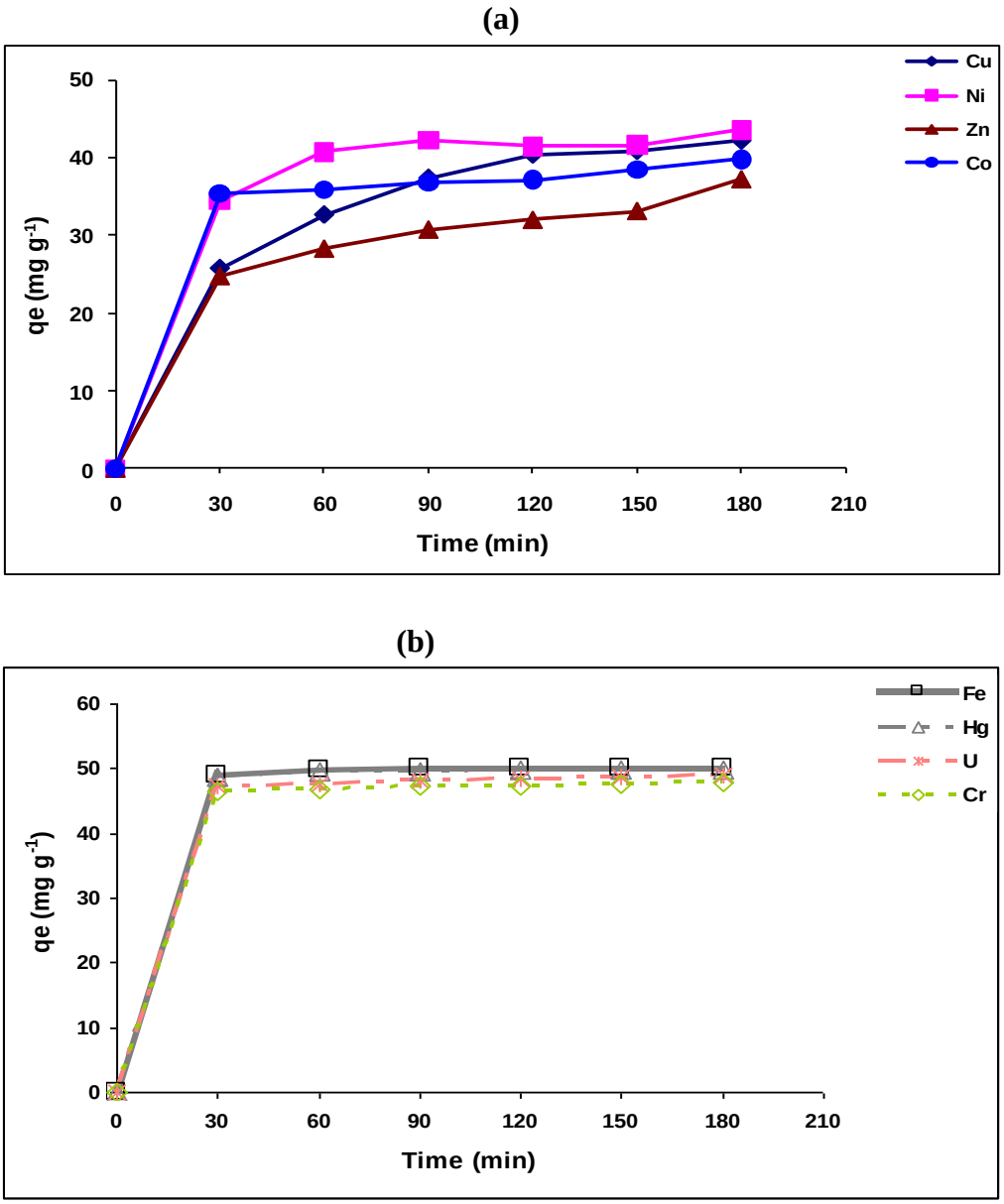

Figure 4.104 Effect of contact time on the biosorption of (a) Cu, Co, Ni and Zn (b) Cr, Fe, Hg and U for *Oedogonium* sp. in single-component solutions (C_i = 100 mg L^{-1}, pH = 3, algal mass = 1 g, Temp = 25^{o}C)

The biomass in contact with each metal solution decreased the metal concentration until equilibrium was reached after 3 h. A maximum adsorption was reached after 30 minutes of contact. The biosorption occurred in 2 steps: the first step corresponding to the dissociation of the complexes formed between metals in solution and water hydronium ions followed by the interaction of the metal with algal functional groups. Since biosorption is a metabolism-independent process, it would be expected to be a very fast reaction. Experimental kinetic data for the free biomass coincided with this expectation, with more than 99% of metal ions

removed in the first 30 min. This initial quick phase was followed by slow attainment of equilibrium as a large number of vacant binding sites were initially available for sorption; but thereafter, the occupation of the remaining vacant sites were difficult to occupy due to the repulsive forces between the metal ions in the solid and bulk phases. Most importantly, the metal ions should have access to all possible binding sites, even at a slower rate.

The preference or selectivity of metals by algae depends on the number of functional groups present in the algal cell walls. From the IR characteristics, *Oedogonium* sp. has functional groups as: ester (C-O), amine (C-N), hydroxyls (O-H) and alkyne (C≡C). Carboxyls and hydroxyls (Ligands of Class A) form strong bonds with soft ions whereas ester and amides (Ligands of Class B) form strong bonds with hard ions. Except for Hg and U which are soft and hard ions, respectively, the rest of the metals studied fall under the category of borderline/intermediate ions. They do not form strong bonds with Class A and B ligands. Live algae cells induce metabolism-dependent biosorption, where metal adsorption could be attributed to extra/intracellular accumulation, precipitation or cell surface sorption (Afkar *et al.*, 2010).

The biosorption in a multi-ion system is shown in Figure 4.105. A similar trend was observed as for the adsorption in single-ion system with an increase of adsorption capacity.

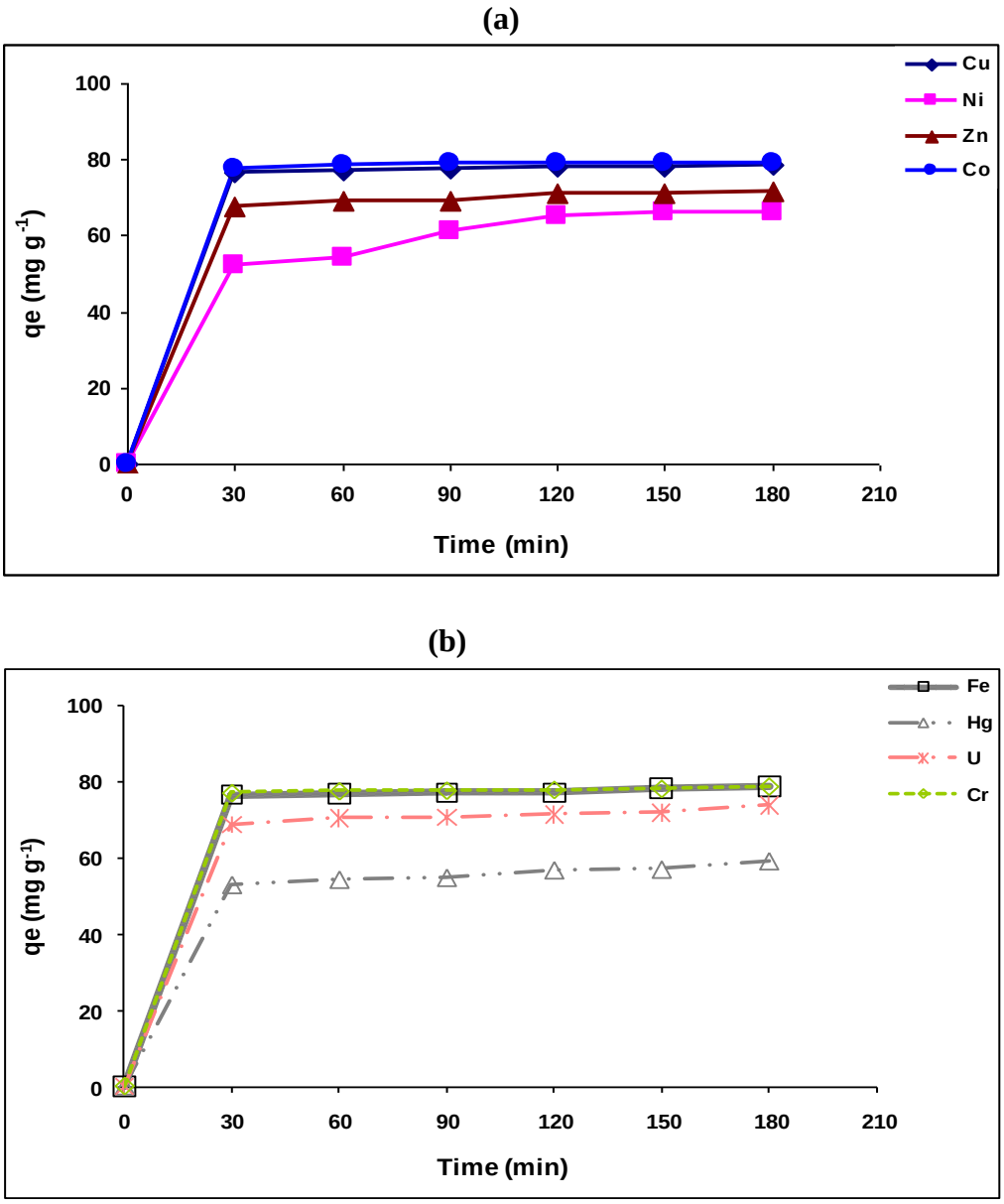

Figure 4.105 Effect of contact time on the biosorption of (a) Cu, Co, Ni, Zn (b) Cr, Fe, Hg, U for *Oedogonium* sp. in multi- component solutions (C_i = 100 mg L^{-1}, pH = 3, algal mass = 25 g, Temp = 25^{o}C)

ii) Kinetic modelling of the adsorption of metal ions on Odoegonium sp.

In order to reach a conclusion about the controlling mechanism of the biosorption process, kinetic models are used to test the experimental data. The high heterogeneity of surface groups on the algal cell wall (carboxyl, hydroxyl, phosphate, imidazole and amino groups) suggests that there are many types of biosorbent-metal ion interactions. The sorption kinetic

models used in this study are: pseudo first-order, pseudo second-order, Elovich, intraparticle diffusion and film diffusion models. The parameters and constants obtained from the experimental data (in single-ion systems) are presented in Table 4.86.

Table 4.86 Kinetic constants for the adsorption of metal ions on *Oedogonium* sp. (in single-ion system)

Pseudo-first order								
	Fe	***Cu***	***Co***	***Hg***	***Ni***	***Zn***	***U***	***Cr***
A	-2.711	-2.604	-2.065	-3.750	-2.184	-2.413	-3.428	-2.453
B	-0.019	-0.005	-0.004	-0.012	-0.004	-0.003	-0.006	-0.007
q_e (mol/kg)	0.002	0.002	0.009	0.003	0.007	0.004	0.001	0.004
K_1	0.044	0.013	0.010	0.028	0.009	0.007	0.014	0.016
Δq (%)	91.12	79.54	85.13	91.19	86.73	81.57	90.36	89.64
r	0.874	0.860	0.744	0.841	0.614	0.779	0.706	0.747
Pseudo – second order								
	Fe	***Cu***	***Co***	***Hg***	***Ni***	***Zn***	***U***	***Cr***
A	1.728	907.4	90.14	30.88	86.43	907.7	128.4	12.19
B	8.591	70.37	13.79	96.02	14.65	47.68	86.51	11.61
q_e (mol/kg)	0.116	0.014	0.073	0.011	0.068	0.021	0.012	0.086
K_2	42.71	5.457	2.112	298.5	2.482	2.505	58.29	11.05
Δq (%)	0.591	6.804	2.939	0.541	2.847	3.792	0.438	0.227
r	1.000	0.999	0.999	1.000	0.999	0.999	1.000	1.000
Elovich model								
	Fe	***Cu***	***Co***	***Hg***	***Ni***	***Zn***	***U***	***Cr***
A	0.018	0.001	0.009	0.002	0.007	0.001	0.002	0.013
B	0.020	0.002	0.012	0.002	0.012	0.003	0.002	0.015
b	49.31	421.2	81.96	551.5	85.96	298.1	500.2	66.97
a	0.048	0.003	0.025	0.004	0.022	0.005	0.005	0.035
Δq (%)	16.44	8.314	13.51	16.36	12.87	7.428	15.79	16.09
r	0.679	0.878	0.995	0.734	0.779	0.975	0.953	0.951
Intraparticle diffusion model								
	Fe	***Cu***	***Co***	***Hg***	***Ni***	***Zn***	***U***	***Cr***
A	0.046	0.003	0.025	0.004	0.022	0.005	0.004	0.033
B	0.006	0.001	0.004	0.001	0.004	0.001	0.001	0.004
Id	0.046	0.003	0.025	0.004	0.022	0.005	0.004	0.033
Kp	0.006	0.001	0.004	0.001	0.004	0.001	0.001	0.004
Δq (%)	29.38	32.42	30.27	29.40	30.72	32.15	29.57	29.49
r	0.730	0.880	0.768	0.731	0.784	0.845	0.739	0.735
Film diffusion								
	Fe	***Cu***	***Co***	***Hg***	***Ni***	***Zn***	***U***	***Cr***
A	-3.306	-0.934	-0.770	-2.148	-0.746	-0.540	-1.138	-1.305
B	-0.016	-0.004	-0.006	-0.013	-0.007	-0.004	-0.010	-0.011
If	-3.306	-0.934	-0.770	-2.148	-0.746	-0.541	-1.138	-1.305
Kf	0.016	0.004	0.006	0.013	0.007	0.004	0.010	0.011
Δq (%)	38.87	44.28	50.47	41.06	51.82	51.14	49.29	47.24
r	0.874	0.860	0.744	0.841	0.614	0.779	0.706	0.747

The values of the correlation coefficient *(r)* for the pseudo-second-order adsorption model are relatively high (≥ 0.999), and the adsorption capacities calculated by the model (q_e calc) are

also close to those determined by experiments (q_e exp). The experimental data for Co, Cr, Zn and U fitted also the Elovich kinetic model with r > 0.950. Therefore, it can be concluded that the pseudo second-order adsorption model is more suitable to describe the adsorption kinetics of the metal ions over algal biomass.

The kinetics for the adsorption of metal-ions on *Oedogonium* sp. in a multi-ion system was also investigated and the rate constants and different parameters calculated using the kinetic models are listed in Table 4.87.

Table 4.87 Kinetic constants for the adsorption of metal ions on *Oedogonium* sp. (in a multi-ion system)

Pseudo-first order								
	Fe	***Cu***	***Co***	***Hg***	***Ni***	***Zn***	***U***	***Cr***
A	-3.215	-3.279	-3.023	-3.585	-2.571	-2.875	-3.555	-3.153
B	-0.011	-0.014	-0.022	-0.007	-0.018	-0.016	-0.010	-0.013
q_e (mol/kg)	0.002	0.001	0.001	0.002	0.003	0.001	0.003	0.001
K_1	0.031	0.032	0.05	0.015	0.041	0.036	0.023	0.030
Δq (%)	86.22	87.95	85.06	79.19	54.19	81.07	85.80	87.70
r	0.826	0.804	0.928	0.902	0.975	0.924	0.816	0.788
Pseudo – second order								
	Fe	***Cu***	***Co***	***Hg***	***Ni***	***Zn***	***U***	***Cr***
A	114.9	52.82	35.54	6588	1007	145.5	538.6	48.09
B	125.3	105.4	89.45	683.9	150.5	99.87	307.9	84.16
q_e (mol/kg)	0.008	0.009	0.011	0.002	0.007	0.010	0.003	0.012
K_2	136.6	210.4	225.2	71.01	22.49	68.53	176.1	147.3
Δq (%)	0.698	0.294	0.361	6.186	4.935	0.987	1.050	0.346
r	0.999	1.000	1.000	0.988	0.999	0.999	0.999	0.999
Elovich model								
	Fe	***Cu***	***Co***	***Hg***	***Ni***	***Zn***	***U***	***Cr***
A	0.005	0.001	0.001	0.003	0.001	0.001	0.002	0.001
B	0.002	0.002	0.002	0.002	0.001	0.002	0.001	0.002
b	609.8	510.7	432.8	3568	7643	487.8	1508	408.1
a	0.002	0.003	0.004	0.003	0001	0.003	0.001	0.003
Δq (%)	10.89	11.09	11.91	6.796	4.993	10.08	10.41	10.02
r	0.843	0.974	0.989	0.861	0.963	0.960	0.931	0.937
Intraparticle diffusion model								
	Fe	***Cu***	***Co***	***Hg***	***Ni***	***Zn***	***U***	***Cr***
A	0.002	0.002	0.003	0.001	0.001	0.002	0.001	0.004
B	0.001	0.001	0.001	0.003	0.001	0.001	0.003	0.001
Id	0.001	0.002	0.003	0.001	0.001	0.002	0.001	0.004
Kp	0.002	0.001	0.001	0.003	0.001	0.001	0.003	0.001
Δq (%)	33.13	33.08	33.06	34.77	34.46	33.28	38.33	31.02
r	0.853	0.851	0.852	0.915	0.938	0.867	0.862	0.758
Film diffusion								
	Fe	***Cu***	***Co***	***Hg***	***Ni***	***Zn***	***U***	***Cr***
A	-2.111	-2.174	-3.572	-1.080	-3.105	-2.597	-1.585	-2.023
B	-0.012	-0.015	-0.009	-0.004	0.005	-0.007	0.010	-0.015
If	-2.111	-2.174	-3.572	-1.081	-3.105	-2.597	-1.585	-2.023
Kf	0.012	0.015	0.009	0.004	-0.005	0.007	0.011	-0.015
Δq (%)	40.45	41.76	38.22	41.63	39.29	38.28	42.74	42.93
r	0.826	0.804	0.928	0.902	0.975	0.924	0.816	0.788

The biosorption of the metal-ions on the *Oedogonium* sp. biomass in a multi-ion system followed the pseudo-second order model with a correlation coefficient for all the metals > 0.980. The biosorption of Ni may be described by the pseudo-first order, the Elovich and the film diffusion models. In order to assess the nature of the diffusion process responsible for the adsorption of Ni on the biomass, attempts were made to calculate the coefficients of the process as explained by Chabani *et al*. (2006). Assuming spherical geometry for the biosorbent and by considering the appropriate data and the respective overall rate constant, pores and film diffusion coefficients were determined. It clearly appeared that the biosorption of nickel on the *Oedogonium* sp. algal was controlled by film diffusion processes since coefficient values were around 10^{-7} cm^2 s^{-1}.

4.6.3.4 Effect of temperature and thermodynamics parameters

The effect of temperature on the adsorption of metal-ions (in single- and multi-ion systems) on the *Oedogonium* sp. biomass was investigated at 293.15 and 313.15 K. The thermodynamic parameters calculated for a single-ion system are given in Table 4.88. Two trends were observed: an increase of adsorption capacity for Cu, Ni, Zn, Co and Cr, indicating the endothermic nature of the biosorption process; a decrease of the adsorption capacity for Fe, Hg and U with the increase of temperature, prove that the process is exothermic.

Table 4.88 Thermodynamic parameters of metal ions adsorption on *Oedogonium* sp. in a single-ion system

	q_e		Ea	ΔH^o	ΔS^o	ΔG^o	
	mg g^{-1}		kJ mol^{-1}	kJ mol^{-1}	J(K $mol)^{-1}$	kJ mol^{-1}	
	293.15 ^oK	**313.15** ^oK				**293.15** ^oK	**313.15** ^oK
Cu	39.30	49.60	207.7	32.78	-295.8	-2.801	-2.233
Ni	24.20	47.90	170.4	96.15	-832.5	-3.982	-2.318
Zn	23.40	46.10	133.9	95.49	-827.7	-4.064	-2.412
Co	21.81	23.52	4.171	93.64	-864.4	-10.316	-8.695
Fe	43.23	32.00	-67.65	-42.36	330.8	-2.568	-3.301
Hg	42.00	34.50	-45.65	-27.71	208.4	-2.639	-3.118
U	18.20	4.70	-35.13	-190.6	1545.8	-4.677	-7.976
Cr	44.30	46.40	29.30	6.522	-75.08	-2.509	-2.396

The activation energy values for Cu, Ni, Zn, Co and Cr were > 40 kJ mol^{-1}, implying chemisorption, whereas negative values were obtained for Hg, Fe and U. The exothermic

nature could be due to either the damage of active binding sites in the biomass (Ozer and Ozer, 2003) or the increasing tendency to desorb metal ions from the interface to the solution (Sari *et al.*, 2007). Negative ΔG^o values indicate the spontaneous nature of the adsorption process and positive values of ΔS^o reveal the increased randomness at the solid-solution interface during the fixation of the metal ion on the active sites of the algal biomass.

The thermodynamic parameters calculated for the biosorption of metal ions from a multi-ion solution are given in Table 4.89.

Table 4.89 Thermodynamic parameters of metal ions adsorption on *Oedogonium* sp. in a multi-ion system

	q_e		Ea	ΔH^o	ΔS^o	ΔG^o	
	mg g^{-1}		kJ mol^{-1}	kJ mol^{-1}	J(K $mol)^{-1}$	kJ mol^{-}	
	293.15 ^oK	**313.15** ^oK				**293.15** ^oK	**313.15** ^oK
Cu	46.70	44.90	-27.77	-5.535	26.23	-2.380	-2.476
Ni	45.40	42.70	-30.00	-8.634	51.42	-2.449	-2.598
Zn	47.20	47.20	4.345	-0.598	-24.63	-2.364	-2.354
Co	46.60	46.40	3.622	-0.605	-24.95	-2.396	-2.385
Fe	43.30	42.80	-4.730	-1.635	-7.726	-2.564	-2.593
Hg	49.93	49.41	13.46	-1.494	-31.07	-2.243	-2.217
U	45.70	45.30	-5.696	-1.238	-9.934	-2.433	-2.454
Cr	46.30	45.20	-16.54	-3.386	8.189	-2.401	-2.460

The biosorption of metal-ions in a multi-ion system decreases with an increase in temperature. The process is exothermic. The activation energy values are negative for Cu, Ni, Fe, U and Cr, indicating the binding on sites with low energy. The biosorption of Zn, Co and Hg, with Ea < 40 kJ mol^{-1}, is likely physisorption. The enthalpy change $\Delta H\circ$ is negative (exothermic) for all the metal ions studied due to decrease in adsorption on successive increase in temperature. Further, negative entropy change ($\Delta G\circ$) values depict a spontaneous process.

The negative adsorption standard free energy changes ($\Delta G\circ$) and positive standard entropy changes ($\Delta S\circ$) at all temperatures indicated that the adsorption reactions were generally spontaneous processes. The positive value of entropy ($\Delta S\circ$) showed an increased randomness at the solid-liquid interface during the adsorption process, and also suggested the process was entropy-driven and not enthalpy-driven.

4.6.3.5 Effect of adsorbent mass

The effect of algal mass on the biosorption of metal ions was studied using different masses in the range, 0.2–1.2 g as shown in Figure 4.106. Results showed that the biosorption efficiency is highly dependent on the adsorbent mass. The adsorption capacity in single-ion system decreases with the increase of biomass, due probably to the lack of metal in solution. This could explain the opposite effect observed with the metal-ions in multi-component system. This phenomenon has been explained in the section 4.3.

(a)

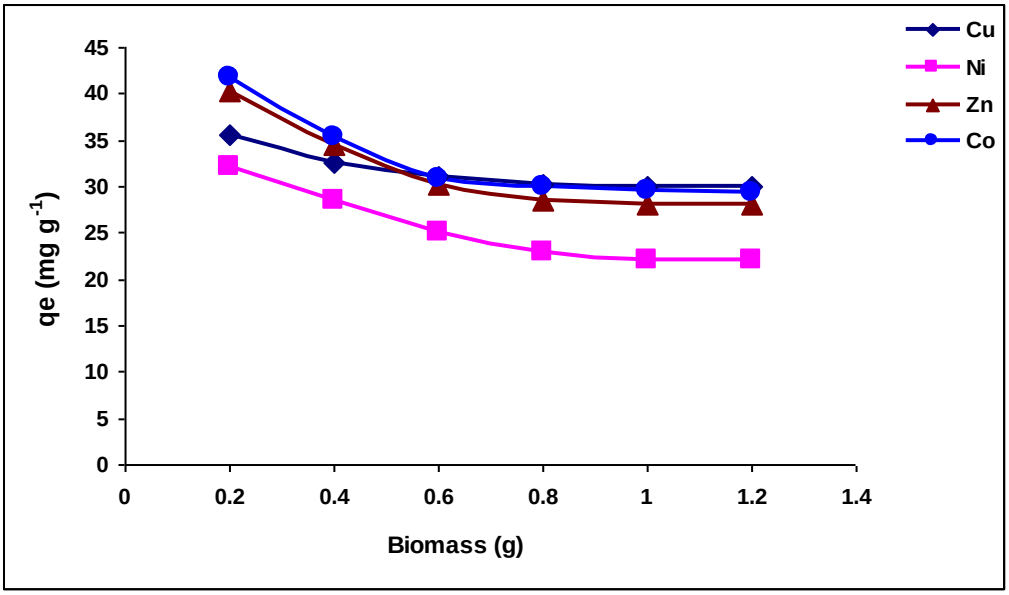

(b)

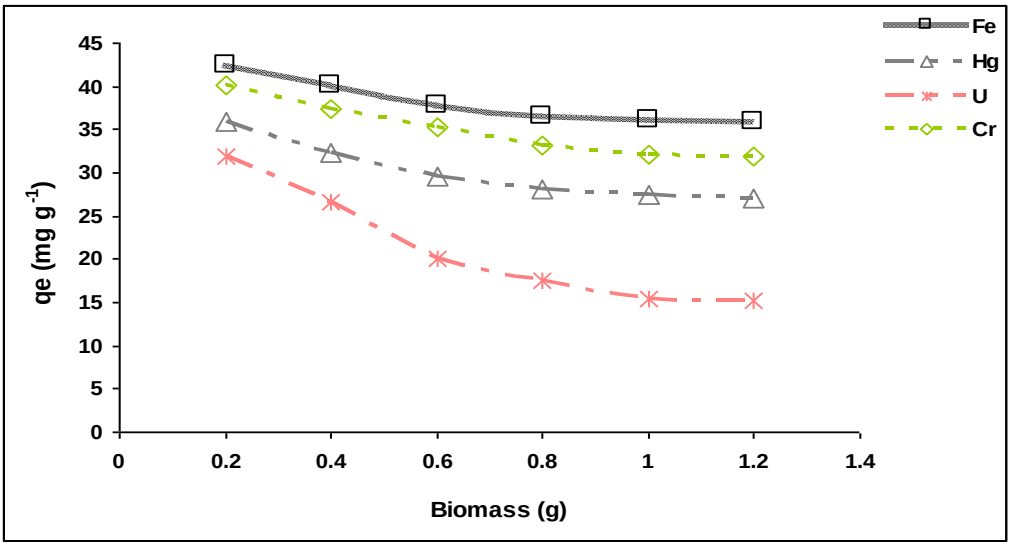

Figure 4.106 Effect of algal mass on the biosorption of (a) Cu, Co, Ni and Zn (b) Cr, Fe, Hg and U for *Oedogonium* sp. in multi-component solutions (C_i = 100 mg L^{-1}, pH = 3, Temp = 25^{o}C)

4.6.3.6 Regeneration and reuse of the algal biomass

In the present study, repeated batch operations were performed to examine the reusability of the algal biomass. 0.1 mol L^{-1} of HCl was used for desorbing the test metals from the metal-loaded biomass of *Oedogonium* sp. The results (Figure 4.107) show that more than 110% of adsorbed metals were eluted; more than 110% of the adsorbed metal ions were eluted from the biomass with 0.1 mol L^{-1} HCl.

(a)

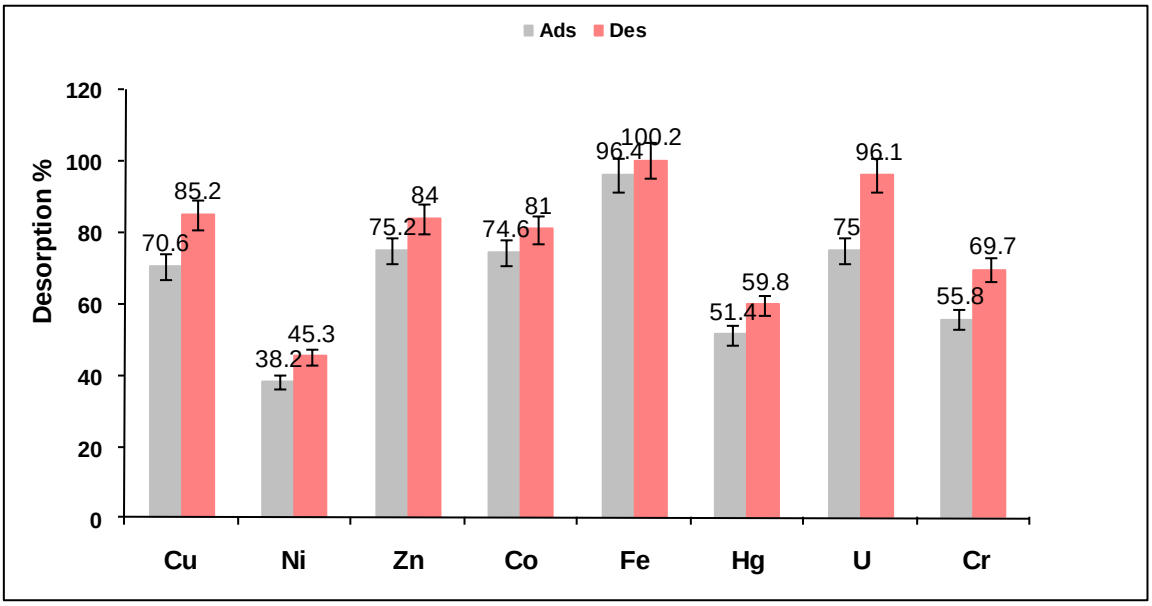

(b)

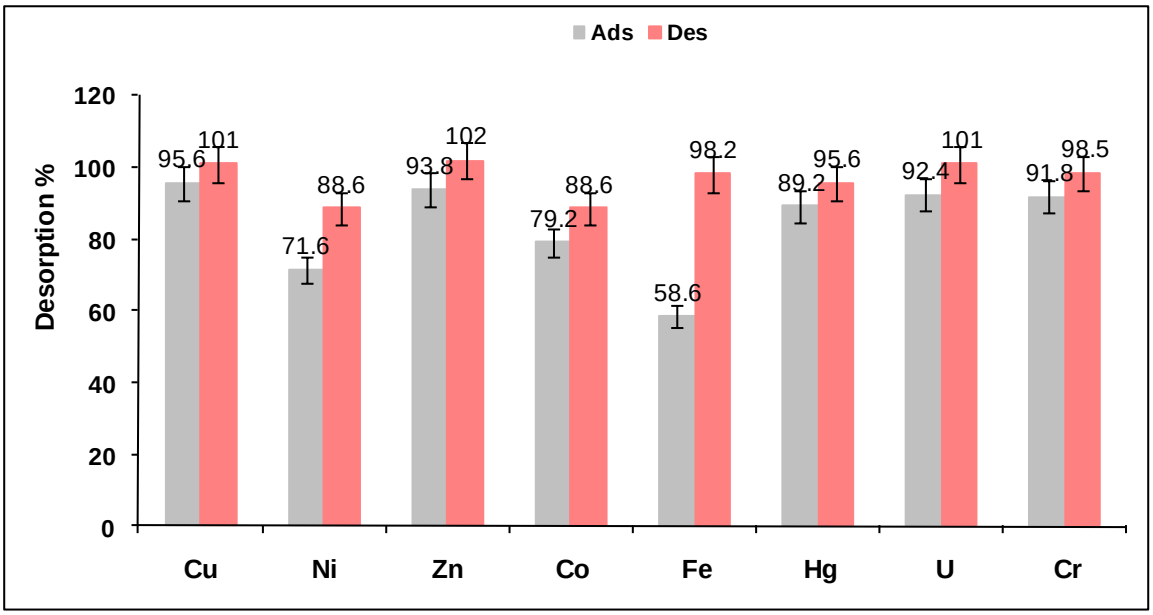

Figure 4.107 Desorption of metals adsorbed in (a) single-ion (b) multi-ion systems by HCl (0.1 mol L^{-1}), contact time = 1 h

These results indicate that there were metals initially adsorbed which were also released during desorption. This virtually increases the adsorption efficiency of the *Oedogonium* sp. during the repeated adsorption-desorption cycles as presented in Figure 4.108.

(a)

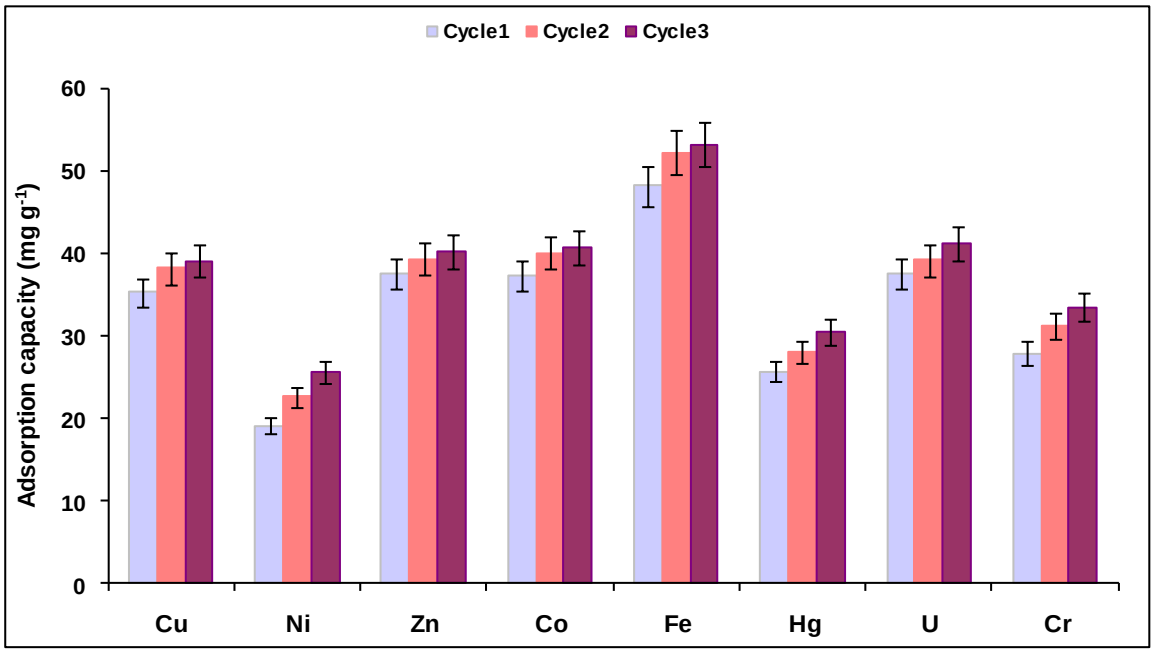

(b)

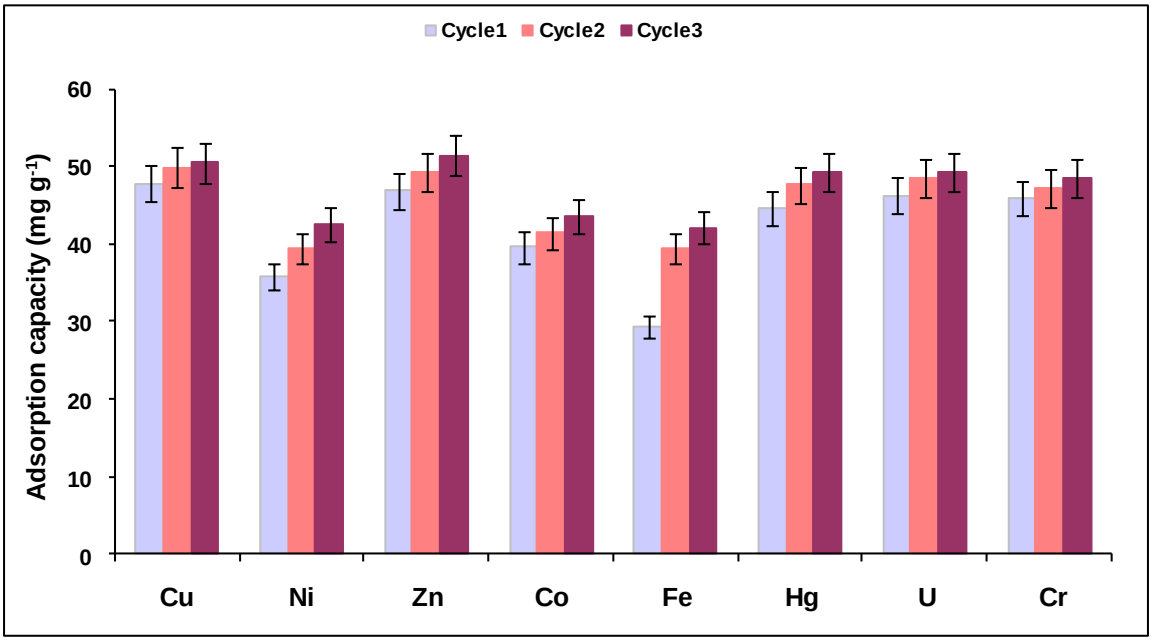

Figure 4.108 Regeneration and re-use of *Oedogonium* sp. biomass (a) single-ion system (b) multi-ion system

The meaning of the cycles is as follows: the biomass was treated with acid to desorb the adsorbed metals. It was then rinsed with de-ionised water, dried and used for adsorption (i.e. cycle 1). It was then treated again with acid following this cycle 1 adsorption, rinsed, dried and re-used (i.e. cycle 2). It was further treated with acid, rinsed, dried and re-used (i.e. cycle 3).

To assess the reusability of the biomass, adsorption-desorption cycles of Cu, Co, Cr, Hg, Fe, Ni, Zn and U were repeated three times by using the test algal biomass. The adsorption capacities of the three test biomasses changed by the following amounts: Cu(10%), Ni(34%), Zn(7.1%), Co(9.4%), Fe(10.4%), Hg(18.7%), U(10.1%), Cr(20.1%) for the single-ion system while for the multi-ion system, the change was about: Cu (5.6%), Ni(18.9%), Zn(9.5%), Co(10.1%), Fe(43.6%), Hg(10.5%), U(6.5%), Cr (5.7%). These results show that the test *Oedogonium* sp. biomass could be repeatedly used for 3 cycles with an increase of the initial adsorption capacities.

4.6.4 Extraction and isolation of alginate from Oedogonium sp.

4.6.4.1 Alginate content of Oedogonium sp.

Alginate, the salt of alginic acid, linear polysaccharides containing 1,4-linked β-D-mannuronic (M) and α-L-guluronic (G) was extracted using the alkaline extraction method described in paragraph 3.2.1.5.

The alginate yield (in weight percent) is defined as:

$$\text{Yield (\%)} = \frac{\text{dried mass of final alginate product}}{\text{dried algal mass before acid extraction}} \text{ x } 100 \qquad (4.17)$$

The alginate yields of *Oedogonium* sp. extracted for this work were in the order of 32 ±1.7%. Few data are available in the literature on the alginates extract from the *Oedogonium* sp. algal, thus these results could not be compared with those for previous studies. It is well-known that the alginate content varies from species to species and depends on such factors as the growth stage (Percival and McDowell, 1967; Black, 1950; Kreger, 1962). In summary, both the alginate content and its conformation determine the metal-binding behaviour of algal biomass.

The alginate was characterized by the IR technique as well as the CHNS elemental analysis. The surface area of the algal biomass was observed to be 1.44 m^2g^{-1} by BET method. The elemental composition was carbon (24.9%), nitrogen (4.12%) and sulphur (5.85%). FTIR spectra (Figure 4.109) depicted the following functional groups: carboxylic acid, hydroxyl and amine. The main functional groups are given in Table 4.90.

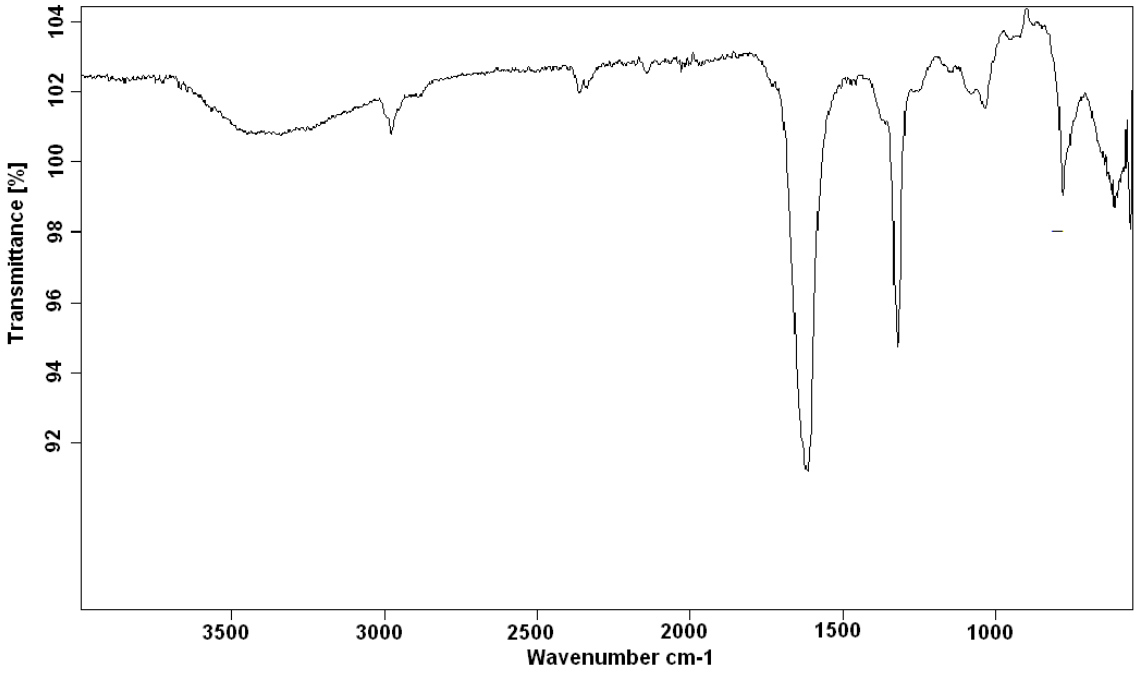

Figure 4.109 FTIR Spectra of the alginates extracted from the *Oedogonium* sp. algal biomass

Table 4.90 IR adsorption bands for Na-alginates extracted from the *Oedogonium* sp.

Wavenumber (cm^{-1}) ***Na-alginates extract***	***Functional groups***
3341	Carboxylic/O-H strech and N-H strech
2980	Phenolic/carboxylic
2364	
1616	amide I band, C=C, >C==N
1319	
1035	=C-N< stretching
780	=C-H bending
644	C-H deformation
610	C-H deformation
559	

4.6.4.2 Estimation of M:G ratios by ^{1}HNMR

The alginate extracted from the green filamentous algae (*Oedogonium* sp.) is a polymer of D-mannuronic acid and L-guluronic acid. The approach of Grasdalen *et al*. (1979) and Santi *et al.* (2008) was adopted to determine the M:G ratio of the alginates extracted in this study. Although solutions of these polymers are usually too viscous to give well-resolved spectra, ^{1}HNMR spectroscopy has proven to be highly effective in the characterization of alginates. The partial hydrolysis can satisfactorily lower the level of the viscosity. Assignments for the ^{1}H signals were readily obtained from a ^{1}H 2-D COSY spectrum. Alternatively, the MestRe Nova software was also used.

^{1}HNMR spectroscopy was used to estimate their ratios and Figure 4.110 represents the ^{1}H spectra of the *Oedogonium* alginates. The signals are due to the anomeric protons of D-mannuronosyl (M) and L-guluronosyl (G) residues, separated at δ 4.35 and 3.79 respectively and have relative intensities corresponding to an M:G ratio of 1.38. For comparison purposes, we also examined the commercial Na-alginates (Figure 4.111 (a)) for which the M:G ratio was about 1.41. These results are close with the ones obtained by Santi *et al*. (2008) on commercial Na-alginates with a M:G ratio of 1.50. The ^{1}H spectra corresponding to the Na-

alginates extracted is presented in Figures 4.110 (b) and 4.110 (c). The Figures 4.111 (a) and 4.111 (b) present the mannuronosyl residue obtained after hydrolysis of the commercial Na-alginates and the alginates from the algae. Additional spectra are presented in APPENDIX I.

Further experiments are needed to determine the block distribution or molar fractions of monads (G, M), diads (GG, MM, GM) and triads (GGG, MMM, GGM, MMG, MGM, GMG) in the copolymer chain. Also, by extending the period of acid hydrolysis and reducing the temperature, well resolved signals could be obtained.

The alginate content, normally expressed as percent dry weight, directly correlates with the metal uptake capacity of algal species. The relevance of these results in the context of remediation of heavy metals derives from the premise that the macromolecular composition, monomer sequencing, and conformation of the alginate biopolymer are key factors in determining the differential affinity of various metals for the biomass. Hence the conformation and sequence of the extracted alginates have to be determined. For instance, a study done by Deramos *et al.* (1997) revealed that the metal-alginate complexation depends on the ratio of the stability constants for metal ion binding with GG blocks or MM blocks. Therefore, the preference of metal ion for GG or MM blocks is a consequence of the extent of its binding to a particular homopolymeric block. The size of the cation appears to be an important variable in metal binding to alginates, both due to the rigid nature of the GG-linkages, as well as to the steric arrangement of the electronegative ions surrounding the divalent cation.

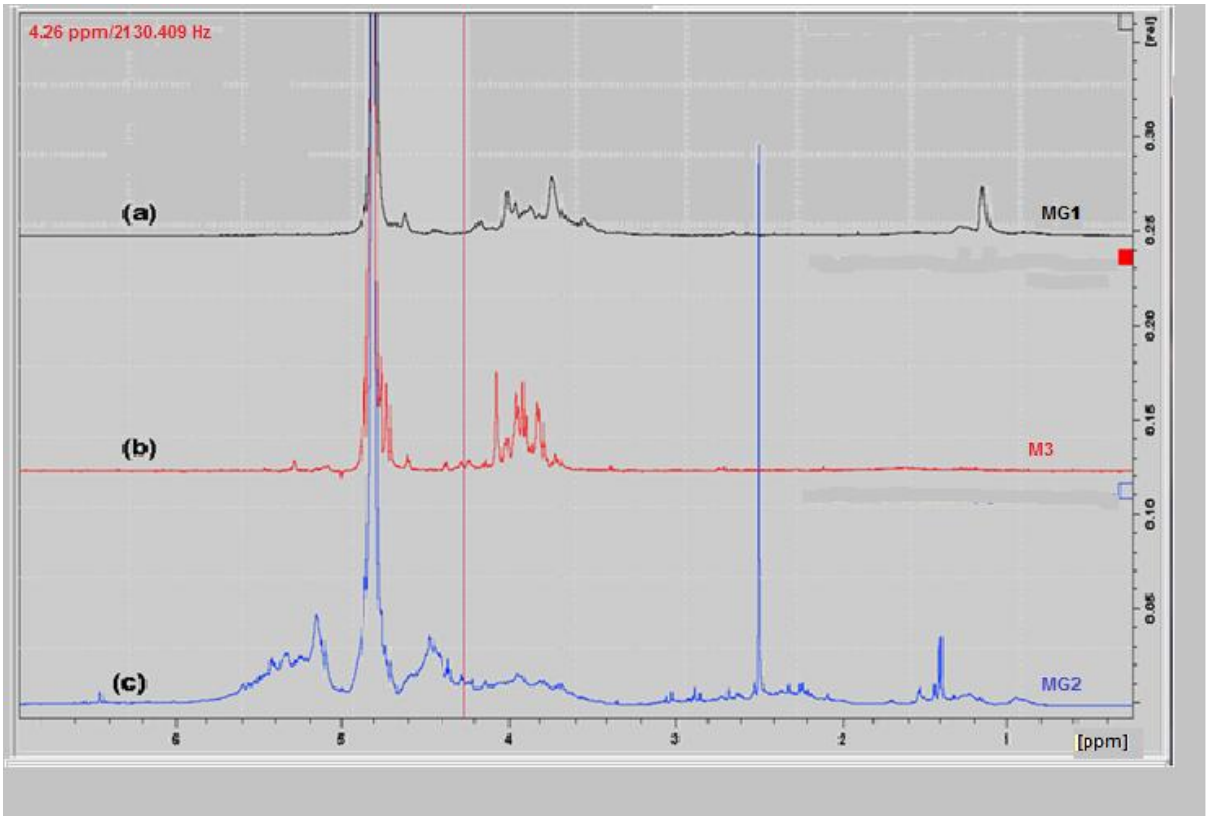

Figure 4.110 ^{1}H NMR spectra of sodium alginates (a) Mannuronic-Guluronic acid from Sigma Aldrich (South Africa) (b) Mannuronic acid (c) Mannuronic-Guluronic acid extracted from *Oedogonium* sp. algal

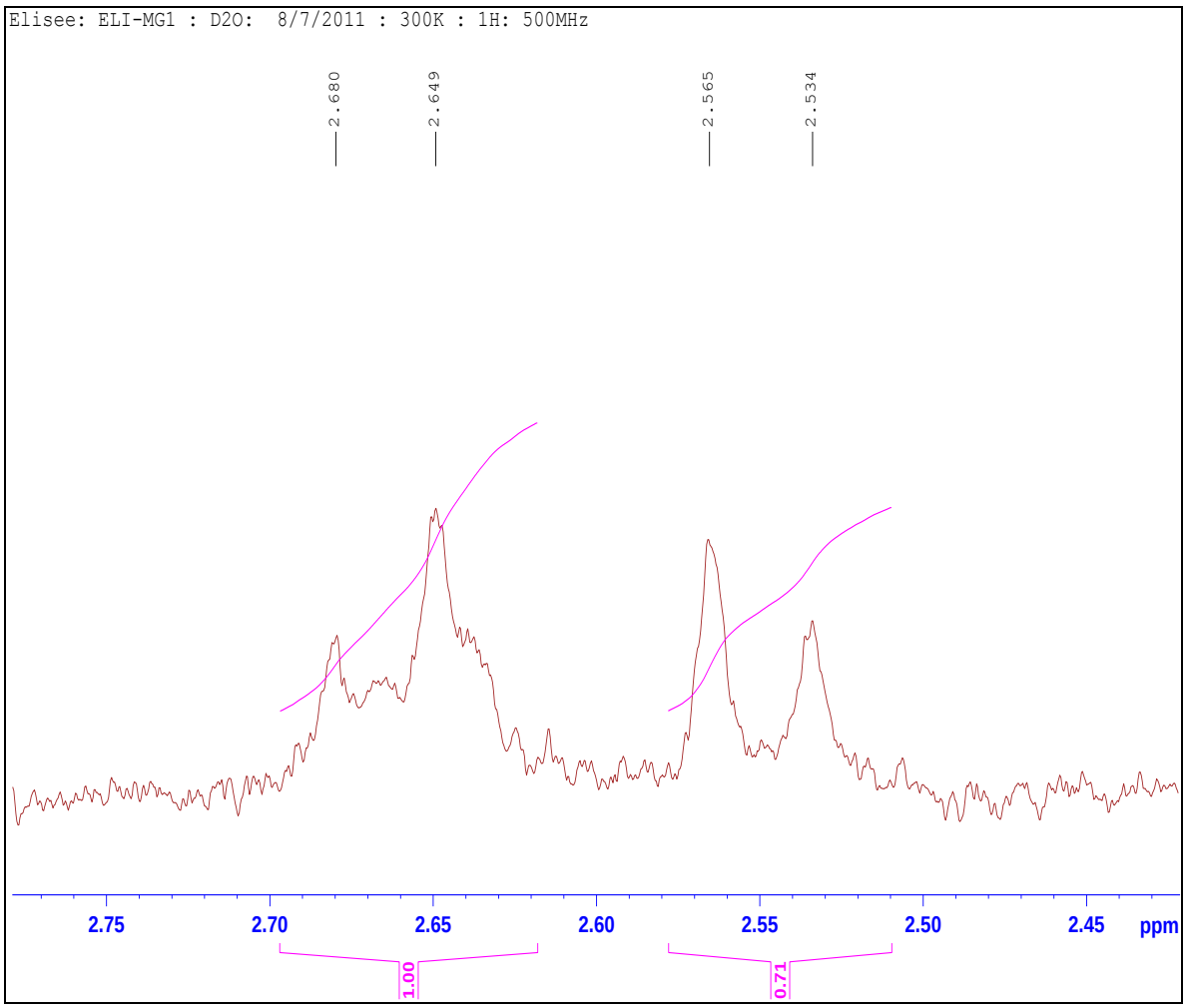

Figure 4.111 (a) Assignment of the ^{1}H signals for M and G residues for the commercial Na-alginates

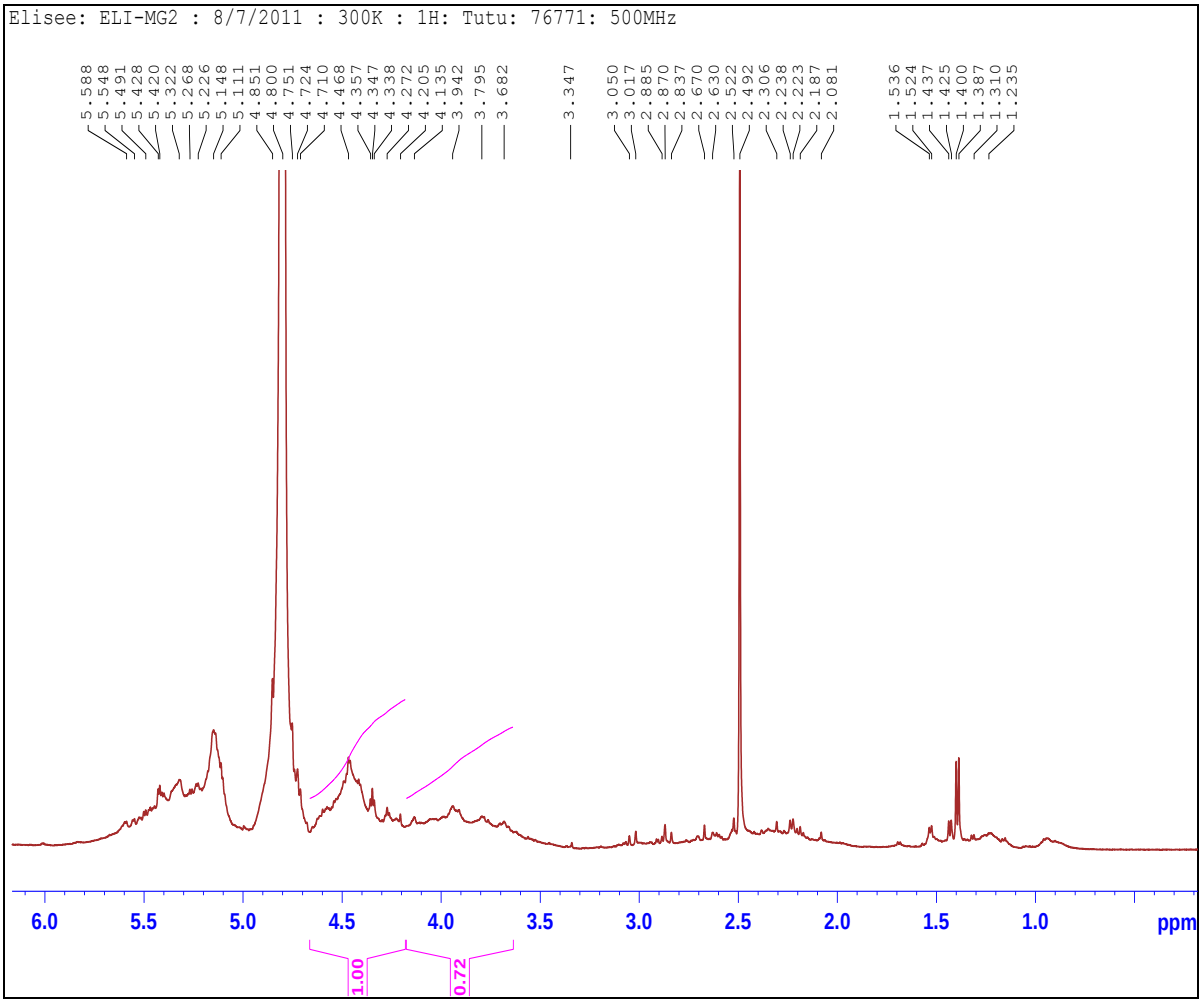

Figure 4.111 (b) Assignment of the ^{1}H signals for M and G residues from *Oedogonium* sp. algal biomass

Future studies should focus on careful characterization of the alginate composition of *Oedogonium* sp. coupled with the determination of the polymeric blocks with a comparison of their performance in competitive metal-binding experiments. The objective would be to relate the percent alginate content and the frequency of GG or MM to their overall multi-metal uptake performance.

4.6.5 Biosorption of metal ions by zeolite impregnated with Na-alginate complex

A novel alginate complex was developed for adsorption of heavy metals. The alginate complex was generated by impregnating synthetic zeolite into alginate gel beads. In order to examine the adsorption capacity of the alginate complex, both equilibrium and kinetic batch studies were performed.

4.6.5.1 Characteristics of the zeolite-alginate

i) FTIR spectral analysis

The FT-IR spectra of the immobilized alginates on zeolite are shown in Figure 4.112 and the different functional groups are listed in Table 4.91.

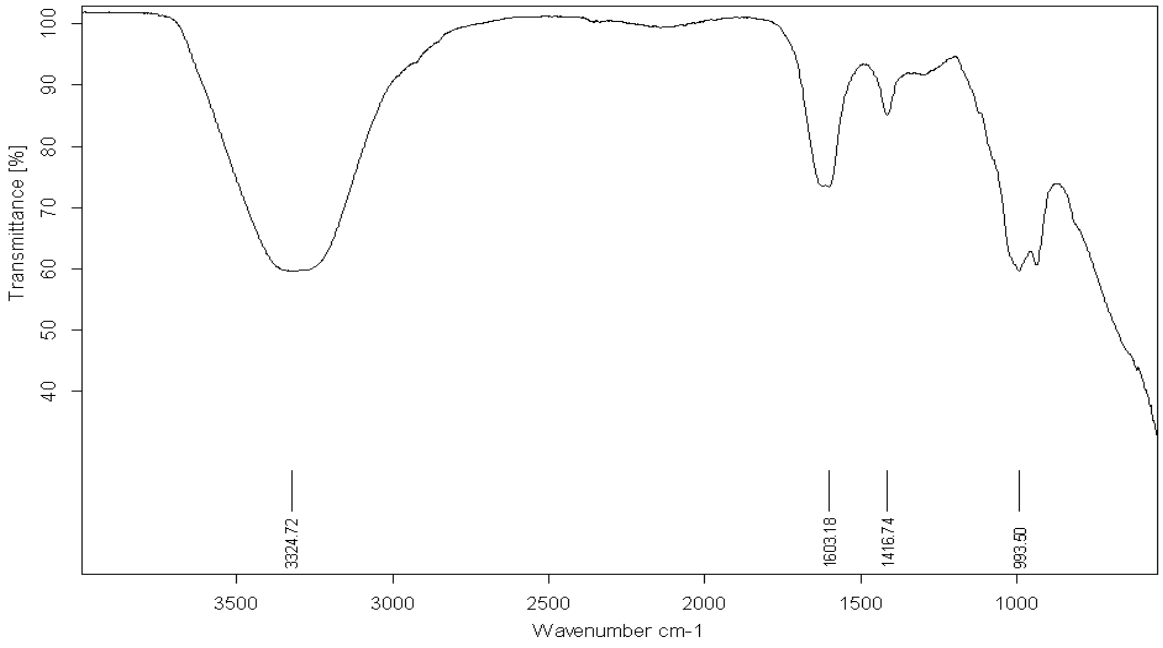

Figure 4.112 FT-IR spectra of the alginates immobilized on zeolite

Table 4.91 IR adsorption bands for zeolite-alginate

Wavenumber (cm^{-1}) ***Na-alginates extract***	***Functional groups***
3324	Carboxylic/O-H strech and N-H strech
1603	COO^- stretching
1416	COO^- stretching
993	Si-O plane vibration

The band assignments depicted are: OH stretching at 3324 cm^{-1} $Si–O^-$ in-plane vibration at 993 cm^{-1}. The O-H stretching and symmetric $–COO^-$ cm^{-1} stretching vibration bands shift to 1603 cm^{-1}. The band shifting may be due to the recombination action between zeolite and sodium alginate. The peak at 1427 cm^{-1} can be assigned to the asymmetric $–COO^-$ stretching vibration and caused by the intercalation role between zeolite and sodium alginate.

ii) Zeta potential measurement of zeolite-alginate

The zeta potential plot for zeolite-alginate is presented in Figure 4.113. The graphs show that the surface of the zeolite-alginate is negatively charged from pH 2 to 8. The point of zero charge was depicted between pH 4 and 5.2.

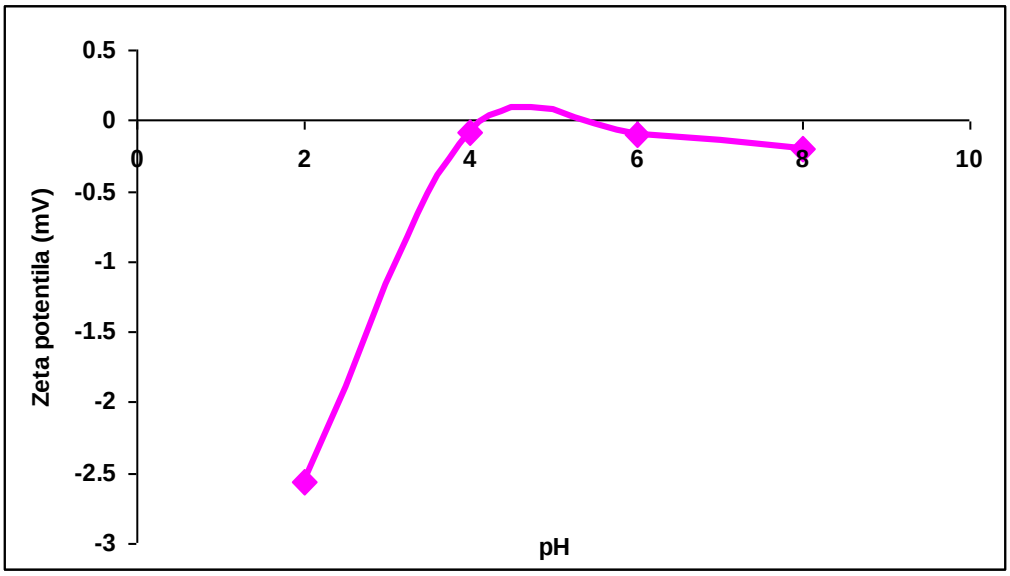

Figure 4.113 Zeta potential of zeolite-alginate

4.6.5.2 Sorption capacities, pH and isotherms

i) Effect of pH

The initial pH value of a solution may change the surface charge of an adsorbent, the degree of ionization of an adsorbate molecule, and the extent of dissociation of functional groups on the active sites of an adsorbent (Nandi *et al.*, 2009), therefore it plays a major role in the adsorption of metal ions by zeolite-alginate. In order to study the pH effect, 100 mg L^{-1} of Cu, Co, Cr, Fe, Hg, Ni, Zn and U in single-ion and multi-ion systems were adsorbed at different pH: 2, 4, 6, and 8 as shown in Figures 4.114 and 4.115.

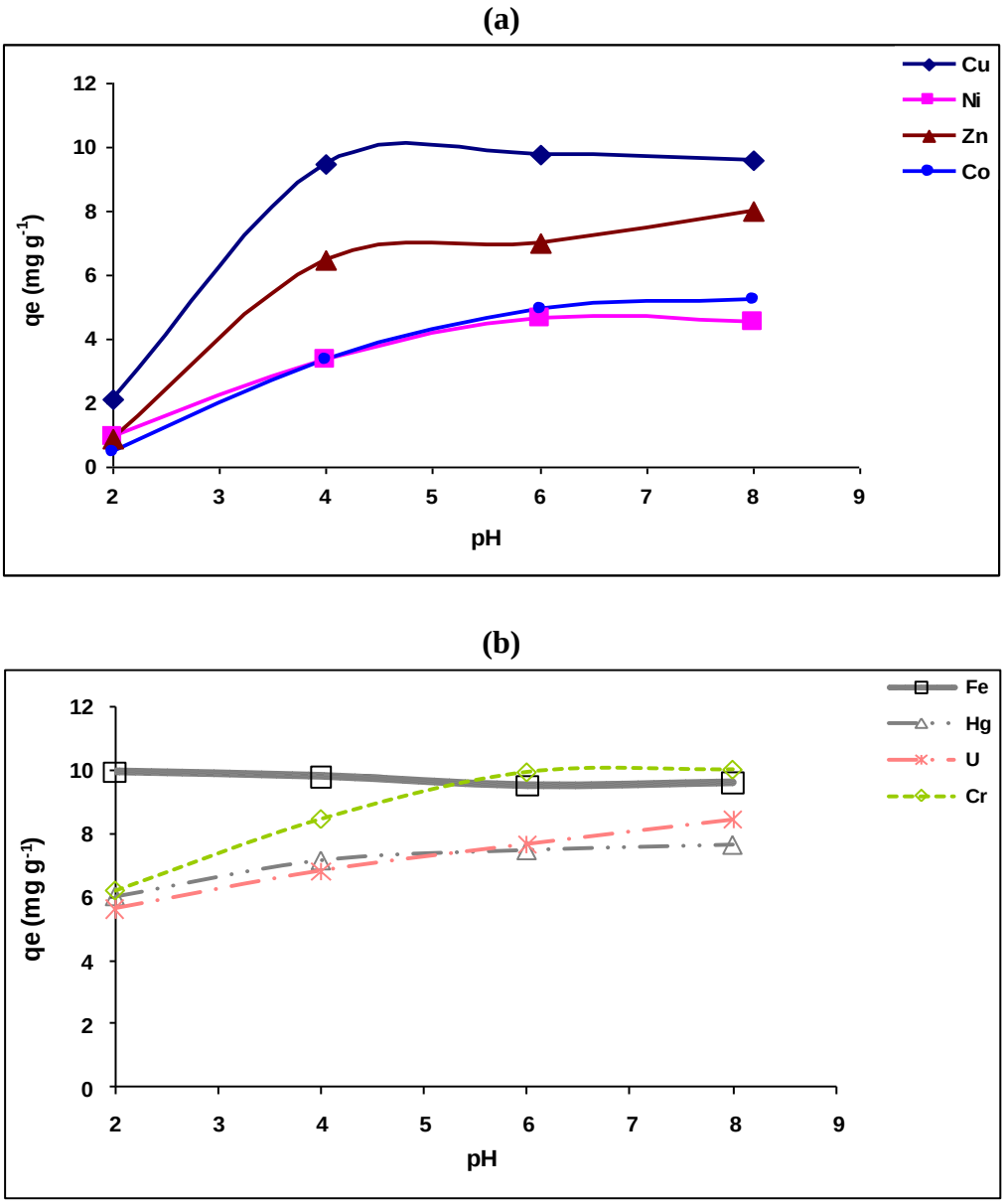

Figure 4.114 Effect of pH on the adsorption of (a) Cu, Co, Ni and Zn (b) Cr, Fe, Hg and U on zeolite-alginate in a single-ion system (C_i = 100 mg L^{-1}, Temp = 25±1^{o}C)

A general trend was observed in a single-ion system, namely an increase of metal ions adsorption when the pH increases from 2 to 5, q_e (mg g^{-1}) was constant after pH 6, explaining a saturation point. Similar results were obtained by Esposito (2001) as well as Yuan and Viraraghavan (2001). In all cases, the maximal heavy metal ions adsorption occurred when the pH was between 4 and 6. Thus, below pH 4 high proton concentrations minimized metal sorption and above pH 7 metal precipitation was favoured.

The adsorption of Fe showed a different trend with a maximum adsorption capacity at pH between 2 and 4, and a slight decrease observed from pH 5 to 8. The first stage of ion exchange is deprotonation of the carboxylic group which is represented by equation 4.18, while equation 4.19 represents the attachment of the metal cation to the reactive carboxylate anion.

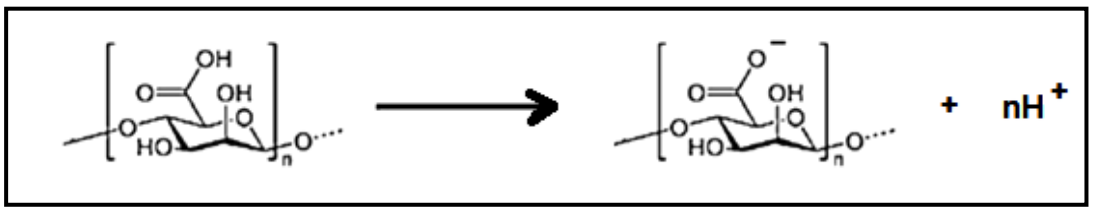

(4.18)

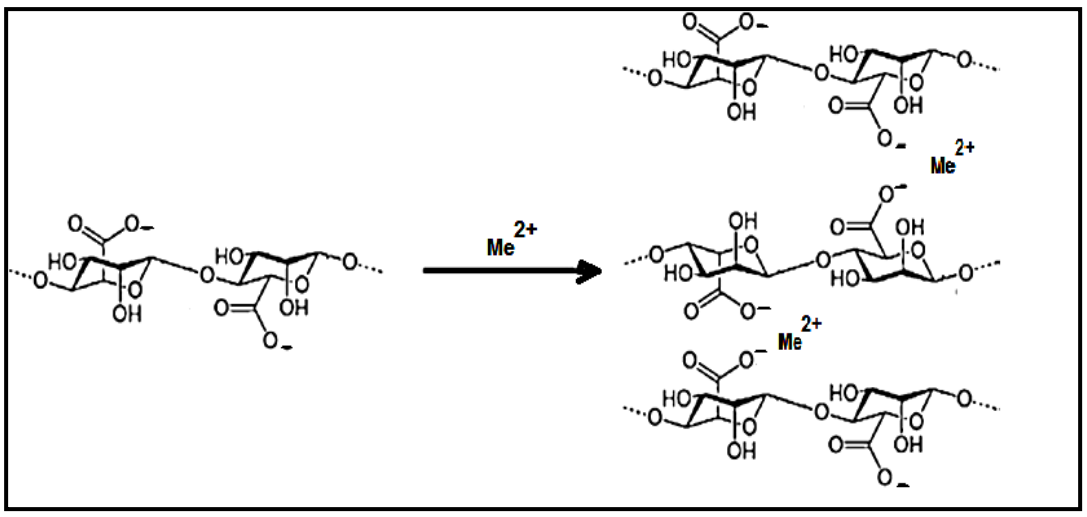

(4.19)

At low pH, the high concentration of H^+ in the medium shifts the equilibrium in Eq. 4.18 to the left direction. This means that the carboxyl groups do not ionize and the ion exchange sites on zeolite-alginate surface are still protonated. Under such conditions the metal ions do not exchange and remain in the solution. As the pH value increases from 3 to 6, the

deprotonation equilibrium in Eq. 4.18 is shifted to the right and, as a result, the adsorption capacity increases according to Eq. 4.19 until it reaches its maximum value at pH 6.

The adsorption of Cu, Co, Cr, Fe, Hg, Ni, Zn and U on zeolite-alginates in a multi-ion system is shown in Figure 4.115. The results showed an increase of adsorption capacity at low pH. Although the maximum was attained at pH 4 for most of the metals studied. The adsorption of Fe, Hg, U and Cr was constant at the range of pH studied.

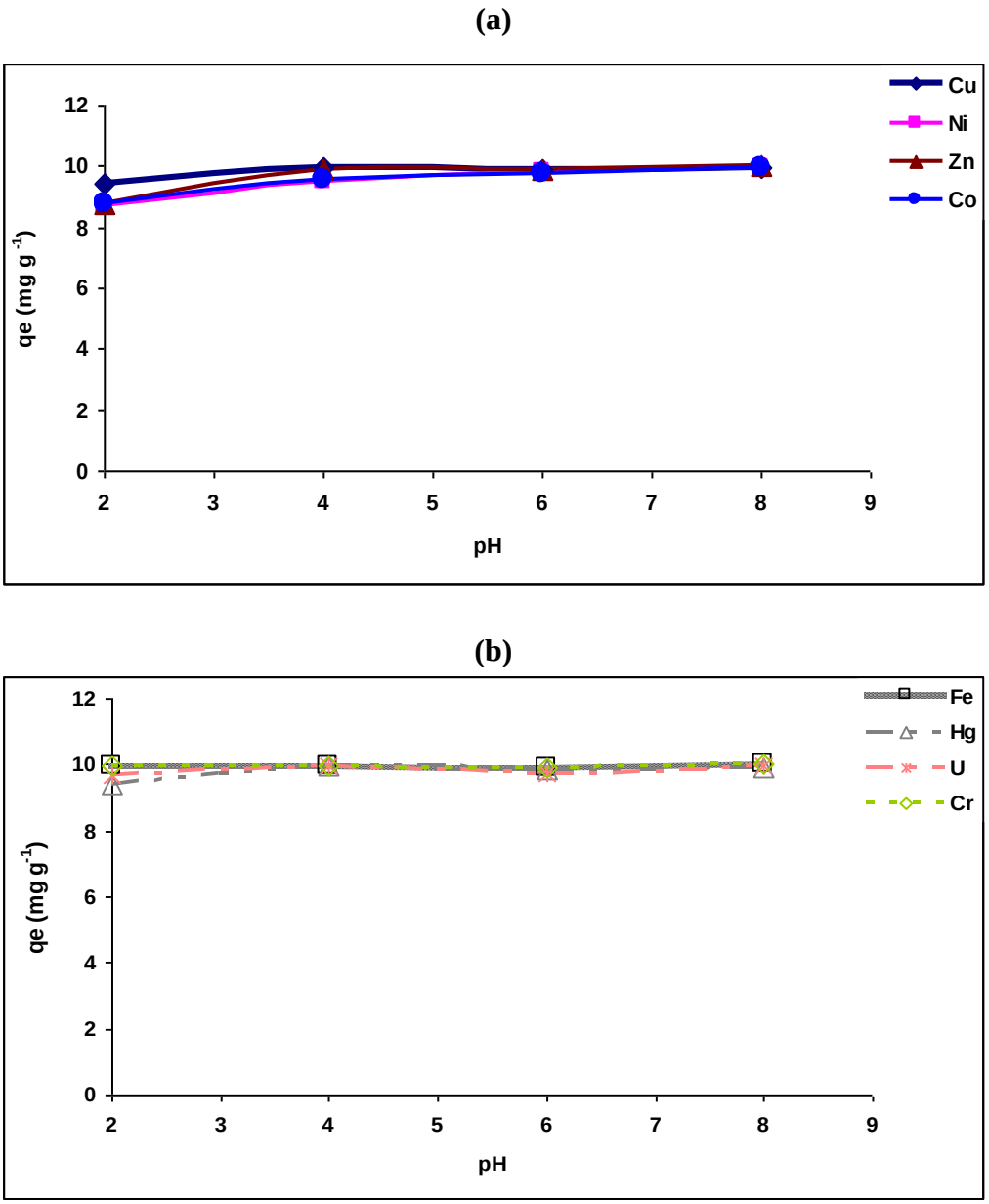

Figure 4.115 Effect of pH on the adsorption of (a) Cu, Co, Ni and Zn (b) Cr, Fe, Hg and U on zeolite-alginate in multi-ion system (C_i= 100 mg L^{-1}, Temp = 298.15^oK, algal mass = 1 g)

ii) Effect of concentration

The adsorption of Cu, Co, Cr, Fe, Hg, Ni, Zn and U on zeolite-alginate was carried out at different concentrations in single- and multi-ion solutions. The results obtained are given in Figures 4.116 and 4.117, respectively.

It was observed that the adsorption capacity of Ni, Fe, U and Hg increases with increase in initial concentration of metal ions in solution. In the case of Cr, Cu, Co and Zn, at the equilibrium concentration of 200 mg L^{-1}, the adsorption would gradually approach saturation levels. It is likely that at the initial concentration of 200 mg L^{-1}, the active adsorption positions of the adsorbents were almost gradually filled by metal ions and hence the adsorption activity of adsorbents is limited (Say *et al.*, 2001). Among the curves, Cu, Co, Zn and Cr showed the lowest adsorption capacity.

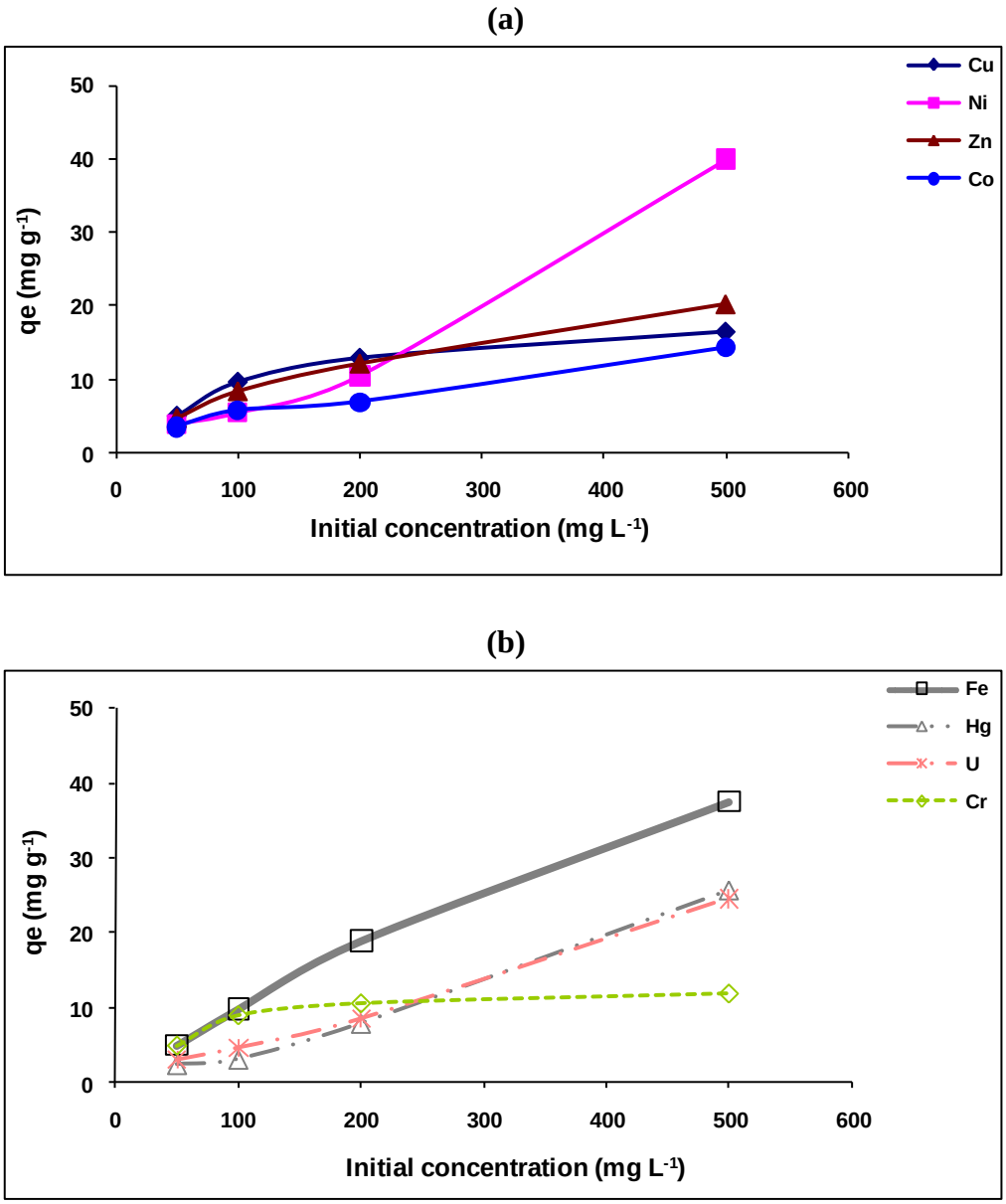

Figure 4.116 Effect of concentration on the adsorption of (a) Cu, Ni, Zn, Co (b) Cr, Fe, Hg, U in single-ion solution on zeolite-alginate (pH = 3, Temp = 298.15±1^{o}K, agitation rate= 150 rpm, agitation time = 12 h, algal mass = 1 g)

The uptake of Cu, Co, Cr, Fe, Hg, Ni, Zn and U on zeolite-alginate in multi-ion solutions (Figure 4.117) increases linearly with an increase in metal concentration. As in the previous observation, all the metals showed a similar trend.

(a)

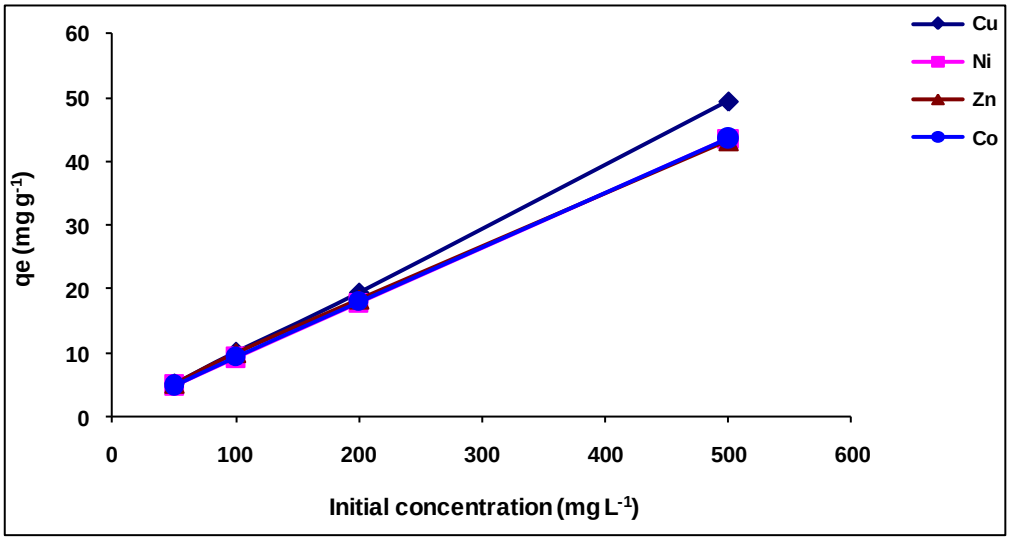

(b)

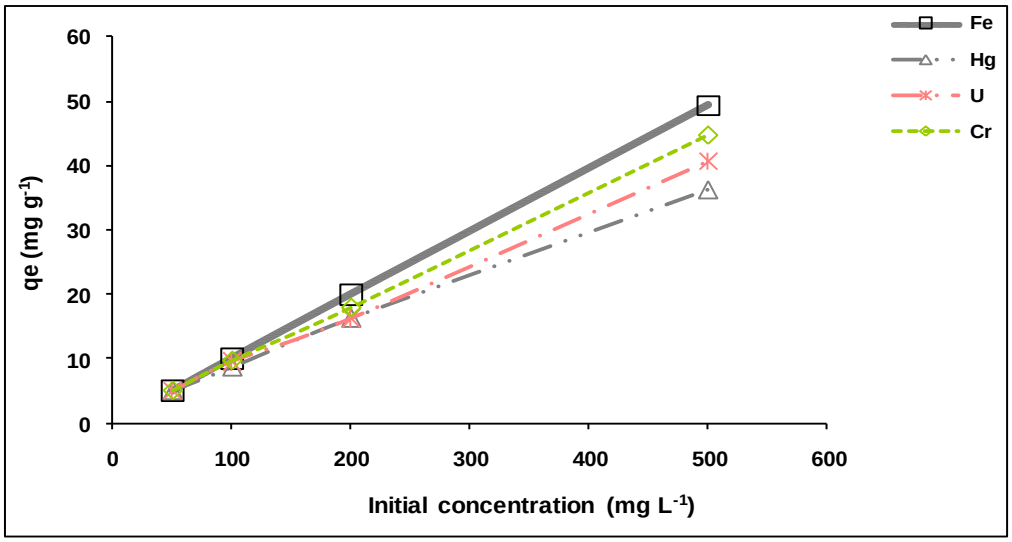

Figure 4.117 Effect of concentration on the adsorption of (a) Cu, Ni, Zn and Co (b) Cr, Fe, Hg, U in multi- component solutions on zeolite-alginate (pH = 3, Temp = 298.15±1^{o}K, agitation rate = 150 rpm, agitation time = 12 h)

iii) Isotherms of adsorption of heavy metals on zeolite-alginate

In order to investigate how metal ions interact with adsorbents, the Langmuir, Freundlich and the Dubinin-Radushkevich models were applied to describe the isotherm. The different constants and parameters obtained for the single and multi ions are listed in Tables 4.92 and 4.93.

Table 4.92 Parameters of Langmuir, Freundlich and D-R models for the adsorption of metals on zeolite-alginate in single-ion systems

Langmuir Isotherms	***Fe***	***Cu***	***Co***	***Hg***	***Ni***	***Zn***	***U***	***Cr***
A	0.041	0.267	0.560	0.573	0.232	0.237	0.427	0.418
B	2.906	7.754	8.127	14.08	6.239	6.357	17.94	8.701
B	70.97	28.98	14.51	24.57	26.91	26.81	41.99	20.81
qm (mol/kg)	0.344	0.129	0.123	0.071	0.160	0.157	0.056	0.115
ΔGo (kJ/mol)	-10.57	-8.346	-6.630	-7.936	-8.161	-8.152	-9.265	-7.525
Δq (%)	67.68	67.67	67.37	67.23	67.30	67.51	67.25	67.66
R	0.998	0.998	0.925	0.403	0.967	0.987	0.746	0.999
Freundlich Isotherms	***Fe***	***Cu***	***Co***	***Hg***	***Ni***	***Zn***	***U***	***Cr***
A	0.044	-0.068	-0.002	0.038	0.039	-0.009	0.028	-0.119
B	0.244	0.277	0.431	0.552	0.371	0.334	0.531	0.257
K_f	1.109	0.855	0.996	1.091	1.096	0.978	1.066	0.760
n	4.101	3.611	2.323	1.810	2.700	2.990	1.884	3.887
ΔGo (kJ/mol)	-10.17	-8.951	-5.758	-4.488	-6.693	-7.413	-4.671	-9.636
Δq (%)	22.89	30.34	11.81	42.97	47.87	6.104	25.65	46.55
R	0.991	0.972	0.971	0.976	0.780	0.997	0.969	0.983
D-R Isotherms	***Fe***	***Cu***	***Co***	***Hg***	***Ni***	***Zn***	***U***	***Cr***
A	-0.079	-0.576	-0.251	-0.010	0.021	-0.339	-0.080	-0.773
B	-0.004	-0.004	-0.009	-0.011	-0.008	-0.006	-0.010	-0.003
Xm (mol/kg)	0.923	0.562	0.778	0.990	1.022	0.712	0.923	0.462
Es (kJ/mol)	11.83	11.77	7.509	6.726	7.904	9.512	7.056	12.99
Δq (%)	10.48	77.71	44.08	36.50	50.20	45.91	26.76	91.94
R	0.999	0.987	0.960	0.920	0.766	0.991	0.956	0.997
K_d	***Fe***	***Cu***	***Co***	***Hg***	***Ni***	***Zn***	***U***	***Cr***
A	4.659	3.989	2.179	1.368	1.593	3.187	1.753	3.926
B	266.3	-116.7	225.7	2724	2060	165.9	2671	-139.8
ΔGo (kJ/mol)	-11.55	-9.889	-5.403	-3.392	-3.951	-7.901	-4.346	-9.732
Kdo	105.5	54.02	8.844	3.928	4.921	24.22	5.774	50.70
Δq (%)	74.02	65.44	67.34	67.22	87.01	69.29	73.59	61.79
R	0.907	0.842	0.864	0.432	0.314	0.857	0.334	0.787

Based on the correlation coefficient (> 0.950), the experimental data fitted well the Freundlich isotherm except for Ni, which was found to obey the Langmuir isotherm. Fe, Cu, Cr, Ni and Zn are also described by the Langmuir model. The adsorption of Fe, Cu, Co, Zn, U and Cr was also described by the D-R isotherm.

The maximum adsorption capacity (mol kg^{-1}) obtained from the Langmuir model is in the order of: Fe (0.344) > Ni (0.160) > Zn (0.157) > Cu (0.129) > Co (0.123) > Cr (0.115) >> Hg (0.071) > U (0.056).

The values of Freundlich constants, K_f and n were calculated and the values of n ($1 < n < 5$) show that the adsorption of metals onto zeolite-alginate is favourable. The D-R isotherm

model was employed to evaluate the energy of sorption which was found to be < 16 kJ mol^{-1}, suggesting a physisorption process.

The distribution coefficient, K_{do} (L g^{-1}) has been used to indicate the adsorption affinity of zeolite-alginate towards metal ions. The distribution coefficient data implicitly indicate the selectivity, capacity, and affinity of metal ions for ion exchange. The distribution coefficient calculated was in the sequence: Fe (105.50 > Cu (54.02) > Cr (50.70) > Zn (24.22) > Co (8.844) > U (5.774) > Ni (4.921) > Hg (3.928).

The Gibbs free energy calculated from the distribution coefficient was negative for all the metals, implying that the adsorption of metal ions on zeolite-alginate was spontaneous.

It is known that alginate is a linear natural polymer constituted by the ß-D-mannuronic (M) and α-L-guluronic (G) through glycosidic bond connection (Ci *et al.*, 1999). The unique chain configuration can form electronegative cavities and a large number of free carboxyl groups in Na-alginate molecules (Athanasekou *et al.*, 2009) which can improve the heavy metal adsorption properties of zeolite. Heavy metal ions could be coordinated to alginate surface functional groups only and the access to functional groups of zeolite (SiO^-).

The adsorption constants and correlation coefficient of Langmuir, Freundlich, D-R and coefficients partition models for the adsorption of metal ions on zeolite-alginate in multi-ion systems were calculated and presented in Table 4.93.

Table 4.93 Parameters of Langmuir, Freundlich and D-R models for the adsorption of metals on zeolite-alginate in a multi-ion system.

Langmuir Isotherms	***Fe***	***Cu***	***Co***	***Hg***	***Ni***	***Zn***	***U***	***Cr***
A	0.002	0.006	0.034	0.078	0.037	0.028	0.051	0.027
B	2.141	4.580	2.558	10.62	2.540	3.015	12.57	2.457
B	1108	821.6	76.05	135.8	67.21	107.8	248.2	90.13
qm (mol/kg)	0.467	0.218	0.391	0.094	0.393	0.332	0.079	0.407
ΔGo (kJ/mol)	-17.38	-16.64	-10.74	-12.17	-10.43	-11.60	-13.67	-11.16
Δq (%)	67.56	67.53	67.35	67.39	67.33	67.48	67.43	67.41
R	0.999	0.836	0.892	0.912	0.859	0.937	0.842	0.836
Freundlich Isotherms	***Fe***	***Cu***	***Co***	***Hg***	***Ni***	***Zn***	***U***	***Cr***
A	0.062	0.053	0.058	-0.011	0.058	0.041	-0.005	0.047
B	0.189	0.212	0.267	0.356	0.273	0.245	0.346	0.232
K_f	1.154	1.129	1.144	0.974	1.143	1.098	0.989	1.116
n	5.267	4.707	3.743	2.808	3.667	4.074	2.888	4.307
ΔGo (kJ/mol)	-13.06	-11.67	-9.279	-6.961	-9.090	-10.09	-7.158	-10.68
Δq (%)	53.88	42.95	31.51	26.51	33.06	19.02	21.95	25.44
R	0.964	0.994	0.983	0.965	0.979	0.978	0.954	0.943
D-R Isotherms	***Fe***	***Cu***	***Co***	***Hg***	***Ni***	***Zn***	***U***	***Cr***
A	0.124	0.018	0.009	-0.501	0.021	-0.187	-0.449	-0.159
B	-0.003	-0.003	-0.004	-0.005	-0.005	-0.003	-0.004	-0.003
Xm (mol/kg)	1.132	1.019	1.010	0.606	1.022	0.829	0.638	0.853
Es (kJ/mol)	14.02	13.24	10.64	10.47	10.38	12.50	10.81	12.70
Δq (%)	29.78	34.46	18.38	74.15	19.78	31.82	75.06	38.10
R	0.973	0.898	0.967	0.905	0.963	0.958	0.936	0.915
K_d	***Fe***	***Cu***	***Co***	***Hg***	***Ni***	***Zn***	***U***	***Cr***
A	6.011	4.906	3.745	3.706	3.560	4.633	4.039	4.353
B	2132	2628	2664	2490	2760	1441	4536	2164
ΔGo (kJ/mol)	-14.89	-12.16	-9.283	-9.187	-8.825	-11.48	-10.01	-10.79
Kdo	407.7	135.1	42.31	40.69	35.17	102.8	56.82	77.69
Δq (%)	79.48	75.44	86.89	73.18	90.58	72.92	68.63	72.73
R	0.977	0.965	0.761	0.669	0.738	0.755	0.764	0.710

The adsorption process is well described by the Freundlich isotherm with r > 0.950. The adsorption of Fe is also described by the Langmuir and the D-R isotherms whereas the adsorption of Co and Ni was found to obey the D-R isotherm. The biosorption of metal ions in a multi-ion system occurs on a heterogenous surface and the coverage might be mono or multilayer depending on the composition of the alginates.

The maximum adsorption capacities calculated from the Langmuir isotherm were higher compared to those for the single-ion system and were followed the sequence: Fe (0.467) > Cr (0.407) > Ni (0.393) > Co (0.391) > Zn (0.332) > Cu (0.218) >> Hg (0.094) > U (0.079). The values of *n* range between 2.808 and 5.267 with $1/n < 1$, indicating that the process is

beneficial and that the metals bind on the zeolite-alginate with weak free energies. These results are confirmed by the values of adsorption free energy ($10.38 \leq Es \leq 14.02$) obtained from the D-R isotherm. At this energy, the adsorption process is meanly by ion exchange. The Gibbs free energies obtained from the distribution coefficient were negative for all the metals, indicating the spontaneous nature of the process. The distribution coefficients (L g^{-1}), indicating the adsorption affinity of metals towards the zeolite-alginate, were higher than the values obtained in single-ion systems and were in the following order: Fe (407.7) > Cu (135.1) > Zn (102.8) > Cr (77.69) > U (56.82) > Co (42.31) > Hg (40.69) > Ni (35.17). This order is not in agreement with the maximum adsorption capacity from the Langmuir isotherm. The presence of other ions could have enhanced the uptake of metal ions on zeolite-alginate.

The Langmuir parameters can be used to predict the affinity between the sorbate and sorbent using the dimensionless separation factor, R_L, as defined in Equation 3.9.
The values of R_L for the biosorption of heavy metals on zeolite-alginate are presented in Figure 4.118 for the single ions and multi ions, respectively.

(a)

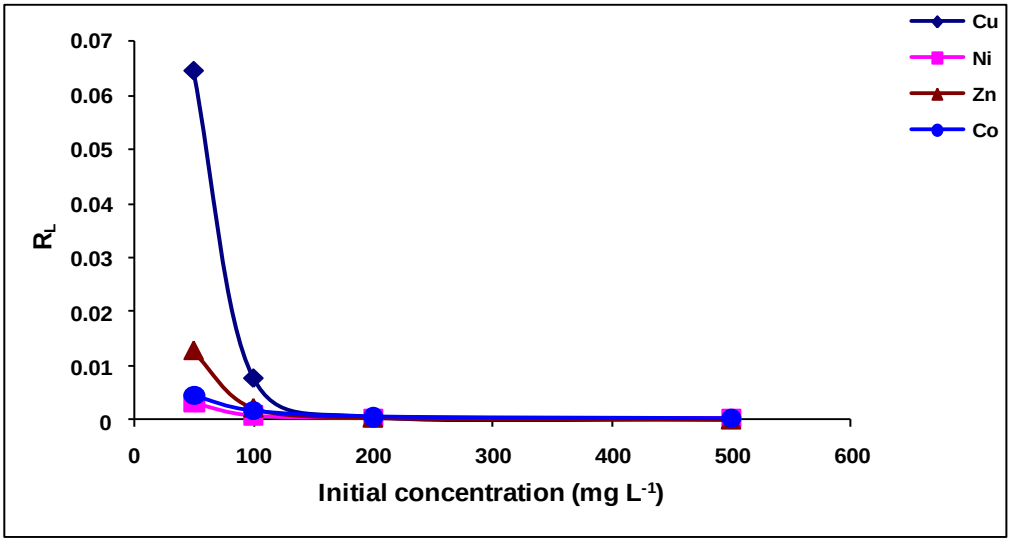

(b)

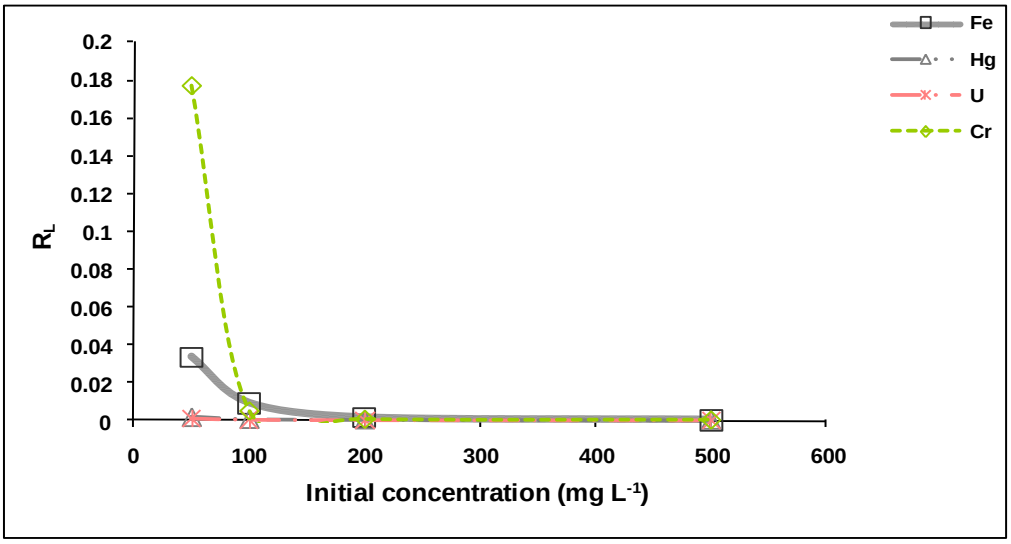

Figure 4.118 (a) and (b) R_L values based on Langmuir isotherm at different metals concentrations in single-ion system

All the values range between 0 and 1, indicating favourable adsorption of Cu, Cr, Co, Fe, Ni, Zn, Hg and U on zeolite-alginate. For an initial concentration of 100 mg L^{-1} for Co, Ni, Zn, Hg, Cr and U, the R_L value was approximately 0, indicating that beyond this concentration the adsorption was irreversible. The adsorption of Cu and Fe on zeolite-alginate is irreversible at a concentration of 200 mg L^{-1}.

The adsorption of metals in a multi-ion system was not described by the Langmuir isotherm for most of the metals studied, so the calculation of R_L was not necessary.

4.6.5.3 Effect of contact time and kinetic studies

i) Effect of contact time

The time taken for the adsorption process to attain thermodynamic equilibrium is very important in characterization and prediction of both the efficiency and feasibility of an adsorbent for its use in water pollution control. The effect of contact time was studied for a concentration of 100 mg L^{-1}. Figure 4.119 shows that the adsorption capacity of metal ions increases sharply with increasing agitation time up to 15 mins and then it increases very slowly and becomes nearly constant after 40 min. The constant adsorption after 45 min means that thermodynamic equilibrium is attained at that extent. We assume that most of the available sites were occupied after 15 min. Zn and Cr had the highest adsorption capacity compared to other metals.

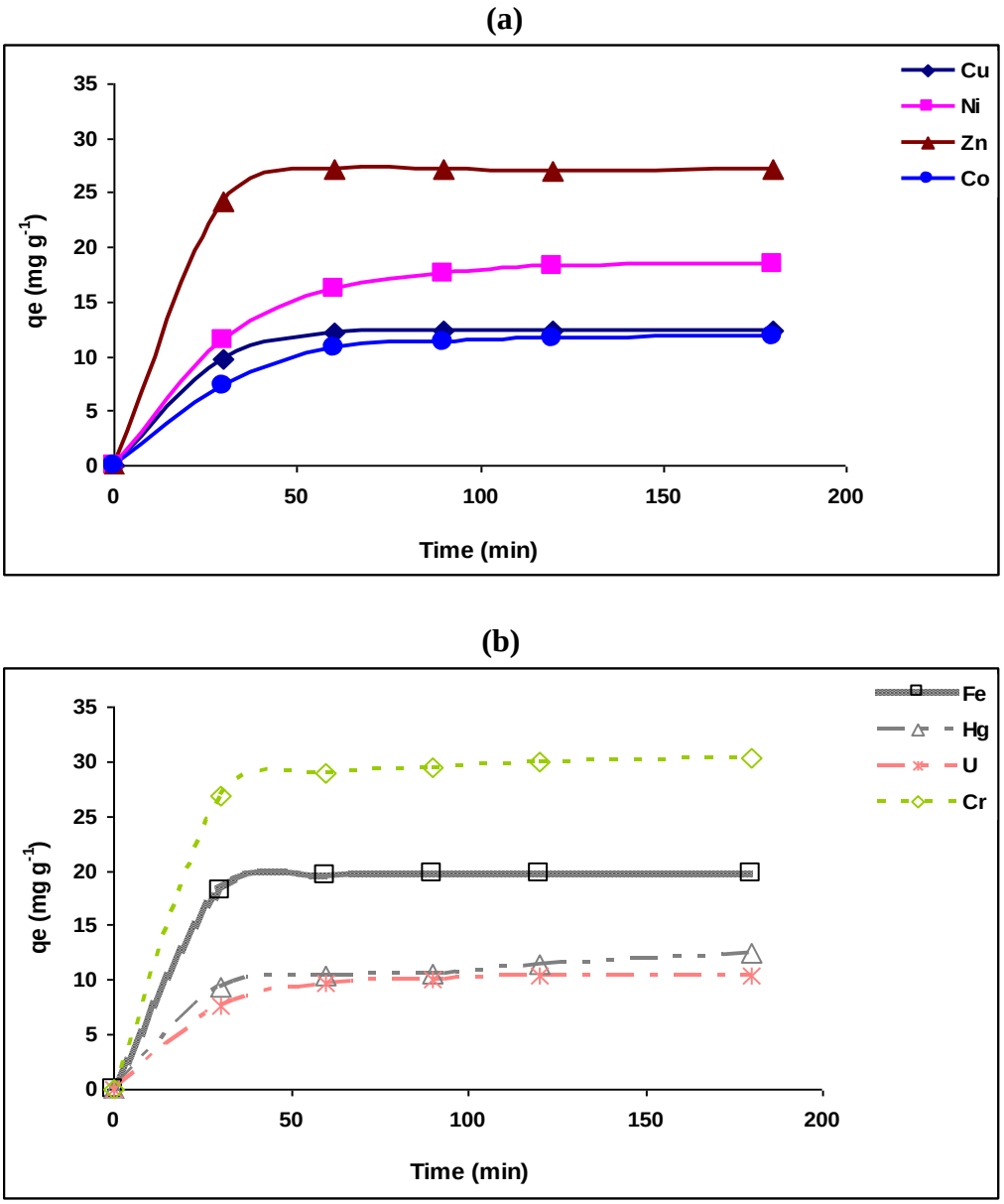

Figure 4.119 Effect of contact time on the adsorption of (a) Cu, Ni, Zn, Co, (b) Cr, Fe, Hg, U on zeolite-alginates in single component solutions (pH = 3, C_i = 100 mg L^{-1}, Temp = 298.15±1^{o}K, agitation rate = 150 rpm)

The biosorption of metals from multi ion solutions are shown in Figure 4.120. A similar trend was observed as for the adsorption in single metal-ion. The maximum uptake reached after 15 min and then the equilibrium was attained after 45 min. In this batch, the uptake of most of the metal ions increases.

(a)

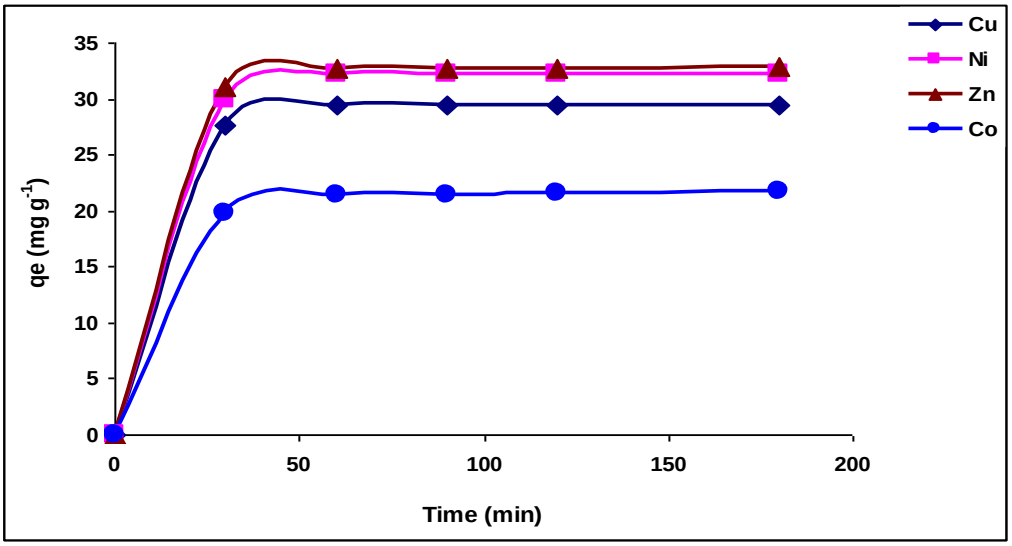

(b)

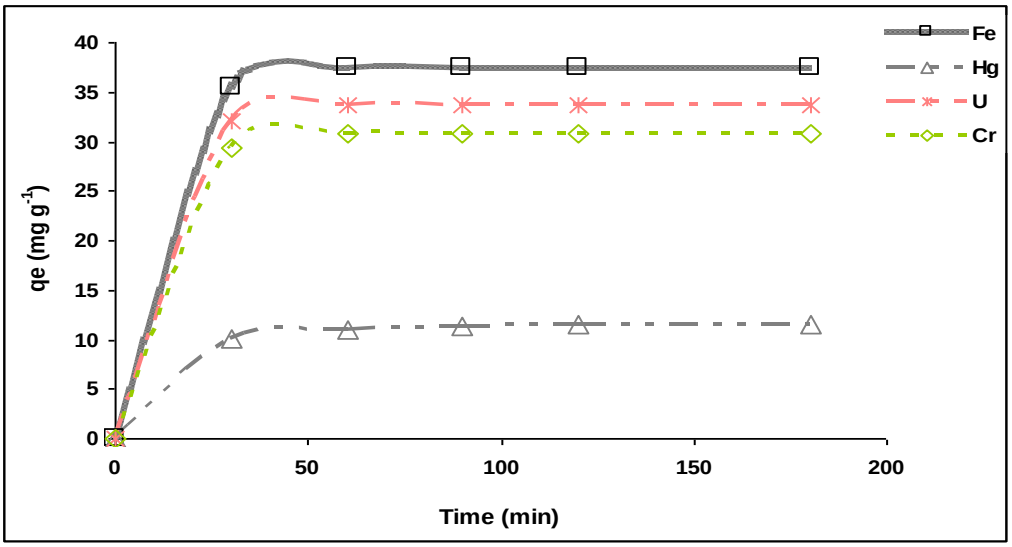

Figure 4.120 Effect of contact time on the adsorption of (a) Cu, Ni, Zn, Co (b) Cr, Fe, Hg, U on zeolite-alginates in multi-components solutions (pH = 3, C_i = 100 mg L^{-1}, Temp = 298.15±1^{o}K, agitation rate = 150 rpm)

ii) Kinetic modelling of the adsorption of metal ions on zeolite-alginate (in single- and multi-component systems)

The experimental data were fitted to the pseudo first- and second-order, Elovich, intraparticle diffusion and the film diffusion models. The corresponding kinetic parameters derived from

these models are shown in Tables 4.94 and 4.95 for the adsorption in single- and multi-component systems, respectively.

Table 4.94 Kinetic constants for the adsorption of metal ions on zeolite-alginates in single-ion system

Pseudo-first order								
	Fe	***Cu***	***Co***	***Hg***	***Ni***	***Zn***	***U***	***Cr***
A	-1.204	-2.114	-1.260	-1.764	-1.093	-1.016	-1.802	-1.283
B	-0.045	-0.001	-0.027	-0.021	-0.026	-0.047	-0.008	-0.001
q_e (mol/kg)	0.063	0.008	0.055	0.017	0.081	0.096	0.016	0.052
K_1	0.103	0.002	0.062	0.048	0.059	0.108	0.018	0.002
Δq (%)	71.91	81.23	86.64	82.13	68.16	124.6	59.52	80.78
R	0.990	0.985	0.993	0.927	0.999	0.998	0.986	0.925
Pseudo – second order								
	Fe	***Cu***	***Co***	***Hg***	***Ni***	***Zn***	***U***	***Cr***
A	18.96	11.36	297.8	984.4	201.7	23.25	86.81	2.984
B	28.29	5.097	49.22	164.4	31.36	24.02	22.69	1.715
q_e (mol/kg)	0.035	0.196	0.021	0.006	0.032	0.042	0.044	0.583
K_2	42.21	2.286	8.133	27.45	4.875	24.81	5.933	0.986
Δq (%)	2.560	7.968	15.41	5.985	14.27	3.651	9.111	3
R	0.999	0.999	0.999	0.996	0.998	0.999	0.999	1.000
Elovich model								
	Fe	***Cu***	***Co***	***Hg***	***Ni***	***Zn***	***U***	***Cr***
A	0.001	0.004	0.001	0.001	0.002	0.001	0.001	0.016
B	0.008	0.041	0.004	0.001	0.006	0.009	0.009	0.123
B	132.05	24.25	244.2	823.7	156.5	112.5	110.3	8.132
A	0.009	0.045	0.004	0.001	0.006	0.010	0.010	0.140
Δq (%)	10.21	7.001	7.127	4.998	5.751	9.440	4.801	8.786
R	0.838	0.843	0.908	0.967	0.941	0.840	0.929	0.968
Intraparticle diffusion model								
	Fe	***Cu***	***Co***	***Hg***	***Ni***	***Zn***	***U***	***Cr***
A	0.009	0.039	0.003	0.001	0.004	0.010	0.008	0.133
B	0.003	0.015	0.002	0.002	0.002	0.003	0.003	0.042
Id	0.009	0.039	0.003	0.001	0.004	0.010	0.008	0.133
Kp	0.003	0.015	0.002	0.002	0.002	0.003	0.003	0.042
Δq (%)	15.98	15.29	11.06	13.13	11.31	16.85	13.67	16.27
R	0.848	0.892	0.939	0.928	0.947	0.859	0.918	0.869
Film diffusion								
	Fe	***Cu***	***Co***	***Hg***	***Ni***	***Zn***	***U***	***Cr***
A	-5.148	-3.898	-2.540	-1.314	-2.512	-5.573	-3.095	-2.426
B	0.015	0.013	0.009	0.001	0.010	0.021	0.012	0.003
If	-5.147	-3.897	-2.539	-1.314	-2.512	-5.573	-3.095	-2.426
Kf	-0.015	-0.013	-0.009	-0.001	-0.001	-0.021	0.012	-0.003
Δq (%)	84.52	41.44	74.21	91.29	91.29	40.24	42.04	40.77
R	0.989	0.985	0.993	0.926	0.999	0.998	0.986	0.951

The correlation coefficients of the pseudo second-order rate model are very close to 1 for all the metals studied, thus suggesting that chemisorption is the controlling step and the biosorption occurred in at least two steps. The first step corresponds to the dissociation of the hydrated metal followed by the interaction of metal with the functional groups on the zeolite-alginate surface. The kinetic uptake for the second-order followed the sequence: Cr > Cu > U > Zn > Ni > Co > Fe > Hg, whereas the sequence of the kinetic rate was as: Fe > Hg > Zn > Co > Cu > U > Ni > Cr. The sequence of the kinetic rate is inconsistent with metal uptake kinetics. The correlation coefficients of the pseudo first-order and film diffusion models for the metals investigated are high (more than 0.900), suggesting that both of the models are applicable to fit the kinetic experimental data. The adsorption of Cr and Hg can be described by the Elovich model, with a correlation coefficient > 0.950, indicating a chemisorption process.

In order to compare the validity of each kinetic model more efficiently, the normalized standard deviation, $\Delta q(\%)$ is used, and the pseudo second-order has the lowest standard deviation error, except for Co, Ni and U.

The high correlation coefficients obtained with the film diffusion kinetic suggest that the kinetics of the adsorption process is controlled by diffusion through the liquid film surrounding the biosorbent.

The different kinetic parameters for the multi-ion system are presented in Table 4.95. As for the previous study, the adsorption followed the pseudo second-order model with correlation coefficients ≥ 0.999, implying a chemisorption process. The metals uptake kinetics was in the order: Fe > Cr > Ni > Zn > Cu > Co > U > Hg while the kinetic rate was in the following sequence: U > Hg > Cr > Cu > Zn > Fe >Ni > Co. The low uptake of U and Hg compared to other metals could be due the nature of functional groups on the surface of the adsorbent as explained in the previously. The adsorption of Cu, Hg and U may be described also by the pseudo first-order as well as by the film diffusion models.

Table 4.95 Kinetic constants for the adsorption of metal ions on zeolite-alginate in A multi-ion system

Pseudo-first order								
	Fe	***Cu***	***Co***	***Hg***	***Ni***	***Zn***	***U***	***Cr***
A	-3.091	-2.950	-1.532	-1.885	-2.469	-1.840	-2.725	-3.106
B	0.005	0.004	-0.003	-0.008	0.002	-0.001	-0.003	0.005
q_e (mol/kg)	0.001	0.001	0.029	0.013	0.003	0.014	0.002	0.001
K_1	0.012	-0.008	0.006	0.019	-0.006	0.003	0.008	-0.011
Δq (%)	81.82	81.83	79.26	68.09	81.93	81.13	81.19	81.80
R	0.940	0.953	0.937	0.991	0.941	0.916	0.953	0.944
Pseudo – second order								
	Fe	***Cu***	***Co***	***Hg***	***Ni***	***Zn***	***U***	***Cr***
A	0.624	1.050	2.918	26.26	1.111	0.984	2.900	0.631
B	1.486	2.155	2.704	17.38	1.816	1.990	7.056	1.687
q_e (mol/kg)	0.673	0.464	0.369	0.058	0.551	0.502	0.142	0.593
K_2	3.542	4.419	2.505	11.50	2.970	4.023	17.17	4.505
Δq (%)	1.793	2.052	2.677	3.522	2.476	1.546	1.662	1.596
R	0.999	0.999	1.000	0.999	0.999	1.000	1.000	1.000
Elovich model								
	Fe	***Cu***	***Co***	***Hg***	***Ni***	***Zn***	***U***	***Cr***
A	0.024	0.016	0.011	0.002	0.018	0.018	0.005	0.021
B	0.145	0.100	0.079	0.012	0.118	0.108	0.030	0.128
B	6.912	10.03	12.69	82.10	8.471	9.267	32.81	7.840
A	0.171	0.117	0.091	0.014	0.138	0.127	0.036	0.151
Δq (%)	10.84	2.718	9.686	8.723	10.33	10.85	10.91	10.98
R	0.813	0.816	0.904	0.937	0.823	0.861	0.825	0.814
Intraparticle diffusion model								
	Fe	***Cu***	***Co***	***Hg***	***Ni***	***Zn***	***U***	***Cr***
A	0.174	0.119	0.089	0.013	0.138	0.130	0.037	0.154
B	0.048	0.033	0.027	0.004	0.040	0.036	0.010	0.043
Id	0.174	0.119	0.089	0.013	0.138	0.130	0.037	0.154
Kp	0.048	0.033	0.027	0.004	0.040	0.036	0.010	0.043
Δq (%)	17.61	17.51	16.89	16.34	17.33	17.57	17.63	17.67
R	0.838	0.841	0.856	0.869	0.846	0.838	0.838	0.836
Film diffusion								
	Fe	***Cu***	***Co***	***Hg***	***Ni***	***Zn***	***U***	***Cr***
A	-5.963	-5.640	-2.850	-3.293	-4.725	-3.490	-5.046	-5.974
B	0.014	0.014	0.003	0.009	0.010	0.003	0.011	0.014
If	-5.963	-5.640	-2.850	-3.293	-4.725	-3.489	-5.046	-5.974
Kf	-0.014	-0.014	-0.003	-0.009	-0.010	-0.003	-0.011	-0.014
Δq (%)	40.32	40.34	40.72	40.63	40.51	40.71	40.43	40.31
R	0.939	0.953	0.937	0.992	0.941	0.916	0.953	0.944

4.6.5.4 Effect of temperature and thermodynamic parameters

An increase of the adsorption capacity was observed with increasing temperature, indicating that the adsorption is endothermic as seen in Table 4.96. In fact, the energy barrier between

metal ions and zeolite-alginate is overcome when the temperature rises. Additional adsorption sites are created on the surface of the biosorbent due to the dissociation of some of the surface components on zeolite (Bhattacharyya and Gupta, 2006). The thermodynamic parameters were calculated and are listed in Table 4.96 for the adsorption of single ions. The adsorption of Co, Hg and U on zeolite-alginate occurred through physisorption process with activation energy < 40 kJ mol^{-1} whereas the rest of the metals with higher activation energies are adsorbed through strong bonds that indicate a chemisorption process.

The positive values of ΔH^o suggest that the interaction of metal ions adsorbed by the zeolite-alginate system is endothermic, which is supported by an increase in adsorption of metals with an increase of temperature. The values of ΔS^o indicate whether the adsorption reaction is through an associative or dissociative mechanism. The value change larger than –10 J mol^{-1} K^{-1} means that adsorption follows a dissociative mechanism (Unuabonah *et al.,* 2008). The values of ΔS^o are in the range of 27.68– 67.15 J mol^{-1} K^{-1} and far larger than the above boundary value, suggesting that the adsorption reaction complies with a dissociative mechanism. The positive values of ΔS^o reveal increased randomness at the solid-solution interface (Nuhoglu and Malkoc, 2009) during the fixation of metal ions on the active sites of the zeolite-alginate. The negative values of ΔG^o indicate that the adsorption process is spontaneous.

Table 4.96 Thermodynamic parameters of metal ion adsorption on zeolite-alginate in a single-ion system

	q_e		Ea	ΔH^o	ΔS^o	ΔG^o	
	mg g^{-1}		kJ mol^{-1}	kJ mol^{-1}	J(K $mol)^{-1}$	kJ mol^{-1}	
	293.15 ^oK	**313.15** ^oK				**293.15** ^oK	**313.15** ^oK
Cu	37.97	44.82	55.86	141.4	0.435	-2.801	-5.248
Ni	29.91	45.72	105.3	276.9	0.866	-0.968	-5.760
Zn	34.81	47.51	118.9	298.1	0.929	-2.019	-7.176
Co	29.01	35.72	28.48	83.39	0.259	-0.787	-2.229
Fe	44.80	48.23	74.40	176.8	0.538	-5.251	-8.310
Hg	15.22	25.14	30.64	123.8	0.395	-2.065	-0.078
U	12.00	24.70	36.27	158.9	0.507	-2.809	-0.058
Cr	43.80	47.20	50.56	122.5	0.369	-4.765	-6.884

The thermodynamic parameters calculated for the biosorption of metal ions from a multi ion solution are given in Table 4.97.

Table 4.97 Thermodynamic parameters of metal ions adsorption on zeolite-alginate in a multi-ion system

	q_e		Ea	ΔH^o	ΔS^o	ΔG^o	
	mg g^{-1}		kJ mol^{-1}	kJ mol^{-1}	J(K $mol)^{-1}$	kJ mol^{-1}	
	293.15 ^oK	**313.15** ^oK				**293.15** ^oK	**313.15** ^oK
Cu	44.80	46.61	27.25	65.41	0.189	-5.248	-6.380
Ni	41.10	46.20	58.85	144.6	0.442	-3.729	-6.231
Zn	46.30	48.21	50.39	119.1	0.355	-5.953	-8.013
Co	41.42	45.10	36.87	91.27	0.274	-3.830	-5.409
Fe	45.80	48.92	84.90	200.5	0.611	-5.820	-9.290
Hg	37.90	41.33	31.44	58.56	0.175	-2.783	-3.796
U	41.10	44.80	45.98	87.82	0.264	-3.729	-5.248
Cr	45.90	46.30	6.510	15.68	0.030	-5.887	-6.158

In general, low values of activation energy were obtained for the adsorption of metal ions on zeolite-alginate in a multi-ion system compared to those for the single-ion system. E_a for Cu, Co, Hg and Cr were < 40 kJ mol^{-1}, indicating physisorption mechanism. A similar trend was seen for the other thermodynamic parameters (ΔS^o, ΔH^o, ΔG^o). Negative ΔG^o values indicate the spontaneous nature of the adsorption process and positive values of ΔS^o reveal the increased randomness at the solid-solution interface.

4.6.5.5 Effect of adsorbent mass

The dependence of metal adsorption on adsorbent mass was investigated by varying the amount of zeolite-alginate from 1 to 6 g, while keeping other parameters (pH, agitation speed and time, temperature and adsorbate concentration) constant. Figure 4.121 shows the adsorption capacity of metal ions as a function of biosorbent mass. The results show a decrease of adsorption capacity with an increase in adsorbent mass. The decrease in equilibrium adsorption capacity per unit mass of adsorbent with increasing mass may be due to the presence of more active sites resulting in the adsorption sites remaining unsaturated during the adsorption reaction (Raji and Anirudhan, 1997). Another possible reason is the decreased total surface area of the adsorbent and an increase in the diffusion path length caused by the aggregation adsorbent particles (Unuabonah *et al*., 2008).

(a)

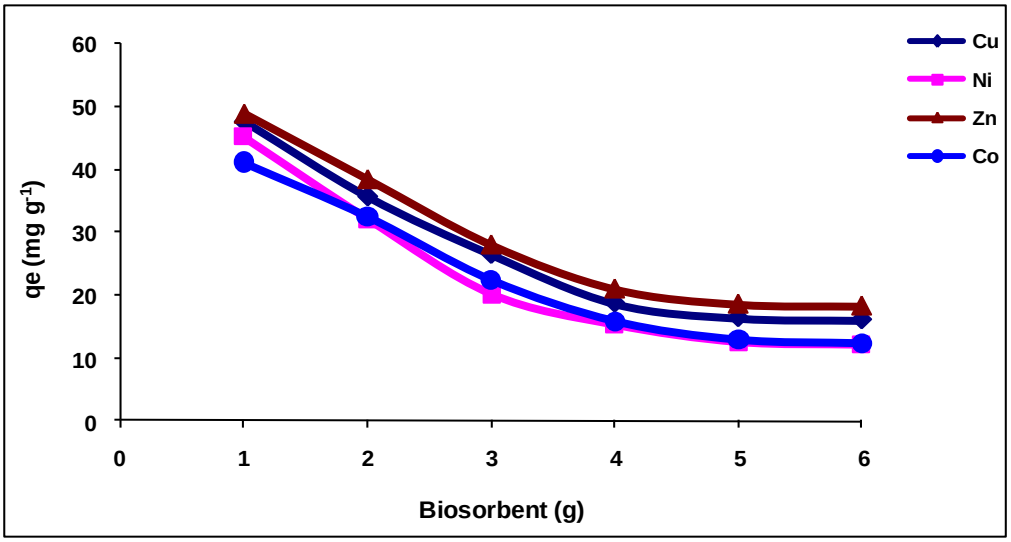

(b)

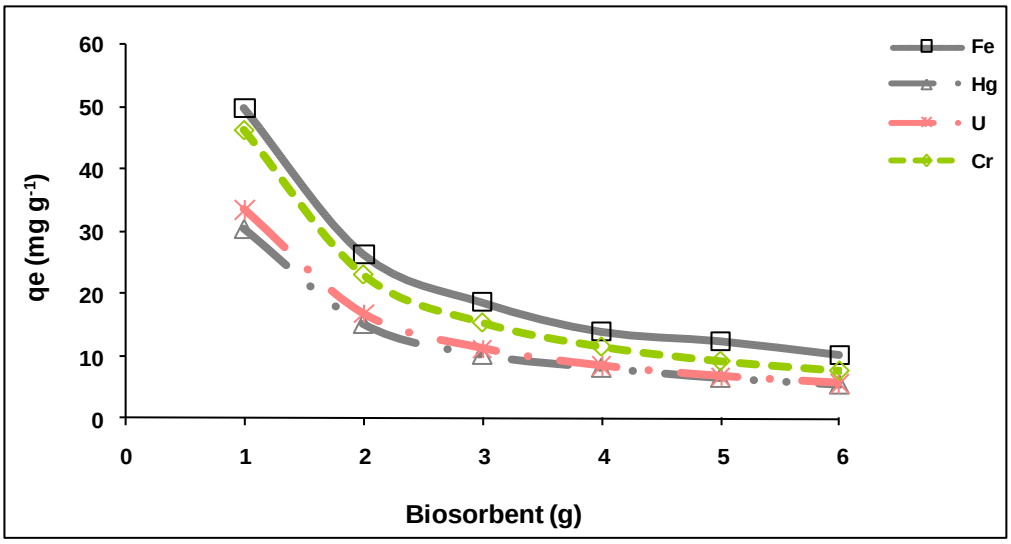

Figure 4.121 Effect of biosorbent mass on the biosorption of (a) Cu, Co, Ni, Zn (b) Cr, Fe, Hg, U for zeolite-alginate in multi-component solutions (C_i = 100 mg L^{-1}, pH = 3, Temp = 25^{o}C)

4.6.5.6 Regeneration and reuse of the zeolite-alginate

The effective desorption of metal ions from the sorbent with regeneration of the latter for reuse is an important economical advantage of sorption processes. Hydrochloric acid 0.1 mol L^{-1} was used for desorption of metal ions from zeolite-alginate beads. The results obtained are shown in Figure 4.122 (a) and (b) for the single and multi-ion system, respectively.

(a)

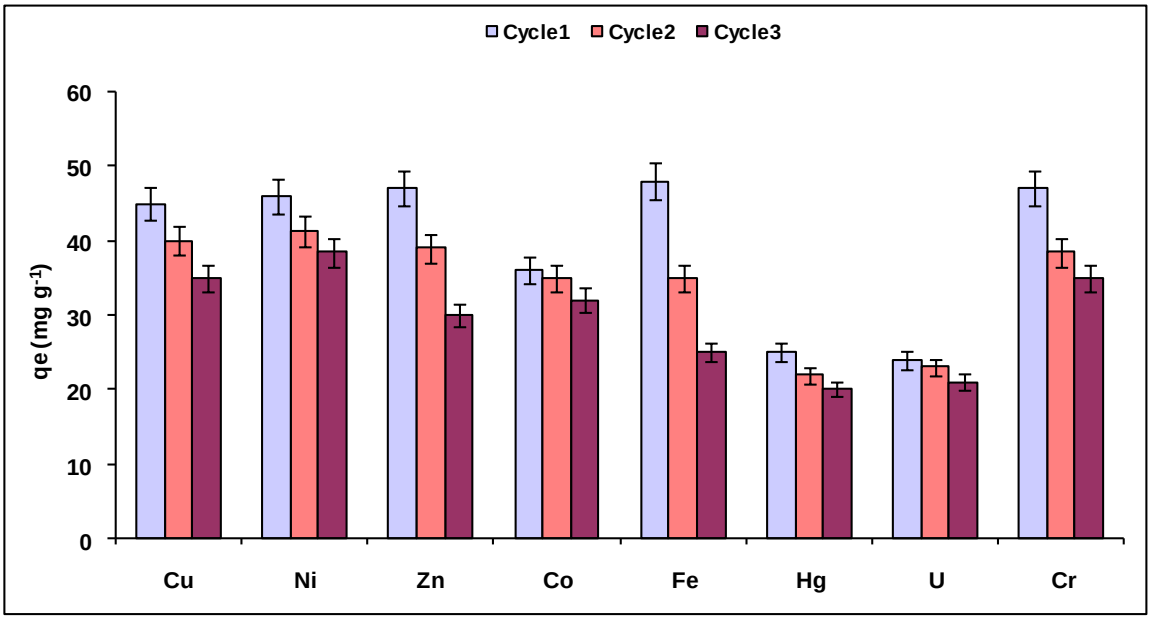

(b)

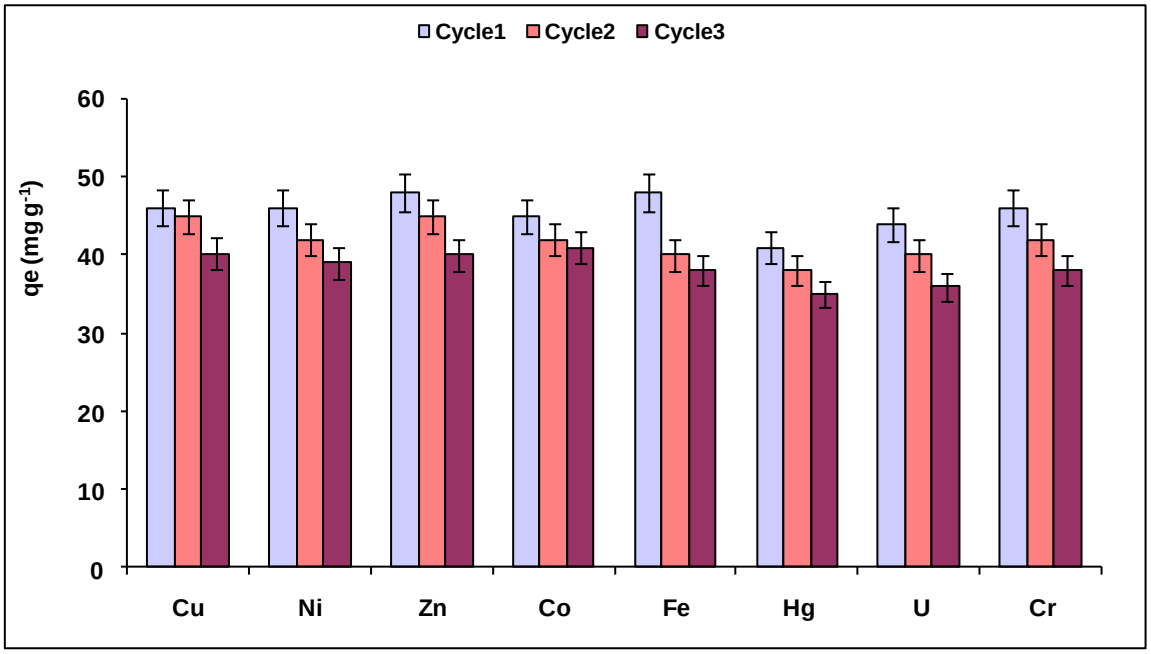

Figure 4.122 Regeneration and reuse of zeolite-alginate (a) single-ion system (b) multi-ion system

A decrease adsorption capacity was observed after the 3rd cycle of: Cu (22.22), Ni (16.31), Zn (36.17), Co (11.11), Fe (47.92), Hg (20), U (12.51), Cr (25.53) in single-ion systems. A decrease in adsorption capacity could be the effect of the acid on the biopolymer. In fact, the acid can dissolve the polysaccharides or alter the morphology of binding sites on the sorbent, reducing its sorption capacity (Esteves *et al.*, 2000). Further studies are recommended to find

out if the desorption process by HCl affects the stability of the zeolite-alginate polymer. From these results, it is clear that uranium and mercury were the less desorbed due to the solvent used. Other solvents (i.e. HNO_3, Na_2CO_3) can be used to desorb these metals.
A decrease of adsorption capacity was observed after the 3rd cycle: Cu (12.61), Ni (15.22), Zn (16.67), Co (8.88), Fe (20.83), Hg (14.63), U (18.18), Cr (17.39) in a multi-ion system. The decrease in terms of adsorption capacity was less than observed in a single-ion system.

Unlike for the single-ion system, the desorption of uranium and mercury were higher in the presence of other ions. It may be possible that the synergistic effect could be reversible.
Most of the metals were desorbed efficiently for the 3 cycles tested and the % of desorption are shown in Figure 4.123 for the single- and multi-ion systems, respectively.

(a)

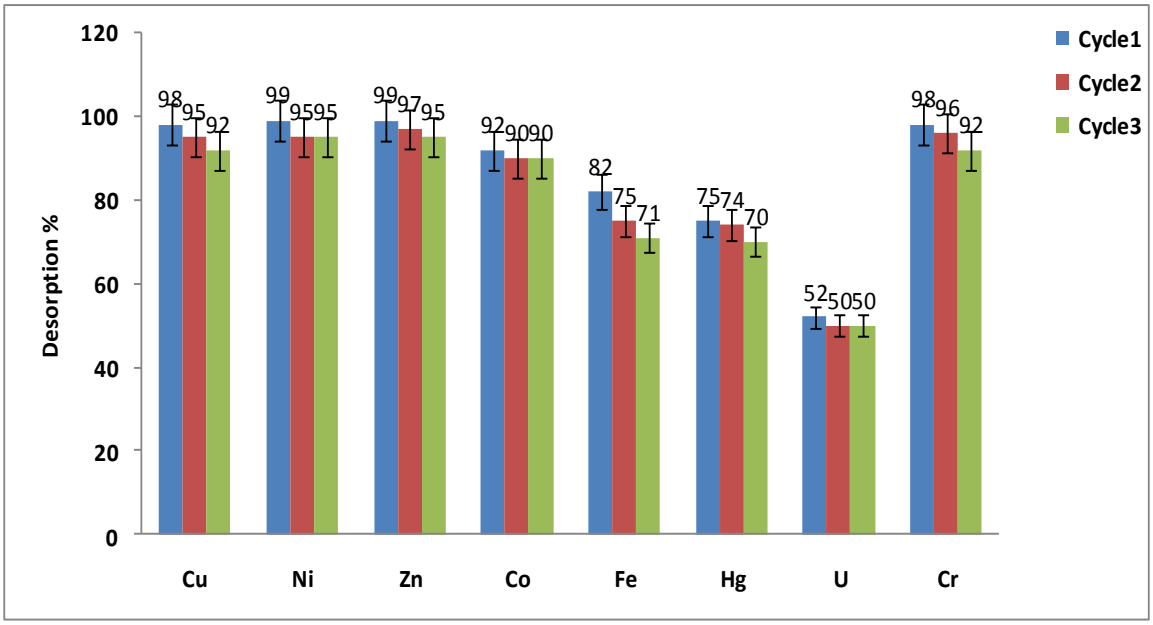

(b)

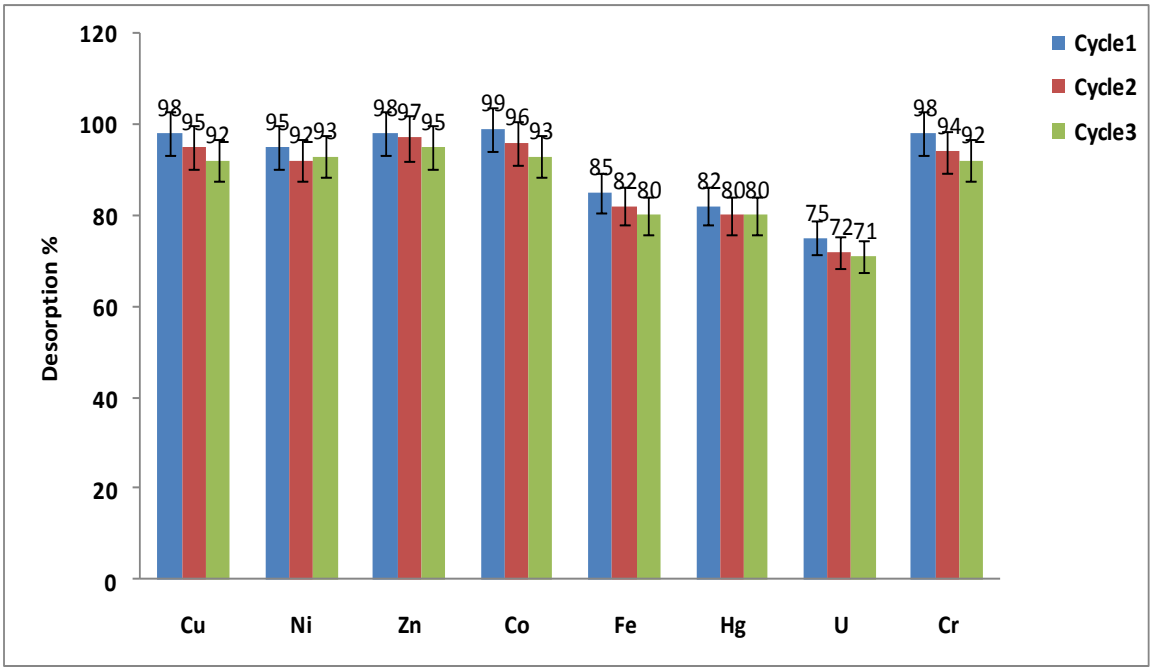

Figure 4.123 Desorption (%) of metal ions from the zeolite-alginate by 0.1 mol L^{-1} HCl

Desorption ratios of Cu, Ni, Zn, Co and Cr from alginate were > 98% with 0.1 mol L^{-1} HCl. Fe, Hg and U gave a desorption < 90%. Iron desorption was incomplete in this case, unlike for most of the adsorbents investigated in this research. Although the alginate beads showed a large uptake capacity for iron, the concentration of this metal in desorption solutions was low, suggesting that iron is partially retained by the biopolymer.

Several studies have reported that the main binding sites for metal ions in alginate molecules are the carboxylic groups from mannuronic and guluronic acid residues. The imino diacetic acid groups in the complex are also weakly acidic. Therefore, the binding sites in the sorbent are converted to the protonated forms at the low pH of the acid desorbents used, thus releasing the previously bound ions.

Conclusion

This study indicated that green alga *Oedogonium* sp. which are widely available, can be an efficient biosorbent material for heavy metals from wastewater.

- The analysis of the FTIR spectra showed the presence of ionisable functional groups (i.e. carboxyl, amino, amide and hydroxyl) able to interact with metal ions.

- The major mechanism of metal ions–sorption interaction is found to be the ionic interactions and complex formation between metal cations and ligands contained within the structure of the biomass.

- The biomasses pre-treated by $H_2C_2O_4$ gave a high adsorption capacity.

- The adsorption process was fast enough, as maximum ions were adsorbed within 30 mins of contact time. The adsorption capacity was solution pH dependent and maximum adsorption capacity was obtained at a solution pH of 5. At pH 3, the maximum biosorption capacity for *Oedonium* sp. has been found to be 50 mg g^{-1} in a multi-ion system for all the metals, whereas, Co and Ni up take were about 4 and 8 mg g^{-1}, respectively in a single–ion system.

- Metals uptake by intact algal cells was found to consist of two processes: (1) a fast surface reaction and (2) a slow transport into walls and cytoplasm. Other variables, such as metal ion size, hydration energy, and electronic structure have to be assessed.

- The equilibrium data fitted well the Freundlich isotherms than the Langmuir isotherm for the single-ion system, thus proving heterogenous adsorption of metals on algal biomass *Oedogonium* sp. The mean free energy of biosorption describes a physisorption process, mainly ion exchange mechanism. Both Freundlich and the

Dubini-Radushkevich describe the biosorption process in a multi-ion system, implying heterogenous process.

- The distribution coefficient values were high for the metal-ions in the multi-ion systems; a synergic effect was observed in this case.

- Analysis of data shows that the process involves pseudo second-order kinetics and the thermodynamic treatment of equilibrium data shows the spontaneous and endothermic nature of the adsorption process for Cu, Ni, Zn, Co and Cr, whereas the biosorption of Fe, Hg and U was exothermic. The biosorption was spontaneous and exothermic in the multi-ion system for the metals studied.

- The biosorption capacity decreases with the increase of biomass, in the single-ion system, probably due to the lack of metals in solution; the opposite effect was obtained with the multi-ion system.

- HCl efficiently desorbed metal from the metal-loaded biomass, interesting is even the initial metals of the *Oedogonium* sp. algal were desorbed, this increases the metals uptake in the next biosorption test. The metal-loading ability of the biomass was not substantially lessen algal during successive sorption/desorption cycles. The test biomass was reused in three biosorption and desorption cycles with an increase (between 9.7% and 16.7%) in its biosorption capacities.

- The IR analysis of this extract revealed the presence of functional groups such as: carboxyl, hydroxy and amine. These results are in agreement with earlier obervations that metals interact with algae primarily by electrostatic bonding to negative sites determined only by pH.

Batch experiments were performed to test the adsorption capacity of the developed alginate complex beads consisting of synthetic Na-alginates and natural zeolite. The following conclusions could be drawn from the experimental investigation:

- Alginate has good formability to immobilize the zeolite to prepare macro-structured material, which can be easily separated from water solution after adsorption using simple filtration method.

- The alginate complex beads developed in this study could adsorb metal ions such as Cu, Co, Cr, Fe, Hg, Ni, Zn and U in single and multi-ion system. The maximum adsorption capacities calculated from the Langmuir model were higher for the multi-ion system.

- In general, the equilibrium isotherm could be described by Langmuir, Freundlich as well as D-R isotherms, except Ni, which obey only the Langmuir isotherm and Hg for which the equilibrium did not fit the Langmuir isotherm, meaning that Ni is adsorbed on monolayer coverage, whereas a multilayer was observed for other metals. For the metals adsorption in multi-ion system, the adsorption equilibrium could be described by the Freundlich and the D-R isotherms.

- All R_L values range between 0 and 1, indicating the favourable adsorption of heavy metals onto zeolite-alginate. Moreover, the adsorption process was also found to obey Freundlich adsorption isotherm. As seen from the results, the values of *n* is $0 < n < 10$ showing that the adsorption of Cu, Co, Cr, Fe, Hg, Ni, Zn and U onto zeolite-alginate is favourable.

- The adsorption of metals was fast and the maximum up take was reached after 15 mins with low adsorption of mercury. The kinetic follows the pseudo-first and second order model. Beside, the film diffusion could be the limiting step in this process. The similar observation is valuable in the multi-ion adsorption system.

- The thermodynamic calculations indicated the feasibility, endothermic, and spontaneous nature of the biosorption of Cu, Co, Cr, Fe, Hg, Ni, Zn and U onto zeolite-alginate is favourable.

- The adsorption capacities decreased with the increase of biosorbent mass, similar results were observed in literature. The regeneration of the biosorbent by 0.1 M HCl was efficient up to 3 cycles of adsorption-desorption.

Chapter 5: General conclusion and recommendations

The biosorbents synthesized, namely: zeolite/bentonite-microbial compounds (histidine, cysteine and sorbitol); zeolite/bentonite-*Penicillium simplicissimum* and zeolite-alginate displayed good adsorption of toxic metals (Cu, Co, Cr, Fe, Hg, Ni, Zn and U) even at low pH values, making them ideal sorbents for metals in gold mine effluents and efficient in areas contaminated by AMD with high metal concentrations. Biosorption was described to be easy, safe, rapid, inexpensive and can be used to recover heavy metals at very low concentration.

Chemical modification of natural zeolite/bentonite by amine coupling agents may be a useful tool for the preparation of new adsorbents with high adsorption capacities and selectivity towards metal ion retention for waste waters from AMD systems. This hybrid organic-inorganic material can be an alternative low-cost material in the treatment of mine wastewater and possibly for the recovery of precious metals for such effluent. The adsorption rate of biofunctionalised zeolite/bentonite was found to be greater than that of natural zeolite/bentonite at high metal concentrations.

Zeolite and bentonite can be used as support media for the culture of fungi and microalgae, resulting in elevated metal-binding capacities. Non-viable microbial biomass has been shown to exhibit higher affinity for metal ions than its viable counterpart, probably due to the absence of competing protons produced during metabolism.

The accumulation of metals from solutions by fungi, as observed in the study, can be divided into three categories:

(1) biosorption of metal ions on the surface of fungi.

(2) intracellular uptake of metal ions.

(3) chemical transformation of metal ions by fungi

In the real environment, the *Penicillium simplicissimum* fungal biomass can grow in the silica matrix, largely constituting tailings material. This can provide an *in situ* or virtual biosorbent which can adsorb metals at the low pH values associated with these facilities. The column experiments closely resembled how this system would behave in the real environment. The breakthrough curves thus gave a perspective as to the loading capacity and expected timeframes at which leaching of the metals into the underlying aquifers would likely occur.

The zeolite-alginate complex showed similar behaviour to the fungal biomass and the initial chemically-modified systems. Elevated adsorption capacities were observed even at low pH regimes, making it a useful biosorbent for metal abstraction from AMD-impacted water. The

algal biomass grows naturally in the vicinity of tailings facilities and water systems, making it possible and cost effective to culture it *in situ* and allow for clean-up of the contaminated water.

For the sorbents studied, adsorption kinetics was shown to be important in establishing the time zones and effective lifetime of adsorbents and also shed information on the need for regeneration. Thermodynamic parameters were also shown to form an important complementary aspect in assessing adsorption mechanisms. The negative activation energies gave an indication that the metals studied prefer to bind to low energy binding sites, therefore adsorption of these metals occurs without an energy barrier which could be a combination of a chemisorption, physisorption or diffusion. The negative Gibbs free energy results indicated that adsorption of the metals was spontaneous. Understanding the interaction of mineral surfaces with the metal ions and hydrated metal ions has been shown to be important in drawing information about the likely adsorption mechanism that will be followed by a particular metal, for instance as shown in the case of Ni.

The study has shown that metals loaded in the biomass can potentially be desorbed in order to regenerate the biosorbent and possibly reclaim valuable metals. As such, these biosorbent systems have great potential in remediation aspects and recovery efforts.

Recommendations

The economic feasibility of applying these materials on a wider scale should be explored further. This will be possible if such an assessment is conducted in conjuction with the recovery of low levels of precious metals e.g. gold and silver from the wastewaters. This way, the costs of water remediation can be traded off by precious metal recovery. Further assessments of the potential of the biosorbents to extract precious metals from other types of mine wastewaters e.g. platinum group elements (PGEs) from platinum mining waste streams could be considered. As it is, the zeolite-cysteine biosorbent from this study is being used in a separate project to assess its potential to recover low levels of PGEs from platinum mining wastewaters. This can be extended to include other biosorbents as well.

Advantage can be taken of the availability of cheap sources of silica e.g. fly ash from the coal mining industry, zeolites, bentonite as well as the quartz matrix which is a major constituent of the gold tailings. These can be used as supports for biomass that is also readily available in gold mining environments of the Witwatersrand Basin. A number of approaches can be

explored, for instance the construction of reactive barriers using these materials for *in situ* water remediation or *ex situ* treatment based on leaching the polluted water through columns. Further studies can be conducted on the regeneration of the biosorbents. It will be recommended that selective desorption of the metals be carried out so as to recover metals that can be useful to specific industries e.g. uranium selectively removed and sent to uranium processing industries.

Publications related to the present study

Published conference proceedings

- **E.N.Bakatula,** E.M. Cukrowska, C.J. Straker, I.M. Weiersbye, H. Tutu. **(2011).** Biosorption of heavy metals from gold mine wastewaters by *Penicillium simplicissimum* immobilized on zeolite: Kinetic, equilibrium and thermodynamic studies. In: Rüde, R. T., Freund, A. & Wolkersdorfer, Ch.: Mine Water – Managing the Challenges. - p. 271 – 275; Aachen, Germany.

- **E.N. Bakatula**, H. Tutu, E.M. Cukrowska, I.M. Weiersbye & C.J. Straker. **(2011).** Application of a biosorbent based on *Penicillium simplicissimum* immobilized on zeolite for the removal of heavy metals from the gold mine wastewater. 40th SACI Convention Gauteng 23–28th January 2011, South Africa.

- **E.N. Bakatula,** H. Tutu, E.M. Cukrowska, I.M. Weiersbye L. Mihaly-Cozmuta and A. Mihaly Cozmuta. **(2009).** Application of bentonite modified with L-Histidine for the adsorption of toxic elements in mine wastewaters. In: Advances in Mineral Resources Management & Environmental Geotechnology – Assessing the Footprint of Resource Utilization and Hazardous Waste Management, Proceedings of the 3rd AMIREG. International Conference, Athens, Greece, 7-9 September 2009. In Press

-H. Tutu, **E.N. Bakatula,** D. Saad, E.M. Cukrowska, I.M. Weiersbye and E. Rosenberg. Engineered materials for the containment of radionuclides and toxic elements in mine leachates and wastewaters, *Environmin* **2012,** Loskop Dam, South Africa, 11 – 15 March 2012.

-A. Peter, E. Indrea, A. Mihaly-Cozmuta, L. Mihaly-Cozmuta, C. Nicula, H. Tutu, **E. Bakatula. (2012)**. Dual Efficiency Of Nano-Structured TiO2 / Zeolyte Systems In Removal Of Copper (II) And Lead (II) Ions From Aqueous Solution Under Visible Light. *American Institute of Physics*, *AIP Conf. Proc*., **1425**, 139 -143.

Published papers

-A. Peter, C. Nicula, A. Mihaly-Cozmuta, L. Mihaly-Cozmuta, E. Indrea, V. Danciu, H. Tutu and **E. N. Bakatula (2011).** Efficiency of amendments based on zeolite and bentonite in reducing the accumulation of heavy metals in tomato organs *(Lycopersicum esculentum)* grown in polluted soils. *African Journal of Agricultural Research***, Vol. 6**(21), pp. 5010-5023, 5 October, 2011.

-M. Marian**,** A. Peter, L. Mihaly-Cozmuta & **E. Bakatula (2012).** Increased survival chances of the species Quercus petrae in terms of pollution with Cd and Cu by using microbiota-Bentonite systems. *Carpathian Journal of Earth and Environmental Sciences*, February 2012, **Vol. 7**, No. 1, p. 231 – 237.

Poster Presentations

-E.N.Bakatula, H.Tutu, E.M.Cukrowska and I.M.Weiersbye **(2009).** Kinetic and thermodynamic studies of the adsorption of heavy metal ions onto the natural bentonite and bentonite-histidine. Kinetics in Analytical Chemistry (KAC), 10th International Symposium, 02-04 December, South Africa.

-E.N.Bakatula, H.Tutu, E.M.Cukrowska and I.M.Weiersbye. **(2010).** Adsorption of heavy metals by *Penicillium simplicissimum* immobilized on zeolite. ANALITIKA Conference. 6th -9th December, South Africa.

Award

Student Oral Presentation Award (2nd best student oral presentation) at the 11th International Mine Water Association Congress – Mine Water – Managing the Challenges", September 4th-11th 2011, Aachen, Germany.

References

Abdel-Fattah, A.F. and Edrees, M. **(1972).** A study on the polysaccharide content of Ulva Lactuca L. *Qual. Plant. Mater. Veg.*, **22**(1), 15-22.

Afkar, E., Ababna, H. & Fathi, A.A. **(2010).** Toxicology response of the green algae *Chlorella vulgaris* to some heavy metals. *American Journal of Environment Sciences*, **6**, 23-31.

AGA. (2008). AngloGold Ashanti, West Wits Country Report 2008, pp 55.

Ahalya, N., Ramachandra, T. V. and Kanamadi, R. D. **(2003).** Biosorption of heavy metals. *Res. J.Chem.Environ.*, **7**(4), 71-79.

Ahluwalia, S.S. and Goyal, D. **(2003).** Removal of lead from aqueous solution by different fungi. *Indian Journal of Microbiology*, **43** (4), 237–241.

Akcil, A. and Koldas, S. **(2006).** Acid Mine Drainage (AMD): causes, treatment and case studies. *Journal of Cleaner Production,* **14,** 1139 – 1145.

Akpor, O. B. and Muchie, M. **(2010).** Remediation of heavy metals in drinking water and waste water treatment systems: Processes and applications. International Journal of the Physical Sciences, **5**(12), 1807-1817.

Aksu Z. **(2001).** Equilibrium and kinetic modeling of cadmium (II) biosorption by C. vulgaris in a batch system: effect of temperature. *Separation and Purification Technology*, **21**, 285–294.

Aksu, Z. and Gönen, F. **(2004).** Biosorption of phenol by immobilized activated sludge in a continuous packed bed: prediction of breakthrough curves. *Process Biochem.,* **39**, 599–613.

Aksu, Z., Acikel, U. and Kutsal, T. **(1997).** Application of multicomponent adsorption isotherms to simultaneous biosorption of iron(III) and chromium(VI) on C. vulgaris. *J. Chem. Technol. Biotechnol.*, **70**, 368–378.

Aksu, Z., Sag, Y. and Kutsal, T. **(1992**). The biosorption of copper (II) by C. vulgaris and Z. ramigera. *Environment Technology*, **13**, 579–586.

Aldor, I., Fourest, E. and Volesky, B. **(1995).** Desorption of cadmium from algal biosorbent. *Can. J. Chem. Eng.*, **73**, 516–522.

Ali, A.A. and El-Bishtawi, R. **(1997).** Removal of lead and nickel ions using zeolite Tuff. *Journal of Chemical Technology and Biotechnology*, **69**, 27 – 34.

Alkorta, I., Hernandez-Allica, J., Becerril, J.M., Amezaga, I., Albizu, I. and Garbisu, C. **(2004).** Recent findings on the phytoremediation of soils contaminated with environmentally toxic heavy metals and metalloids such as zinc, cadmium, lead, and arsenic. *Review in Environmental Science and Biotechnology*, **3**, 71-90.

Allen, S. E., Grimshaw, H. M., Parkinson, J. A. and Quarmby, C. **(1974).** Chemical analysis of ecological materials. *Blackwell Scientific Publications*, Oxford, 49-56.

Angus, C. (2005). Is there genetic evidence for the evolution of a tolerant flora on the polluted soils of South Africa's deep-level gold mines? *MSc Dissertation*. University of the Witwatersrand.

Antures, W.M., Luna, A.S, Henriques, C.A. and da Costa, A.C.A. **(2003)**. An evaluation of copper biosorption by brown seaweed under optimized conditions. *Electr. J. Biotech*., **6**,174-184.

Apiratikul, R., Marhaba, T.F., Wattanachira, S. and Pavasant, P. **(2004).** Biosorption of binary mixture of heavy metals by green macro algae, Caulerpa lentillifera. Songklanakarian. *Journal of Science & Technology*, **26** (1), 199–207.

Argun, **M.E. (2008).** Use of clinoptilolite for the removal of nickel ions from water: Kinetics and thermodynamic. *J. Hazard. Mater.*, **150**, 587–595.

Arienzo M., Chiarenzelli J. and Scrudato R. **(2001).** Remediation of metal-contaminated aqueous systems by electrochemical peroxidation: An experimental investigation, *J. Haz. Mater.*, **87,** 187-198.

Ashan, H. (2004). "Arsenic Exposure from Drinking Water and Risk of remalignant Skin Lesions in Bangladesh: Baseline Results from the Health Effects of Arsenic Longitudinal Study". *American Journal of Epidemiology*, **163** (12).

Athanasekou, C. P., Papageorgiou, S. K., Kaselouri, V., Katsaros, F. K., Kakizis, N. K. and Sapalidis, A. A. **(2009).** Development of hybrid alginate/ceramic membranes for Cd^{2+} removal. *Microporous and Mesoporous Materials*, **120**, 154–164.

Atkins, E. D. T., Mackie, W., Nieduszynski, I. A., Parker, K. D. and Smolko, E.E. **(1973).** Structural components of alginic acid. Part II. The crystalline structure of poly a-l-guluronic acid. Results of X-ray diffraction and polarized infrared studies. *Biopolymers,* **12,** 1879–1887.

Atkinson B.W., Bux F., Kasan H.C. **(1998).** Consideration for application of biosorption technology to remediate metal-contaminated industrial effluents. *Water SA*, **24**: 129-135.

Augustine, A.A., Orike, B.D. and Edidiong, A.D. **(2007).** Adsorption kinetics and modelling of Cu(II) ion sorption from aqueous solution by mercaptoacetic acid modified cassava (*Manihot sculenta cranz*) wastes. *EJEAFChe*, **6**(4), 2221- 2234).

Avery, S. V. and Tobin J. M. **(1992).** Mechanisms of strontium uptake by laboratory and brewing strains of Saccharomyces cerevisiae. *Appl. Environ. Microbiol*., **5**, 3883-3889.

Ayoub, G. M., Semerjian, A., Acra, M., Fadel, E. L. and Koopman, B. **(2001).** Heavy metal removal by coagulation with seawater liquid bittern. *J. Environ. Engin*., **127**,196-202.

Babel, S. and Kurniawan, T.A. **(2003).** Low-cost adsorbents for heavy metals uptake from contaminated water: a review. *Journal of Hazardous Materials*, **97,** 219-243.

Bae, W. and Mehra, R.K. **(1997).** Metal-Binding characteristics of a phytochelatin analog (Glu-Cys)2Gly. *Elsevier Sci*., 201-210.

Bae, W., Chen, W., Mulchandani, A. and Mehra, R.K. **(2000).** Enhanced bioaccumulation of heavy metals by bacterial cells displaying synthetic phytochelatins. *Biotechnol Bioeng*., **70**, 518–24.

Bae, W., Chen, W., Mulchandani, A. and Mehra, R.K. **(2001).** Genetic engineering of *Escherichia coli for enhance uptake and bioaccumulation of mercury. Appl*. *Environ Microbiol.,* **67**, 5335-5338.

Bajpai, A. K. and Sachdeva, R. **(2002).** Study on the adsorption of hemoglobin onto bentonite clay surfaces. *J. Appl. Polym. Sci.*, **85**, 1607–1618.

Bakatula, E.N., Cukrowska, E.M., Chimuka, L. & Tutu, H. **(2012).** Characterization of cyanide in a natural stream impacted by gold mining activities in the Witwatersrand Basin, South Africa. Toxicological & Environmental Chemistry, **94**(1), 7-19.

Banes, P. and Major, V. **(1980).** Trace chemistry of aqueous solutions. Academia/ Preque.

Banke, S., Rosendahl, S. and Frisvad, J.C. **(1997).** Taxonomy of *Penicillium chrysogenum* and related xerophilic species, based on isozyme analysis. *Mycological Research*, **101**, 617–624.

Benguella, B. and Ben asissa, H. **(2002).** Cadmium removal from aqueous solutions by Chitin: Kinetics and equilibrium studies, *Water Res.*, **36**, 2463.

Berthon, G. **(1995).** 'Critical Evaluation of the Stability Constants of Metal Complexes of Amino Acids with Polar Side Chains'. Technical Report, *Pure Appl. Chem.,* **67**, 1117–1240.

Beveridge, T.J. and Murray, R.G.E. **(1980).** Sites of metal deposition in the cell walls of Bacillus subtilis. *Journal of Biotechnology*, **141**, 876–887.

Bhattacharyya, K. G. and Gupta, S. S. **(2006).** Kaolinite, montmorillonite, and their modified derivatives as adsorbents for removal of Cu(II) from aqueous solution. *Separation and Purification Technology*, **50**, 388–397.

Black, W. A. P. (1950). The seasonal variation in weight and chemical composition of the common British Laminariaceae. *J. mar. biol. Ass*. U.K., **29**, 45-72.

Blowes, D. W., Ptacek, C.J., Benner, S. G., Waybrant, K. R., Bain, J. G. **(1998).** Permeable reactive barriers for the treatment of mine tailings drainage water, *Proceedings of the International Conference and Workshop on Uranium Mining and Hydrogeology*, Freiberg, Germany, September, 1998, **2**, 113-119.

Bogacka, E. K. (2011). Surface properties of yeast cells during heavy metal biosorption. *Cent. Eur. J. Chem.*, **9**(2), 348-351.

Bohart, G. S., Adams, E. Q. **(1920).** Some aspects of the behaviour of charcoal with respect to chlorine. *J. Am. Chem. Soc.*, **42** (3), pp 523–544.

Bold, H. C., Wynne, M. J. **(1985).** Introduction to the algae. Englewood Cliffs, NJ: Prentice-Hall, pp. 516.

Borro, D.M. and Fein, J.B. **(2005).** The impact of ionic strength on the adsorption of protons, Pb, Cd, and Sr onto the surfaces of gram negative bacteria: testing non-eletrostatic, diffuse, and triple-layer models. *J. Colloid Interf. Sci.,* **286**, 110-126.

Bose, P., Bose, M.A. and Kumar, S. **(2002).** Critical evaluation of treatment strategies involving adsorption and chelation for wastewater containing copper, zinc, and cyanide. *Advances in Environmental Research,* **7**, 179–195.

Borchardt, M. A. (1996). Nutrients, *In* R.J. Stevenson, M. L. Bothwell, and R. L. Lowe [eds.], Algal ecology: Fresh-water benthic ecosystems. Academic, pp. 182-227.

Brev, W.S. (1958). *Surface Chemistry. Processes.*

Calarge, L., Meunier, A., Lanson, B. & Formoso, M. **(2006).** Chemical signature of two Permian volcanic ash deposits within a bentonite bed from Melo, Uruguay. *Anais da Academia Brasileira de Ciências*, **78**(3): 525-541.

Cambra, J. and Aboal, M. **(1992).** Filamentous green algae of Spain: distribution and ecology. *Limnetica,* **8**, 213-220.

Caratzoulas S., Vlachos D.G. and Tsapatsis M. **(2005).** Molecular dynamics studies on the role of tetramethylammonium cations in the stability of the silica octamers Si_8O_{208}- in solution. *J. Phys. Chem.,* **B 109** (20), 10429–10434.

Chabani, M., Amrane, A. and Bensmaili, A. **(2006).** Kinetic modelling of the adsorption of nitrates by ion exchange resin. Chem. Eng. J., **125**(2), 111.

Champion, J. T, Gilkey, C.J, Lamparski, H, Retterer, J, Miller, R.M. **(1995).** Electrom microscopy of rhamnolipid (biosurfactant) morfphology: Effects of pH, cadmium, and octadecane. *J. Colloid and interface science,* **170**, 569-574.

Chang, L., Meier, J. and Smikth, M. **(1997).** Application of plant and earthworm bioassays to evaluate remediation of a lead-contaminated soil. Arch. Environ. *Contam. Toxicol*, **32**, 166-171.

Chapman, H.D. (1965). Cation-exchange capacity. *In:* C. A. Black (ed.) Methods of soil analysis - Chemical and microbiological properties. *Agronomy*, **9**, 891-901.

Chen, C. and Wang, J. **(2008).** Removal of Pb^{2+}, Ag^{+}, Cs^{+}, and Sr^{2+} from aqueous solution by brewery s waste biomass. *J. Hazard. Mater.*, **151**, 65-70.

Chen, W. and Georgiou, G. **(2002).** Cell-surface display of heterologous proteins: from highthroughput screening to environmental applications. *Biotechnol Bioeng.*, **79**, 496–503.

Chmielewská, E., Sabová, L., H. Peterlik, H.,Wu, A. **(2011).** Batch-wise adsorption, saxs and microscopic studies of zeolite pelletized with biopolymeric alginate. *Braz. J. Chem. Eng*., 28(1), 63-71.

Choi, J., Yang, K., Kim, D. and Lee, Ch. **(2009).** Adsorption of zinc and toluene by alginate complex impregnated with zeolite and activated carbon. *Current Applied Physics*, **9**, 694–697.

Chong, K.H. and Volesky, B. **(1995).** Description of 2-metal biosorption equilibrium by Langmuir-type models. *Biotechnol. Bioeng*., **47**, 451–460.

Chrishnan, K.A. and Anirudhan, T.S. **(2003).** Removal of cadmium(II) from aqueous solutions by steamactivated sulphurised carbon prepared from sugar-cane bagasse pith: Kinetics and equilibrium studies. Water S.A. **29**, 2, 2003.

Christensen, B. E., Indergaard, M., Smidsrod, O. **(1990).** Polysaccharide research in Trondheim. *Carbohyd. Poly.*, **13**, 239–55.

Christensen, M., Miller, S.L. and Tuthill, D.I. **(1994).** Colour standards: a review and evaluation in relation to *Penicillium* taxonomy. *Mycol. Res.*, **98**, 635–644.

Chu, K.H. (2004). Improved fixed bed models for metal biosorption. *Chem. Eng. J.*, **97**, 233–239.

Ci, S. X., Huynh, T. H., Louie, L. W., Yang, A., Beals, B. J. and Ron, N. **(1999).** Molecular mass distribution of sodium alginate by high-performance size-exclusion chromatography. *Journal of Chromatography A*, **864**, 199–210.

Clem A. G. and Doehler, R.W. **(1961).** Industrial applications of bentonite. *10th National conference on clays and clay minerals.* **10,** 272-283.

Cobbett, C., Goldsbrough, P. **(2002).** Phytochelatins and Metallothioneins: Roles in heavy metal detoxification and homeostasis. *Annu. ReVol. Plant Biol.,* **53**, 159-182.

Coetzee, H. (1995). Airborne radiometric mapping of the environmental impact of gold and uranium mining in the Gauteng Province, South Africa. *In: Proceedings to the Symposium on the application of geophysics to environmental and engineering problems*, Orlando, Florida, U. S. A.

Costa, A.C.A. & Leite, S.G.F**. (1991).** Metals biosorption by sodium alginate immobilized Chiarella homosphaera cells. *Biotechnol Left*, **13**, 555-562.

Costello, C. (2003). Acid Mine Drainage: Innovative Treatment Technologies. U.S. Environmental Protection Agency, Washington.

Cox, P.W., Paul, G.C., Thomas, C.R. **(1998).** Image analysis of the morphology of filamentous micro-organisms. *Microbiology.*, **144**, 817–827.

Cozmuta, L. M., Cozmuta, A. M., Peter, A., Nicula, C., Bakatula, E., Tutu, H. **(2012).** The influence of pH on the adsorption of lead by Na-clinoptilolite: Kinetic and equilibrium studies. *Water SA*, **38**, 269-278.

Crank, J. (1956). Mathematics of Diffusion. Oxford at the Clarendon Press, London, England.

CSRI, Council for Scientific and Industrial Research. Acid mine drainage in South Africa. **(2009).** Briefing note 2009/02.

D'onmez, G.C., Aksu, Z., Ozturk, A. Kutsal, T. **(1999).** A comparative study on heavy metal biosorption characteristics of some algae. *Process Biochem.,* **34**, 885–892.

Das, N., Vimala, R., Karthika, P. **(2007).** Biosorption of heavy metals-An overview. *Indian Journal of Biotehnology*, **7,** 159-169.

Da Silva, G., Lastra, M.R., Budden, J.R. **(2003).** Electrochemical passivation of aphalerite during bacterial oxidation in the presence of galena. *Miner Eng*., **16**, 199–203.

Daszkiewicz, K. and Voelkel, A. **(2009).** Theoretical and experimental methods of determination of the breakthrough volume of SPE Sorbents. *Talanta,* **80**, 614 – 621.

Davidson, C. (2003). Catchment diagnostic framework for the Klip River catchment, Vaal barrage, October 1998 - September 1999, Unpublished MSc Research Report, University of the Witwatersrand, Johannesburg, 154.

Davis, T. A., Collanes, F., Volesky, B. and Mucci, A. **(2003).** Metal selectivity of *Sargassum* spp. and their Alginates in relation to their r-L-Guluronic acid content and conformation. *Environ. Sci. Technol.*, **37**, 261-267.

De Ramos, C. M., Irwin, A. E., Nauss, J. L. and Stout, B. E. **(1997).** ^{13}C NMR and molecular modeling studies of alginic acid binding with alkaline earth and lanthanide metal ions. ions. *Inorganica Chimica Acta*, **256**, 69.

De Rome, L. and Gadd, G.M. **(1987).** Copper adsorption by Rhizopus arrhizus, Cladosporium resinae and Penicillium italicum. *Applied Microbiology Biotechnology*, **26**, 84–90.

De Rosa, C. and Lyon, J. **(1997).** *Golden Dreams, Poisoned Streams*. Mineral Policy Center, Washington DC, pp 61-75.

Deng, S. and Ting, Y.P. **(2005).** Characterization of PEI-modified biomass and biosorption of Cu (II), Pb (II) and Ni (II). *Water Research,* **39**(10), 2167-2177.

Dias, M.A., Lacerda, I.C.A., Pimentel, P.F., Castro, H.F. and Rosa, C.A. **(2002).** Removal of heavy metals by an Aspergillus terreus strain immobilized in a polyurethane matrix. *Lett Appl. Microbiol.*, 34, 46-50.

Dinger, D.R. (2005). *Characterization Techniques for Ceramists.* (Morris Publishing, U.S.A), pp.3-4, 71-72, 175-176, 223-224.

Dobson, R.S. and Burgess, J.E. **(2007).** Biological treatment of precious metal from refinery wastewater: A review. *Minerals Eng.*, **20**(6), 519-532.

Dorge, T., Carstensen, J.M. and Frisvad, J.C. **(2000).** Direct identification of pure *Penicillium* species using image analysis. *J. Microbiol. Meth.*, **41**: 121–133.

Eckenfelder, W. W. (2000). *Industrial Water Pollution Control*, (McGraw-Hill Companies), pp. 451-457.

EEB. (2000). The environmental performance of the mining industry and the action necessary to strengthen European legislation in the wake of the Tisza-Danube pollution. *European Environmental Bureau.* Document No. 2000/016. pp.32.

Ehrlich, H. L. (1996). *Geomicrobiology,* Dekker, New York, pp.719.

Ehrlich, H. L. (1997). Microbes and metals. *Appl Microbiol Biotechnol*, **48**, 687-692.

El-Kamash, A.M., Zaki, A.A. and El Geleel, M. A. **(2005).** Modeling batch kinetics and thermodynamic of zinc and cadmium ions removal from waste solutions using synthetic zeolite A. *Journal of Hazardous Materials*, **B127**, 211.220.

EPA, (**2000).** Wastewater technology sheet: chemical precipitation. United State Environmental Protection, EPA 832-F-00-018. Available from http://www.epa.Gov/own/ mtb/chemical_precipitation.pdf. Accessed: 07/07/2010.

Ercole, C. Veglio, F. Toro, L., Ficara, G. and Lepidi, A. **(1994).** Immobilisation of microbial cells for metal adsorption and desorption. *In: Mineral Bioprocessing II*. Snowboard. Utah.

Esposito, F., A. Pagnanelli, C. Lodi, O. Solisi, and Vegilo, F. **(2001).** Biosorption of heavy metals by Sphaerotilus natants: An equilibrium study at different pH and biomass concentration. *Hydrometallurgy*, **60**, 129 – 141.

Esteves, A.J.P., Valdman, E. and Leite, S.G.F. **(2000).** Repeated removal of cadmium and zinc from an industrial effluent by waste biomass Sargassum sp. *Biotechnology letters*, **22**(6), 499-502.

Faghihian, H. and Nejati, Y. M. **(2009).** Equilibrium study of adsorption of L-cysteine by natural bentonite. *Clays Minerals*, **44**, 125-133.

Fan, T., Liu, Y., Feng, B., Zeng, G., Yang, C., Zhou, M. **(2008).** Biosorption of cadmium(II), zinc(II) and lead(II) by *Penicillium simplicissimum*: Isotherms, kinetics and thermodynamic. *Journal of Hazardous Materials*, **160**, 655–661.

Farkas, V. (1980). Biosynthesis of cell wall of fungi. *Microbiological Reviews*, **44**, 117–141.

Feather, C. and Koen, G.M. **(1975).** The mineralogy of the Witwatersrand reefs. *Minerals Science and Engineering*, **7**, 189–224.

Fomina, M., Charnock, J., Bowen, A.D. and Gadd, G.M. **(2007).** X-ray absorption spectroscopy (XAS) of toxic metal mineral transformations by fungi. Environmental Microbiology (2007),Volume: 9, Issue: 2, Publisher: Wiley-Blackwell, pp 308-321.

Fourest, E. and Roux. J.C. **(1992).** Heavy metal biosorption by fungal mycelial by-products mechanisms and influence of pH. *Appl Microbiol Biotechnol*, **37**, 399-403.

Fourest, E., Canal, C. and Roux, J.C. **(1994).** Improvement of heavy metals biosorption by mycelial dead biomass (Rhizopus arrhizus, Mucor meihi and Penicillium chrysogenum): pH control and cationic activation. *Microbiology Reviews*, **14**, 325–332.

Forstner, U. and Wittmann, G. T. W. **(1976).** Metal accumulations in acidic waters from gold mines in South Africa. Geoforum 7, 44 - 49.

Freundlich, H.M.F. **(1906).** *Über die adsorption in lösungen*. Z. Phys. Chem., **57**, 385-470.

FSE, Federation for a sustainable environment, **(2006).** Comment on behalf of the FSE regarding the national waste management strategy. Department of Environmental Affairs., South Africa.

Funke, J. W. (1990). The water requirements and pollution potential of South African gold and uranium mines, Water Research Commission Report ISBN 0 947447 27X, Pretoria, South Africa.

Gadd, G.M. (1988). Accumulation of metals by microorganisms and algae. In: Rehm, H.J. (Ed.), *Biotechnology, special Microbial Processes*, **6b**, 401–433.

Gadd, G.M., White C. and de Rome, L. **(1988).** Heavy metals and radionuclide uptake by fungi and yeast, In: Norries, P.R., Kelly, D.P. (Eds.). *Biohydrometallurgy Science and Technology Letters, Kew*, Surrey, UK, pp. 421–435.

Gadd, M. G. (2000). Bioremediation potential of microbial mechanisms of metal mobilization. *Current Opinion in Biotechnology*, **11**, 271-279.

Gadd, M. G. (2010). Metals, minerals and microbes: geomicrobiology and bioremediation. *Microbiology*, **156**(3), 609-643.

Gaikward, R.W. and Gupta, D.V. **(2007).** Review on removal of heavy metals from acid mine drainage. Applied Ecology and Environmental Research, 6(3), 81-98.

Galun, M., Keller, P., Malki, D., Feldstein, H., Galun, E., Siegel, S.M. and Siegel, B.Z. **(1983).** Removal of uranium(VI) from solution by fungal biomass and fungal wall-related biopolymers. *Science*, **219**, 285–286.

García-Mendieta, A., Solache-Ríos, M. and Olguín, M.T. **(2009).** Evaluation of the sorption of a Mexican clinoptilolite-rich tuff for iron, manganese and iron – manganese systems. *Microporous and Mesoporous Materials*, **118**(1-3), 489-495.

Gardea-Torresdey, J. l., Peralta-Videa, J. R., Rosa, G. D. and Parsons, J. G. **(2005).** Phytoremediation of heavy metals and study of the metal coordination by X-ray absorption spectroscopy. Coord. Chem. Rev., **249**(17-18), 1797-1810.

Gavrilescu, M. (2004). Removal of heavy metals from the environment by biosorption. *Eng. Life Sci*., **4**(3), 219-232.

Gazsó, L.G. (2001). The key microbial processes in the removal of toxic metals and radionuclides from the environment. *Mini ReVol. CEJOEM*, **7**, 178-185.

Ghosh, S.K., Chaudhuri, R., Gachhui, R., Mandal, A. and Ghosh, S. **(2006).** Effect of mercury and organo-mercurials on cellular glucose utilization: a study using resting mercury resistant yeast cells. *J. Appl. Microbiol.*, **102**, 375-383.

Gillman, G.P. and Sumpter, E.A. **(1986).** Modification to the compulsive exchange method for measuring exchange characteristics of soils. *Aust. J. Soil Res*., **24**, 61-66.

Gök, ö**.,** özcan, A., Erdem, B, and özcan, A.S. **(2008).** Prediction of the kinetics, equilibrium and thermodynamic parameters of adsorption of copper(II) ions onto 8-hydroxy quinoline immobilized bentonite. *Colloids and Surfaces A: Physicochemical and Engineering Aspects*, **317**(1-3), 174-185.

Golden Environmental Services (2007). Natural processes: bioremediation. Available from: *http://www.goldenenviro.ca/bioremediation*. *htmL*. Accessed 12/06/2010.

Grampton, H. (1982). Reverse osmosis in the metal finishing industry. *Metal finishing*, **80**, 21- 27.

Guiry, M.D. **(2009).** "Monographie und Iconographie der Oedogoniaceen" in *Acta Soc.Sci.Fenn.*, **27**(1), 1-394.

Gupta, V.K., Shrivastava, A.K. and Jain, N. **(2001).** Biosorption of chromium(VI) from aqueous solutions by green algae Spirogyra species. *Water Research*, **35** (17), 4079–4085.

Gupta, A.K., Yunus, M. and Pandey, P. **(2003).** Bioremediation in ecotechnology for the present century. *Inter. Soc. Environ*. Botanists Environnews, **9**(2).

Gupta, D.K., Tohoyama, H., Joho, M. and Inouhe, M. **(2005).** Changes in the levels of phytochelatins and related metal-binding peptides in chickpea seedlings exposed to arsenic and different heavy metal ions. *J. Plant Res.,* **17**, 253- 256.

Gupta, V. K. and Rastogi, A. **(2008).** Biosorption of lead(II) from aqueous solutions by non-living algal biomass *Oedogonium* sp. and Nostoc sp.--a comparative study. *Colloids Surf Biointerfaces*, **64**(2), 170-178.

Gunaya, A., Arslankaya, E. and Tosun, I. **(2007).** Lead removal from aqueous solution by natural and pretreated clinoptilolite: Adsorption equilibrium and kinetics. *Journal of Hazardous Materials,* **146**, 362.371.

Hallberg, K.B. and Johnson, D.B. **(2005).** Microbiology of a wetland ecosystem constructed to remediate mine drainage from a heavy metal mine. *Science of the total environment*, **338**(1-2), 53-66.

Hamdaoui, Q. and Naffrechoux, E. **(2007).** Modeling of adsorption isotherms of phenol and chlorophenols unto granular activated carbon. Part 1. Two parameter models and equations allowing determination of thermodynamic parameters. *Journal of Hazardous*, **147**, 381- 394.

Han, R., Zou, W., Li, H., Li, Y. and Shi, J. **(2006).** Copper (II) and lead (II) removal from aqueous solution in fixed-bed columns by manganese oxide coated zeolite. *Journal of Hazardous Materials,* **B137**(1), 934 – 942.

Harholt, J., Suttangkakul, A., Scheller, H.V. **(2010).** Biosynthesis of Pectin. *Plant and Physiology*, **153** (2), 384-395.

Haug, A. **(1961).** The affinity of some divalent metals to different types of alginates. *Acta Chem Scand*, **15**, 1794–1795.

Haug, A. and Smidsrod, O. **(1965).** The effect of divalent metals on the properties of alginate solutions II. Comparison of different metal ions. *Acta Chem. Scand.*, **19** (2), 341–351.

Haug, A., Larsen, B. and Smidsrod, O. **(1974).** Uronic acid sequence in alginate from different sources. *Carbohyd. Res.*, **32**, 217–225.

Haug, A., Myklestad, S. Larsen, B. and Smidsrod, O. **(1967).** Correlation between chemical structure and physical properties of alginates. *Acta Chem. Scand.*, **21**, 768–178.

Heather, E. J., Shannon, S. C. and Clark, A. H. **(1995).** Mineralogical factors controlling metal release from tailings at Geco, Manitouwadge, Ontario. In: Proceedings Sudbury Mining and Environment Conference, Sudbury, Canada, May 28 - 01 June 1995, 405 - 413.

Hermond, H.F. and Fechner-Levy, E.J. **(2000).** Chemical fare and transport in the environment. San Diego: Academic Press.

Hernandez-Ramirez, O. and Holmez, S.M. **(2007).** Novel and modified materials for wastewater treatment applications. *Journal of Materials Chemistry*, **18**, 2751-2762.

Hinchman, R.R. and Negri, M. C. **(1997).** Providing the Baseline Science and Data For Real-Life Phytoremediation Applications – Partnering for Success, Chapter 1.5. *In, Proceedings of the 2nd Intl. Conference on Phytoremediation*, Seattle WA, June 18-19, 1997.

Ho, Y.S. (1995). Adsorption of heavy metals from waste streams by peat. Ph.D. Thesis, University of Birmingham, Birmingham. U.K.

Ho, Y.S. and Wang, C.C. **(2004**). Pseudo-isotherms for the sorption of cadmium ion onto tree fern. *Process. Biochem.*, **39**, 759–763.

Ho, Y.S., McKay, G. **(1998).** Kinetic model for lead(II) sorption on to peat. *Adsorption Science and Technology*, **16** (4), 243–255.

Ho, Y.S., Wase, D.A.J., Forster, C.F. **(1996a).** Removal of lead ions from aqueous solution using sphagnum moss peat as adsorbent. *Water SA*, **22** (3), 219–224.

Ho, Y.S., Wase, D.A.J., Forster, C.F. **(1996b).** Kinetic studies of competitive heavy metal adsorption by sphagnum moss peat. *Environmental Technology*, **17** (1), 71–77.

Hoek van den, C., Mann, D.G. and Jahns, H.M. **(1995).** *Algae An introduction to phycology*. Cambridge University Press, Cambridge. ISBN 0 521 30419 9.

Huang, C. and Huang, C.P. **(1996).** Application of Aspergillus oryzae and Rhizopus oryae for Cu (II) removal. *Water Res.*, **30**, 1958-1990.

Huang, C.P. and Morehart, A.L. **(1990).** The removal of Cu(II) from dilute aqueous solutions by Saccharomyces cerevisiae. *Water Research*, **24**, 433–439.

Hughes, M. N. and Poole, R. K. **(1989).** Metals and Microorganims. Chapman and Hall, London. Pp 245-248.

Humar, M. and Pohleven, F. **(2006).** Bioremediation of waste wood - Overview of advantages and disadvantages. Available from http://*www.bfafh.de/inst4/45/ppt/bioremd.pdf*. Accessed: 10/06/2010.

Hutchins, R.A. (1974). New method simplifies design of activated carbon systems. Chemical Engineering, 80, 133–138.

Inouhe, M. (2005). Phytochelatins. *Braz. J. Plant Physiol.,* **17**(1), 650-678.

Inglezakis, V.J., Loizidou, M.M. and Grigoropoulou, H.P. **(2004).** Ion exchange studies on natural and modified zeolites and the concept of exchange site accessibility. *Journal of Colloid and Interface Science*, **275**, 570 – 576.

IWQS (Institute of Water Quality Studies) (1995). The impact of diffuse load reduction from the Vaal Reefs, Hartebeesfontein Gold Mine, Buffelsfontein and Stilfontein mines on the water quality in the Vaal River, Report to the Department of Water Affairs and Forestry: Pollution Control (Highveld Region).

Jambor, J. J. and Blowes, D.W. **(1998).** Theory and applications of mineralogy in environmental studies of sulphide-baring mine waste. In: Cabri, L. J. and Vaughan, D. J. (eds): Short Course Handbook on Ore and Environmental Mineralogy. *Mineralogical Association of Canada Nepean,* **27**, 367-401.

Jokela, P. and Keskitalo, P. **(1999).** Plywood mill water system closure by dissolved air flotation treatment. *Water Science &Technology,* **40**, 33–42.

Jones, G. A., Brierley, S. E., Geldenhuis, S. J. J. and Howard, J. R. **(1988).** Research on the contribution of mine dumps to the mineral pollution load in the Vaal Barrage, Report to the Water Research Commission, WRC Report No. 136/1/89, Pretoria, South Africa.

Jüttner, K., Galla, U. and Schmieder, H. **(2000).** Electrochemical approaches to environmental problems in the process industry. *Electrochimica Acta,* **45**, 2575–2594.

Kefala, M.I., Zouboulis, A.I.E. and Matis, K.A. **(1999).** Biosorption of cadmium ions by Actinomycetes and separation by flotation. *Environ. Pollut.*, **104**(2), 283-293.

Keleşoğlu, S. (2007). Comparative adsorptions studies of heavy metal ions on chitin and chitosan biopolymers. MSc Thesis submitted to the Graduate School of Engineering and Science of Izmir Institute of Technology, Turkey.

Khalfaoui, M., Knani, S., Hachicha, M.A. and Lamine, A. B. **(2003).** New theoretical expressions for five adsorption type isotherms classified by BET based on statistical physics treatment. *Journal of Colloid and Interface Science*, **263**(2), 350-356.

Kim, S.K., Lee, B.S., Wilson, D.B. and Kim, E.K. **(2005).** Selective cadmium accumulation using recombinant E. coli. *J. Biosci. Bioeng.,* **99**(2), 109-114.

Kim, S.U., Cheong, Y.H., Seo, D.C., Hu, J.S., Heo, J.S. and Cho, J.S. **(2007).** Characterisation of heavy metal tolerance and biosorption capacity of bacterium strain CPB4 (Bacillus spp.). *Water Sci. Tech.,* **55**(1-2), 105-111.

Klimiuk, E. and Kuczajowska-Zadrożna, M. **(2002).** The Effect of Poly(vinyl Alcohol) on Cadmium Adsorption and Desorption from Alginate Adsorbents. *Polish Journal of Environmental Studie,***11**(4), 375-384.

Kondo, A. and Ueda, M, **(2004).** Yeast cell-surface display-applications of molecular display. *Appl. Microbiol. Biotechnol*., **64**, 28-40.

Kotrba, P. and RumL, T. **(2000).** Bioremediation of heavy metal pollution exploiting constituents, metabolites and metabolic pathway of livings. *Appl. Environ. Microbiol*., **65**(80) 1205-1247.

Kozlowski, H., Urbanska, J., Sóvágó, I., Varnagy, K., Kiss, A., Spychala, J. and Cherifi, K. **(1990).** Cadmium ion interaction with sulphur containing amino acids and peptide ligands. *Polyhedron,* **9**, 831–837.

Kratochvil, D. and Volesky, B. **(1998).** Advances in the biosorption of heavy metals. *Tibtech*, **16**, 291–299.

Kreger, D. R. (1962). In: *Physiology and biochemistry of algae*. Lewin, R. A., Ed.; Academic Press: New York, pp 315-335.

Kumar, P.S., Ramalinga, S., Abhinaya, R.V., Kirupha, S.D., Murugesan, A. and Sivanesan, S. **(2011).** Adsorption of metal ions onto the chemically modified agricultural waste. *Clean-Soil, Air, Water,* **40**(2) 188-197.

Kumar, K.K., Prasad, M.K., Sarma, G.V.S. and Murthy, C.V.R. **(2009).** Removal of Cd (II) from aqueous solution ssing immobilized Rhizomucor Tauricus. *J Microbial Biochem Technol,* 1(1), 15-21.

Kurniawan, T.A., Chan, G.Y.S., Lo, W.H., Babel, S. **(2006).** Physico–chemical treatment techniques for wastewater laden with heavy metals. *Chemical Engineering Journal*, 118, 83–98.

Kuroda, K., Shibasaki, S., Ueda, M. and Tanaka, A. **(2001).** Cell surface engineered yeast displaying a histidine oligopeptide (hexa-His) has enhanced adsorption of and tolerance to heavy metal ions. *Appl. Microbiol. Biotechnol*., **57**, 697-701.

Kuroda, K. and Ueda, M. **(2010).** Engineering of microorganisms towards recovery of rare metal ions: Mini Review. *Appl Microbiol Biotechnol.*, **87**, 53-60.

Kuroda, K. and Ueda, M. **(2011).** Yeast Biosorption and Recycling of Metal Ions by Cell Surface Engineering. *Microbial Biosorption of Metals*, 10, 235-247.

Kuyucak, N. and Volesky, B. **(1989).** Accumulation of cobalt by marine alga. *Biotechnology & Bioengineering*, **33** (7), 809–814.

Kuzniatsova, T., Yanghee Kim, Y., Shqau, K., Dutta, P.K. and Verweij, H. **(2007).** Zeta potential measurements of zeolite Y: Application in homogeneous deposition of particle coatings. *Microporous and Mesoporous Materials*, **103,** 102–107.

La Grega, M.D., Buckingham, P.L. and Evans, J.C. **(1994).** Hazardous waste management. McGraw Hill. pp.1315.

Lagergren, S. (1898). Zur theorie der sogenannten adsorption gelo¨ster stoffe. Kungliga Svenska Vetenskapsakademiens. *Handlingar Band*, **24** (4), 1– 39.

Laglay, G., M. Ogawa, M. and Dékány, I. **(2006).** Clay Mineral Organic Interactions, *Development in clay Science*, **1**, 309-377.

Langmuir, D. (1997). *Aqueous environmental geochemistry*. Prentice Hall, Upper Sadle River, N. J.

Lasat, M. M. (2000). Phytoextraction of metals from contaminated soil: a review of plant/soil/metal interaction and assessment of pertinent agronomic issues. *J. Hazard. Subst. Res.*, **2**(5), 1-25.

Laskowski, J.S. **(1993).** Electrokinetic measurements in aqueous solutions of weak electrolyte type surfactants. *J. Colloid Interface Sci*., **159** (2), 349–353.

Lee, R.E. **(1989).** *Phycology*. Cambridge, UK: Cambridge University Press, pp.645.

Leitão, A.L. (2009). Potential of *Penicillium* Species in the Bioremediation Field. *Int J Environ Res Public Health,* **6**(4), 1393–1417.

Levine, H. and Slade, L. **(1988).** Water as a plasticizer: physico-chemical aspects of low-moisture polymeric systems. ***In:*** *Water Science Reviews,* 3, 79–185, F. Franks, editor, Cambridge University Press, Cambridge.

Levinson, A. A. (1974). *Introduction to exploration geochemistry*, 2nd edn, Photopress Inc., USA, 689-697.

Liefferink, M. (2007). Environmental risks and hazards pertaining to AMD and radioactivity within the Witwatersrand goldfields. Department of Mineral Resources. Regional Mine Closure Strategy for the West Rand Goldfield. 35pp.

Liefferink, M. (2011). Acid mine drainage documentary**,** Technical presentation.

Liu, J., Zhang, Y., Huang, D. and Song, G. **(2005).** Cadmium induced MTs synthesis via oxidative stress in yeast Saccharomyces cerevisiae. *Mol. Cell Biochem.*, **280**(1-2), 139-145.

Li, X., Tang, Y., Xuan, Z., Liu, Y. and Luo, F. **(2007).** Study on the preparation of orange peel cellulose adsorbents and biosorption of Cd^{2+} from aqueous solution, **55** (1), 69-75.

Li, Y., Li, B. **(2011).** Study on fungi-bacteria consortium bioremediation of petroleum contaminated mangrove sediments amended with mixed biosurfactants. *Adv.Mat. Res*., **183-185,** 1163-1167.

Li, Y.H., Di, Z.C., Ding, J., Wu, D.H., Luan, Z.K. and Zhu, Y.Q. **(2005).** Adsorption thermodynamic, kinetic and desorption studies of Pb^{2+} on carbon nanotubes. *Water Res.*, **39**, 605.

Licskó, I. (1997). Realistic coagulation mechanism in the use of aluminium and iron (III) salts. *Water Science and Technology*, **27**, 103-110.

Lone, M.I., He, Z., Stoffella, P. J. and Yang, X. **(2008).** Phytoremediation of heavy metals polluted soils and water: progress and perspectives. *J. Zhejiang Univ. Sci.,* **B 9**(3), 210-220.

Lopez-Bautista (2011). Biology of Algae. *Laboratory Guide*. University of Alabama. USA.

Lövkvist, P. and Jöensson, J. Ä. **(1987).** Capacity of sampling and preconcentration columns with a low number of theoretical plates. *Anal.Chem.,* **59**(6), 818-821.

Lucia Leitao, A. (2009). Potential of *Penicillium* species in the bioremediation field. *Int. J. Environ. Res. Public Health* 2009, **6**(4), 1393-1417.

Lloyd, J.R. and Lovley, R.D. **(2001).** Microbial detoxification of metals and radionuclides. Current Opinion in Biotechnology, **12**, 248–253.

Machado, M.D., Santos, M.S.F., Gouveia, C., Soares, H.M.V.M. and Soares, E.V. **(2008).** Removal of heavy metal using a brewer's yeast strain of Saccharomyces cerevisiae: The flocculation as a separation process. *Bioresour. Technol.,* **99**, 2107-2115.

Mackie, W., Preston, R.D. **(1974).** Cell wall and intercellular region polysaccharides. In: Stewart WDP, editor, *Algal physiology and biochemistry*. Oxford, UK, Blackwell Scientific Publications, 58–64.

Mackie, W., Perez, S., Rizzo, R., Taravel, F. and Vignon, M. **(1983).** Aspects of the conformation of polyguluronate in the solid state and in solution. *Int J Biol Macromol*, **5**, 329–41.

Malik, A. (2004). Metal bioremediation through growing cells. *Enkviron. Int.,* **30**(2), 261-278.

Malkoc, E. and Nuhoglu, Y. **(2005).** Investigations of nickel(II) removal from aqueous solutions using tea factory waste. Journal of Hazardous Materials, **B127**, 120–128

Mameri, N., Boudries, N., Addour, L., Belhocine, D., Lounici, H., Grib, H. and Pauss, A. **(1999).** Batch zinc biosorption by a bacterial nonliving Streptomyces rimosus biomass. *Water Res.*, **33**, 1347-1354.

Marandi, R. (2011). Biosorption of Hexavalent Chromium from Aqueous Solution by Dead Fungal Biomass of Phanerochaete crysosporium: Batch and Fixed Bed Studies. *Canadian Journal on Chemical Engineering & Technology*, **2**(2), 8-22.

Marsden, D. D. (1986). The current limited impact of Witwatersrand gold-mine residues on water pollution in the Vaal River system. *Journal of the South African Institute of Mining and Metallurgy*, **86**, 481-504.

Matheickal, J.T., Yu, Q., Feltham, J. **(1987).** Cu (II) binding by E. radiata biomaterial. *Environ. Technol.*, **18**, 25-34.

Matis, K.A., Zouboulis, A.I., Lazaridis, N.K. and Hancock, I.C. **(2003).** Sorptive flotation for metal ions recovery. *International Journal of Mineral Processing*, **70**, 99–108.

Matsuhiro, B., Torres, S. E. and Guerrero, J. J. **(2007).** Block structure in alginic acid from Lessoia vadosa (Laminariales, Phaeophyta). *J. Chil.Chem.Soc*, 52(1), 1095.

Mehta, S.K., Tripathi, B.N. and Gaur, J.P. **(2002).** Enhanced sorption of Cu^{2+} and Ni^{2+} by acid-pretreated *Chlorella vulgaris* from single and binary metal solutions. *J. Appl. Phycol.*, **14**, 267–273.

Mendoza-Cózatl, D., Tavera, H.L., Navarro, A.H. and Sánchez, R.M. **(2005).** Sulfur assimilation and glutathione metabolism under cadmium stress in yeast, protists and plants. *FEMS Microbiol.*, **29**(4), 653-671.

METALSORB (2004). Heavy metal chelating agents. Available from http://*www.snf-group.com/IMG/pdf/Heavy_Metal_-METALSORB_E.pdf.* Accessed: 09/07/2010.

Metcalf and Eddy, (2003). *Wastewater Engineering: Treatment and Reuse*. (McGraw Hill International Edition, New York). pp. 478-483.

Mohandrao, G.J., Subrahmanyam P.V., Srinivasan M. **(1972).** Treatment and utilization of wood-hydrolysate wastes. *Biochem. J.*, **128**, 37–38.

Montgomery, J.M. (1985). *Water Treatment Principles and Design*, (Consulting Engineers Inc. USA). pp. 312-326.

Morin, A. K. and Hutt, N.M. **(1997).** Environmental geochemistry of minesite drainage. Practical theory and case studies. MDAG Publishing, Vancouver, 333 pp.

Morris, E. R, Rees, D. A. and Thom, D. **(1980).** Competitive inhibition of interchain interactions in polysaccharide systems. *Carbohydr. Res.*, **81**, 305–14.

Moses, C. O., Nordstrom, D. K., Herman, J. S. and Mills, A. L. **(1987).** Aqueous pyrite oxidation by dissolved oxygen and by ferric iron. *Geochimica et Cosmocimica Acta*, **51**, 1561-1571.

Mphephu, N. F. (2004). Geotechnical environmental evaluation of mining impacts on the Central Rand. PhD Thesis submitted to the University of the Witwatersrand, Johannesburg.

Mugo, R.K. and Orians, K.J. **(1983).** Seagoing methods for the determination of chromium (III) and total chromium in sea water by electron-capture detection gas chromatography. *Analytica Chimica Acta*, **271**, 1–9.

Mulligan, C.N. **(2005).** Environmental applications for biosurfactants. *Environ. Pollut.*, **133**(2), 183-198.

Mumpton, F.A. (1999). La roca magica: Uses of natural zeolites in agriculture and industry. Proc. *National Academy of Sciences*, **96**, 3463 – 3470.

Myklestad, S. (1968). Ion-exchange properties of brown algae. I. Determination of rate mechanism for calcium-hydrogen ion exchange for particles from Laminaria hyperborea and Laminaria digitata. *J Appl Chem,* **18**, 30–36.

Naeem, A., Woertz, J.R. and Fein, J.B. **(2006).** Experimental measurement of proton, Cd, Pb, Sr, and Zn adsorption onto the fungal species Saccharomyces cerevisiae. *Environ. Sci. Technol.*, **40**(18), 5724-5729.

Naja, G.M. and Volesky, B. **(2006).** Behavior of the mass transfer zone in a biosorption column. *Environ. Sci. Technol.,* **40**(12), 3996-4003.

Nandi, B. K., Goswami, A. and Purkait, M K. **(2009).** Adsorption characteristics of brilliant green dye on kaolin. *Journal of Hazardous Materials*, **161**, 387–395.

Ndasi, M. B. (2004). The geochemistry and mineralogy of mine tailings sediments in the Fleurhof Dam and their contribution to pollution in the Fleurhof Wetland, Central Rand, BSc Honours Report, University of the Witwatersrand, Johannesburg.

NEESA. (1993). Precipitation of metals from ground water. NEESA Document Number 20.2-051.6. *Novel Energy and Environmental Support Activity*, Port Hueneme, CA.

Nengovhela, A.C., Yibas, B. and Ogola, J.S. **(2006).** Characterisation of gold tailings dams of the Witwatersrand Basin with reference to their acid mine drainage potential, Johannesburg, South Africa. Water SA, 32(4), 499-506.

Nieboer, E. and Richardson, D.H.S. **(1980).** The replacement of the no-descript term 'heavy metals' by a biologically and chemically significant classification of metal ions. *Environ Pollut Series B,* **1**, 3-26.

Nikolakis, V. (2005). Understanding interactions in zeolite colloidal suspensions: "A review". *Curr. Opin. Colloid Interf. Sci.,* **10** (5-6), 203**.**

Nishitani, T., Shimada, M., Kuroda, K. and Ueda, M. **(2010).** Molecular design of yeast cell surface for adsorption and recovery of molybdenum, one of rare metals. *Appl Microbiol Biotechnol.,* **86**, 641–648.

Nomanbhay, S.M. and Palanisamy, K. **(2005).** Removal of heavy metal from industrial wastewater using chitosan coated oil palm shell charcoal. *Electron. J. Biotechnol.,* **8** (1), Issue 15.

Nordstrom, D. K., Jenne, E. A. and Ball, J. W. **(1979).** Redox equilibria of iron in acid mine waters. In: Jenne, E.A. (Ed.): *Chemical modeling in aqueous systems*. Am. Chem. Soc. Symp. Washington, D.C., **93**, 51-79.

Nordstrom, D. K. and Alpers, C. N. **(1999).** Geochemistry aof acid mine waste. In: PlumLee, G.S. and Logsdon, M. J. (Eds). Reviews in Economic Geology. The environmental geochemistry of ore deposits. Part A: *Processes, techniques, and heath issues*, **6A**, 133-168.

Nourbakhsh, M., Sag, Y., Ozer, D., Aksu, Z., Katsal, T. and Calgar, A. **(1994).** A comparative study of various biosorbents for removal of chromium (VI) ions from industrial wastewater, *Process Biochemistry*, **29**, 1–5.

Nuhoglu, Y., E. Malkoc. ***(*2009).** Thermodynamic and kinetic studies for environmentally friendly Ni(II) biosorption using waste pomace of olive oil factory. *Bioresource Technology,* **100**, 2375-2380.

Ochieng, G.M., Seanego, E.S., Nkwonta, O.I. **(2010).** Impacts of ining on water resources in South Africa: A review. *Scientific Research and Essays*, **5**(22), 3351-3357.

Olmez A.S., Akyil, S. and Eral, M. **(2004).** Adsorption and thermodynamic behavior of uranium on natural zeolite. *Journal of Radio analytical and Nuclear Chemistry*, **260**(1), 119-125.

Ouki, S.K. and Kavannagh, M. **(1997).** Performance of natural zeolites for the treatment of mixed metal-contaminated effluents. *Waste Management. Res.*, **15**, 383–394.

Özer, A., Ibrahim, Ekiz, I.H., Özer, D., Kutsul, T. and Caglar, A. **(1997).** A comparative study of the biosorption of cadmium(II) ions to S. leibleinil and R. arrhizis. *Chimica Acta Ture*, **25** (1), 63–67.

Özer, A. and Özer, D. **(2003).** Comparative study of the biosorption of Pb(II), Ni(II) and Cr (VI) ions onto S. cerevisiae: Determination of biosorption heats. *J.Hazard.Mater*. **100**(1-3), 219-229.

Öztürk, N., Ahmet Tabak, A., Sinan Akgöl,, S., Uzun, L. and Denizli, A**.(2007).** Preparation of Bentonite-Cysteine (Bent-Cys) micro-composite affinity sorbents for Ferritin adsorption. *Hacettepe J. Biol. & Chem.*, **35**(1), 65-73.

Pagnanelli, F., Toro, L. and Veglio, F. **(2002).** Olive mill solid residues as heavy metal sorbent material: a preliminary study. *Waste Management*, **22** (8), 901–907.

Palmer, J.D., Soltis, J.E. and Chase, M.W. **(2004).** The plant tree of life: an overview and some points of view. *Am J Bot.*, **91**, 1437–1445.

Panayotova, M., Velikov, B. **(2003).** Influence of zeolite transformation in a homoionic form on the removal of some heavy metal ions from wastewater. *Journal of Environmental Science and Health Part A*, **38**(3), 545-554.

Paskins-Hurlburt, A. J., Tanaka, Y., Skoryna, S. C. **(1976).** Carrageenan and the binding of lead. *Bot Mar.*, **19,** 327–328.

Pattus, F. and Abdallah, M. **(2000).** Siderophores and iron-transport in microorganisms: Review. *J. Chin. Chem. Soc.*, **47**, 1-20.

Pearlmutter, N.L. and Lembi, C.A. **(1980).** Structure and composition of pithophora Oedogonia (Chlorophyta) cell walls. *Journal of Phycology*, **16,** 602-616.

Pearson, R.G. **(1963).** Hard and soft acids and bases. *J Am Chem Soc.*, **85**, 3533–3539.

Penninckx, M.A. (2000). A short review on the role of glutathione in the response of yeasts to nutritional, environment, and oxidative stresses. *Enzyme Microbiol. Technol*., **26**, 737-742.

Percival, E. and McDowell, R. H. **(1967).** *Chemistry and enzymology of marine algal polysaccharides*, Eds.; Academic Press: London, U.K., pp. 137-143.

Permien, T. and Lagaly, G. **(1994).** The rheological and colloidal properties of bentonite dispersions in the presence of organic compounds IV. Sodium montmorillonite and acids. *Applied Clay Science*, **9**(4), 251-263.

Persin, F. and Rumeau, M. **(1989).** Le traitement électrochimique des eaux et des effluents. *Tribune de l'eau,* 3 (42), 45–46.

Perpetuo, E.A., Cleide Barbieri Souza, C.B. and Nascimento, C.A.O. **(2011).** Engineering Bacteria for Bioremediation. Progress in molecular and environmental bioengineering-From Analysis and Modeling to Technology Applications, ISBN: 978-953-307-268-5.

Pinetown K.L., Ward C.R. and van der Westhuisen, W.A. **(2007).** *International Journal of Coal Geology*, **70**, 166-167.

Pitt, J.I. (1979). *The genus Penicillium and its teleomorphic states Eupenicillium and Talaromyces,* Academic Press, London, UK.

Pivetz, B. E. (2001). Phytoremediation of contaminated soil and groundwater at hazardous waste sites. *EPA, Ground Water Issue*, EPA/540/S-01/500.

Pócsi, I. (2011). Toxic Metal/Metalloid Tolerance in Fungi—A Biotechnology-Oriented Approach, G. Bánfalvi (ed.), *Cellular Effects of Heavy Metals*, DOI 10.1007/978-94-007-0428-2_2

Prescott, L.M., Harley, J. P. and Klein, D. A. **(2002).** Microbiology. McGraw-Hill Science/ Engineering/Math; 2002. Ed. Fifth.

Quintelas, C., Rocha, Z., Silva, B., Fonseca, B., Figueiredo, H. and Tavares, T. **(2009).** Biosorptive performance of an Escherichia coli biofilm supported on zeolite NaY for the removal of Cr (VI), Cd (II), Fe (III) and Ni (II). Chem Eng J, 152, 110-115.

Raji, C. and Anirudhan, T. S. **(1997).** Kinetics of Pb(II) adsorption by polyacrylamide grafted sawdust. *Indian Journal of Chemical Technology*, **4**, 157–162.

Ramesh, S. T., Gandhimathi, R., Nidheesh, P. V., Nagendra B. and Bharathi, K. S. **(2011).** Breakthrough data analysis of adsorption of Cd(II) on coir pith column. *EJEAFChe*, **10**(7), 2487-2506.

Raper, K.B. and Thom, C. **(1949).** *Manual of the Penicillia.* Williams and Wilkins, Baltimore, USA.

Rees, D A. (1981). Polysaccharide shape and their interactions - some recent advances. *Pure Appl. Chem*, **53**, 1–14.

Remacle, J. (1990). The cell wall and metal binding. In: Volesky B, editor. *Biosorption of heavy metals.* Boca Raton: CRC Press, pp. 83–92.

Ribeiro, F. R., Rodrigues, A. E, Rollmann, L. D. and Naccache, C. **(1984).** *Zeolites: Science and Technology*. Martinus Nijhoff Publishers, the Hague.

Richardson, J.F., Harker, J.H., Backhurst, J.R. **(2002).** *Particle Technology and Separation Processes*. Coulson & Richardson's Chemical Engineering, **2**, 5th edition, Butterworth Heinemann, pp. 1208.

Roane, T.M. and Pepper, I.L. **(2001).** Environmental Microbiolology In: ROANE, T. M, PEPPER, I.L. (Ed.). Microorganisms and Metal Pollutants. *Academic Press*, **17**, 403-423.

Roberto, S.T. and Rubio, J. **(2009).** On the removal of Mn^{2+} ions by adsorption onto natural and activated Chilean zeolites. *Minerals Engineering*, **22**, 336-343.

Rome, L. and Gadd, G.M. **(1987).** Copper adsorption by *Rhizopus arrhizus*, *Cladosorium resinae* and *Penicillium Italicum. Applied Microbiology Biotechnology***, 20,** 84-90.

Rosell, K.G. and Srivastava, L.M. **(1984).** Seasonal variation in the chemical constituents of the brown algae *Macrocystis integrifolia* and *Nereocystis luetkeana. Canadian Journal of Botany*, **62**(11), 2229-2236.

Rosner,T. (2001). The environmental impact of seepage from gold mine tailings dams near Johannesburg, South Africa University of. Pretoria (Thesis - D.phil.). 184p.

Rouquerol, F. (1999). *Adsorption by Powders and Porous Solids*. (Academic Press, London), pp. 1-21, 355-361, 378-382.

Rutherford, N. and Mourez, M. **(2006).** Surface display of proteins by Gram-negative bacterial autotransporters. *Microbiol. Cell Factores*, 5(22).

Samuelson, P., Gunneriusson, E., Nygren, P.P.A. and Stahl, S. **(2002).** Display of proteins on bacteria. *J. Biotechnol.*, **96**(2), 129-154.

Santi, C., Coppetta, D., and Santoro, S. **(2008).** NMR Analysis of Non Hydrolyzed Samples of Sodium Alginate. 12th International Electronic Conference on Synthetic Organic Chemistry, 1-30 Nov. 2008.

Sari, A., Tuzen, M., Uluozlu, O.D. and Soylak, M. **(2007).** Biosorption of Pb(II) and Ni(II) from aqueous solution by lichen (Cladonia furcata) biomass. *Biochem. Eng. J.*, **37**, 151-158.

Sato, M. (1960). Oxidation of sulphide orebodies, II. Oxidation mechanisms of sulphide minerals at 25°C. *Economic Geology,* **55**, 1202-1231.

SAWQG. (1996). South Africa Water Quality Guidelines. 2nd ed. DWAF, S.A.

Sawyer, N.C., Mc Carty, P.L. and Parkin, G.F. **(1994).** *Chemistry for Environmental Engineering.* (Mc. Graw Hill International Edition, Singapore).

Say, R., Denizli, A. and Arica, M.Y. **(2001).** Biosorption of cadmium (II), lead (II) and copper (II) with the filamentous fungus *Phanerochaete chrysosporium*. *Bioresource Technology*, **76**, 67–70.

Scheller, H.V. and Ulvskov, P. **(2010).** Hemicelluloses. *Annu Rev Plant Biol.*, **61,** 263–289.

Schwarzenbach, R.P, Gschwend, M.P and Imboden, D.M. **(2003).** *Environmental Organic Chemistry* (John Willey & Sons, Inc. Publication, Canada, 2003).

Selatnia, A., Boukazoula, A., Kechid, B.N., Bakhti, M.Z., Chergui, A. and Kerchich, Y. **(2004).** Biosorption of lead (II) from aqueous solution by a bacterial dead *Streptomyces rimosus* biomass. *J. Eng. Biochem.*, **19**(2), 127-135.

Semerjian, L. and Ayoub, G.M. **(2003).** High-pH-magnesium coagulation–flocculation in wastewater treatment. *Advanced Environmental Research,* **7**, 389– 403.

Semmens, M.J., Seyfarth, M., Sand, L.B. and F.A. Mumpton (Eds.) **(1978).** Natural Zeolites. Occurence, Properties and Use. Pergamon Press, New York.

Shammas, N.K. (2004). "Coagulation and flocculation" in *Physicochemical Treatment Processes*, **3**, Humana Press, New Jersey, pp. 394.

Shumate, S. E.H and Strandberg, G. W. **(1985).** Accumulation of metals by microbial cells. In *M. Moo-Young, C. N. Robinson, and J. A. Howell (ed.), Comprehensive biotechnology*, **4**, Pergamon Press, New York, 235-247.

Sillen, L. G. and Martell, A. E. **(1971).** *Stability Constants of Metal-Ion Complexes,* Suppl. 1, Spec. Publ., **25**, *Chem. Soc.* London, Alden, Oxford.

Silva, E., Fialho, A.M., Sá-Correia, I., Burns, R.G. and Shaw, L.J. **(2004).** Combined bioaugmentation and biostimulation to cleanup soil contamined with high concentrations of atrazine. *Environ. Sci. Technol.,* **15-38**(2), 632-637.

Sing, H. (2006). *Mycoremediation,* John Wiley & Sons, Inc; New Jersey, USA.

Sing, K., Rouquerol, F. and Rouquerol, J. **(1990).** Adsorption by Powders & Porous Solids: Principles, Methodology and Applications (Academic, San Diego).

Singer, P. C. and Stumm W. **(1970).** Acid mine drainage: rate determining step. *Science,* **167**, 1121-1123.

Smidsrød, O. and Draget, K.I**. (1996).** Chemistry and physical properties of alginates. *Carbohydr. Europe,* **14**, 6–13.

Smith, M.C., Sumner, E.R. and Avery, S.V. **(2007).** Gluthatione and Gts1p drive beneficial variability in the cadmium resistances of individual yeast cells. *Mol. Microbiol*., **66**(3), 699-712.

Soares, E.V., Hebbelinck, K. and Soares, H.M**. (2003).** Toxic effects caused by heavy metals in the yeast Saccharomyces cerevisiae: a comparative study. *J. Microbiol.,* **49**(5), 336-343.

Song, S. H. and Vieille, C. **(2009).** Recent advances in the biological production of mannitol. *Appl. Microbiol. Biotechnol.,* **84**, 55–62.

Sprynskyy, M., Kowalkowski, T., Tutu, H., Cukrowska, E., and Buszewski, B. **(2011).** Adsorption performance of talc for uranium removal from aqueous solution. *Chem.Eng.J.,* **117**(3), 1185-1193.

Steginsky, C. A., Beale, J. M., Floss, H. G. and Mayar, R.M. **(1992).** Structural determination of alginic acid and the effects of calcium binding as determined by high-field NMR. *Carbohydr Res*, **225**(1), 11–26.

Stiason, M. K. (1979). Emerging technologies for the treatment of electroplating wastewaters, Water-1978. *AICHE symp. Ser*. **75**(190), 270-284.

Stolk, A.C. and Samson, R.A. **(1983).** The ascomycete genus *Eupenicillium* and related *Penicillium* anamorphs. *Stud. Mycol.,* **23**, 1–149.

Straker, C. J., Weiersbye, I. M. & Witkowski, E. T. F. **(2004a).** Arbuscular mycorrhizal (AM) status of gold and uranium tailings and polluted soils of South Africa's deep level gold mines: I. Root colonization and sporulation. *Journal of Applied Soil Ecology.* Submitted.

Straker, C. J., Weiersbye, I. M., Witkowski, E. T. F., Freeman, A., Whitfield, B., Costas, T., Forbes, N. M., Magagula, L., Hilditch, A. J., Groenewald, C. **(2004b).** Plant growth-promoting-micro-organisms and the vegetation of gold and uranium tailings and polluted soils in South Africa. Plant Ecology & Conservation Series. *Series of Reports to AngloGold Ashanti Ltd & Harmony Ltd.*

Stumm, W. and Morgan, J. J. **(1970).** Aquatic chemistry, An Introduction Emphasising Chemical Equilibria in Natural Waters, 2nd edition, Wiley, New York.

Strandberg, G.W., Shumate, S.E. and Parrott, J.R. **(1981).** Microbial cells as biosorbents for heavy metals: accumulation of uranium by *Saccharomyces cerevisiae* and *Pseudomonas aeruginosa*. *Applied Environmental Microbiology*, **41**, 237–245.

Stricks, W. and Kolthoff, I.M. **(1953).** Reactions between mercuric mercury and cysteine and glutathione. Apparent dissociation constants, heats and entropies of formation of various forms of mercuric mercapto-cysteine and -glutathione. *J. Am. Chern. Soc.,* **75**, 5673-5680.

Tabak, H.H., Lens, P., Hullebusch, E.D.V. and Dejonghe, W. **(2005).** Developments in bioremediation of soil and sediments polluted with metals and radionuclides–1. Microbiolal processes and mechanisms affecting bioremediation of metal contamination and influencing meal toxicity. *Rev. Environ. Sci. Biotechnol.,* **4**, 115-156.

Takagi, H., Yoshioka, K., Awano, N., Nakamori, S., Ono, B. **(2002).** Role of Saccharomyces cerevisiae serine O-acetyltransferase in cysteine biosynthesis. *FEMS Microbiology Letters*, **218**, 291-297.

Talaro, K.P. and Talaro, A. **(2002).** *Foundations in microbiology*. Blacklick, Ohio, U.S.A.: McGraw-Hill College, ed. 4th.

Tan, I.A.W., Hameed, B.H. and Ahmad, A.F. **(2007).** Equilibrium and kinetic studies on basic dye adsorption by oil palm fiber activated carbon. Chem.Eng.J, **127**, 11-119.

Taylor, J., Pape, S. and Murphy, N. **(2005).** A summary of passive and active treatment technologies for acid and metalliferous drainage (AMD). Fifht Australian workshop on acid drainage, 29-31 August 2005, Fremantle, Australia.

Teng, H. and Hsieh, C. **(1999).** Activation energy for oxygen chemisorption on carbon at low temperatures. *Ind. Eng. Chem. Res.,* **38**, 292-297.

Teutli-Sequeira, A., Solache, R. M. and Olguín, M.T. **(2009).** Influence of Na^{+}, Ca^{2+}, Mg^{2+} and NH_4^{+} on the sorption behaviour of Cd^{2+} from aqueous, solutions by a Mexican zeolitic material. *Hydrometallurgy*, **97**, 46-52.

Thirumoorthy, N., Kumar, K.T.M., Sundar, A.S., Panayappan, L.and Chatterjee, M. **(2007).** Metallothionein: An overview. *World J. Gastroenterol*., **13**(7), 993-996.

Thomas, D. (2002). *Seaweeds.* The Natural History Museum, London.

Tiffany, L.H. (1936). The Oedogoniales. *The botanical Review.* **2**, 456-473.

Ting, F., Yunguo, L., Baoying, F., Guangming, Z., Chunping, Y., Ming, Z., Haizhou, Z., Zhenfeng, T. and Xin, W. **(2008).** Biosorption of cadmium(II), zinc(II): thermodynamic. *Journal of Hazardous Materials,* **160**, 655–661.

Tobin, J. M., Cooper, D. G. and Neufeld, R. J. **(1990).** Investigation of the mechanism of metal uptake by denatured Rhizopus arrhizus biomass. *Enzyme Microb. Technol.,* **12**, 591-595.

Tsitsishvili, G.V., Andronikashvili, T.G., Kirov, G.N. and Filizova, L.D. **(1992).** *Natural Zeolites.* Ellis Horwood Limited, Great Britain.

Tunali, S., Çabuk, A. and Akar, T. **(2006).** Removal of lead and copper ions from aqueous solutions by bacterial strain isolated from soil. *J. Eng. Chem.*, **115**, 203-211.

Tutu, H. (2006). Determination and geochemical modeling of the dispersal of uranium in gold mine polluted land on the Witwatersrand. *PhD Thesis*, University of the Witwatersrand, Johannesburg.

Tutu, H., McCarthy, T.S. and Cukrowska, E. **(2008)**. The chemical characteristics of acid mine drainage with particular reference to sources, distribution and remediation: The Witwatersrand Basin, South Africa as a case study. *Applied Geochemistry*, **23**, 3666–3684.

UNEP (2010). United Nations Environmental Programme. Phytoremediation, an environmentally sound technology for pollution prevention, control and remediation: an introductory guide to decision makers. *United Nations Environment Programme, Newsleter and Technical Publication*, Freshwater Management Series N^{o} 2.

Unuabonah, E. I., Adebowale, K. O., Olu-Owolabi, B. I., Yang, L. Z. and Kong, L. X. **(2008).** Adsorption of Pb(II) and Cd(II) from aqueous solutions onto sodium tetraborate-modified Kaolinite clay: Equilibrium and thermodynamic studies. *Hydrometallurgy*, **93**, 1–9.

Uslu, G. and Tanyol, M. **(2006).** Equilibrium and thermodynamic parameters of single and binary mixture biosorption of lead(II) and copper(II) ions onto Pseudomonas putida: effect of temperature. *J. Hazard. Mater*., **135**, 87-93.

Vadivelan, V. and Vasanth kumar, K. **(2005).** Equilibrium, kinetics, mechanism and process design for the sorption of methylene blue onto rice husk. *J Colloid Interface Sci*, **286**(1), 91-100.

Valls, M. and Lorenzo, V. **(2002)**. Engineering a mouse exploiting the genetic and biochemical capacities of bacteria for the remediation of heavy metal pollution. *FEMS Microbiol. Rev.*, **26**(4), 327- 338.

Vaughan, D. E. W. (1978). "Properties of Natural Zeolites", pp. 353-371 in Natural Zeolites - Occurrence, Properties, Use, L. B. Sand and F. A. Mumpton, Eds., Pergamon Press, Oxford.

Veglio, F. and Beolchini, F**. (1997).** Removal of metals by biosorption: a review. *Chem. Hydrometallurgy*, **44**, 301-316.

Viladi, M. (2001). Bioremediation: an overview. *Pure Appl. Chem.*, **73**(7), 1163–1172.

Violante, A., Cozzolio, V., Perelomov, L., Caporale, A. G. and Pigna, M. **(2010).** Mobility and bioavailability of heavy metals and metalloids in soil environments. *J. Soil. Sci. Plant Nutr.* **10** (3): 268 – 292.

Viraraghavan, T. and Dronamrajum **(1993).** Removal of copper, nickel and zinc from wastewater by adsorption using peat. *J. Environ. Sci. Health*, Part **A 28**, 1261.

Vijayaraghavan, K. and Yun, Y.S. **(2008).** Bacterial biosorbents and biosorption. Biotechnology Advances, **26**, 266–291.

Volesky, B. (1990a). Biosorption and biosorbents. In: *Biosorption of heavy metals*. Boston, USA, CRC press, pp. 3-5.

Volesky, B. and Holan, Z.R. **(1995).** Biosorption of heavy metal. Biotechnol. Prog., **11**, 235-250.

Volesky, B. (2001). Detoxification of metal-bearing effluents: biosorption for the next century. *Hydrometallurgy*, **59**(2-3), 203-216.

Volesky, B. (2003). Sorption and Biosorption, BV Sorbex, St. Lambert, Que., Inc., Canada, cerevisiae. *Applied Microbiology & Biotechnology*, **42**, 797–806.

Wang, L. K., Fahey, E. M. and Wu, Z. C. **(2004).** Dissolved air flotation. In: Wang, L.K., Hung, Y.T, Shammas NK (eds) Physicochemical treatment processes, **3**. Humana Press, NJ, USA, pp 431–500.

Wang, J. and Chen, C. **(2006).** Biosorption of heavy metals by Saccharomyces cerevisiae: A review. *Biotechnology Advances*, **24**(5), 427-451.

Wang, Q., Li, L., Chen, M., Qi, Q. and Wang, P.G. **(2007).** Construction of a novel system for cell surface display of heterologous proteins on Pichia pastoris. *J. Biotechnol. Lett*., **29**(10), 1561-1566.

Wang, B.E., Hu, Y.Y., Xie, L., & Peng, K. **(2008).** Biosorption behavior of azo dye by inactive CMC immobilized Aspergillus fumigatus beads. *Bioresour. Technol.*, **99**(4), 794-800.

Wang, J.L. and Chen, C. **(2009).** Biosorbents for heavy metals removal and their future. *Biotechnol. Advances*, **27**(2), 195-226.

Wasewar, K.L. **(2010).** Adsorption of metals onto tea factory waste: A review. IJRRAS, **3** (3), 303-322.

Weber, T.W and Chakraborti, R.K. **(1974).** Pore and solid diffusion models for fixed bed adsorbents. *J.Amer.Inst. Chem.Eng*, **20**, 228–238.

Weiersbye, I.M. (2007). Global review and cost comparison of conventional and phyto-technologies for mine closure. in A.B. Fourie, M. Tibbett and J. Wiertz (eds). *Proceedings of the 2nd international Seminar on Mine closure 2007*, Santiago, chilli, 13-29.

Weiersbye, I. M. and Witkowski, E. T. F. **(1998).** The structure, diversity and persistence of naturally-colonizing and introduced vegetation on gold tailings. *Plant Ecology & Conservation Series*, **8**, AngloGold Limited, pp. 224.

Weiersbye, I.M. and Witkowski, E. T. F. **(2002).** Seed fate and practical germination methods for 46 perennial species that colonize gold mine tailings and acid mine drainage-polluted soils in the grassland biome. *In: AHW Seydeck et al. (eds) Multiple use management of natural forests and woodlands*: *Policy refinements and scientific progress.* Department of Water Affairs & Forestry, 221-255.

Weiersbye, I. M. and Witkowski, E. T.F. **(2003).** Acid rock drainage (ARD) from gold tailings dams on the Witwatersrand Basin impacts on tree seed fate, inorganic content and seedling morphology. In: D. Armstrong et al. (eds). Mine Water and the Environment. *Proceedings of the 8th International Mina Water Association (IMWA) Congress*, Johannesburg, 311-318.

Weiersbye, I. M., Witkowski, E. T. F. & Reichardt, M. **(2005).** Floristic composition of gold and uranium tailings dams, and adjacent polluted areas, on South Africa's deep-level mines. Bothalia. In Press.

Weiersbye, I. M., Witkowski, E. T. F. & Straker, C. J**. (2005).** Growth of leguminous trees in gold mine tailings is enhanced by treatment with rhizobia and arbuscular mycorrhizal fungi. *International Journal of Phytoremediation*. Manuscript.

Wieczorek, M., Jesionowski, T., Krysztafkiewicz, A. **(2003).** Influence of organic polymer modification on physicochemical properties of bentonites. *Physicochemical Problems of Mineral Processing*, **37**, 131-140.

Wingenfelder, U., Hansen, C., Furrer, G. and Schulin, R. **(2005).** Removal of heavy metals from mine water by natural zeolites. *Environmental Science and Technology*, **39**, 4606 – 4613.

Wipplinger, P.E. and Horn, G.F.T. (eds) **(1998).** Zeolite minerals: In Wilson, MGC. And Anhausser (eds) The mineral resources of South Africa: Handbook, **16**, 671- 675.

Witkowski, E. T. F. & Weiersbye, I. M. **(1998).** The seed biology of naturally-colonizing and introduced vegetation on gold tailings dams, tailings-polluted soils and unpolluted soils. *Plant Ecology & Conservation Series*, **9**, AngloGold Ltd. pp 210.

Witkowski, E.T.T. & Weiersbye, I.M. **(1998).** Establishment of plants on gold slimes dams: characterization of the slimes and adjacent soils. Plant Ecology & Conservation Series, **6**, AngloGold Ltd, 111 pp.

Witkowski, E.T.T. & Weiersbye, I.M. **(1999).** The seed biology of naturally-colonizing and introduced vegetation on gold tailing dams, tailings polluted soils and adjacent veld. Plant Ecology & Conservation Series, **9**, AngloGold Ltd, 210 pp.

Witkowski, E. T. F. & Weiersbye, I. M. **(2005).** Variation in geochemistry and soil features of South African gold slimes dams and polluted soils in relation to rehabilitation efforts. Environmental Pollution (submitted). Plant Ecology & Conservation Series, **6**, AngloGold Limited, pp 200.

Witteveen, C. F. B. and J. Visser. **(1995).** Polyol pools in Aspergillus niger. *FEMS Microbiol. Lett.,* **134,** *57*-62.

Woolard, C.R. and Irvine, RL. **(1995).** Treatment of hypersaline wastewater in the sequencing batch reactor. *Water Res.*, **29**, 1159–1168.

Wu, C.H., Wood, T.K., Mulchandani, A. and Chen, W. **(2006).** Engineering Plant-microbe symbiosis for rhizoremediation of heavy metal. *Appl. Environ. Microbiol.,* **72**(2), 1129-1134.

Wurdack, M. E**. (1923).** Chemical composition of the walls of certain algae. *Ohio journ.Sc.,* **23**, 181-191.

Xiao-ming, L., De-xiang, L., Xue-qin, X., Qi, Y., Guang-ming, Z., Wei, Z., Liang, G. **(2008).** Kinetic studies for the biosorption of lead and copper ions by *Penicillium simplicissimum* immobilized within loofa sponge. *Journal of Hazardous Materials*, **159**(2-3), 610-615.

Xu, Y. and Xu, T. **(2008).** Heavy metal complexes wastewater treatment with chelation precipitation. *IEEE Xplore*, 2789-2793.

Yamada, O. K. H., Mukumoto, Y., Katsuyaya, Y., Saiganji, A. and Tani, Y. **(2001).** Degradation of polyethylene by a fungus, *Penicillium simplicissimum* YK. *Polym. Degrad. Stabil*, **72**, 323–327.

Yang, W., Wang, X., Tang, Y., Wang, Y., Ke, C. and Fu, S. **(2002).** Chemistry on modified oxide and phosphate surfaces. *J. Macromol. Sci. Pure Appl. Chem.*, **39**, 509-526.

Yang, X.J., Fane, A.G. and MacNaughton, S. **(2001).** "Removal and recovery of heavy metals from wastewater by supported liquid membranes". *Water Science and Technology*, **43**, 341–348.

Yee, N., Benning, L.G., Phoenix, V.R., Ferris, F.G. **(2004).** Characterization of metal-cyanobacteria sorption reactions: a combined macroscopic and infrared spectroscopic investigation.*Environ. Sci. Technol.,* **38,** 775.

Yu, Q.Z. and Kaewsarn, P. **(2001).** Desorption of Cu2+ from a biosorbent derived from the marine alga Durvillaea potatorum. *Separ. Sci. Technol.,* **36**(7), 1495-1507.

Yuan, Y. and Viraraghavan, T. **(2001).** Heavy metal removal in a biosorption column by immobilised M. rouxii biomass. Bioresource Technology, **78**, 243-249.

Yun-guo, L., Cui, P., Wen-bin, X., Zeng, G., Ming, Z., Yuan-yuan, L., Jie, K. and Chao, H. **(2008).** Simultaneous removal of Cr(VI) and phenol in consortium culture of Bacillus sp. and Pseudomonas putida Migula (CCTCCAB92019) Trans.Nonferrous Met.Soc.China, 1014-1020.

Zabel, T. (1984). Flotation in water treatment in "*The Scientific Basis of Flotation*", edited by K.J. Ives, (Martinus Nijhoff Publishers, The Hague), pp. 349–378.

Zamzow, M.J., Eichbaum, B.R., Sandgren, K.R. and Shanks D.E. **(1990).** Removal of heavy metals and other cations from wastewater using zeolites. *Separation Science and Technology*, **25**, 1555 – 1569.

Zielinski, R. A., AsherBolinder, S., Meier, A. L., Johnson, C. A. and Szabo, B. J. **(1997).** Natural or fertilizer-derived uranium in irrigation drainage: A case study in southeastern Colorado, U. S. A. *Applied Geochemistry*, **12**(1), 9-21

Zouboulis, A.I., Matis, K.A. and Lazaridis, N.K. **(2001).** Removal of metal ions from simulated wastewater by Saccharomyces yeast biomass: Combining biosorption and flotation processes. *Separ. Sci. Technol*., **36**(3), 349-365.

Appendix A

Fungal biomass for removal of heavy metals from aqueous solution

Biosorbent	*Metals*	*Adsorption capacity (mg g^{-1})*	*References*
Aspergillus foetidus	Cr(VI)	2	Prasanjit and Sumathi (2005)
Aspergillus niger	Cu	5	Townsley and Ross (1986)
		-	Modak *et al.* (1996)
	Co	95	Kuyucak and Volesky (1989)
	Au	200	Kuyucak and Volesky (1989)
	Co	2.4	Sakaguchi and Nakajima (1991)
	Cr, Fe	–	Goyal *et al.* (2003)
	Pb	30	Kim *et al.* (1995)
	Th	22	Tsezos and Volesky (1981)
		162	Gadd (1988)
	U	29	Sakaguchi and Nakajima (1991)
		27	Kuyucak and Volesky (1989)
	Zn	-	Luef *et al.* (1991), Modak *et al.* (1996), Muter *et al.* (2002)
Aspergillus terreus Th,	U	60, 10	Tsezos and Volesky (1981)

Aureobasidium pullulans	Cu	6	Gadd and Mowll (1995)
	Pb	56.9	Suh *et al.* (1998)
		-	Ahluwalia and Goyal (2003)
Cladosporium resinae	Cu	18	Gadd (1988) de Rome and Gadd (1987)
	Pb	-	Ahluwalia and Goyal (2003)
Candida utilis	Cr, Cu, Pb	–	Muter *et al.* (2002)
Ganoderma lucidum	Cu	24	Muraleedharan and Venkobachar (1990)
Mucor meihi	Cr	–	Tobin and Roux (1998)
Mucor rouxii	Pb, Zn, Cd, Ni	17, 4.89, 6.94, 5.24	Yan and Viraraghavan (2003)
	Pb	769	Lo *et al.* (1999)
Penicillium chrysogenum	Cd, Cu, Pb	11, 9, 116	Niu *et al.* (1993)
	Cd	56	Holan and Volesky (1995)
		39	Fourest *et al.* (1994)
	Th	142	Tsezos and Volesky (1981) Gadd and White (1992)
	U	70	Tsezos and Volesky (1981)
	Zn	6.5	Niu *et al.* (1993)
		-	Luef *et al.* (1991)
	Cd, Zn, Cu, Pb	-	Skowronôski *et al.* (2001)

Pleurotus sapidus	Cd, Hg	127, 287	Yalcinkaya *et al.* (2002)
Streptoverticillium cinnamoneum	Pb, Zn	57.7, 21.3	Puranik and Paknikar (1997)
Penicillium italicum	Cu	-	de Rome and Gadd (1987)
	Th	–	Gadd and White (1989)
Penicillium spinulosum	Cu, Zn	0.4–2, 0.2	Townsley and Ross (1985)
Phanerochaete chrysosporium	Cd	84.5	Gabriel *et al.* (1996)
	Pb	2	Say *et al.* (2001)
	Cu	–	Yetis *et al.* (2000)
Rhodotorula glutinis	Pb	73.5	Cho and Kim (2003)
Rhizopus nigricans	Cr, Pb	47	Bai and Abraham (2002)
	Zn	14	Zhang *et al.* (1998)
	Cd, Ni, Pb	19, 5, 166	Fourest and Roux (1992) Holan and Volesky (1995)
R. oligosporus	Cr	126	Ariff et al. (1999)
	Cd	17.09	Aloysius et al. (1999)

R. arrhizus	Ni, Cd, Zn, Pb, Cu	18, 27, 14, 56, 9.5	Fourest and Roux (1992)
	Cd	30	Holan and Volesky (1995)
	Cr	11	Bai and Abraham (1998)
		36	Nourbakhsh *et al.* (1994)
	Co	2.9	Sakaguchi and Nakajima (1991)
		–	Niyogi *et al.* (1998)
		–	Sag and Kutsal (1998)
		–	Prakasham *et al.* (1999)
	Cu	10	Gadd (1988)
		-	de Rome and Gadd (1987),Sag and Kutsal (1998), Zhou and Kiff (1991)
	Th	185	Tsezos and Volesky (1981)
		97	Gadd *et al.* (1988)
		-	Gadd and White (1992)
	U	220	Tsezos and Volesky (1981)
		–	Tsezos *et al.* (1989)
		–	Tsezos and Deutschmann (1990)

Saccharomyces cerevisia			
	Cd	–	Volesky *et al.* (1993)
	Cr	–	Nourbakhsh *et al.* (1994)
		11.4	Omar *et al.* (1996)
	Co	5.8	Sakaguchi and Nakajima (1991)
	Pb	–	Suh *et al.* (1998)
	Th	119	Gadd (1988)
	Cu	17–40	Volesky and May-Phillips (1995)
	U	55–140	
	Cu	10	Mattuschka *et al.* (1993)
		0.4	Huang *et al.* (1990)
	Zn	14–40	Volesky and May-Phillips (1995)
	Cr	–	Bayramoglu *et al.* (2003)
	Cd	109	Gabriel *et al.* (1996)

Appendix B

Algal biomass for removal of heavy metals from aqueous solution

Biosorbent	*Metals*	*Adsorption capacity (mg g^{-1})*	*References*
Ascophyllum nodosum	Cd	215	Holan *et al.* (1993)
	Co	156, 100	Kuyucak and Volesky (1988, 1989)
	Ni, Pb	30, 270–360	Holan and Volesky (1995)
	Cd	30	Volesky and Prasetyo (1994)
Aphanothece halophytica	Zn	133	Incharoensakdi and Kitjaharn (2002)
Chlorella vulgaris	Ag	–	Harris and Ramelow (1990)
	Cd	111	Aksu (2001)
	Cu	43	Aksu *et al.* (1992)
	Cr	3.5	Nourbakhsh *et al.* (1994)
	Cr, Cu, Ni		Donmez *et al.* (1999)
		3.95	Sakaguchi and Nakajima (1991)
		–	Greene *et al.* (1986)
Chlorella fusca	Pb	293	Wehreim and Wettern (1994)
Chlorella sorokiniana	Cd	-	Akhtar *et al.* (2003)

Cladophoracrispate	Cr	3	Nourbakhsh *et al.* (1994)
Caulerpa lentillifera	Cu, Cd, Pb, Zn	–	Apiratikul et al. (2004)
***Dunaliella* sp.**	Cr	58.3	Donmez and Aksu (2002)
Fucus vesiculosus	Cd	73	Holan *et al.* (1993)
	Ni, Pb	17, 220–371	Holan and Volesky (1995)
Fucus spiralis	Cd	64	Cordeo *et al.* (2004)
Ecklonia maxima	Cd	–	Stirk and Staden (2002)
Laminaria japonica	Cd	-	Yun *et al.* (2001)
Laurencia obtuse	Cr	-	Hamdy (2000)
Lyngbya taylorii	Cd, Pb, Ni, Zn	-	Klimmek *et al.* (2001)
Phormidium laminosum	Cu, Ni, Zn	-	Blanco *et al.* (1998)
Pilayella littoralis	Al, Cd, Co, Cr, Ni, Zn	-	Carrilho and Gilbert (2000)
***Pachymeniopis* sp.**	Cr(VI)	225	Lee *et al.* (2000)
Oscillatoria anguistissima	Zn	641	Ahuja *et al.* (1999)
	Zn, Cu, Co	-	Mohapatra and Gupta (2005)
***Spirogyra* sp.**	Cr	-	Gupta *et al.* (2001)
Scenedesmus quadricula	Cd, Cu, Zn	-	Harris and Ramelow (1990)
Scenedesmus obliquus	Cr, Cu, Ni	-	Donmez *et al.* (1999)
Scenedesmus abundans	Cd, Cu	-	Terry and Stone (2002)
Scenedesmus incrassatulus	Cr, Cd, Cu	-	Pena-Castro *et al.* (2004)
Sargassum fluiyans	Cu	-	Schiwer and Volesky (1996)
		51	Kratochvil *et al.* (1997)

Sargassum natans	U	–	Kuyucak and Volesky (1989)
	Cd	135	Holan *et al.* (1993)
	Ni, Pb	24–44, 220–270	Holan and Volesky (1995)
Sargassum sp.	Zn	–	da Costa *et al.* (2001)
***Sargassum* sp.**	Cu	38, –	Volesky *et al.* (2003), Padilha *et al.* (2005)
	Cd, Zn, Cu	157, 118, 77	Valdman and Leite (2000)
	Cd	120	Cruz *et al.* (2004)
Tetraselmis suecica	Cd	–	Perez-Rama *et al.* (2002)
Ulothrix zonata	Cu	–	Nuhoglu *et al.* (2002)

Appendix C

FTIR spectra of: (a) Bentonite-Histidine (b) Bentonite-Cysteine (c) Bentonite-Sorbitol (d) Bentonite-Fungi

(a)

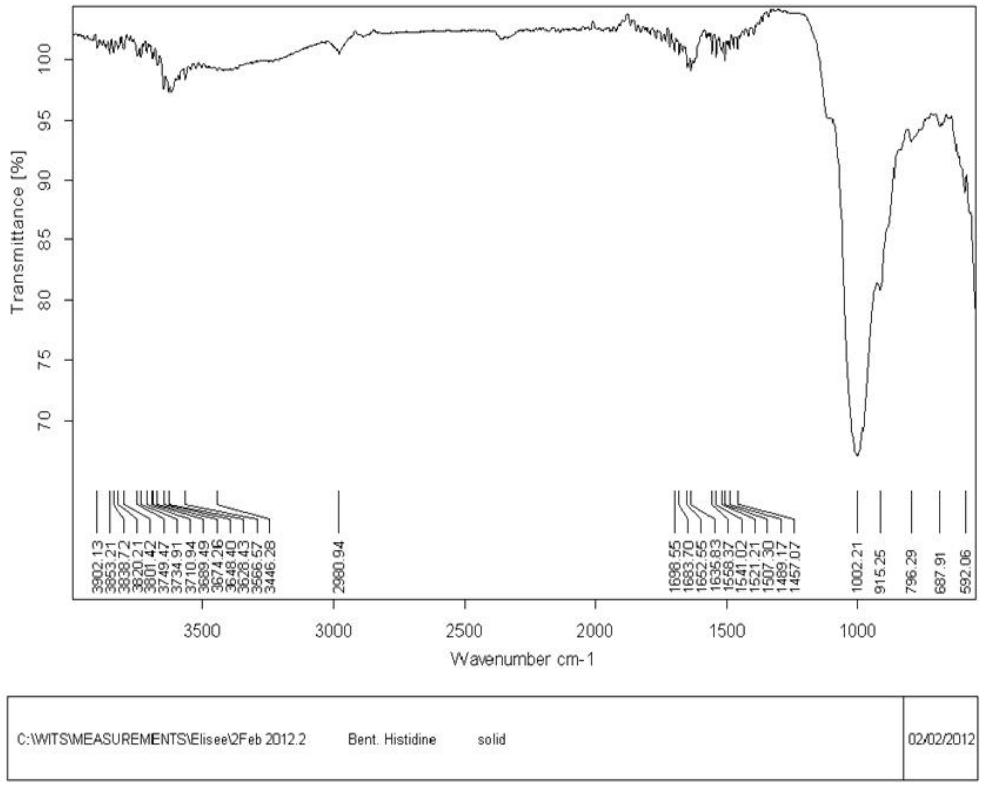

(b)

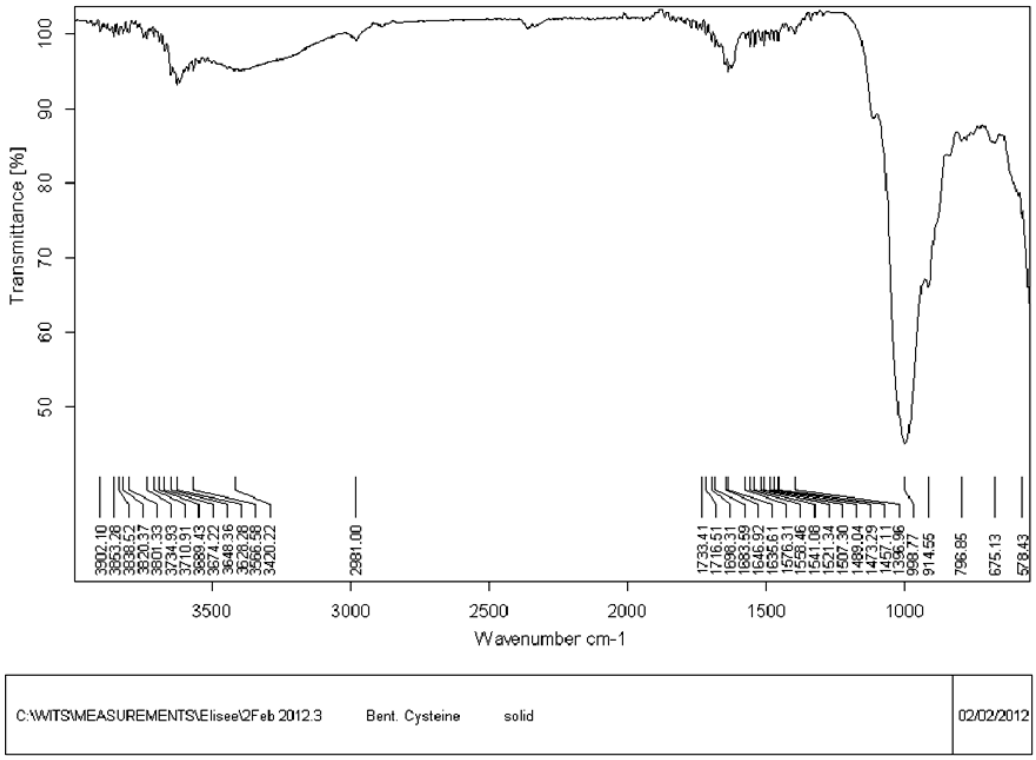

C:\WITS\MEASUREMENTS\Elisee\2Feb 2012.3	Bent. Cysteine	solid	02/02/2012

(c)

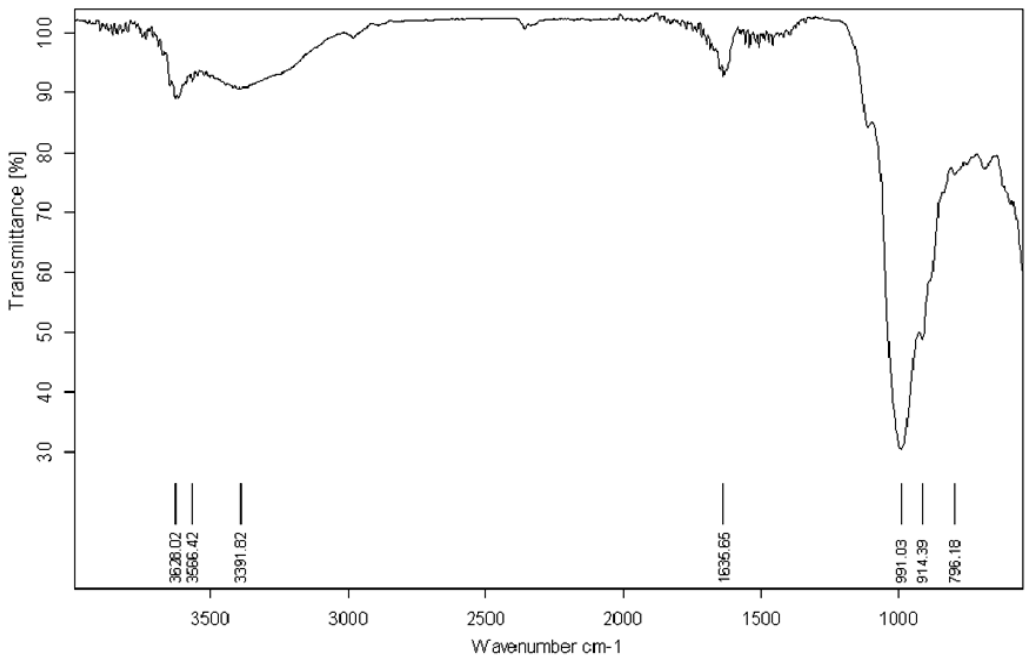

C:\WITS\MEASUREMENTS\Elisee\2Feb 2012.4	Bent. Sorbitol	solid	02/02/2012

(d)

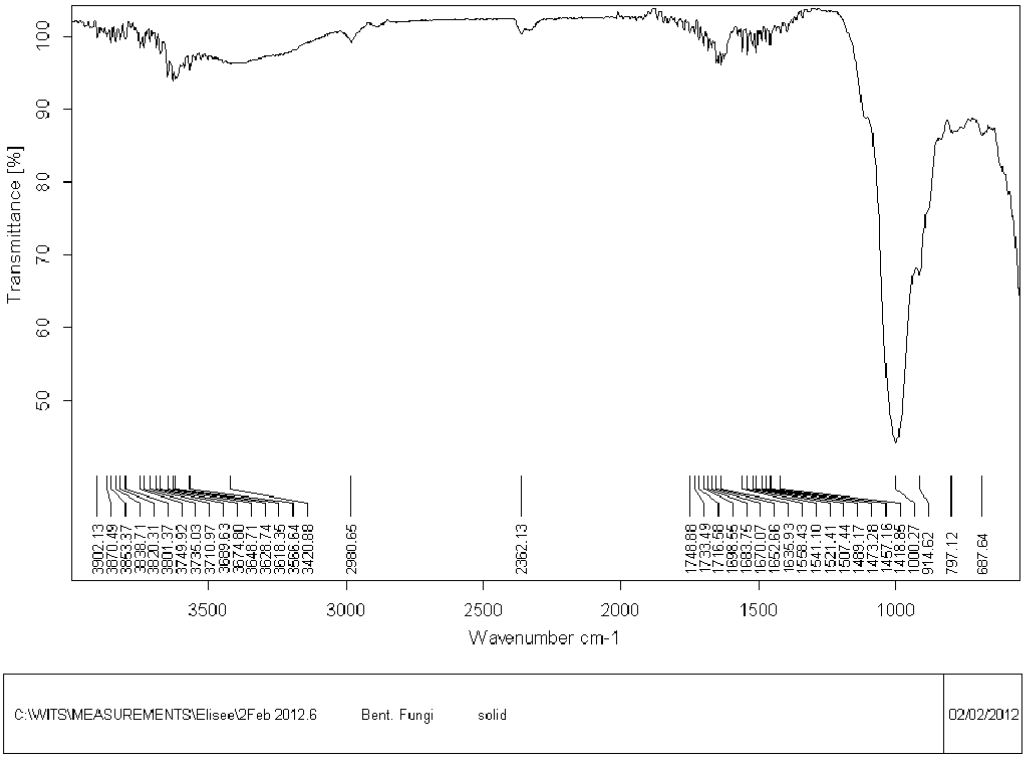

C:\WITS\MEASUREMENTS\Elisee\2Feb 2012.6 Bent. Fungi solid	02/02/2012

Appendix D

FTIR spectra of: (a)Zeolite- Histidine (b) Zeolite-Cysteine (c) Zeolite-Sorbitol (d) Zeolite-Mannitol

(a)

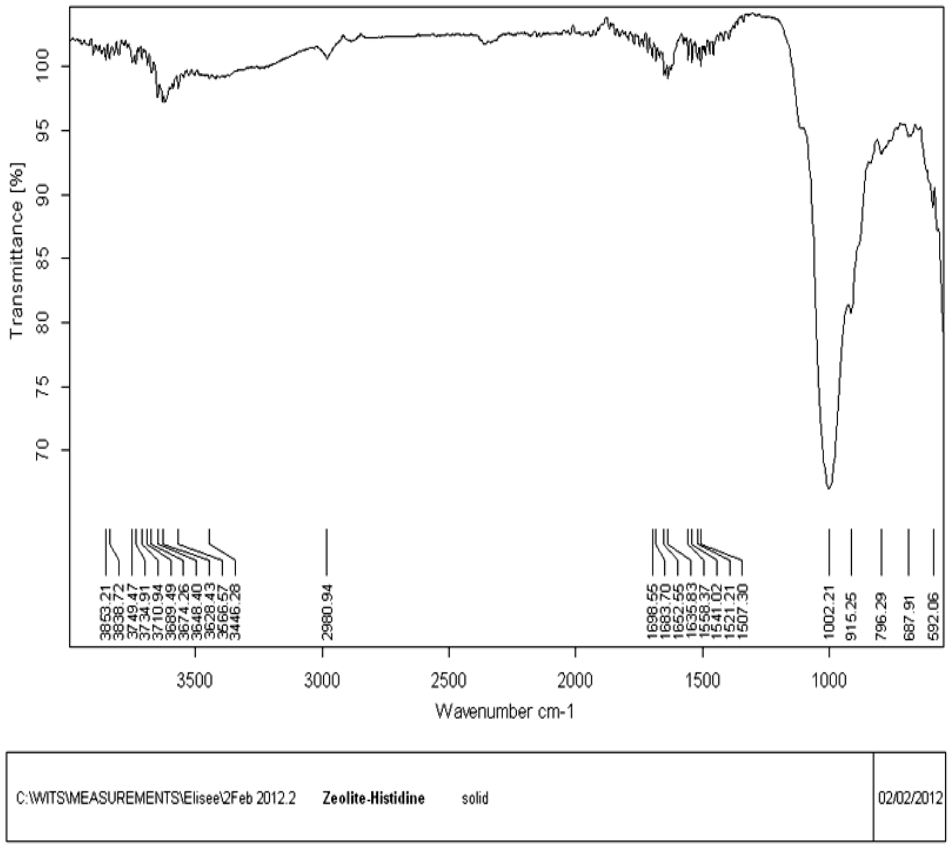

(b)

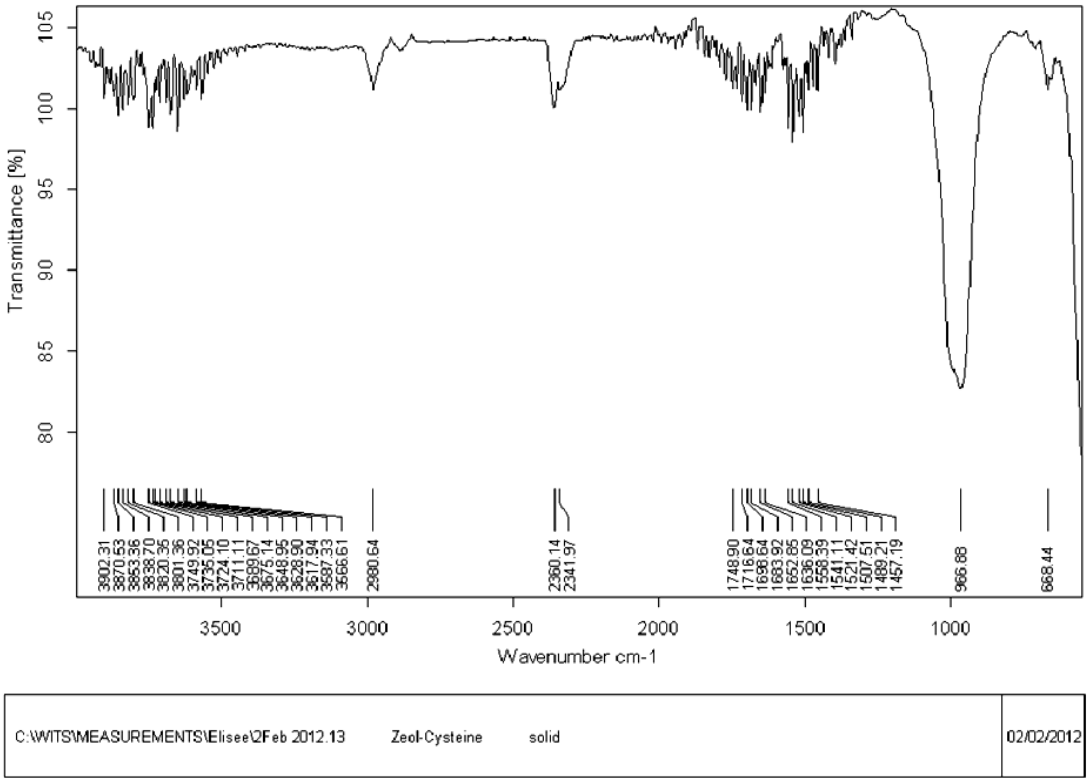
Transmittance [%]
105
100
95
90
85
80
3902.31
3870.53
3853.36
3838.70
3820.35
3801.36
3749.92
3735.05
3724.10
3711.11
3689.67
3675.14
3648.95
3628.90
3617.34
3587.33
3566.61
2980.64
2360.14
2341.97
1748.90
1716.64
1698.64
1683.92
1652.85
1636.09
1558.39
1541.11
1521.42
1507.51
1489.21
1457.19
966.88
668.44
3500
3000
2500
2000
1500
1000
Wavenumber cm-1
C:\WITS\MEASUREMENTS\Elisee\2Feb 2012.13
Zeol-Cysteine
solid
02/02/2012

(c)

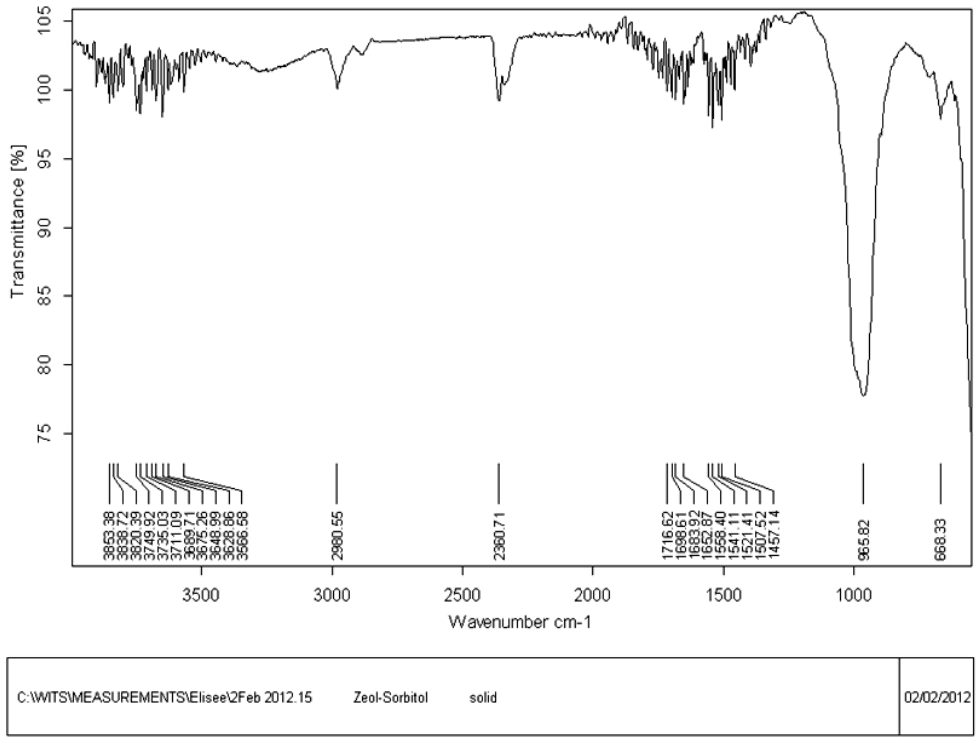
Transmittance [%]
105
100
95
90
85
80
75
3853.38
3838.72
3820.79
3749.92
3735.03
3711.09
3689.71
3675.26
3648.99
3628.86
3566.58
2980.55
2360.71
1716.62
1698.61
1683.92
1652.87
1558.40
1541.11
1521.41
1507.52
1457.14
965.82
668.33
3500
3000
2500
2000
1500
1000
Wavenumber cm-1
C:\WITS\MEASUREMENTS\Elisee\2Feb 2012.15
Zeol-Sorbitol
solid
02/02/2012

(d)

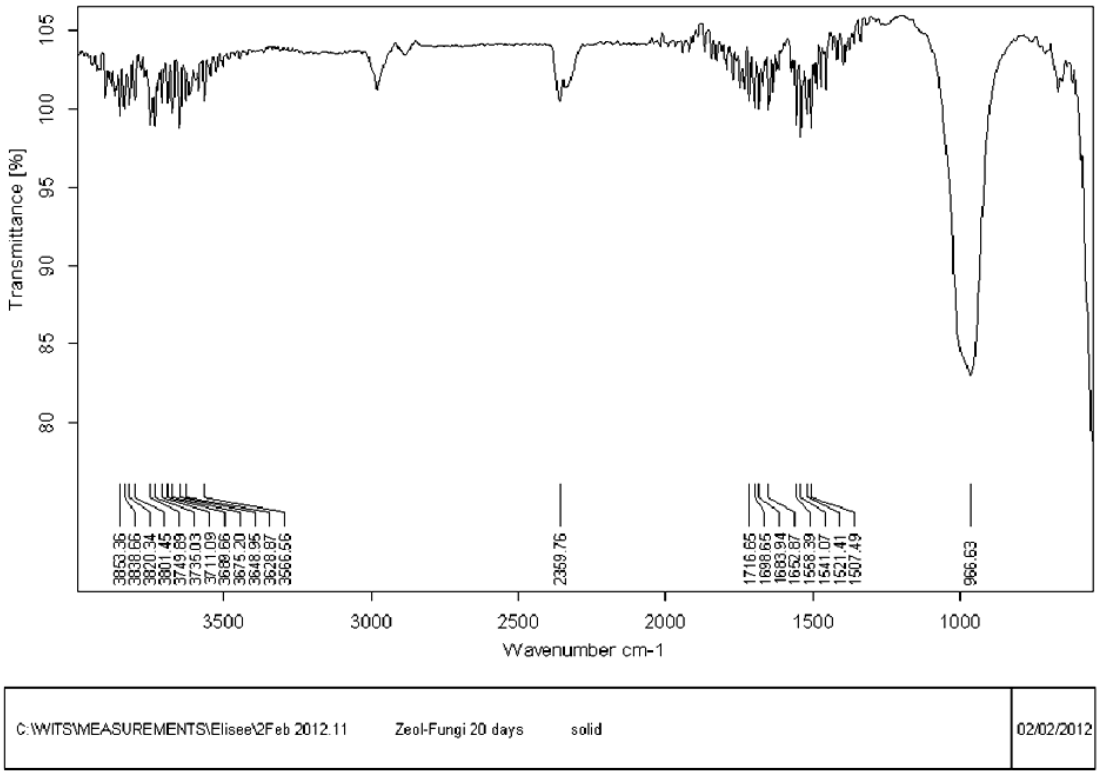
Transmittance [%]
105
100
95
90
85
80
3853.36
3838.66
3820.34
3801.45
3749.89
3735.03
3711.09
3688.66
3675.20
3648.95
3628.87
3566.56
2359.76
1716.65
1698.65
1683.94
1652.87
1558.39
1541.07
1521.41
1507.49
966.63
3500
3000
2500
2000
1500
1000
Wavenumber cm-1
C:\WITS\MEASUREMENTS\Elisee\2Feb 2012.11
Zeol-Fungi 20 days
solid
02/02/2012

Appendix E

Column desorption curves of Cu, Cr, Co, Fe, Hg, Ni, Zn and U for the natural bentonite, column bed height 15 cm, cycle 1.

1. Natural bentonite

(a)

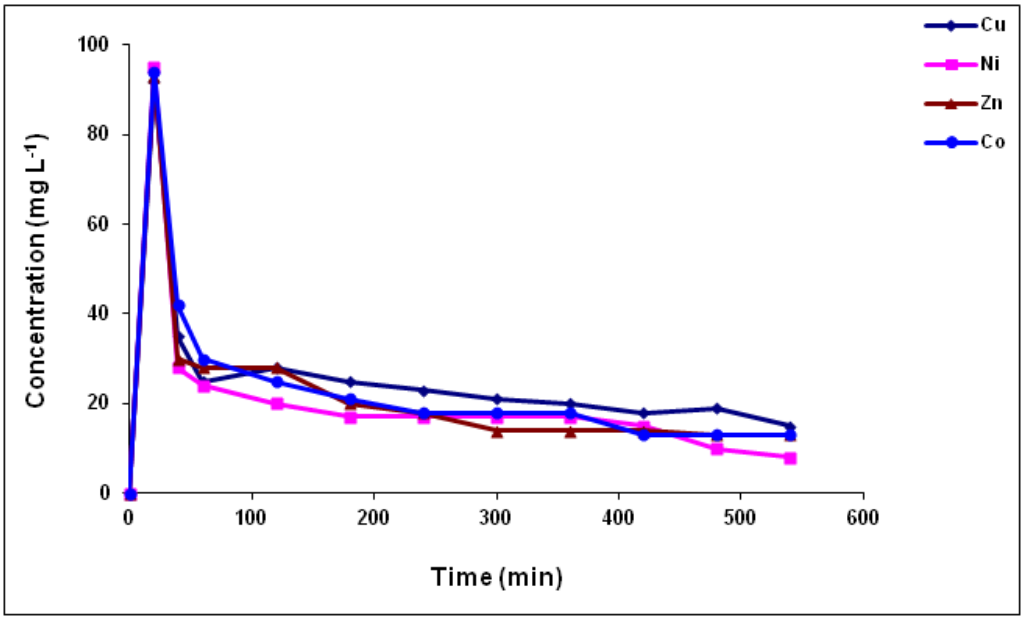

(b)

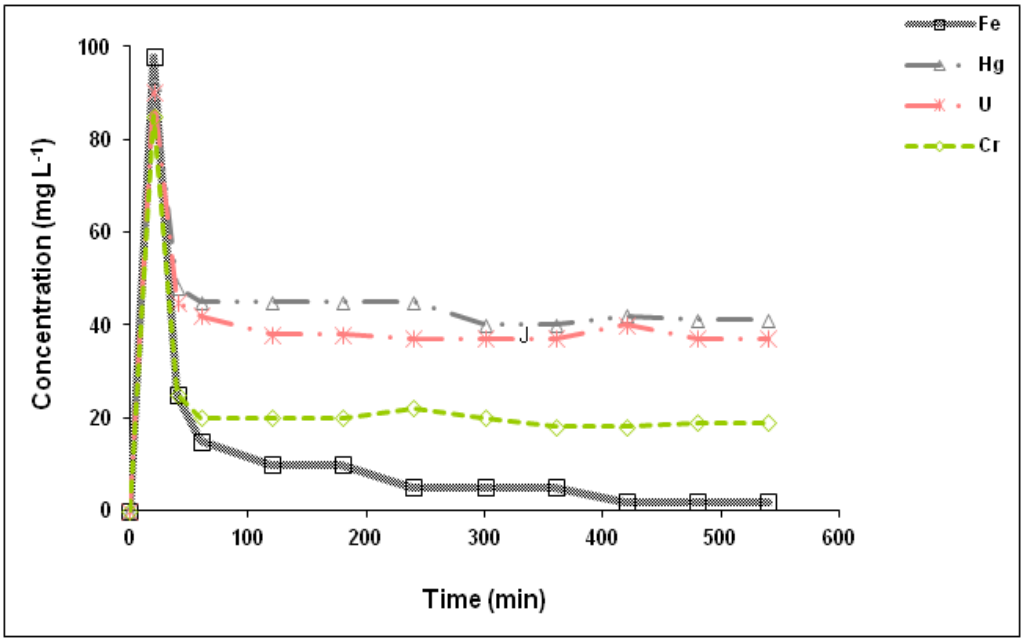

Appendix F

Column desorption curves of Cu, Cr, Co, Fe, Hg, Ni, Zn and U for the natural zeolite, column bed height 15 cm, cycle 1.

2. *Natural zeolite*

(a)

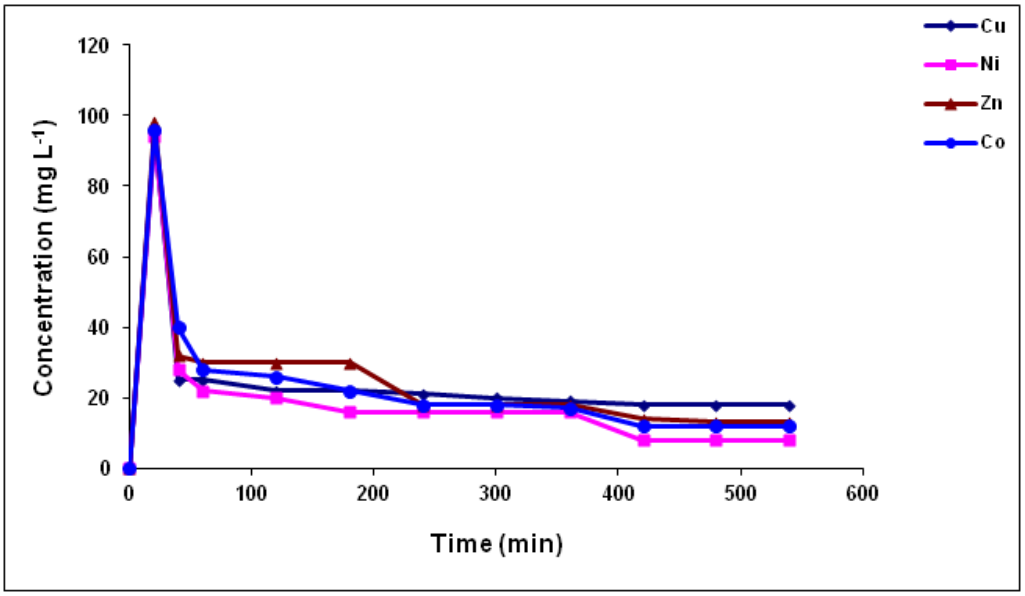

(b)

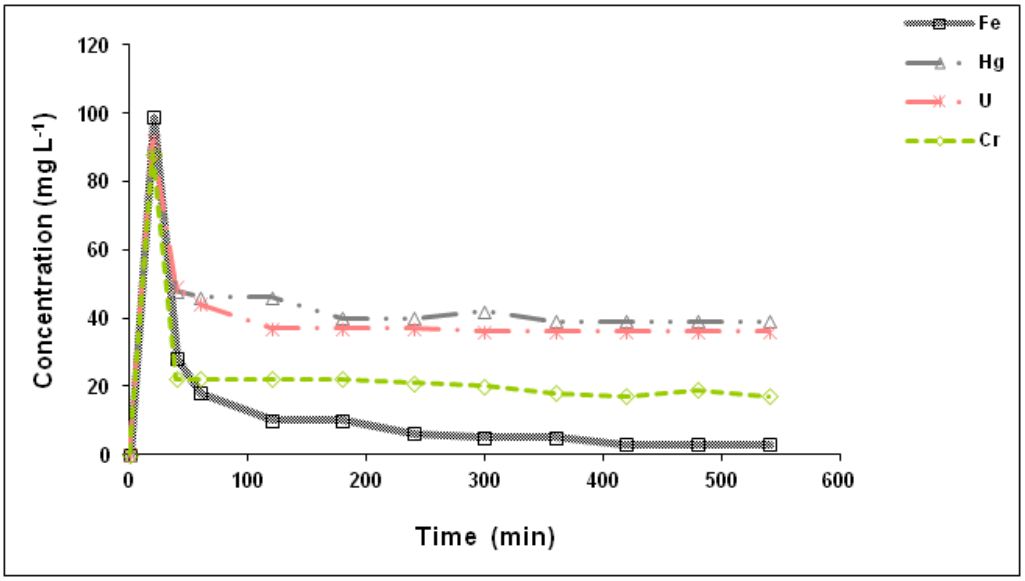

Appendix G

Column desorption curves of Cu, Cr, Co, Fe, Hg, Ni, Zn and U for the bentonite - *P.simplicissimum*, column bed height 15 cm, cycle 1.

3. Bentonite-P.simplicissimum

(a)

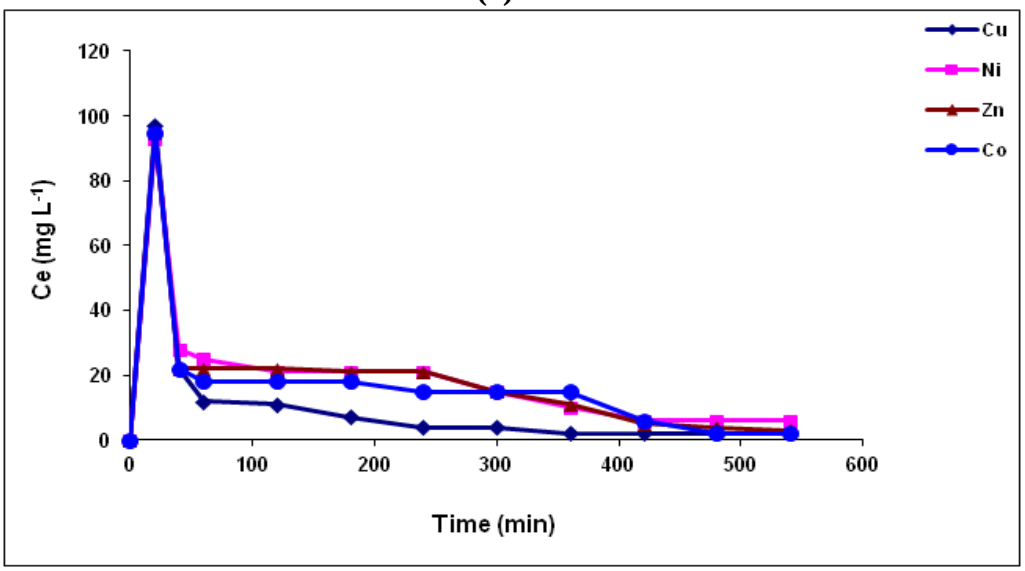

(b)

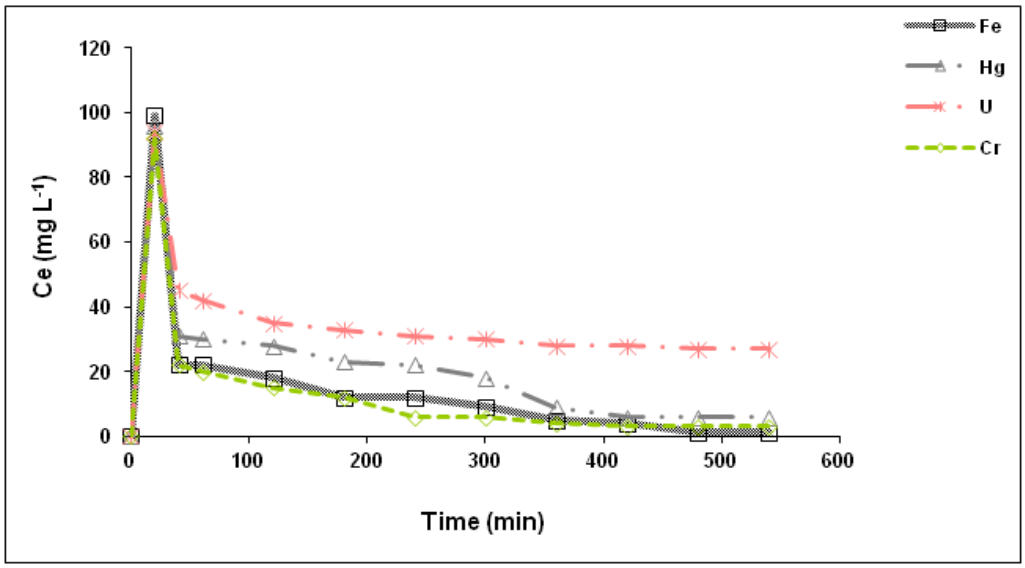

Appendix H

Column desorption curves of Cu, Cr, Co, Fe, Hg, Ni, Zn and U for the zeolite-*P.simplicissimum*, column bed height 15 cm, cycle 1.

4. Zeolite-P.simplicissimum

(a)

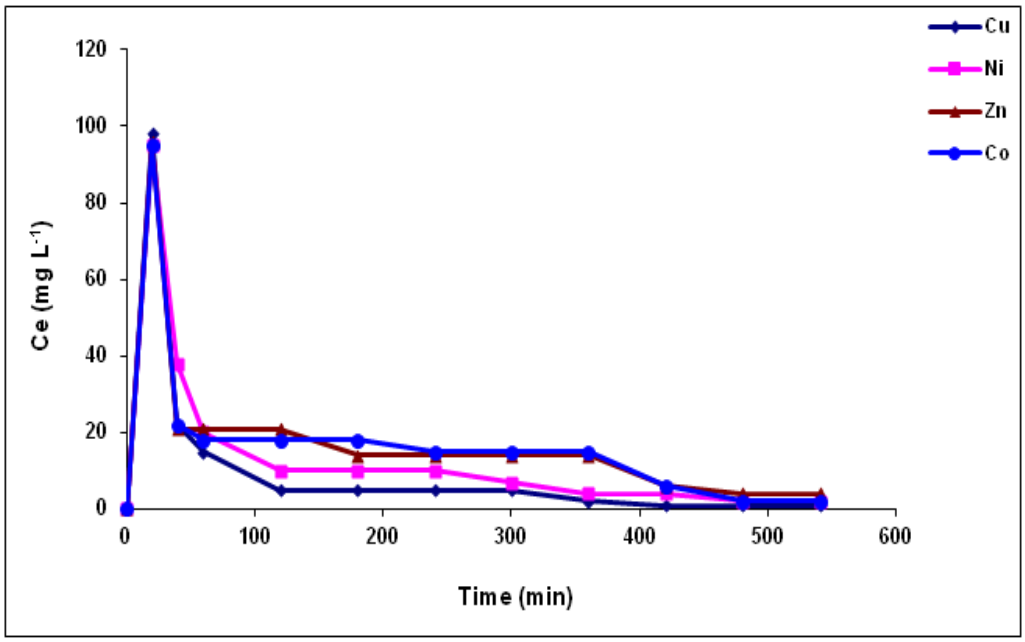

(b)

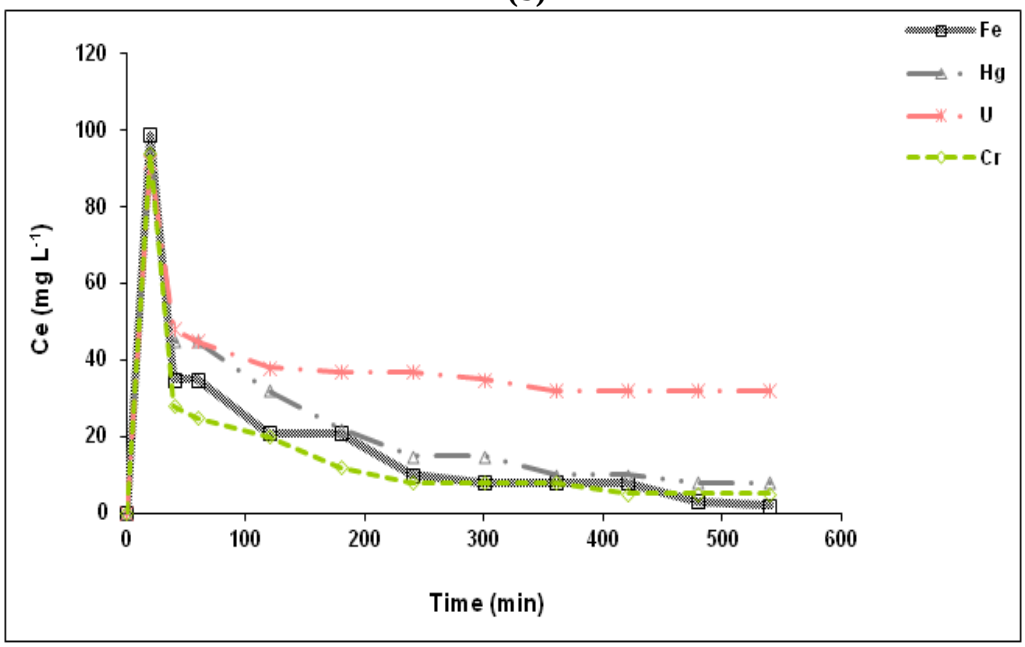

Appendix I

^{1}H-NMR spectra of alginates

Assignment of the ^{1}H signals for M and G residues from *Oedogonium* sp. algal

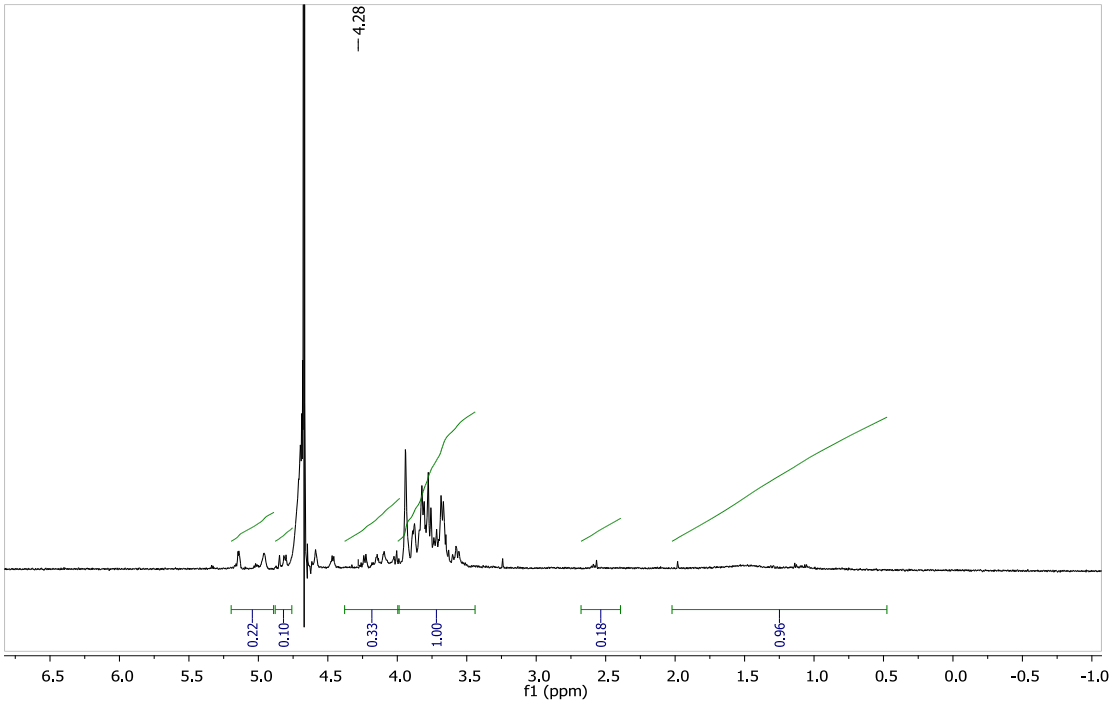

M3

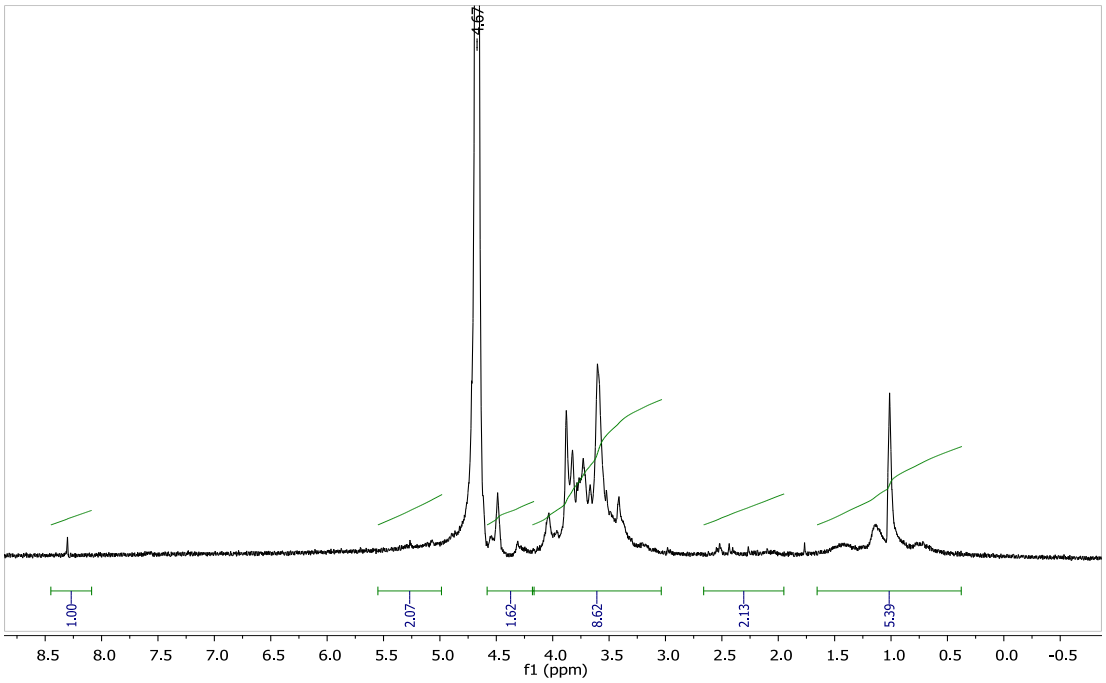

MG1

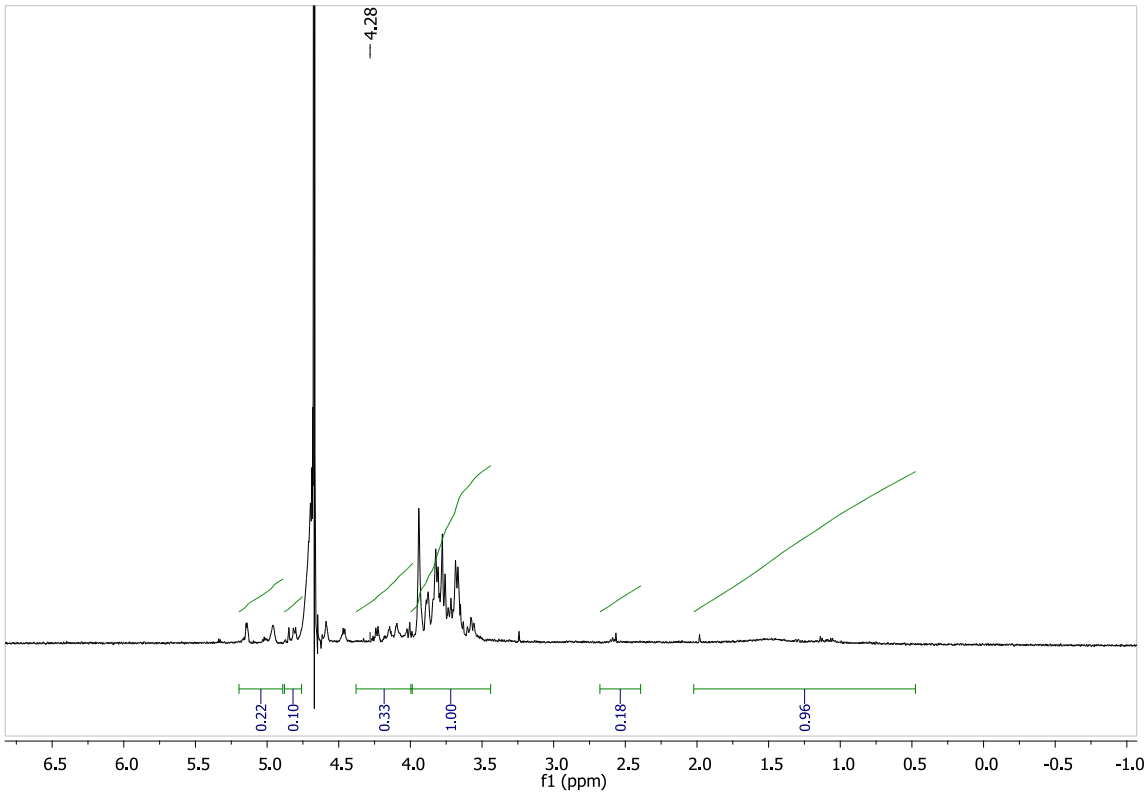
4.28
0.22
0.10
0.33
1.00
0.18
0.96
6.5
6.0
5.5
5.0
4.5
4.0
3.5
3.0
2.5
2.0
1.5
1.0
0.5
0.0
-0.5
-1.0
f1 (ppm)

MG2